



**Technische Universität München**

**Fakultät für Chemie**

**Influence of aging on binder systems and chemical admixtures  
in cementitious building materials**

**Florian Andreas Hartmann**

Vollständiger Abdruck der von der Fakultät für Chemie der Technischen Universität  
München zur Erlangung des akademischen Grades eines

**Doktors der Naturwissenschaften (Dr. rer. nat.)**

genehmigten Dissertation.

Vorsitzender: Prof. Dr.-Ing. Kai-Olaf M. Hinrichsen

Prüfer der Dissertation:

1. Prof. Dr. Johann P. Plank
2. apl. Prof. Dr. Anton Lerf

Die Dissertation wurde am 23.11.2021 bei der Technischen Universität München eingereicht  
und durch die Fakultät für Chemie am 03.05.2022 angenommen.

Die vorliegende Arbeit entstand in der Zeit von Oktober 2017

bis Oktober 2020 unter der Anleitung von

**Herrn Prof. Dr. Johann Plank**

am Lehrstuhl für Bauchemie der Technischen Universität München.

*"Seize the time, Meribor – live now! Make now always the most precious time.  
Now will never come again."*

*Patrick Stewart, Star Trek: The Next Generation „The Inner Light“*

*They treat me like a fox, a cunning fellow of the first rank.*

*But the truth is that with a gentleman I am always a gentleman and a half,  
and when I have to do with a pirate, I try to be a pirate and a half.*

*Man cannot control the current of events. He can only float with them and steer.*

*Otto von Bismarck*

Mein besonderer Dank gilt

**Herrn Prof. Dr. Johann Plank**

für die Aufnahme am Lehrstuhl für Bauchemie und das Vertrauen, mir die Zuständigkeit für ein drittmittelgefördertes Forschungsprojekt und die Position des Sicherheitsbeauftragten zu übertragen. Auch möchte ich ihm für die Vermittlung eines Forschungsaufenthaltes in Japan bei der Firma Denka während meines Masterstudiums danken.

Mein weiterer Dank gilt:

- der *Deutschen Forschungsgemeinschaft* (DFG) für die Förderung dieses Forschungsvorhabens mit Sachbeihilfen unter der Projektnummer PL-472 / 9-2
- den Firmen *HeidelbergCement, Imerys, Nabaltec* und *Quarzwerke* für die großzügige Versorgung mit Bindemitteln und Rohstoffen für die Klinkersynthese

Persönlich möchte ich mich bedanken bei:

- meinen Laborkollegen **Marlene Schmid, Alexander Engbert, Christopher Schiefer** und **My Linh Vo** für die gute Zusammenarbeit
- im Besonderen Herrn **Christopher Schiefer** für die Unterstützung bei der Instandhaltung der Labor- und Messausrüstung
- und Herrn **Alexander Engbert** für die vielen Gespräche nach Feierabend zum Philosophieren und Dampf ablassen
- allen anderen (Post-)Doktoranden während unserer gemeinsamen Zeit, Dr. **Lei Lei, Timon Echt, Manuel Ilg, Steffi Gruber, Claudia Chomyn, Matthias Theobald, Johann Mekulanetsch, Matthias Werani, Dominik Staude** und nicht zuletzt Dr. **Oksana Storcheva** für die Einarbeitung zu Beginn meines Aufenthalts am Lehrstuhl für Bauchemie
- der Laborantin **Dagmar Lettrich** für die experimentelle Unterstützung

- meinem Mentor und ersten Praktikumsbetreuer am Lehrstuhl Dr. **Thomas Hurnaus**
- den Studenten **Abdul Rahman, Pia Peitl, Sebastian Schleser, Philip Deng, Jiang Jingwen** und **Lucia Mengel** für die Projektmitarbeit im Rahmen ihrer Forschungspraktika und Abschlussarbeiten
- **Myriam Reif** vom Lehrstuhl für Siedlungswasserwirtschaft (Prof. Dr. Jörg Drewes) und **Max Koch** vom Arbeitskreis Synthese und Charakterisierung innovativer Materialien (Prof. Dr. Tom Nilges) für die abteilungsübergreifende Zusammenarbeit
- den Lehrstuhl-Alumni Dr. **Elina Dubina** und Dr. **Markus Meier** für ihre umfassenden und sorgfältigen Arbeiten als meine Vorgänger auf dem Forschungsgebiet Zementalterung, die eine stabile Grundlage für meine eigene Tätigkeit geliefert haben

Ferner möchte ich meinen Freunden außerhalb der Universitätssphäre danken, die mich zum Teil schon begleiten, seitdem ich zum ersten Mal das Wort Chemie gehört habe. Auf dass uns noch zahlreiche weitere Jahre miteinander vergönnt sind!

Der letzte und für mich wichtigste Dank gebührt meinen Großeltern und meinen Eltern **Monika** und **Dr. Klaus-Peter Hartmann**, ohne die ich auf meinem Lebensweg nie so weit gekommen wäre. Sie haben mein Interesse für die Naturwissenschaften geweckt und mich auch in ihren schwersten Zeiten nach Kräften unterstützt. Ihnen sei diese Arbeit gewidmet.

## List of journal articles and conference contributions

The present thesis is based upon the following scientific publications:

Articles in peer-reviewed journals:

1. F. A. Hartmann, J. Plank  
**Impact of aging on the hydration of tricalcium aluminate (C<sub>3</sub>A) / gypsum blends and the effectiveness of retarding admixtures**  
*Zeitschrift für Naturforschung B*, 75 (8), **2020**, 739–753  
<https://doi.org/10.1515/znb-2020-0087>
2. F. A. Hartmann, J. Plank  
**New insights into the effects of aging on Portland cement hydration and on retarder performance**  
*Construction and Building Materials*, 274, **2020**, 122104  
<https://doi.org/10.1016/j.conbuildmat.2020.122104>
3. F. A. Hartmann, L. C. Mengel, J. Plank  
**Effects of exposure to atmospheric moisture and CO<sub>2</sub> on the performance of a ternary binder system and chemical admixtures in a self-levelling underlayment**  
Submitted to *Construction and Building Materials* on 15 May **2022**

Contributions to international conferences:

1. F. A. Hartmann, M. R. Meier, J. Plank  
**Wirksamkeit von Verzögerern in gealtertem Zement und reinen Klinkerphasen**  
*20. Internationale Baustofftagung*, Weimar, Germany, 12–14 September **2018**  
in: H.-M. Ludwig (pub.), Proceedings, volume 1, 590–597
2. F. A. Hartmann, M. R. Meier, J. Plank  
**The impact of cement and clinker prehydration on retarder performance**  
*15<sup>th</sup> International Congress on the Chemistry of Cement*, Prague, Czechia, 16–20 September **2019**  
in: J. Gemrich (ed.), Papers and posters proceedings, 1–8
3. F. A. Hartmann, A. A. Engbert, J. Plank  
**Towards understanding the ageing behaviour of SLU formulations: Impact of prehydration on individual components and the role of admixtures**  
*5<sup>th</sup> International Conference on Calcium Aluminates*, Cambridge, United Kingdom, 01–03 June **2020** (postponed to 18–20 July **2022**)  
in: C. H. Fentiman, R. J. Mangabhai (eds.), Proceedings, part 6 – Ternary binders (accepted)

## LIST OF CONTENTS

---

### List of contents

List of journal articles and conference contributions.....	I
List of contents.....	II
List of figures .....	V
List of abbreviations.....	VII
Cement chemist notation.....	IX
<b>1      Introduction to cementitious building materials.....</b>	<b>1</b>
1.1     A brief history of cement .....	1
1.2     Chemical admixtures for cement.....	3
1.3     On cement aging .....	4
<b>2      Relevant knowledge of cement chemistry .....</b>	<b>5</b>
2.1     Chemical composition of cement .....	5
2.1.1     Major constituents of Portland cement: The clinker phases.....	5
2.1.1.1     Tricalcium oxy silicate C <sub>3</sub> S.....	5
2.1.1.2     Dicalcium silicate C <sub>2</sub> S .....	6
2.1.1.3     Tricalcium aluminate C <sub>3</sub> A.....	6
2.1.1.4     Tetracalcium alumino ferrite C <sub>4</sub> AF .....	7
2.1.2     Minor components of Portland cement.....	8
2.1.3     Industrial Portland cement production .....	8
2.1.3.1     Synthesis of the clinker phases .....	8
2.1.3.2     Milling the cement clinker.....	9
2.1.4     Non-Portland cements and cement blends .....	11
2.2     Chemistry of cement hydration .....	13
2.2.1     Role of the water / cement ratio .....	13

## LIST OF CONTENTS

---

2.2.2	Chemical reactions during Portland cement hydration .....	14
2.2.2.1	Hydration of the silicate phases .....	14
2.2.2.2	Properties of silicate phase hydrates .....	17
2.2.2.3	Hydration of C <sub>3</sub> A.....	20
2.2.2.4	Hydration of C <sub>4</sub> AF .....	24
2.2.3	Setting and hardening of Portland cement .....	25
2.2.4	Hydration of calcium aluminate cement and cement blends .....	25
2.3	Chemical admixtures in cement hydration.....	27
2.3.1	General information.....	27
2.3.2	Accelerators.....	28
2.3.3	Retarders .....	31
2.3.4	Dispersing agents.....	34
2.4	Impact of cement aging on hydration.....	39
2.4.1	Background information .....	39
2.4.2	Aging impact on binders.....	40
2.4.3	Aging impact on admixtures.....	42
<b>3</b>	<b>Scope of the present thesis.....</b>	<b>45</b>
3.1	Research objectives .....	45
3.2	Experimental work .....	48
3.2.1	Synthesis procedures.....	48
3.2.1.1	Clinker phases C <sub>3</sub> A and C <sub>3</sub> S.....	48
3.2.1.2	Binders, ternary binder system and self-levelling underlayment.....	51
3.2.1.3	Synthetic ettringite .....	52
3.2.2	Aging procedure .....	52
3.2.3	Investigation of the aging impact .....	53
3.2.3.1	Sample characterization.....	53
3.2.3.2	Examining the hydration behavior.....	55

## LIST OF CONTENTS

---

<b>4</b>	<b>Results and discussion.....</b>	<b>61</b>
4.1	Outline.....	61
4.2	Topic 1: Impact of aging on retarder performance in clinker phases and OPC.....	62
4.2.1	Journal article 1: Clinker phase C <sub>3</sub> A .....	62
4.2.1.1	Content overview for journal article 1 .....	62
4.2.1.2	Reprint of journal article 1 .....	65
4.2.2	Journal article 2: Portland cement .....	81
4.2.2.1	Content overview for journal article 2 .....	81
4.2.2.2	Reprint of journal article 2 .....	84
4.2.3	Further investigations on topic 1 .....	96
4.2.3.1	Compilation of the results.....	96
4.2.3.2	Reprint of conference contribution 1 .....	99
4.2.3.3	Reprint of conference contribution 2 .....	108
4.3	Topic 2: Impact of aging on the TBS and chemical admixtures in a model SLU.....	121
4.3.1	Journal article 3: Aging of various components of a model SLU .....	121
4.3.1.1	Content overview for journal article 3 .....	121
4.3.1.2	Reprint of journal article 3 .....	124
4.3.2	Further investigations on topic 2 .....	147
4.3.2.1	Compilation of the results.....	147
4.3.2.2	Reprint of conference contribution 3 .....	149
<b>5</b>	<b>Conclusion .....</b>	<b>163</b>
5.1	Summary of the project and outlook for future research.....	163
5.2	Official project report (in German) .....	167
<b>6</b>	<b>References .....</b>	<b>183</b>

**List of figures**

<b>Figure 1:</b> Comparative tests between Roman cement and Portland cement .....	2
<b>Figure 2:</b> An $\text{Al}_6\text{O}_{18}$ puckered ring, structural element of the $\text{C}_3\text{A}$ clinker phase .....	7
<b>Figure 3:</b> Transformation of raw materials into clinker in a rotary kiln .....	9
<b>Figure 4:</b> Diagram of a ball mill and a vertical mill.....	10
<b>Figure 5:</b> Filling gaps between cement particles with fine limestone to increase flowability .....	11
<b>Figure 6:</b> Application of self-levelling underlays (SLUs).....	12
<b>Figure 7:</b> Formation of cement hydration products .....	13
<b>Figure 8:</b> Hydration of a cement paste as a closed system or with an external water source .....	14
<b>Figure 9:</b> Stages of the $\text{C}_3\text{S}$ hydration process by heat release and free $\text{Ca}^{2+}$ concentration .....	15
<b>Figure 10:</b> Idealized structures of 1.4 nm tobermorite and jennite.....	18
<b>Figure 11:</b> SEM images after hydrating $\text{C}_3\text{S}$ at a w/s ratio of 1.0 and 20 °C.....	19
<b>Figure 12:</b> SEM images showing a ‘normal’ and a ‘flash’ set of Portland cement.....	20
<b>Figure 13:</b> Stages in the hydration of $\text{C}_3\text{A}$ with gypsum by heat release and conductivity .....	22
<b>Figure 14:</b> SEM images of ettringite and monosulfoaluminate in cement pastes at high w/c ratios ...	23
<b>Figure 15:</b> Schematic representation of the structure of trigonal ettringite .....	24
<b>Figure 16:</b> Heat flow diagram of OPC hydration and impacts of accelerating admixtures .....	29
<b>Figure 17:</b> Effect of various accelerating admixtures on Portland cement hydration .....	31
<b>Figure 18:</b> Impact of glucose retarder on Portland cement hydration at various dosages .....	32
<b>Figure 19:</b> Sodium tartrate retarder and non-retarding sodium caprate .....	33
<b>Figure 20:</b> Transformation of D-glucose between $\alpha$ and $\beta$ ring via the open intermediate .....	34
<b>Figure 21:</b> Photographs of suspended cement particles before and after superplasticizer addition ..	35
<b>Figure 22:</b> Effects of superplasticizer addition on rheological properties and water demand .....	35

## LIST OF FIGURES

---

<b>Figure 23:</b> Structural elements of a comb-shaped copolymer superplasticizer .....	36
<b>Figure 24:</b> Major synthesis routes for PCE superplasticizers .....	37
<b>Figure 25:</b> Impact of superplasticizing admixtures on mortars containing Portland cement .....	38
<b>Figure 26:</b> Schematic representation of the cement aging process.....	39
<b>Figure 27:</b> Main experimental work carried out over the course of the DFG project PL 472/9-2.....	46
<b>Figure 28:</b> Overview of the preparation of the clinker phases C <sub>3</sub> A and C <sub>3</sub> S .....	48
<b>Figure 29:</b> Comparison between clinker phases synthesized from quarried or precipitated CaCO <sub>3</sub> ..	49
<b>Figure 30:</b> Effects of pregrinding CaCO <sub>3</sub> on the particle size distributions of the C <sub>3</sub> A polymorphs....	50
<b>Figure 31:</b> Overview of the preparation of the TBS and the SLU .....	51
<b>Figure 32:</b> Overview of the preparation of the aged samples .....	52
<b>Figure 33:</b> Overview of the methods used to characterize fresh and aged samples .....	54
<b>Figure 34:</b> Overview of the methods used to analyze the hydration of fresh and aged samples .....	56
<b>Figure 35:</b> Preparation of powder XRD and in situ XRD samples .....	56
<b>Figure 36:</b> Schematic representation of the operating principle of a TOC analyzer.....	57
<b>Figure 37:</b> Vicat apparatus with glass vessel holding the hydrating sample .....	59
<b>Figure 38:</b> Preparation of prisms from hydrated paste for compressive strength tests .....	59
<b>Figure 39:</b> Overview of the scientific publications associated with each project topic .....	61
<b>Figure 40:</b> Overview of journal article 1 on the aging of the C <sub>3</sub> A clinker phase .....	62
<b>Figure 41:</b> Overview of journal article 2 on the retarder performance in aged CEM I 52.5 N .....	81
<b>Figure 42:</b> Depletion of NaGluc retarder from the liquid by fresh and aged synthetic ettringite.....	97
<b>Figure 43:</b> Admix ampoule after removal from the calorimeter .....	98
<b>Figure 44:</b> Overview of journal article 3 on the aging of TBS and SLU .....	121
<b>Figure 45:</b> Impact of OPC aging on the performance of NaGluc and KPPhos (not to scale) .....	163
<b>Figure 46:</b> Impact of aging TBS / admixture combinations or the full SLU on the hydration.....	165

**List of abbreviations**

AH	anhydrite
bwob	by weight of binder
bwoc	by weight of cement
bwoe	by weight of ettringite
bwof	by weight of formulation
c or cub	cubic
CAC	calcium aluminate cement
cm <sup>(-1)</sup>	(reciprocal) centimeter
°C	degree Celsius
d	days
d <sub>10/50/90</sub>	mass-median-diameter in particle-size distribution
DIN	German standard
EN	European standard
(E)SEM	(environmental) scanning electron microscopy
FTIR-ATR	Fourier transformed infrared - attenuated total reflection
g	gram
h	hours
ICP-OES	inductively coupled optical emission spectroscopy
J	joule
kg	kilograms
KPPhos	potassium pyrophosphate
L	liter
m or mono	monoclinic
MAS	magic angle spinning
mg	milligrams
min	minutes
mL	milliliter

## LIST OF ABBREVIATIONS

---

mW/g	milliwatt per gram
N/mm <sup>2</sup>	newton per square millimeter
NaGluc	sodium gluconate
nm	nanometer
NMR	nuclear magnetic resonance
o or orth	orthorhombic
OPC	ordinary Portland cement
PCE	polycarboxylate ester / ether
PDI	polydispersity index
PEG	polyethylene glycol
pH	pondus hydrogenii
RH	relative humidity
rpm	revolutions per minute
s or sec	seconds
SCPS	synthetic cement pore solution
SLU	self-levelling underlayment
t or tric	triclinic
TBS	ternary binder system
TGA	thermogravimetric analysis
TG-MS	thermogravimetry coupled with mass spectroscopy
TOC	total organic carbon
µm	micrometer
UV-Vis	ultraviolet - visible
w/b	water-to-binder ratio
w/c	water-to-cement ratio
w/f	water-to-formulation ratio
w/s	water-to-solid ratio
wt.%	weight percent
XRD	X-ray diffraction

**Cement chemist notation**

A aluminum oxide,  $\text{Al}_2\text{O}_3$

C calcium oxide,  $\text{CaO}$

F iron oxide,  $\text{Fe}_2\text{O}_3$

H water,  $\text{H}_2\text{O}$

S silicon oxide,  $\text{SiO}_2$

\$ sulfur oxide,  $\text{SO}_3$

$\text{C}_3\text{A}$  tricalcium aluminate,  $\text{Ca}_3\text{Al}_2\text{O}_6$

$\text{C}_{12}\text{A}_7$  mayenite,  $\text{Ca}_{12}\text{Al}_{14}\text{O}_{33}$

CA calcium aluminate,  $\text{CaAl}_2\text{O}_4$

CA<sub>2</sub> calcium dialuminate,  $\text{CaAl}_4\text{O}_7$

$\text{C}_4\text{AF} / \text{C}_2(\text{A},\text{F})$  tetracalcium aluminoferrite,  $\text{Ca}_2(\text{Al}_x\text{Fe}_{1-x})_2\text{O}_5$

$\text{C}_3\text{S}$  tricalcium oxysilicate,  $\text{Ca}_3\text{SiO}_5$

$\text{C}_2\text{S}$  dicalcium silicate,  $\text{Ca}_2\text{SiO}_4$

$\text{C}\$\text{H}_2$  calcium sulfate dihydrate,  $\text{CaSO}_4 \cdot 2 \text{H}_2\text{O}$

AH<sub>3</sub> aluminum hydroxide,  $\text{Al}(\text{OH})_3$

CAH<sub>10</sub>  $\text{Ca}[\text{Al}(\text{OH})_4]_2 \cdot x \text{H}_2\text{O}$ ,  $\text{CaAl}_2(\text{OH})_8(\text{H}_2\text{O})_2 \cdot x \text{H}_2\text{O}$

$\text{C}_2\text{AH}_8$   $\text{Ca}_2[\text{Al}(\text{OH})_5]_2 \cdot x \text{H}_2\text{O}$ ,  $[\text{Ca}_2\text{Al}(\text{OH})_6]^+[\text{Al}(\text{OH})_4 \cdot x \text{H}_2\text{O}]^-$

$\text{C}_4\text{AH}_{13/19}$   $\text{Ca}_2[\text{Al}(\text{OH})_7] \cdot x \text{H}_2\text{O}$ ,  $2([\text{Ca}_2\text{Al}(\text{OH})_6]^+\text{OH}^- \cdot x \text{H}_2\text{O})$

$\text{C}_3\text{AH}_6$   $\text{Ca}_3[\text{Al}(\text{OH})_6]_2$

$\text{C}_6\text{A\$}_3\text{H}_{32}$  ettringite,  $\text{AF}_t$ ,  $[\text{Ca}_3\text{Al}(\text{OH})_6]_2 \cdot (\text{SO}_4)_3 \cdot 26 \text{H}_2\text{O}$

$\text{C}_4\text{A\$H}_{12}$  monosulfoaluminate,  $\text{AF}_m$ ,  $[\text{Ca}_2\text{Al}(\text{OH})_6]_2 \cdot \text{SO}_4 \cdot 6 \text{H}_2\text{O}$

C–S–H calcium silicate hydrate,  $\text{Ca}_x\text{Si}_y\text{O}_z$

CH calcium hydroxide,  $\text{Ca}(\text{OH})_2$

# 1 Introduction to cementitious building materials

## 1.1 A brief history of cement

The origins of modern cements can be traced back to the first use of lime, clay and gypsum as building materials several millennia ago. At the time of writing, the oldest such structures are believed to have been created in Neolithic Anatolia in modern-day Turkey. Pillars made of burnt limestone and clay at the site of Göbekli Tepe date from 12,000–10,000 BCE while gypsum plaster from at least 9,000 BCE was found in Çatalhöyük. The technological progress of this era culminated in the development of an early concrete-like material in which hydrated lime bonded pieces of stone. Remains of its production dating from around 7,000 BCE were discovered in Galilee in the eastern Mediterranean [1].

The first binders lacked the clinker phases of modern cements, so their adhesive capabilities relied almost exclusively on the transition from quicklime to slaked lime. At the time, only wood-fired kilns that could not exceed temperatures of 850–1000 °C were available, which limited the treatment of limestone to just calcination [2]. To make matters worse, in many cradles of civilization along the Fertile Crescent wood was too scarce to be used as fuel. There, primarily calcium sulfate plasters were used, taking advantage of the low temperatures required to partially dehydrate gypsum which would reform on contact with water. The arid climate of the region guaranteed a reasonable durability for these soluble plasters [3].

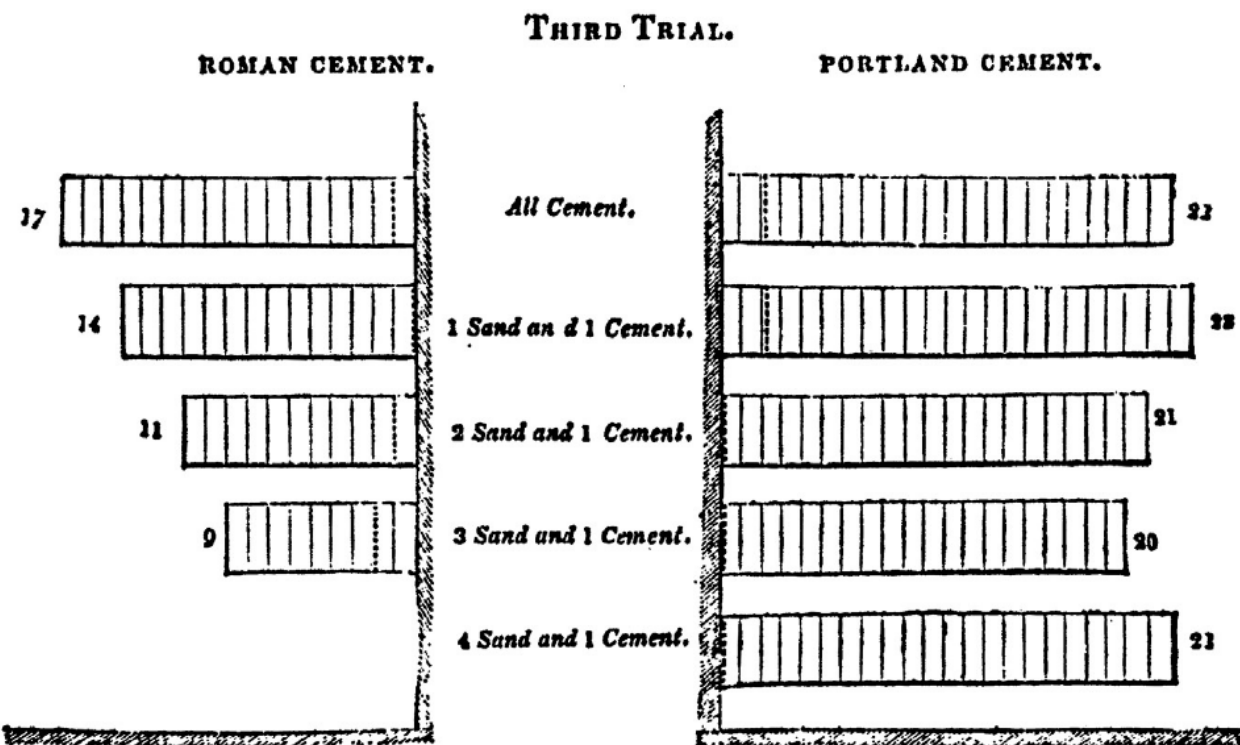
The transition from Neolithic binders to antique cements (from Latin *opus caementitium*) was achieved in Greece around 500 BCE. Specifically, limestone was in part replaced by volcanic ash from the island of Thera, today known as Santorini, which had been devastated about 1000 years earlier by the Minoan eruption, one of the largest in human history. The combination of the two materials greatly increased the durability of the hydrated binder, with some structures having persevered until the present day. Famous examples remain from the Roman empire, where the technology had made its way shortly after being discovered. The Romans were no strangers to volcanic activity, which is why these ashes are known today as *pozzolana*. The name is derived from Pozzuoli – a town located both in the middle of the Phlegraean fields and around 30 km west of Mount Vesuvius [4].

The downfall of the western Roman empire arrested the development of cementitious building materials for over a millennium. The immigrating Germanic tribes were more familiar with wooden constructions and smaller, sometimes temporary settlements due to the abundance of timber in their ancestral territories. With the spread of Christianity in Europe, places of worship in Romanesque, gothic, renaissance and ultimately baroque architecture helped maintain the – albeit diminished – knowledge of antique cements through the Medieval ages and early modern period.

Against this background, in 18<sup>th</sup> century England John Smeaton set out to uncover the science behind the hydraulic properties of certain binders, which allowed them to harden under water. This research was motivated by the need of the growing naval power Great Britain for durable seaports and lighthouses. The most famous example of the latter was constructed on the Eddystone Rocks after Smeaton had compared the performance of over 300 different sources of limestone and extensively tinkered with the ratio of pozzolana, trass and ferrous materials additions. The finished building guided ships through the western approaches of the British Channel from 1759 to 1882, when it was not

destroyed but deemed insufficient in size. After relocation to Plymouth, it serves as a tourist attraction until this day [5, 6].

Among the most familiar names associated with the development of cement in the modern era are that of John Aspdin and his son William. In 1824, Aspdin Sr. filed a patent for 'Portland' cement, a rather ambiguously defined mix of limestone and argillaceous earth or clay [7]. The name was chosen purely for marketing reasons, it likened the material to a popular sort of limestone from the namesake isle off Dorset. Portland cement was not immediately superior to known limestone binders, but over the following decades its performance was found to greatly increase with rising calcination temperatures, which were provided by the potent coal-fired kiln designs of the Industrial revolution [3, 8–10]. Compared to Roman cement, Portland was up to 50% more expensive [11], but had the crucial advantage to develop sufficient strength at low ratios of binder to aggregate (**Figure 1**), thus alleviating its higher cost by the reduced amount of cement required [6, 12].



**NOTE.**—The figures denote the number of bricks each specimen carried before it broke from the wall. The trials of adhesion were worked without a centre. The dotted lines indicate the points of fracture.

**Figure 1:** Comparative tests between Roman cement and Portland cement from 1843 [12].

Reprinted from [1] with permission.

Portland cement performance was consistently improved over the remainder of the 19<sup>th</sup> century. For example, German cements of 1885 developed around twice the strength of British ones from 20 years earlier, mainly due to advances in the calcination process [12–14]. The British responded in kind with a prototype rotary kiln, which after further improvement in the United States started to be used all around the world. During this period, Edouard Candlot discovered that calcium sulfate delayed cement setting and Henry Louis Le Chatelier published his groundbreaking findings on the hydration of cement clinker [10, 13, 15]. These developments culminated in the first standardizations of cements on a

scientific basis, notably the German standard of 1887, the 1904 British BS 12 and the American ASTM C9, also of 1904.

International cement production has skyrocketed since the beginning of the 20<sup>th</sup> century, reaching over 4 billion tons per annum and thus surpassing oil as the world's most produced commodity at the time of writing [16]. Improvements in the milling technology enabled a strength classification of cements based on particle fineness. Cement production has also diversified with binders becoming increasingly tailored towards specific demands in application. Examples for sought-after properties are water repellency, rapid hardening, and / or high sulfate resistance. Cements can be designed for high-temperature and -pressure environments such as encountered when reinforcing deep bore holes [17, 18]. To reduce CO<sub>2</sub> emissions without compromising performance, cement producers aim to lower both limestone requirements and kiln temperatures by incorporating materials with pozzolanic properties such as pulverized fly ash, blast furnace slag and rice husk ash. Moreover, blending cements with other binders such as calcium sulfates can combine multiple desirable properties such as good workability, fast strength development and self-levelling. However, success in application is often not only a question of choice and composition of the binder but also requires deliberate modification of certain properties via chemical admixtures.

## 1.2 Chemical admixtures for cement

Both inorganic and organic admixtures were added to cement almost from its first use. They are not to be confused with additives, for example pozzolans, or aggregates such as stone. The earliest admixtures were plant and animal products. Blood, fat and milk improved the workability of concrete and entrained air. Urea was found to affect the setting and hardening process. Most admixtures probably first came into contact with cements accidentally. Once identified, beneficial effects were documented for targeted use. Several centuries BCE, the Romans gave instructions to add eggs and blood to the binders in concrete [19, 20] and in the 13<sup>th</sup> century, gothic architects reported the use of vegetable oil addition to waterproof exposed surfaces [21].

Following the start of industrialized cement production, lubricant oils used in the bearings of clinker mills sometimes found their way into the cement and were reported to increase air-entrainment [20] which improved freeze-thaw resistance [22]. Tallow, added to the clinker during milling to improve grinding efficiency, was suspected to cause a comparable effect.

Coloring of concrete used for highway construction unintentionally resulted in a similarly increased freeze-thaw resistance of the road surface. It was found that polynaphthalene sulfonate, which had been used to homogeneously disperse the solid color particles in the concrete, also dispersed entrained air bubbles. Moreover, this colored concrete reportedly displayed increased flowability which ultimately resulted in polynaphthalene being patented as a cement dispersing agent in the US [23].

The main difference between admixtures on one side and additives and aggregates on the other is that the former can influence the binder's properties at quantities low enough that they essentially do not constitute a weight fraction in concrete. Similar to the discovery of the first admixtures, binder performance can thus unintentionally be impacted by accidental contamination of concrete batches with materials active in cement hydration. In one case, it was reported that a concrete experienced

significant retardation because it was produced with aggregates that had been transported by a truck which previously carried sugar wastes. The problem quickly subsided after the truck bed was thoroughly cleaned before switching the loads [24].

Admixture use is constantly increasing as the knowledge of the chemistry of cement hydration improves and the field of concrete applications broadens. In the bulk business that is concrete production, the choice of admixture usually boils down to a cost-performance analysis. The use of cheap industrial by-products, such as lignosulfonate plasticizers, is continuously competing with highly sophisticated synthetic compounds, in this case for example polycarboxylate ether superplasticizers, which are higher in cost but usually require lower dosages and might be tailored towards specific demands and tolerances.

## 1.3 On cement aging

In chemical terms, “aging” describes the change of material properties over time as a result of environmental influence. These changes can be both intentional or unintentional and beneficial or detrimental to the substance’s intended use. Common triggers are exposure to light, heat, moisture and / or air. With regards to cement and concrete, two forms of aging may be distinguished:

The first and generally better known one encompasses aging effects *after* the hydration of the binder has started. For one thing, concrete is exposed to atmospheric CO<sub>2</sub> following placement and hardening. Hence in surviving Neolithic and antique structures the hardened slaked lime has been converted to calcium carbonate over the millennia. As another example, the exposure of reinforced concrete to saline water weakens the passivation provided by the hydrated cement and leads to corrosion of the steel bars.

The second, less known form of cement aging is the subject of this PhD thesis. It specifies the impact of binder exposure to environmental factors *before* the application. This relates principally to the contact with atmospheric moisture and CO<sub>2</sub>. Modern binders possess high reactivity towards water as a result of advanced calcination and milling technologies. Depending on the application, chemical admixtures might be added as solids even before hydration. When these materials are unintentionally exposed to elevated humidity, a partial hydration occurs on the cement surface. This process is also known as “prehydration”. Like regular hydration products, prehydrates are susceptible to subsequent carbonation.

## 2 Relevant knowledge of cement chemistry

### 2.1 Chemical composition of cement

Cementitious building materials are mass products which require large supplies of raw materials. The outermost layer of the Earth's crust that is available for exploitation contains five elements with an abundance of more than 3% by weight, in decreasing order oxygen, silicon, aluminum, iron and calcium. From these, four principal oxides – CaO, SiO<sub>2</sub>, Al<sub>2</sub>O<sub>3</sub> and Fe<sub>2</sub>O<sub>3</sub> – are derived which comprise the main building blocks of cements. In a cement chemist's notation, they are commonly abbreviated C, S, A and F when describing the mineralogical composition of cement clinker alongside H for water in hydrates and \$ for sulfate, among others.

Portland cement is produced by the calcination of limestone with clay, shale, and sand [25]. Containing all four principal oxides, it is the most common type of cement. It is also the main binder in this work's investigations, as such it will be described in detail in the following sections. Non-Portland cements as relevant for the present thesis are briefly introduced at the end of the chapter.

#### 2.1.1 Major constituents of Portland cement: The clinker phases

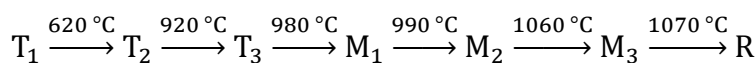
During cement production, certain binary combinations of the principal oxides emerge as the so-called clinker phases. In Portland cement, four different phases appear in significant quantities:

- Tricalcium oxy silicate Ca<sub>3</sub>SiO<sub>5</sub>, combining 3 CaO with SiO<sub>2</sub>, abbreviated C<sub>3</sub>S
- Dicalcium silicate Ca<sub>2</sub>SiO<sub>4</sub>, combining 2 CaO with SiO<sub>2</sub>, abbreviated C<sub>2</sub>S
- Tricalcium aluminate Ca<sub>3</sub>Al<sub>2</sub>O<sub>6</sub>, combining 3 CaO with Al<sub>2</sub>O<sub>3</sub>, abbreviated C<sub>3</sub>A
- Tetracalcium aluminoferrite Ca<sub>2</sub>(Al<sub>x</sub>Fe<sub>1-x</sub>)<sub>2</sub>O<sub>5</sub>, combining 4 CaO with Al<sub>2</sub>O<sub>3</sub> and Fe<sub>2</sub>O<sub>3</sub>, abbreviated C<sub>4</sub>AF

All four phases are crystalline. Following discovery, they were assigned the names alite (C<sub>3</sub>S), belite (C<sub>2</sub>S), celite (C<sub>3</sub>A) and felite (C<sub>4</sub>AF), [26] due to the latter being considered as celite containing iron (Fe). Today, alite and belite are still commonly used while C<sub>3</sub>A is mostly referred to as the aluminate and C<sub>4</sub>AF as the ferrite phase.

##### 2.1.1.1 Tricalcium oxy silicate C<sub>3</sub>S

C<sub>3</sub>S is the most abundant clinker phase in Portland cement. A polymorphic mineral, it undergoes a series of phase transformations with increasing temperature from variants of triclinic (T<sub>1</sub>–T<sub>3</sub>) and monoclinic (M<sub>1</sub>–M<sub>3</sub>) symmetry to a rhombohedral (R) high-temperature modification [27, 28]:



Since all clinker phases of Portland cement are produced *in situ*, foreign ions are incorporated into the C<sub>3</sub>S crystal lattice. Apart from aluminum and iron, this also includes ions from impurities in the natural raw materials, primarily magnesium. For this reason, the term alite is sometimes used for the technical grade clinker phase to distinguish it from pure C<sub>3</sub>S. Due to the uptake of foreign ions at high

## 2.1 CHEMICAL COMPOSITION OF CEMENT

---

temperature the phase transitions during the cooling process change from those during temperature increase. This leads to the emergence of monoclinic alite when returning to ambient temperature [29, 30] instead of the triclinic modification for pure  $C_3S$ . Furthermore, both alite and pure  $C_3S$  are metastable below 1250 °C and decompose to  $C_2S$  and  $CaO$  [31, 32]. However, this process is kinetically restricted and can be arrested by quenching the clinker after it passed the burning zone of the kiln. A high alite content in Portland cement is generally favored since  $C_3S$  confers significantly more strength to the hydrating binder than  $C_3A$  and  $C_4AF$ , and develops this strength much faster than  $C_2S$ .

### 2.1.1.2 Dicalcium silicate $C_2S$

The second silicate clinker phase,  $C_2S$ , is polymorphic as well. The main modifications are designated  $\gamma$  (orthorhombic),  $\beta$  (monoclinic) and  $\alpha$  (hexagonal) in order of increasing temperature [33]. On cooling from maximum kiln temperature,  $\alpha$ - $C_2S$  will first transform to orthorhombic  $\alpha'$  below 1425 °C [34], which subsequently changes to the  $\beta$  modification at 630 °C. The transition of  $\beta$ - to  $\gamma$ - $C_2S$  occurs slowly below 500 °C. Unlike  $C_3S$ ,  $\gamma$ - $C_2S$  is stable and would not decompose even on slow cooling, but it is quite unreactive towards water at ambient temperature and thus useless in binders relying on hydraulic activity.  $C_2S$  however, like  $C_3S$ , incorporates foreign ions such as aluminum, iron and magnesium at high temperatures. Combined with quenching this results in the stabilization of  $\beta$ -belite, which is much more reactive in hydration. Still, it hydrates much slower than alite and primarily contributes to cement strength at later stages of the hardening process.

### 2.1.1.3 Tricalcium aluminate $C_3A$

$C_3A$  can crystallize in cubic, orthorhombic or monoclinic modification [32, 35–37]. Unlike the silicate phases, below the melting point of 1542 °C its polymorphism is independent of temperature and quenching. The deciding factor is the amount of foreign ions, in this case mostly  $Na^+$  and  $K^+$ , incorporated into the  $C_3A$  lattice. From pure  $C_3A$  up until 1.9 wt.% of  $Na_2O$ , a cubic modification, designated C I, is obtained. Between 1.9 and 3.7 wt.%  $Na_2O$  uptake,  $C_3A$  crystallizes in a combination of a modified cubic (C II) and an orthorhombic (O) polymorph. Above 3.7 wt.%  $Na_2O$  only the orthorhombic and above 4.6 wt.%  $Na_2O$  eq. only a monoclinic (M) modification is formed. The  $Na_2O$  uptake of  $C_3A$  generally does not surpass 5.9 wt.% [38].

The basic C I structure consists of stacked  $Al_6O_{18}$  rings (**Figure 2**) which are connected via  $Ca^{2+}$  [39]. The distance between the rings is sufficient that on  $Ca^{2+}$  substitution by  $Na^+$ , a second  $Na^+$  can occupy a cavity site in the center of the ring, restoring charge balance. The substitution distorts the ring stacking, with increasing  $Na^+$  content the cubic structure can only initially be preserved (C II) before the symmetry gradually deteriorates, first to orthorhombic and subsequently to monoclinic modification [31, 40, 41].

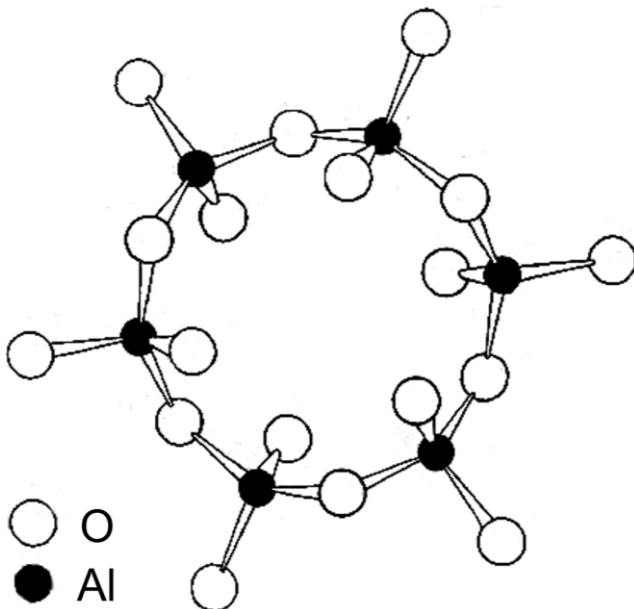


**Figure 2:** An  $\text{Al}_6\text{O}_{18}$  puckered ring, structural element of the  $\text{C}_3\text{A}$  clinker phase [39].  
Reprinted in modified form with permission.

In Portland cement production,  $\text{C}_3\text{A}$  is usually obtained as cubic and orthorhombic polymorphs, their relative share depending on the amount of sodium and potassium entering the kiln in the raw materials. Unlike the silicate phases,  $\text{C}_3\text{A}$  contributes only marginally to cement strength. However, both  $\text{C}_3\text{A}$  modifications possess vastly superior reactivity towards water than the silicate phases, the cubic form even more so than the orthorhombic one. This is problematic in cement application since the rapid development of calcium aluminate hydrates quickly stiffens the paste / concrete which reduces workability. As mentioned in the history of cement (chapter 1.1), the presence of sulfate during clinker hydration was found to slow the setting process. This will be described in detail in chapter 2.2.2 on Portland cement hydration.

#### 2.1.1.4 Tetracalcium alumino ferrite $\text{C}_4\text{AF}$

Unlike the other three clinker phases,  $\text{C}_4\text{AF}$  possesses a somewhat variable stoichiometry. It is more accurately described as a solid solution  $\text{C}_2\text{A}_{1-x}\text{F}_x$  with  $x$  ranging from 1 to  $\sim 0.3$  at atmospheric pressure [42]. At  $x = 1$ , pure  $\text{C}_2\text{F}$  would be obtained with  $\text{Fe}^{3+}$  occupying tetrahedral and octahedral sites in an orthorhombic lattice.  $\text{Al}^{3+}$  first substitutes  $\text{Fe}^{3+}$  in the tetrahedral sites. As there are only half as many of these than orthorhombic sites, the tetrahedral  $\text{Fe}^{3+}$  is fully replaced already at  $x = 0.67$ . Only at higher rates of  $\text{Al}^{3+}$  substitution is  $\text{Fe}^{3+}$  in octahedral sites replaced. The crystal modification remains orthorhombic below  $x = 0.67$ , but switches from a principal (P) to a body centered (I) lattice type.

$\text{C}_2\text{A}_{1-x}\text{F}_x$  can incorporate foreign ions, mostly  $\text{Mg}^{2+}$  and  $\text{Ti}^{4+}$ , the latter due to a distant structural similarity with perovskite  $\text{CaTiO}_3$  [43]. Unlike in the silicate and aluminate phases, the foreign ions tend to accumulate locally instead of distributing throughout the phase, conferring perovskite-like character to isolated areas but not changing the polymorphism as a whole.

## 2.1 CHEMICAL COMPOSITION OF CEMENT

---

### 2.1.2 Minor components of Portland cement

Due to Portland cement being produced from natural raw materials, the clinker contains various oxides apart from the four principal ones. MgO, Na<sub>2</sub>O, K<sub>2</sub>O, SO<sub>3</sub>, TiO<sub>2</sub>, P<sub>2</sub>O<sub>5</sub>, SrO and Mn<sub>2</sub>O<sub>3</sub> contents generally range from 0.2–2 wt. %, while ZnO, Cr<sub>2</sub>O<sub>3</sub>, Rb<sub>2</sub>O, Cs<sub>2</sub>O, V<sub>2</sub>O<sub>5</sub>, As<sub>2</sub>O<sub>3</sub>, CuO, PbO, CdO, BaO and TiO<sub>2</sub> appear in traces, usually between 0.5 and 200 ppm [43].

As discussed in the previous sections, these are partially incorporated into the crystal lattices of the individual clinker phases. However, depending on the cation and its abundance, some minor oxides may not dissolve in the clinker at high temperatures and instead be obtained in pure form after cooling. As such they can act as fluxing agents during cement production, nucleate the crystallization of clinker phases and influence the phase composition. Thus, their influence on the reactivity of cement must not be underestimated. This also signifies that no two batches of Portland cement have perfectly matching compositions and hydrate precisely in the same way.

### 2.1.3 Industrial Portland cement production

#### 2.1.3.1 Synthesis of the clinker phases

In industrial Portland cement production, the main sources for the four principal oxides CaO, SiO<sub>2</sub>, Al<sub>2</sub>O<sub>3</sub> and Fe<sub>2</sub>O<sub>3</sub> are limestone, clay materials (including shales), sands, slags and ashes [25]. The Portland clinker is obtained via solid-state synthesis in a rotary kiln at a maximum temperature of 1420–1450 °C (**Figure 3**). As the raw materials are heated up, the CaCO<sub>3</sub> decomposes to CaO under liberation of CO<sub>2</sub> and the clay materials dehydrate to fine silica and alumina. As a result, β-C<sub>2</sub>S is the first clinker phase formed from about 800 °C alongside C<sub>12</sub>A<sub>7</sub> and C<sub>2</sub>(A,F) as intermediates for C<sub>3</sub>A and C<sub>4</sub>AF [44].

## 2.1 CHEMICAL COMPOSITION OF CEMENT

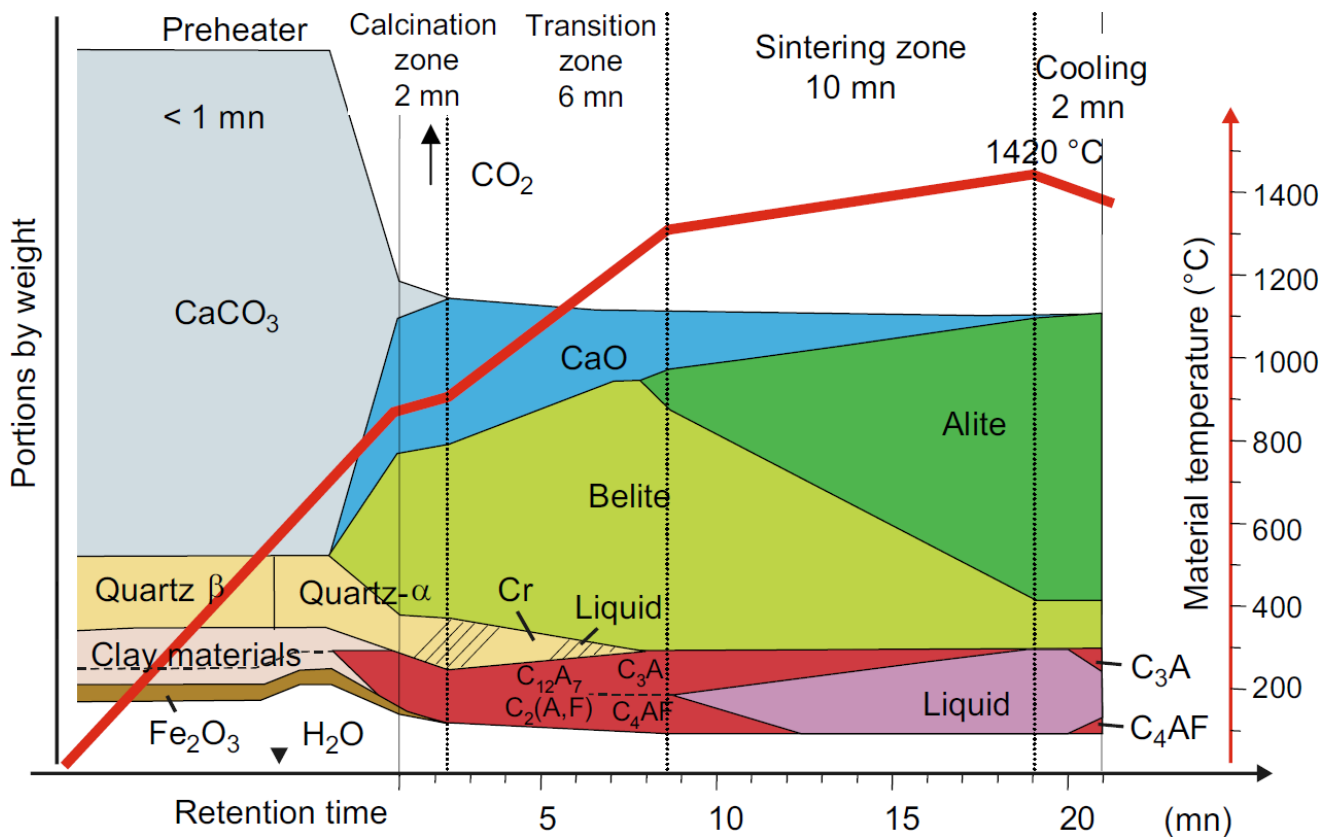


**Figure 3:** Transformation of raw materials into clinker in a rotary kiln [45].

Reprinted from [46] in modified form with permission.

If the clinker phases were synthesized individually, a temperature of 1420 °C would be sufficient to yield each of C<sub>2</sub>S, C<sub>3</sub>A, and C<sub>4</sub>AF, but not C<sub>3</sub>S which could only be obtained from 2100 °C upwards. However, industrial cement production takes advantage of the *in situ* synthesis of all clinker phases. At 1420 °C the aluminate and ferrite phases are molten as are some of the minor oxides. They form a liquid flux which transports C<sub>2</sub>S and CaO, thus enabling their combination to C<sub>3</sub>S at this temperature. At least 20–25% of the material in the kiln needs to be in liquid state for sufficient conversion to C<sub>3</sub>S.

During quenching, the melt surrounding the grains of C<sub>3</sub>S and C<sub>2</sub>S solidifies under recrystallization of C<sub>3</sub>A and C<sub>4</sub>AF. For this reason, in clinker a distinction is commonly made between an aluminous, so-called ‘interstitial’ phase and a silicate phase. A typical Portland cement contains 15+ wt.% of C<sub>3</sub>A and C<sub>4</sub>AF in addition to 75+ wt.% of silicate phase. The ratio of C<sub>3</sub>S to C<sub>2</sub>S is approximately 80 to 20 by weight.

### 2.1.3.2 Milling the cement clinker

After the phases have stabilized, the clinker is ground to a powder in ball or vertical mills (**Figure 4**). During hydration, water interacts with the clinker surface, thus the reactivity of a cement is proportional to its particle fineness. Portland cements usually possess a specific surface area between 3000 and 5000 cm<sup>2</sup>/g. Coarse cements are used in mass concreting where slow curing without heat release spikes is desired to avoid cracking. Fine cements are preferred in the production of prefabricated concrete parts since the rapid strength development allows for a fast demolding and thus high turn-over frequencies. An example for the use of cements with intermediate particle sizes is ready-mix

## 2.1 CHEMICAL COMPOSITION OF CEMENT

application. There, a quick achievement of load-bearing capacity to reduce construction downtime is aimed for, but only after the concrete has arrived and been processed at the job site.

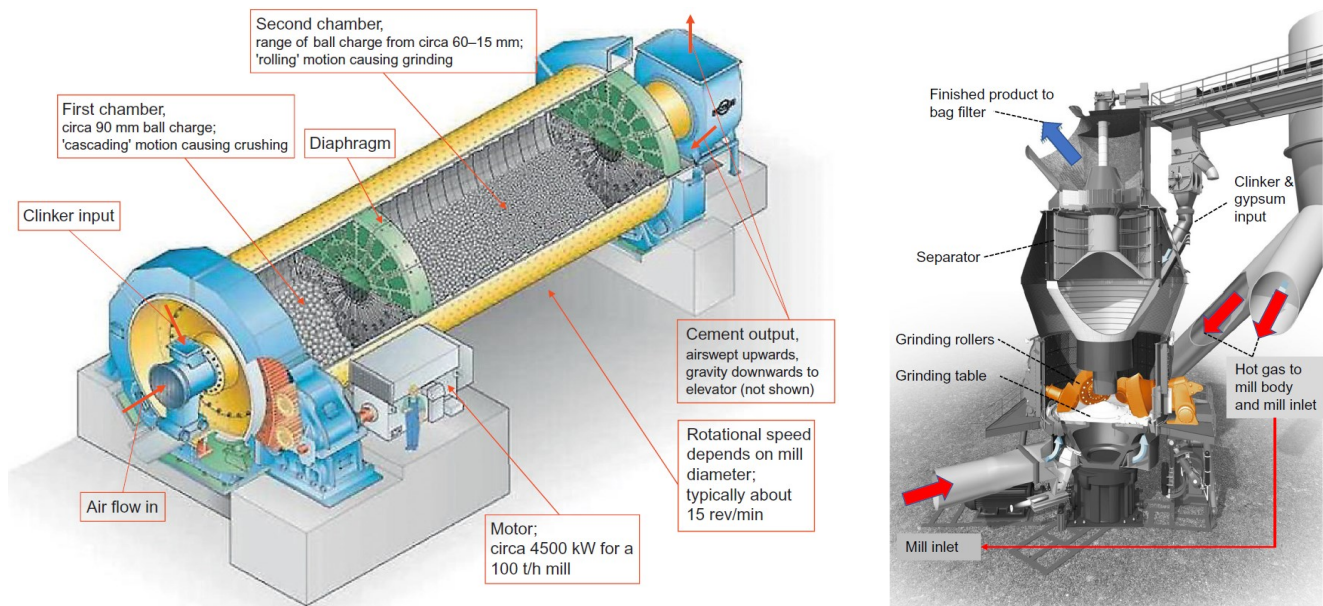


**Figure 4:** Diagram of a ball mill (left) and a vertical mill (right) [47].

Reprinted with permission.

Modern milling and sieving technologies allow cements to possess tight particle size distributions. While this is beneficial in terms of obtaining stable hydration profiles, it is detrimental for the workability. The packing of uniformly sized cement particles leaves large gaps filled with air which is replaced with water during mixing. In consequence, less water is available to provide flowability to the cement. The most efficient countermeasure is to fill the gaps with fine solids that do not negatively affect the early hydration behavior (**Figure 5**). The clinker is interground with a soft material that does not increase the energy demand of the milling process significantly while being reduced to a small particle size. A combination of limestone and gypsum is commonly used for this purpose.

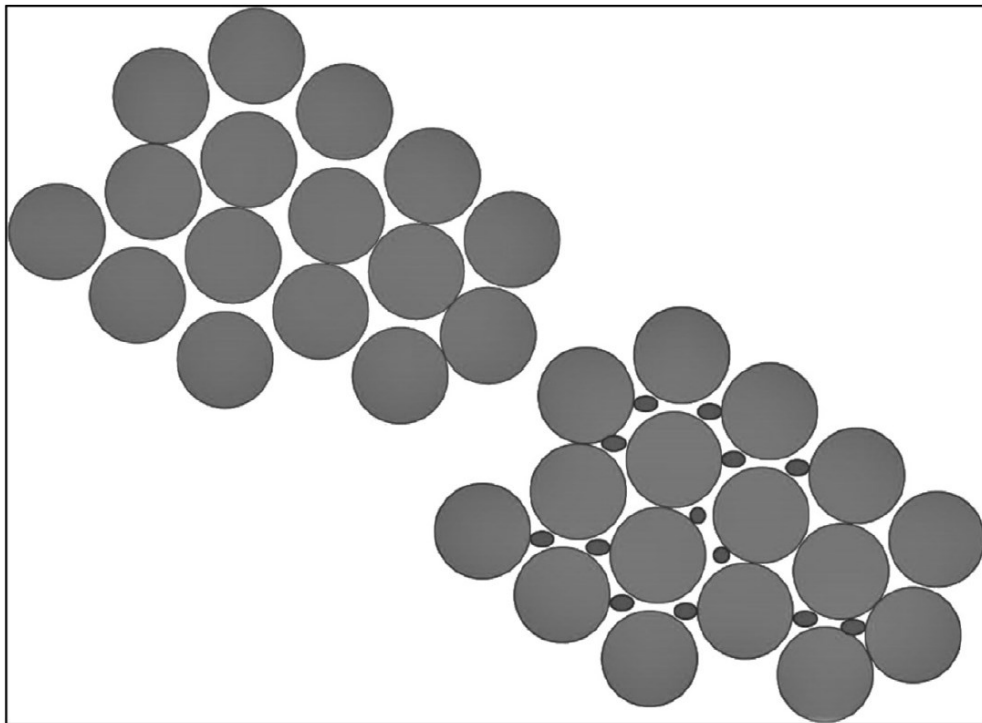


**Figure 5:** Filling gaps between cement particles with fine limestone to increase flowability [43].  
Reprinted with permission.

As previously mentioned, gypsum or calcium sulfate in general has to be interground with Portland clinker in any case to control the hydration of the  $C_3A$  phase. In Portland cement, calcium sulfate is encountered as the dihydrate (gypsum), the hemihydrate (bassanite) and as “anhydrite” (near-dehydrated hemihydrate, available in large quantities as a by-product of hydrofluoric acid production). Hemihydrate results from the dehydration of gypsum above 42 °C [48]. Since the clinker is usually fed into the mill after quenching, but before cooling to ambient temperature, intergrinding it with a mixture of gypsum and anhydrite will lead to the formation of hemihydrate *in situ*.

### 2.1.4 Non-Portland cements and cement blends

Currently, there are two major types of cements besides Portland whose mineralogical compositions allow for mass industrial production with regards to raw material availability. These are calcium aluminate cement (CAC) and calcium sulfoaluminate cement (CSA). CAC clinker contains aluminate phases with a higher ratio of  $Al_2O_3$  to  $CaO$  than  $C_3A$ . Generally, the most abundant is monocalcium aluminate (CA), followed by calcium dialuminate ( $CA_2$ ) and mayenite ( $C_{12}A_7$ ). CAC tends to swiftly harden, but only a couple of hours after the start of hydration, which is attractive from a workability viewpoint.

Raw materials with high alumina and low silica content are required for CAC manufacture. A cement from limestone and bauxite was developed in France and patented as ‘ciment fondu’ (melted cement) in 1909 [49]. The limited availability of suitable materials is one reason why the annual production of CAC only amounts to one thousandth of that of Portland cement.

## 2.1 CHEMICAL COMPOSITION OF CEMENT

The first use of CAC was in applications where Portland cement would suffer from durability loss due to sulfate attack. Today, two fields of use account for 80% of CAC production [50–52]. One is the production of castable refractories, taking advantage of the superior tolerance of CACs to high temperatures and sharp fluctuations thereof. The second use is in dry-mixed blends of binders and additives which are marketed as ready-to-use products for repairs and special applications. A self-levelling floor screed (illustrated in **Figure 6**) based on a ternary binder system consisting of Portland cement, CAC and anhydrite was investigated as part of this work.



**Figure 6:** Application of self-levelling underlays (SLUs) [53]. Reprinted with permission.

CSA containing calcium sulfoaluminate clinker phases, primarily ye'elite ( $C_4A_3S$ ), has been introduced as an eco-friendly alternative to Portland cement. CSA can be manufactured at lower kiln temperatures and has a lower limestone content. This however reduces the amount of portlandite formed during hydration which results in a faster carbonation of CSA concrete. Attempts are being made to hydrate combinations of CSA and  $\gamma$ -belite under  $CO_2$  ingress. The latter, while mostly inactive in hydration, readily forms expansive carbonates possibly providing additional strength while lowering the porosity [54].

## 2.2 Chemistry of cement hydration

### 2.2.1 Role of the water / cement ratio

The water-to-cement (w/c) ratio describes the relative amount of water used to hydrate a cement sample and is usually expressed as mass [water] divided by mass [cement]. The term water-to-binder (w/b) is used if the binder wholly or partially consists of non-cementitious materials while water-to-formulation (w/f) is applied if solid admixtures are present.

The w/c ratio is arguably the most important parameter in cement and concrete hydration, directly affecting workability, the rates of setting and hardening as well as the strength and durability of the final product [55–57]. At the start of hydration, the w/c ratio controls the suspension of the cement particles in the water [58] (**Figure 7**). The higher the w/c ratio, the greater is the distance between individual grains, allowing the hydrates developing from the interaction between water and particle surface to grow larger. The lower the w/c ratio, the closer are the grains and the smaller is the interparticle space [59–61]. In the latter case, small but numerous individual hydrate growths confer higher load-bearing capacity and durability on a cement due to the development of stronger attractive forces (especially van der Waals) and lower porosity in comparison to large hydrates.

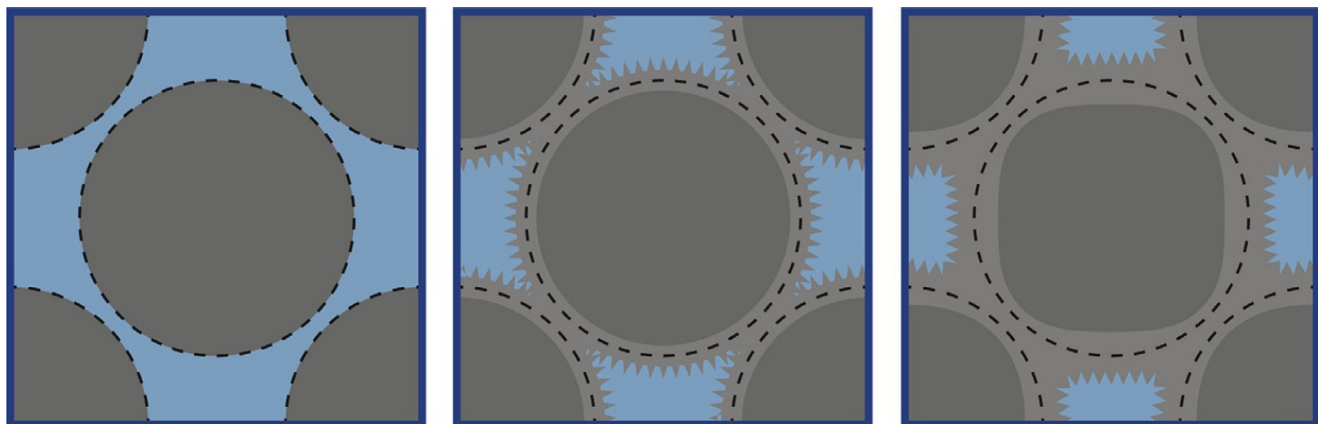


**Figure 7:** Formation of cement hydration products [62, 63]. Reprinted from [63] with permission.

At an average phase composition as given in chapter **2.1.3** on industrial cement production, to fully convert the clinker phases of a Portland cement to their respective hydrates, a w/c ratio of ~0.42 is needed [64, 65]. During hydration, water is gradually removed from the interparticle space. This results in the development of strong capillary forces leading to a decrease of the apparent volume of the cement paste which is referred to as autogenous shrinkage. The final product of cement hydration consists of a porous mass of clinker hydrates which has been described as a ‘solid gel’. Additional water is bonded to the pores’ inner walls as a ‘water gel’, while the pore volume (~8% of the hydrated cement) is filled with gaseous H<sub>2</sub>O (**Figure 8**, left).

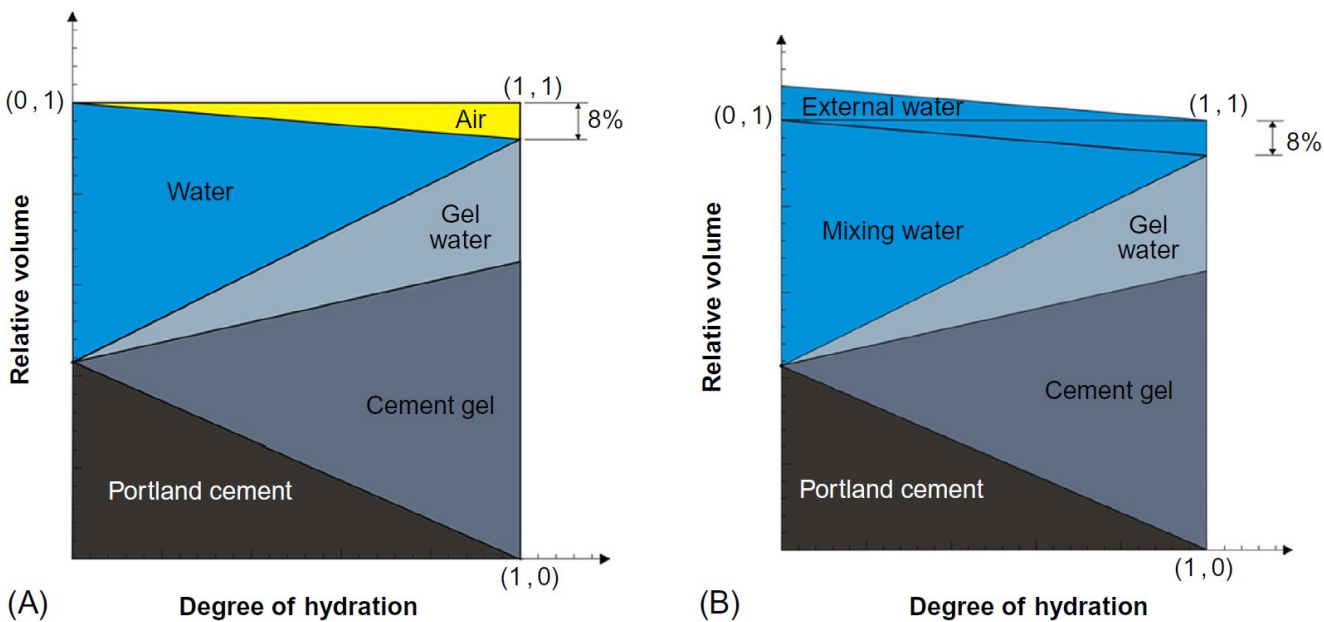


**Figure 8:** Hydration of a cement paste at a w/c ratio of 0.42 as a closed system (left, A) or in the presence of an external water source (right, B) [66, 67]. Reprinted from [63] with permission.

To avoid autogenous shrinkage, hydrating cements and concretes are provided with an additional external source of water, e. g. by curing prefabricated parts under water after demolding. In so doing, the consumed mixing water is continuously replaced by external water in the interparticle spaces and as hydration progresses, in the pores which prevents the contraction of hydrating cement. Thus, at a w/c ratio of 0.42 no autogenous shrinkage is observed and the pores, while of a similar volume as before, are filled with liquid water instead of vapor (**Figure 8**, right). This means that the external source of water needs to provide at least an additional ~8% of the cement paste's volume in water for it to take up in order to avoid autogenous shrinkage.

### 2.2.2 Chemical reactions during Portland cement hydration

Portland cement consists of four major clinker phases and a variety of minor constituents; therefore its hydration process involves a plethora of chemical reactions occurring in both parallel and succession. The hydration starts as soon as water and cement come into contact during mixing. Broadly speaking, the clinker phases are dissolved which results in the precipitation of associated hydrates under release of heat. Hydrate formation also controls the engineering properties of the hydrating binder: Aluminate hydrates determine the workability of cement paste while silicate hydrates are the main source of a hardened cement's strength.

#### 2.2.2.1 Hydration of the silicate phases

Alite and belite reactions with water are fundamentally similar, with the belite hydration progressing at a significantly slower pace [68]. The hydration process of the silicate phase can be divided into 5 stages (**Figure 9**): Initial dissolution (0) and preinduction period (I), induction / dormant period (II), post-induction / acceleration period (III), deceleration period (IV) and final period (V) [69].

## 2.2 CHEMISTRY OF CEMENT HYDRATION

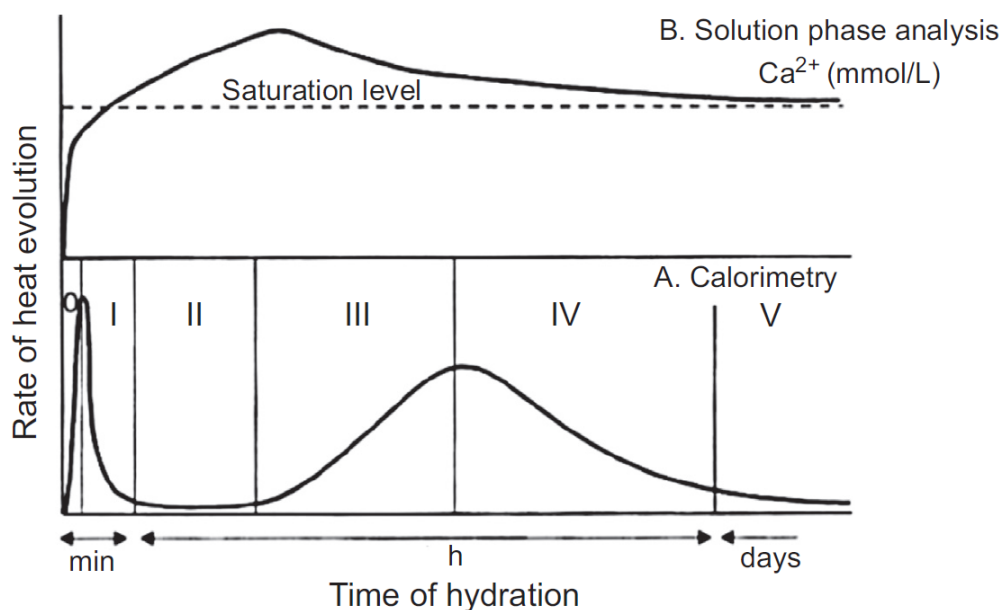
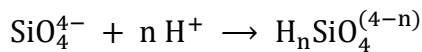
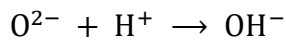


**Figure 9:** Stages of the  $\text{C}_3\text{S}$  hydration process as defined by heat release and free  $\text{Ca}^{2+}$  concentration [69]. Reprinted from [70] with permission.

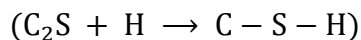
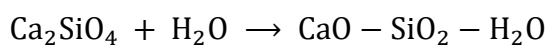
It remains a matter of debate whether calcium silicates dissolve congruently or incongruently during the preinduction period. A congruent dissolution [71–74] begins with protonolysing silicate and oxygen anions at the alite surface directly after the contact of water and alite:



$\text{Ca}^{2+}$  and  $\text{OH}^-$  enter the liquid phase at a much higher rate than protonolyzed silicate anions. Heat flow calorimetry reveals that the initial dissolution is highly exothermic (**Figure 9**, 0). The dissolution rate is sufficiently high to cause a local ion oversaturation in the water layer directly above the dissolving surface. As a result, calcium silicate hydrate ( $\text{C}-\text{S}-\text{H}$ ) quickly starts to precipitate on the solid silicate.

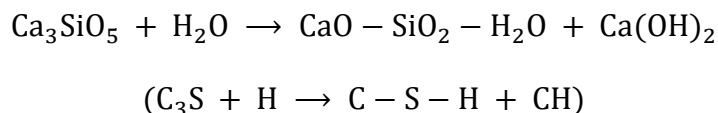
On the other hand, if the silicate phase dissolves incongruently [75–77], the silicate anions are not protonolyzed. They instead adsorb dissolved  $\text{Ca}^{2+}$ , forming  $\text{C}-\text{S}-\text{H}$  as an electric double layer on the silicate surface.

Calcium silicate hydrate has a variable composition hence why the ambiguous abbreviation  $\text{C}-\text{S}-\text{H}$  is used. The  $\text{CaO}$  to  $\text{SiO}_2$  ratio of  $\text{C}-\text{S}-\text{H}$  is generally between 1.2 and 2.1 [70], most commonly it is slightly below 2. Thus, most of the  $\text{CaO}$  molar equivalent in belite contributes to the growth of silicate hydrates but only about two thirds in alite. Excess  $\text{CaO}$  from the alite and ‘free’ lime (residual  $\text{CaO}$  from clinker production) form calcium hydroxide  $\text{Ca}(\text{OH})_2$ , which in mineralogy is called portlandite.



## 2.2 CHEMISTRY OF CEMENT HYDRATION

---



Initial dissolution and preinduction period together only last for a few minutes, during which between 2 and 10 wt.% of the calcium silicates hydrate [78, 79]. The end of this stage is marked by a decrease of the heat release rate to almost zero [80] (**Figure 9, I**). The subsequent lull in the hydration process is called the induction or dormant period and usually continues for a couple of hours (**Figure 9, II**). The reasons for the low rate are still debated. One theory states that metastable C–S–H forms a layer on the silicate surface that slows the ongoing dissolution of the clinker phase [72, 74, 77, 80–87]. At the end of the induction period this C–S–H transforms into a stable state that is also more permeable [88, 89]. Alternatively, the layer breaks down either from the imbibition of water by the underlying silicate surface [90] or from the osmotic pressure generated between the two [70, 90, 91].

Another hypothesis is centered around the calcium silicate dissolution [92, 93]. It distinguishes different processes based on the ion saturation of the liquid phase. At the start of hydration, the mixing water is so strongly undersaturated that calcium silicate dissolves even at non-defective surfaces despite the high activation energy barrier. As the ion concentration in the liquid phase increases, etch pit opening becomes restricted to surface defects before it stops altogether. From this point onwards, further dissolution is limited to the slow expansion of existing etch pits [70]. According to this model, the end of the dormant period is reached when the ion saturation of the liquid phase triggers the precipitation of portlandite and ‘second-stage’ C–S–H. Unlike C–S–H, portlandite does not precipitate early in calcium silicate hydration. It is assumed that, while nuclei are formed, their growth is inhibited by the adsorption of silicate ions [75, 80, 94]. Only as the liquid phase reaches a high enough calcium hydroxide oversaturation is this poisoning overcome and portlandite starts to grow. The increasing calcium hydroxide concentration in the liquid phase also has a slowing effect on C–S–H precipitation, thus as soon as portlandite precipitates, a second stage of intense C–S–H formation commences [80, 95–97].

This renewed precipitation and growth of hydrates marks the start of the acceleration period (**Figure 9, III**). The ion consumption lowers the oversaturation of the liquid phase [76, 98], thus calcium silicate dissolution and reaction rate continue to increase until reaching a maximum around 5–10 hours after the dormant period ended [99]. The rate determining step of this stage is also still the subject of debate: Some authors attribute the highest impact to the early C–S–H precipitate, which enables heterogeneous nucleation and promotes hydrate growth [69, 70, 100]. Others emphasize the significance of the not yet hydrated silicate phase [99], which controls the dissolution rate in this stage since the ions are continuously removed from solution. This prevents the local ion oversaturation above the dissolving surface observed in the preinduction period. As a result, hydrates can precipitate throughout the liquid phase, depending only on the availability of dissolved ions.

After reaching a maximum in the acceleration period, heat release decreases again during the subsequent deceleration period (**Figure 9, IV**). The hydration process is at an advanced stage, with the hydrates increasingly overgrowing the interparticle space and replacing the liquid phase. Thus, the availability of dissolved ions becomes limited by diffusion which decreases the reaction rate exponentially. For this reason, the final period of the hydration process lasts much longer than all

## 2.2 CHEMISTRY OF CEMENT HYDRATION

---

previous stages (**Figure 9**, V). It ends when, depending on the w/c ratio, either all calcium silicate has hydrated or the liquid phase has been fully consumed.

The hydration of the silicate phase can be accelerated by the addition of *ex situ* synthesized C–S–H nuclei [101, 102]. The presence of C–S–H ‘seeds’ at the start of hydration provides additional sites for hydrate growth, which reduces ion oversaturation of the liquid phase and accelerates calcium silicate dissolution. In this case, the early hydration is more comparable to the acceleration period without C–S–H seeding. This is also reflected in that no induction period occurs.

### 2.2.2.2 Properties of silicate phase hydrates

C–S–H possesses a poorly crystalline to amorphous structure, hence why hydrated clinker is likened to a solid gel. The main building block of the silicate phase are  $\text{SiO}_4$  tetrahedra. During the hydration process, the separated tetrahedra become corner connected via Si–O–Si bonds. Thus, C–S–H can be regarded as a polymer of calcium silicates. The degree of polymerization increases over the course of hydration. While C–S–H is X-ray amorphous, the structural changes can be monitored via the chemical shift in  $^{29}\text{Si}$  MAS NMR [103, 104]. Separated tetrahedra (designated  $Q_0$ , –71 ppm) transform into end groups ( $Q_1$ , –79 ppm) and links ( $Q_2$ , –85 ppm) of tetrahedra chains. Higher levels of branching are generally not encountered in C–S–H.

The structure of C–S–H is related to those of 1.4 nm tobermorite  $[\text{Ca}_4(\text{Si}_3\text{O}_9\text{H})_2]\text{Ca} \cdot 8\text{H}_2\text{O}$  and jennite  $[\text{Ca}_8(\text{Si}_3\text{O}_9\text{H})_2(\text{OH})_8]\text{Ca} \cdot 6\text{H}_2\text{O}$  (**Figure 10**). In these crystalline phases the tetrahedra chains are bent in such a way that a structural motif consisting of three  $\text{SiO}_4$  tetrahedra repeats itself. This  $\text{Si}_3\text{O}_9$  unit is called a ‘dreierkette’. The tetrahedra chains form layers by surrounding sheets of calcium and oxygen, in jennite this further includes  $\text{OH}^-$ . The layers are separated by calcium and water [37].

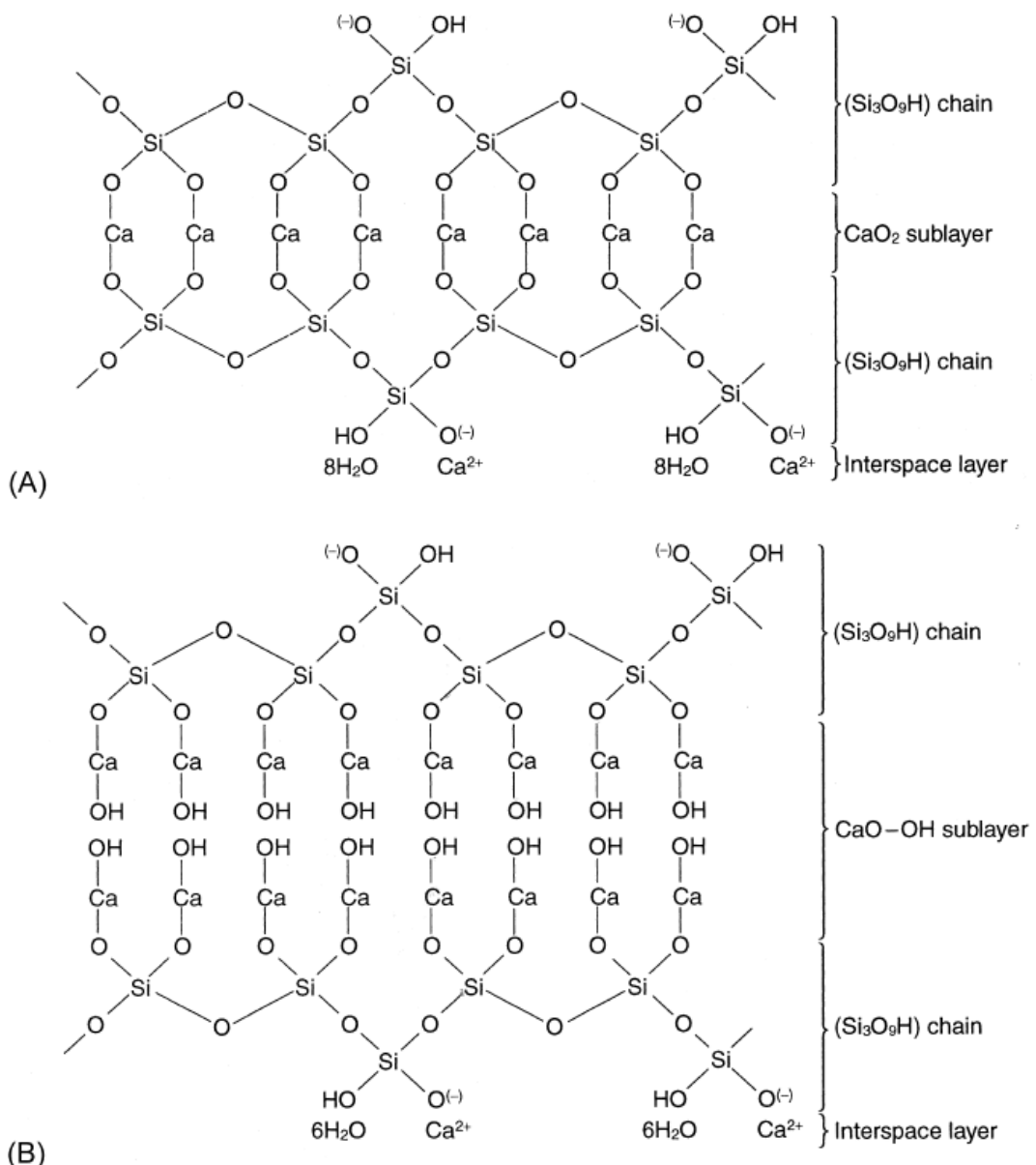


**Figure 10:** Idealized structures of 1.4 nm tobermorite (A) and jennite (B) [99].  
Reprinted with permission.

However, both phases have a lower  $\text{CaO}$  to  $\text{SiO}_2$  ratio [61, 105–107] (tobermorite ~0.8 and jennite ~1.5) than C–S–H (~2). The reason is that in the C–S–H structure some of the spaces occupied by  $\text{SiO}_4$  tetrahedra in tobermorite and jennite remain empty. This also results in the poor crystallinity of C–S–H compared to the other two.

Zooming out from atomic to microscopic level, the first C–S–H precipitates in hydration appear foil-like. They subsequently grow into a fibrous or needle-like appearance [99, 108] (**Figure 11**). The maximum heat release during the acceleration period corresponds with the complete covering of the calcium silicate surface with hydrates [109, 110].

## 2.2 CHEMISTRY OF CEMENT HYDRATION

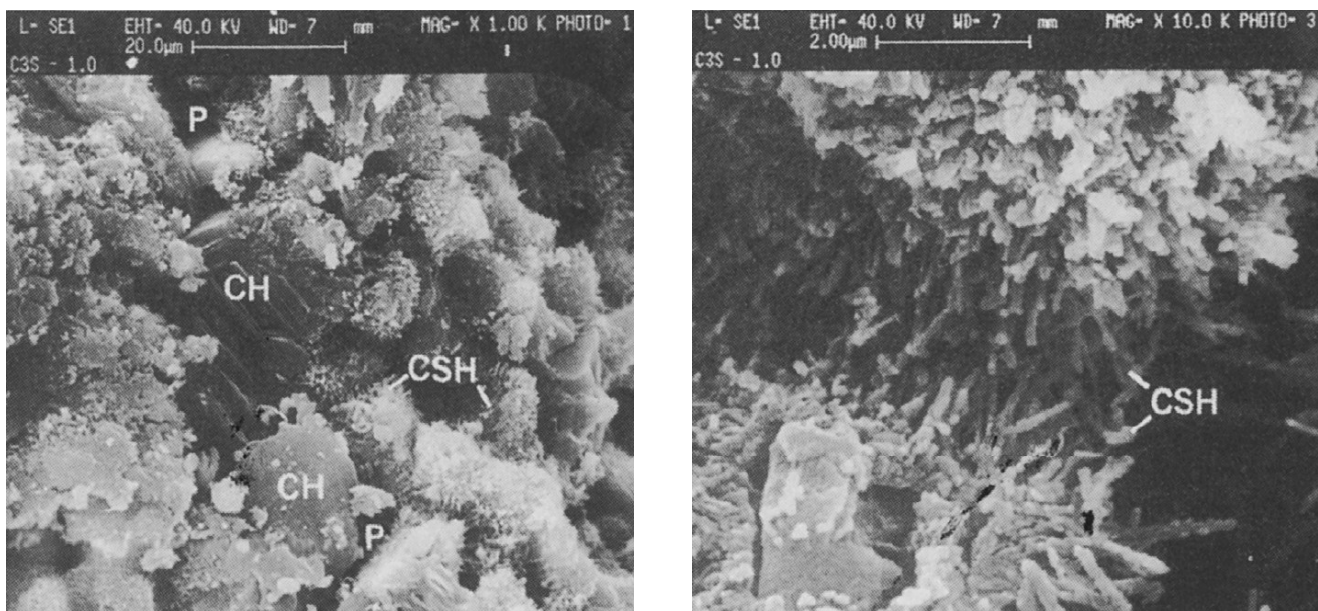


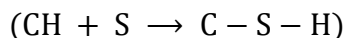
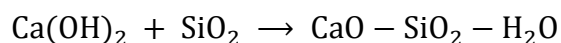
**Figure 11:** SEM images after hydrating  $\text{C}_3\text{S}$  at a w/s ratio of 1.0 and 20 °C [99].

Reprinted with permission.

As previously explained, the hydration of the silicate phase also yields calcium hydroxide (portlandite). Unlike the amorphous C–S–H, portlandite is a crystalline phase, which possesses hexagonal symmetry (**Figure 11**). Its structure contains alternating layers of calcium in octahedral coordination and layers of hydrogen-bound oxygen in tetrahedral configuration.

Depending on the ratio between alite and belite and the relative amount of the silicate phase in the Portland clinker, portlandite makes up between 20 and 30 wt.% of the hydrated cement. It is soluble in water, conferring a pH value of ~13 to the pore solution. This promotes the use of Portland cement in reinforced concrete since the alkaline environment protects the steel bars from corrosion. However, it also signifies that portlandite can be leached out in underwater applications and carbonates when exposed to atmospheric  $\text{CO}_2$ , gradually removing this protection.

Portlandite lacks the fiber-like morphology of C–S–H, whose needles can interlock and entangle easily, developing strong attractive forces in the process. Thus, its contribution to compressive and tensile strength of hydrated cement is largely negligible. Portlandite can however be transformed to C–S–H in a secondary hydration reaction, which provides additional strength:

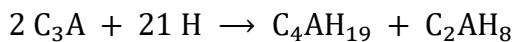


Since all  $\text{SiO}_2$  in the silicate phase has already been consumed in the primary hydration reaction, it is necessary to provide an external source of silica for the Portlandite conversion. This is the explanation for the beneficial effects of pozzolanic materials on the mechanical properties of cement discovered in antiquity and the reason why this secondary formation of C–S–H is usually called the ‘pozzolanic reaction’. In applications where additional strength gain is not required, pozzolanic materials can still be included to decrease the necessary amount of clinker in the binder, thus reducing its carbon footprint.

### 2.2.2.3 Hydration of C<sub>3</sub>A

#### Absence of sulfate

The hydration of C<sub>3</sub>A initially resembles that of the silicate phase with an amorphous calcium aluminate hydrate gel being formed on the dissolving surface. Unlike C–S–H however, this gel quickly gains crystalline character and the hexagonal phases C<sub>2</sub>AH<sub>8</sub> and C<sub>4</sub>AH<sub>19</sub> emerge:



C<sub>2</sub>AH<sub>8</sub> is comprised of [Ca<sub>2</sub>Al(OH)<sub>6</sub>]<sup>+</sup> layers with the remaining OH<sup>-</sup> and Al<sup>3+</sup> (as Al(OH)<sub>4</sub><sup>-</sup>) located in the interlayer alongside H<sub>2</sub>O. C<sub>4</sub>AH<sub>19</sub> possesses a similar structure with an additional layer of water between the [Ca<sub>2</sub>Al(OH)<sub>6</sub>]<sup>+</sup> sheets. Depending on water activity, this layer can be released (generally at relative humidities below 80%), which results in the conversion of C<sub>4</sub>AH<sub>19</sub> to C<sub>4</sub>AH<sub>13</sub>. Similar to the calcium silicate hydration, the covering of the C<sub>3</sub>A surface with aluminate hydrates results in a temporary drop of the reaction rate [111–116]. The C<sub>3</sub>A hydration accelerates again after the metastable C<sub>2</sub>AH<sub>8</sub> and C<sub>4</sub>AH<sub>19</sub> / C<sub>4</sub>AH<sub>13</sub> transform into the stable C<sub>3</sub>AH<sub>6</sub>, which possesses a cubic structure of the hydrogarnet type [37, 117–120].

The introduction of foreign ions into the C<sub>3</sub>A lattice (primarily Na<sup>+</sup>) during Portland clinker production lowers the reactivity towards water. Therefore, the hydration of pure, cubic C<sub>3</sub>A is faster than that of the doped orthorhombic polymorph [116, 121]. Among all clinker phases in Portland cement, C<sub>3</sub>A is the most reactive towards water. As a result, during hydration the calcium aluminate hydrates quickly overgrow the interparticle space (**Figure 12**) and the formerly suspended cement particles come in direct contact with each other. This results in a stiffening of the cement paste within minutes of the start of hydration. Preempting the setting and hardening process of the silicate phase, it is thus called a ‘flash set’. The stiffening cannot be reversed by application of mechanical force. For this reason, a flash set is generally undesired in most applications since it strongly reduces paste workability.

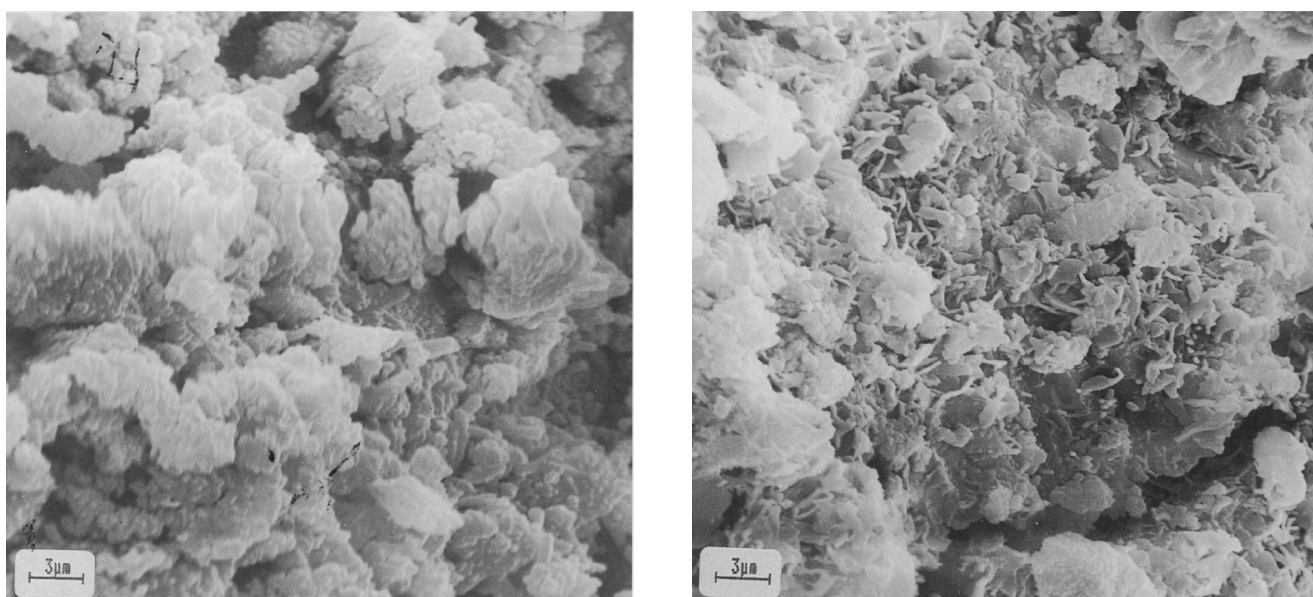


**Figure 12:** SEM images showing a ‘normal’ (left) and a ‘flash’ set (right) of Portland cement [99].  
Reprinted with permission.

### Presence of sulfate

As mentioned in the history of cement (chapter 1.1), Edouard Cailletet discovered that a flash set did not occur had a sulfate source been present during hydration. As it turned out, sulfate (in the following equation exemplified by gypsum) leads to the emergence of a different hydration product of the  $\text{C}_3\text{A}$  phase, a calcium sulfoaluminate hydrate [122–124]:



This phase is called ettringite or ‘trisulfate’ since in its formation for every unit of  $\text{C}_3\text{A}$  three molar equivalents of  $\text{CaSO}_4$  ( $\text{C}\$\text{}$ ) are consumed. It is also known as ‘AFt’, an abbreviation for the trisulfoaluminoferrite hydrate family, of which it is the most prominent member. Ettringite incorporates a comparatively large amount of  $\text{H}_2\text{O}$  into its crystal structure. Different entries about the exact number of molecules are found in literature, generally varying between 30 and 32. In fact, 30 water molecules are strongly anchored to the unit cell while another two are more loosely bound and can detach if the ettringite is dried intentionally or accidentally prior to characterization [46].

In Portland cement, the formation of ettringite is secured by adding calcium sulfate to the mill during clinker grinding. This practice has become so common that the term ‘Portland cement’ nowadays generally refers to the co-ground mix of clinker and calcium sulfate instead of the clinker powder alone. The calcium sulfate source is required to dissolve rapidly in the liquid phase to guarantee that the  $\text{C}_3\text{A}$  reacts to ettringite instead of  $\text{C}_2\text{AH}_8$  and  $\text{C}_4\text{AH}_{19}$ . This is especially important if part of the  $\text{C}_3\text{A}$  is in orthorhombic modification, whose hydration was found to be more difficult to control than that of cubic  $\text{C}_3\text{A}$ , despite being less reactive towards water [46, 99]. Hemihydrate dissolves the quickest among the calcium sulfates in Portland cement, followed by gypsum and anhydrite. Hemihydrate was also observed to increase the solubility of gypsum [43]. The amount of hemihydrate obtained during clinker grinding from the dehydration of gypsum above 42 °C depends on the milling process. It was observed to be minimized in high-pressure environments which are encountered when using certain roller mill designs instead of ball mills. Cements ground in these roller mills possessed low amounts of hemihydrate and tended to stiffen faster in comparison to ball mills [125, 126]. On the other hand, if too much hemihydrate is formed during grinding, a ‘false set’ can occur during early cement hydration. It is caused by the recrystallization of excessively dissolved sulfate in the dihydrate form, which is appropriately called ‘secondary gypsum’ [127]. This recrystallization decreases the workability of the paste. However, unlike the ‘flash set’ described previously the ‘false set’ is reversible by continued mixing which dissolves the secondary gypsum again. The impact of hemihydrate signifies that both the milling technology and the control of the temperature during grinding are determining factors for the setting behavior of Portland cement.

Like the hydration of the silicate phase, the reaction of  $\text{C}_3\text{A}$  and sulfates with water is exothermic. Isothermal heat flow calorimetric analysis of the process allows for distinguishing three distinct stages [128] (Figure 13):

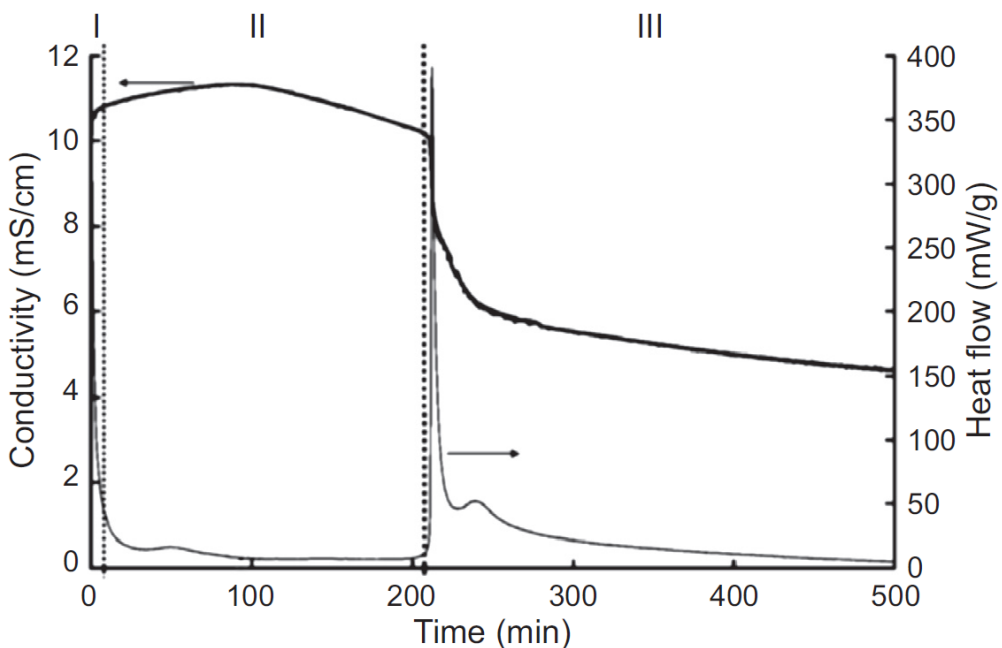


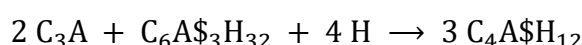
**Figure 13:** Stages in the hydration of  $\text{C}_3\text{A}$  with gypsum as defined by heat release and conductivity [128]. Reprinted from [70] with permission.

The stark increase and drop in heat release over a short time period in stage I resemble the preinduction period of the silicate phase hydration. Also similarly, the reasons for this deceleration after a strong initial reaction are still the subject of controversial debate. Most authors again suggest that ettringite formation creates a hydrate barrier which restricts water access to the not yet reacted  $\text{C}_3\text{A}$  [37, 117, 122–124, 129–131]. Others conclude that the sulfate ions poison dissolution sites on the  $\text{C}_3\text{A}$  surface [70, 128, 132–134].

Throughout stage II the heat release remains relatively low. This dormant period again closely resembles its counterpart from the silicate phase hydration. It lasts the longer the higher the ratio of sulfate to aluminates was at the start of hydration. Albeit at a much reduced rate, the formation of ettringite continues in the second half of stage II as shown by the decreasing conductivity [128]. Due to the decelerated reaction only up to 25% of the  $\text{C}_3\text{A}$  in Portland cement hydrates in stage I and II [78, 79, 135–138] which means that the workability of the paste does not decrease considerably during this time. This signifies the effect of sulfate as a set regulator in Portland cement.

The beginning of stage III is marked by a sharp increase in heat release. Compared to the acceleration stage in the hydration of the silicate phase, in  $\text{C}_3\text{A}$  this period is very short. In the formation of ettringite, sulfate is consumed at three times the rate of  $\text{C}_3\text{A}$  due to its stoichiometry as a ‘trisulfate’ [122, 124, 139]. Thus, once the calcium sulfate is completely dissolved, the sulfate saturation level in the liquid phase immediately starts to decrease. This ends the deceleration of the ettringite formation and therefore also the dormant period. The remaining dissolved sulfate rapidly reacts in what is called the ‘final ettringite crystallization’ or the ‘sulfate depletion’, marked by the heat release peak.

After the final crystallization, ettringite starts to redissolve since it is only stable in the presence of dissolved sulfate. It reacts with the remaining  $\text{C}_3\text{A}$  to a different calcium sulfoaluminate hydrate:



## 2.2 CHEMISTRY OF CEMENT HYDRATION

This phase contains only one molar equivalent of sulfate (\$) per  $\text{C}_3\text{A}$  and is thus called 'monosulfoaluminate' or 'monosulfate'. The basic member of the monosulfoaluminoferrite hydrate family, it is commonly abbreviated 'AFm'.

The amount of sulfate available during hydration also impacts the morphology of the aluminate hydrate phases. At low sulfate oversaturation, the ettringite appears as stout hexagonal prisms, retaining some semblance to the sulfate-free hexagonal  $\text{C}_2\text{AH}_8$  and  $\text{C}_4\text{AH}_{19}$ , while at high oversaturation trigonal needle-like structures are formed [140, 141] (**Figure 14**, top). Low sulfate oversaturation conditions require the absence of dissolved calcium hydroxide and thus are generally not encountered in Portland cement. The ettringite structure consists of  $\text{H}_2\text{O}$  surrounded  $\text{Ca}_3[\text{Al}(\text{OH})_6]_2$  repeating units arranged in columns (**Figure 15**). The channel-shaped interspaces contain the sulfate and the remaining incorporated water molecules.

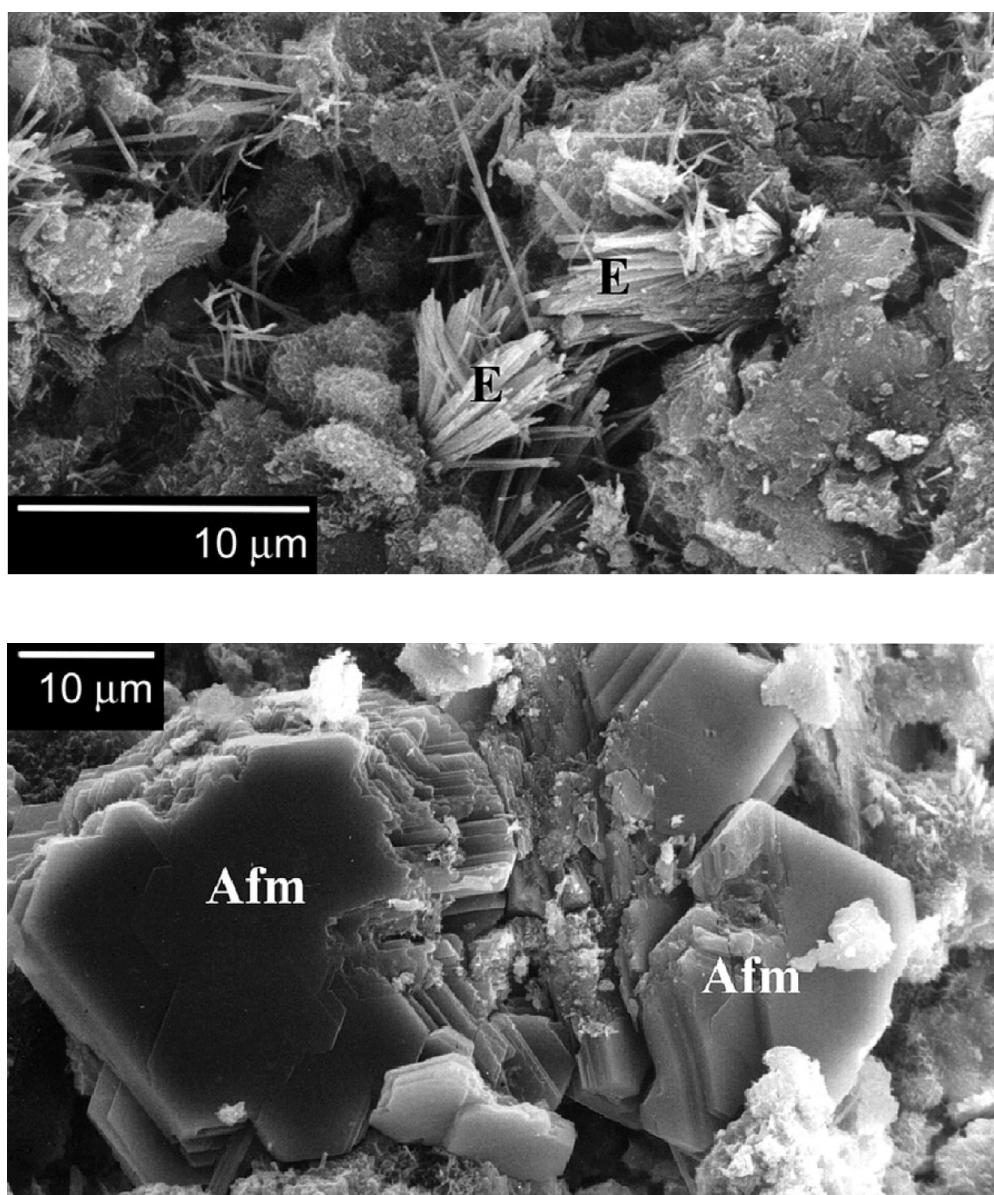


**Figure 14:** SEM images of ettringite (E) and monosulfoaluminate (AfM) in cement pastes hydrated at high w/c ratios [46]. Reprinted with permission.

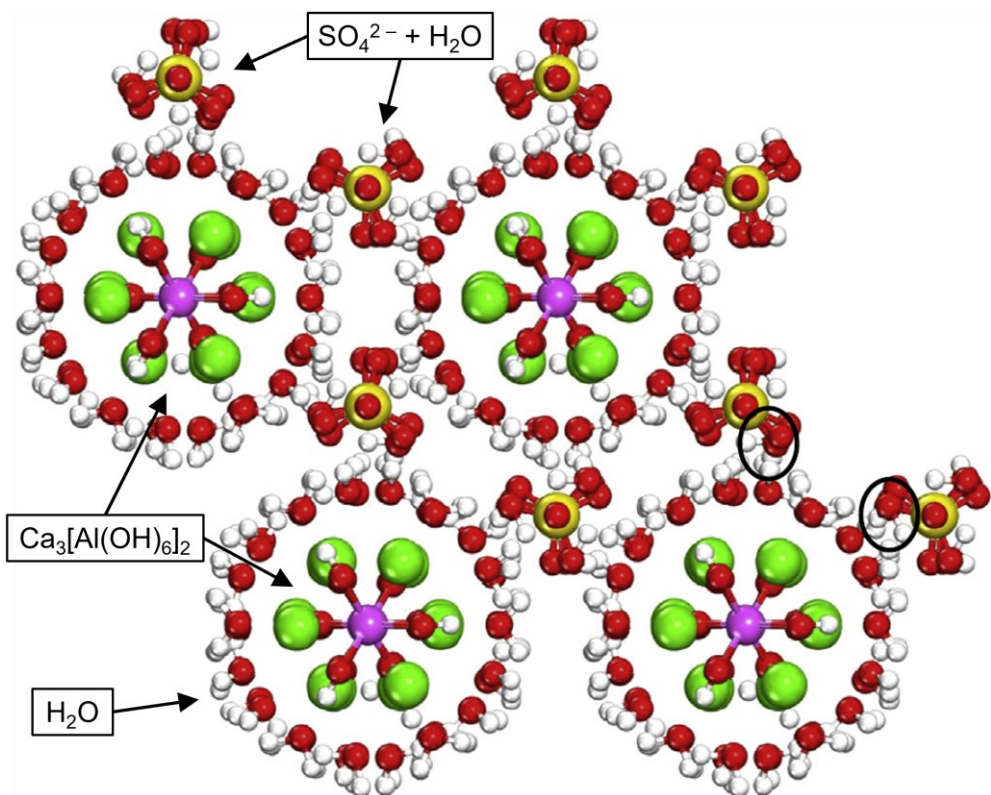


**Figure 15:** Schematic representation of the structure of trigonal ettringite [46].  
Reprinted with permission.

Monosulfoaluminate crystallizes as hexagonal plates (**Figure 14**, bottom). Having a lower sulfate concentration than ettringite, its structure can be regarded to some degree as an intermediate between the calcium aluminate hydrates and ettringite. Like  $C_2AH_8$  and  $C_4AH_{19}$  it is comprised of a layered structure, but with repeating units of  $Ca_3[Al(OH)_6]_2$  similar to ettringite. Sulfate and  $H_2O$  are again located in the interlayer space.

#### 2.2.2.4 Hydration of $C_4AF$

Provided that the hydration conditions are similar, the hydrates of the aluminoferrite phase are closely related to those of the aluminate phase. In the absence of sulfate,  $C_2(A_{1-x}F_x)$  reacts to hexagonal  $C_2(A_{1-x}F_x)H_8$  and  $C_4(A_{1-x}F_x)H_{19}$  which subsequently transform into the cubic hydrogarnet  $C_3(A_{1-x}F_x)H_6$  [142–145].

If sulfate is present, the metastable trisulfoaluminoferrite hydrate  $C_6(A_{1-x}F_x)S_3H_{32}$  is formed [142, 145–148] which reacts with the remaining  $C_2(A_{1-x}F_x)$  to the monosulfoaluminoferrite hydrate  $C_4(A_{1-x}F_x)SH_{12}$  after the sulfate has been depleted [142, 146, 149]. In the hydration of Portland cement, the reactivity of  $C_2(A_{1-x}F_x)$  is lower than that of  $C_3A$  and dependent on the ratio between  $Fe_2O_3$  and  $Al_2O_3$ . Generally, the more iron the aluminoferrite phase contains, the lower the reaction rates are for both the precipitation of  $C_6(A_{1-x}F_x)S_3H_{32}$  and its conversion to  $C_4(A_{1-x}F_x)SH_{12}$  [150, 151]. Furthermore, not all iron in  $C_2(A_{1-x}F_x)$  enters the aluminoferrite and sulfoaluminoferrite hydrates. Part of it is left separate from the hydrate phases as a mix of amorphous iron oxides and hydroxides [146, 148].

### 2.2.3 Setting and hardening of Portland cement

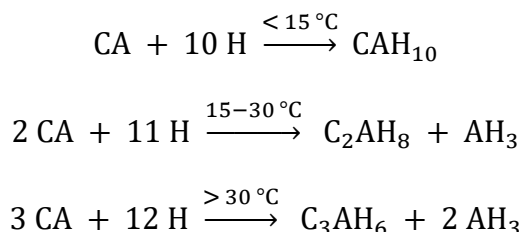
Immediately after the start of hydration, the cement paste is freely deformable or ‘workable’. Its rheological properties can range from an adhesive consistency to free-flow ability, depending on the w/c ratio and admixture use. If no flash or false sets are encountered, the cement paste stiffens in what is called a ‘normal set’. After contact with the mixing water, suspended cement particles experience mutual attraction due to opposite surface charges, the polarity of water as well as van der Waals forces and start to flocculate [152–154]. The flocks remove water by entrapment which weakens the suspension of the cement grains. As a result, the viscosity of the cement paste increases. The flocculation is initially weak and reversible by application of mechanical force. This changes after the start of the acceleration period when the share of clinker phase hydrates in the paste quickly increases. The hydrate growth consumes the liquid phase in the interparticle space and establishes chemical bonds between the cement grains. These particle connections are irreversible and develop into a three-dimensional network over time. This process marks the setting of the cement paste. The deformability or ‘workability’ gets lost and a solid, yet still plastic material is obtained.

At this stage, barely any compressive strength has developed which results in the paste crumbling under pressure [99]. Over time, load-bearing capacity is attained when the initial particle network consolidates into a rigid matrix. This ‘hardened’ cement paste possesses high strength, hardness and elastic modulus.

### 2.2.4 Hydration of calcium aluminate cement and cement blends

As previously mentioned, apart from pure Portland cement a ternary binder system further including calcium aluminate cement and calcium sulfate anhydrite is also subject of the present thesis.

If aluminate cement is hydrated individually, the clinker phase CA is protonolyzed to  $\text{Ca}[\text{Al}(\text{OH}_4)]_2$  and dissolves congruently. Similar to the hydration of Portland clinker phases, the main reaction is preceded by a dormant period which in aluminate cements can last up to multiple hours. Once the reaction rate has increased again, the hydration of aluminate cement finishes quicker as that of Portland cement. There, C–S–H nucleates in the pore solution only after the acceleration period has started. In comparison, the aluminate hydrates nucleate simultaneously on the cement grains and in the pore solution in the preinduction period, which provides more sites for hydrate growth during the acceleration. During the hydration of CA, the following hydrate phases are formed depending on ambient temperature:

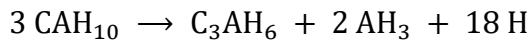


The initial distribution of the hydrate phases  $\text{CAH}_{10}$ ,  $\text{C}_2\text{AH}_8$  and  $\text{C}_3\text{AH}_6$  depends on the amount of  $\text{C}_{12}\text{A}_7$  in aluminate cement clinker [53].  $\text{C}_{12}\text{A}_7$  shifts the dissolution of pure CA from congruency

## 2.2 CHEMISTRY OF CEMENT HYDRATION

---

towards a CaO preference. Thus, the more  $C_{12}A_7$  is present, the larger is the share of phases with a higher ratio of CaO to  $Al_2O_3$  ( $C_3AH_6 > C_2AH_8 > CAH_{10}$ ). Above 20 °C,  $C_2AH_8$  and  $CAH_{10}$  are metastable and redissolve after precipitation, converting to  $C_3AH_6$  and amorphous  $AH_3$  gel as the final hydration products [155]:



As mentioned in chapter 2.1.4, due to the rapid hardening of aluminate cements one of their major applications is as repair binders. Blends with Portland cement are used as well for this purpose. To this binary system, a sulfate source such as calcium sulfate anhydrite can be added if a more controlled setting process is desired. The joint hydration of aluminate cement and calcium sulfate results in the formation of ettringite. Therefore, much higher volumes of ettringite are produced in such ternary systems as compared to pure Portland cement. Due to the ability to incorporate numerous  $H_2O$  molecules into its structure, this large amount of ettringite can significantly reduce the loss of mixing water due to evaporation [99]. Ternary binder systems are thus frequently used as underlays and generally in applications which involve large exposed surface areas. Furthermore, if the hydration process is adjusted for the bulk of ettringite and C–S–H formation occurring simultaneously, then the volume expansion associated with the high water uptake can be used to counterbalance a potential autogenous shrinkage of the silicate phase [156–158]. This makes ternary systems attractive not only for underlays, but also for tile adhesives and grouts and allows them to be hydrated at very low w/c ratios.

## 2.3 Chemical admixtures in cement hydration

### 2.3.1 General information

The cement hydration can be modified by the addition of chemical admixtures. For example, accelerators shorten the period between the start of hydration and the setting and / or hardening of the cement paste. They can potentially reduce the duration of these processes as well. If an opposite effect is required in application, retarders are used [24, 159]. Dispersing and viscosity-modifying agents influence the rheology of the hydrating binder and are used to ease the placement and increase the pumpability [160, 161]. If the degree of workability is already satisfactory, admixtures can be instead used to lower the water demand. A reduction in the w/c ratio (while staying above 0.30) generally increases the durability and compressive strength of the concrete as explained in chapter 2.2.1. This can result in a reduction of the binder amount required for a construction and thus decrease its carbon footprint [162]. Durability can be further improved with admixtures affecting the air entrainment during hydration which determines the porosity and permeability of the hardened material [163, 164].

A single admixture can possess multiple of the properties listed. For example, certain plasticizing admixtures can also cause a delay in setting, while some retarders further act as dispersants. All admixtures have in common that they impact the interaction between the liquid mixing water and the solid binder or the entrained air bubbles in the case of durability enhancers. This enables admixtures to be effective at low quantities which explains why they present a very small constituent of the binder, often amounting to less than 1% by weight.

As described in the introduction, cement admixtures have traditionally been everyday commodities and later by-products of industrial processes. This is due to the availability of these materials in sufficient quantities and the comparatively small cost increase of the binder they cause. The increasing knowledge of cement hydration and admixture working mechanisms has since enabled the development of synthetic compounds geared towards high efficiency and / or specific applications. As a result, the classification of chemical admixtures has expanded significantly over time [165]. In 2001, the Canadian Cement Association described no less than 27 types of admixtures, among them for example five different classes of water-reducers: normal, accelerating, retarding as well as high and low-range.

For this reason, calls have increased for a classification of chemical admixtures based on their working mechanism rather than their actions in cement hydration. An example of such a classification is as follows [165–167]:

1. Active admixtures, that chemically react with the binder and the mixing water to form small amounts of ‘derivative’ hydrates which impact the bulk hydration process. These admixtures are often subcategorized according to their effect on individual parts of the hydration process such as the silicate phase hydration or the pozzolanic reaction. Accelerators, retarders and water-proofers are mostly but not necessarily exclusively active admixtures.
2. Interactive admixtures, which act in hydration via adsorption and as surfactants, affecting the suspension of cement grains in the liquid phase and the air content of the cement paste. Thus, unlike active admixtures they do not undergo structural changes during the hydration process and

instead end up enclosed in the final product. Examples are rheology and durability enhancing admixtures such as superplasticizers, air-entraining agents and shrinkage reducers.

3. Passive admixtures, they predominantly interact with the cement or its hydration products physically. This includes effects such as the light absorption and reflection of pigments as well as the temperature-dependent enclosure of fluid by viscosity-modifying polymers.

Depending on application, admixtures are generally administered in two ways: In dry-mix products, the admixtures are blended as powders with the cement. The mixing water is subsequently added at the job site. The second method is to add the admixtures during the mixing of binder and water. In this case, the admixtures are generally administered as aqueous solutions. To not increase the w/c ratio, the volume of the mixing water is reduced accordingly. Both methods have distinct advantages and disadvantages. An incorrect admixture dosing by the end user is impossible when using the dry-mix method, but it does not allow for any dosage adjustments which might be needed due to changing environmental conditions such as temperature. While not as easy, the addition of admixtures during the mixing of binder and water makes fine-tuning the hydration process possible. Apart from the dosage, the performance of many admixtures depends on the exact time of addition relative to the start of hydration. An admixture added to the binder 30 seconds after the mixing water affects a solid-liquid interface that already contains early hydrate nuclei. If the admixture is added simultaneously with the mixing water, it encounters a neat clinker surface and might display a stronger or weaker effect.

As mentioned above, modern admixtures are purpose-designed chemicals that are tailored towards specific demands in application. For example, dispersing agents used in ready-mix concreting need to be able to uphold their effect over an extended period of time, which is commonly called ‘slump retention’, in case delays occur during the transport. That way, they would however be useless in precast application where the plasticizing action must be very strong initially but only last as long as the mold is being filled [168]. The advances in admixture technology also allow for a broader range of application temperature, making it possible to place more concrete in hot or cold climate, deep boreholes and permafrost soil. Nowadays admixtures can be designed to exclusively affect individual reactions during the hydration process. This enables the simultaneous usage of previously antagonistic admixtures such as accelerators and retarders if setting and hardening of a cement paste need to be modified differently.

A more detailed description of the state of the art regarding accelerators, retarders and dispersing agents is provided in the following subchapters. Only these types of admixtures are subject of the present thesis.

### 2.3.2 Accelerators

Admixtures have traditionally been defined as accelerators if they cause a measurable increase in compressive strength as early as 1 day after the start of hydration. Over time it was found that accelerators can affect various reactions during hydration, often simultaneously. Most accelerators increase the dissolution and hydrate formation rates of individual clinker phases and / or shorten the dormant period (**Figure 16**).

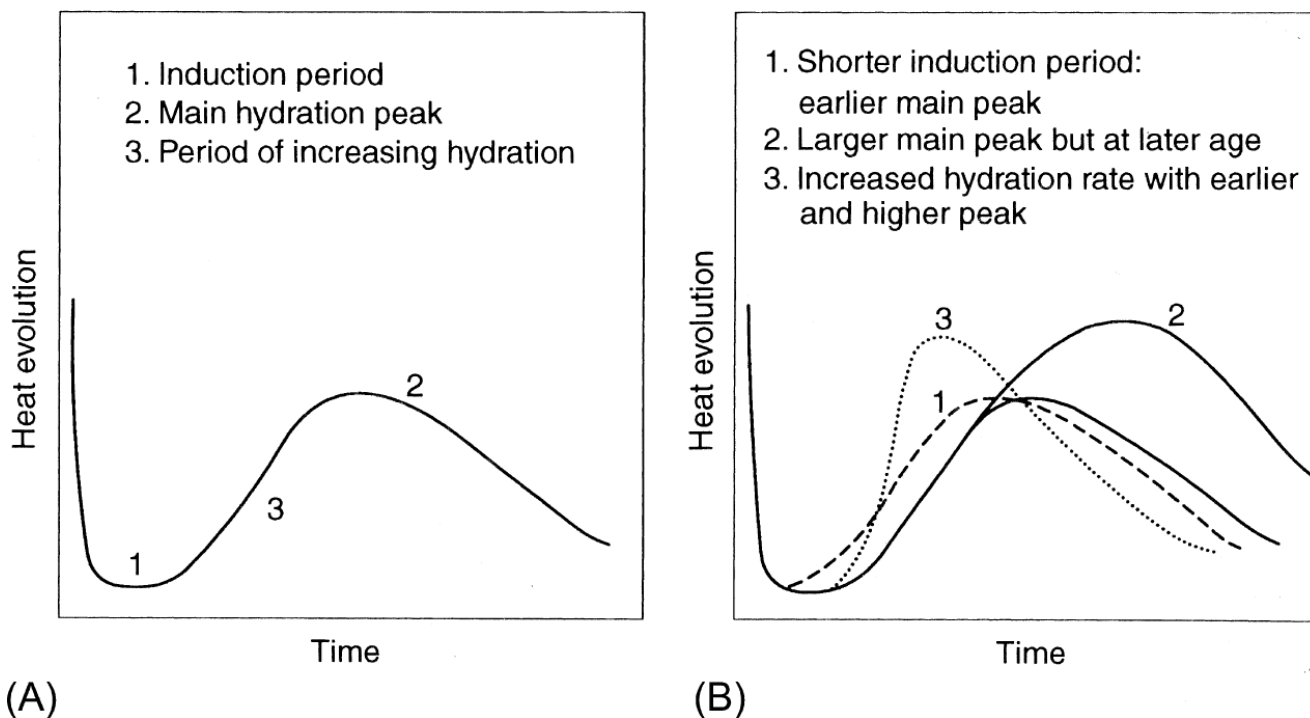


**Figure 16:** Generic heat flow diagram of Portland cement hydration (A) and potential impacts of accelerating admixtures (B) [169]. Reprinted from [167] with permission.

The preferred method of action often depends on a variety of factors, including the chemical composition, dosage and physical state of the accelerator as well as environmental factors. As with admixtures in general, the knowledge of accelerators has evolved over time which resulted in somewhat convoluted systems of classification. For example, the four classes of accelerating admixtures listed by the American Concrete Institute (ACI) partially overlap, meaning the individual admixtures can appear in more than one category [159]:

1. Inorganic salts, such as chloride, bromide, fluoride, carbonate, nitrate, nitrite, formate, thiosulfate, thiocyanate, silicate, aluminate and alkaline hydroxide
2. Soluble organics, such as triisopropanolamine, triethanolamine, calcium formate, calcium acetate, calcium propionate, and calcium butyrate
3. Setting accelerators, such as sodium silicate, sodium aluminate, aluminum chloride, sodium fluoride, and calcium chloride
4. 'Various' solid accelerators, such as calcium aluminate, calcium silicate, finely divided magnesium carbonate, and calcium carbonate

Generally, strong acids based on chloride and nitrate are the best accelerators for alkaline binders like Portland cement. Weak acids / strong bases from carbonate, hydroxide and amines are superior in less basic binders such as sulfoaluminate cement. The most widely used accelerator for calcium aluminate cement is lithium carbonate ( $\text{Li}_2\text{CO}_3$ ), although recent studies have identified certain alginates and carrageenans as viable alternatives [170, 171].

In general, there are two major incentives to accelerate the cement hydration with chemical admixtures: The first is the reduction of construction downtime or respectively the increase of prefabricated concrete

## 2.3 CHEMICAL ADMIXTURES IN CEMENT HYDRATION

---

output that an acceleration of the compressive strength development provides. Appropriate admixtures thus primarily promote the hydration of the silicate phase. Amines are frequently used in ready-mix concretes where only a weak acceleration is required. A powerful effect is necessary in precasting, thus strongly acidic inorganic salts are applied [172].

Second, accelerators are indispensable in applications that require a very fast setting to maintain cohesion against external forces including gravity. This mostly concerns binders used to plug leaks and / or sprayed against walls or ceilings, for example in tunnels. There, highly flowable 'shotcrete' needs to stiffen immediately after being projected against the tunnel walls in order to adhere to the surface and not flow down. For this reason, admixtures need to be applied that specifically increase the hydration rate of the aluminate clinker phase to rapidly induce setting. Accelerators for shotcreting are usually silicates or aluminum salts.

Most of the investigations into the working mechanisms of accelerators have focused on calcium chloride, which at the time of writing is the most efficient accelerator in ordinary Portland cement with regards to increasing early compressive strength [159] (**Figure 17**). The effects of accelerators on cement hydration are complex. So far, textbooks have collected reports of no less than 12 different interactions of calcium chloride and Portland cement that could contribute to an acceleration of the hydration process [159, 167, 173]:

1. Calcium chloride activates nucleation sites for C–S–H formation on the surface of  $C_3A$  and  $C_4AF$
2. ...promotes hydration of the interstitial phase, creating a pull effect on silicate phase hydration
3. ...reacts with C–S–H formation by-product portlandite to  $3CaO \cdot CaCl_2 \cdot 12 H_2O$
4. ...changes the  $CaO/SiO_2$  ratio of early C–S–H
5. ...reacts with the interstitial phase and sulfate to an ettringite derivative
6. ...creates complex chloride salts (e. g. Friedel's salt) that promote alite hydration
7. ...catalyzes  $C_3A$  hydration in cement pore solution
8. ...increases the activation energy barrier for the conversion of  $C_4AH_{13}$  to  $C_3AH_6$  in the absence of sulfates
9. ...promotes coagulation of  $H_nSiO_4^{(4-n)}$  on the cement grain surface
10. ...lowers pH of the liquid phase, affecting dissolution / precipitation kinetics of portlandite
11. ...universally increases dissolution rates of the clinker phases
12. ...decreases hydroxide diffusion limitations, thereby promoting portlandite precipitation and subsequently silicate phase dissolution

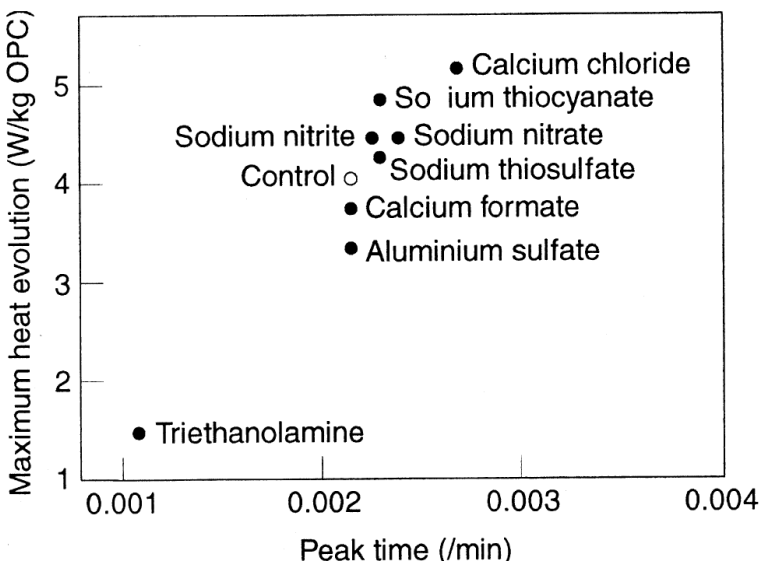


**Figure 17:** Effect of various accelerating admixtures on Portland cement hydration [174].

Reprinted from [167] with permission.

The use of calcium chloride has a major drawback: It negatively affects the durability of concrete, especially if it is reinforced with steel bars. The surface of these bars is usually covered by a passivating oxide layer that is stabilized by the basicity of the cement pore solution. The iron oxide reacts with calcium chloride to iron chloride salts which dissolve and expose the underlying metal to corrosion. Calcium chloride also lowers the Portland cement's resistance to sulfate attack [175]. For these reasons, the employment of chloride-containing admixtures is prohibited in reinforced concrete and limited in various other applications. Producers have transitioned to different calcium salts which, while not as effective as the chloride, have become increasingly attractive pricewise. Examples are calcium nitrate for reinforced concrete as well as the non-hygroscopic calcium formate and calcium thiocyanate for tile adhesives and grouts.

The application of most conventional accelerators leads to a lower final strength of the hydrated binder since the sped-up hydration process usually yields products with a less ordered atomic structure. Accelerating the hydration by adding *ex situ* synthesized nuclei as described in chapter 2.2.2.1 largely avoids this problem [70]. Stabilized dispersions of nano-sized C–S–H seeds have already entered the market (for example 'X-seed' by BASF). Due to the nuclei's tendency to merge in order to minimize energy, the shelf-life of these commercial products may be limited compared to conventional accelerators [167]. The research into suitable seeding materials and effective stabilizers for them will remain a key investigative topic in construction chemistry for the foreseeable future.

### 2.3.3 Retarders

Although a fast cement hydration is often desirable as described above, application can require certain steps of the hydration process to be delayed. For example, postponing the setting of fresh cement extends the time window for processing the paste. This is necessary when ready-mix concrete is transported over a longer period to the job site. It also allows construction work to be carried out at high temperatures where setting would occur too soon otherwise. Such a prolonged workability can be

obtained with retarding admixtures that increase the induction period during cement hydration (**Figure 18**). Retarders can also affect the rate of heat release during setting and hardening. As mentioned in chapter **2.1.3.2**, mass concreting often requires a slow curing without heat release spikes in order to avoid cracking.

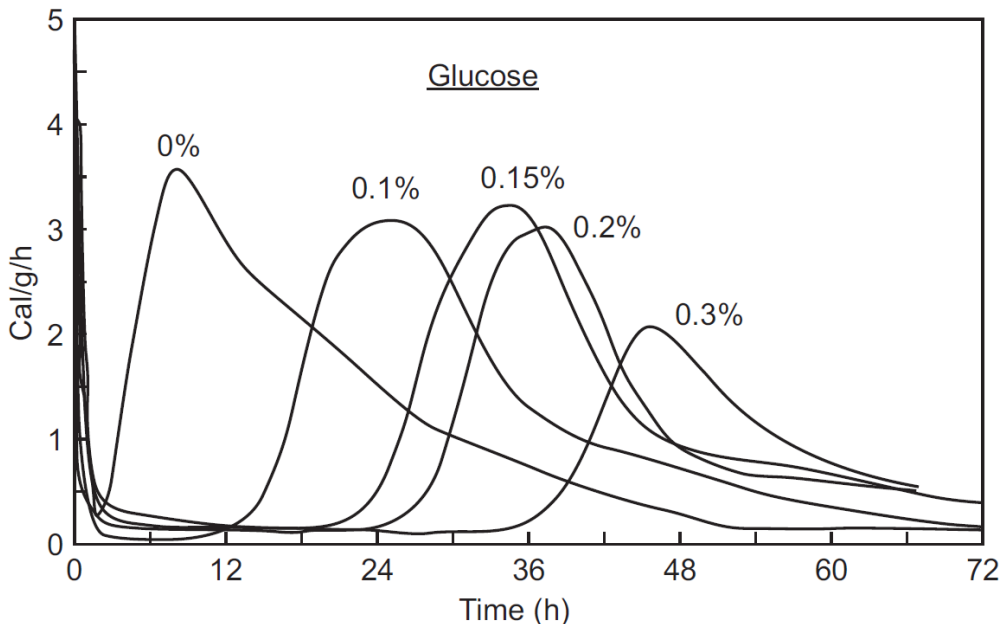


**Figure 18:** Impact of glucose retarder on Portland cement hydration at various dosages [177].  
Reprinted from [176] with permission.

These examples show that retarding admixtures affect the cement hydration on a fundamental level. Many studies have investigated the working mechanisms of retarders and identified the following major actions [167, 176]:

- Retarders delay the dissolution of clinker phase
- ...chelate or salt out dissolved calcium ions
- ...slow nucleation and growth of hydrates

The clinker dissolution can be slowed by increasing ion saturation with an appropriate admixture, for example a calcium salt [178, 179]. This is mechanistically related to the prevention of a flash set by adding calcium sulfate. An admixture might also retard the dissolution process by adsorbing on the clinker surface which poisons dissolution sites and reduces water access [180]. Similarly, some retarders can adsorb on the hydrate phases, poisoning growth sites and limiting water consumption.

In order to chelate or salt out calcium ions, retarders need to possess suitable functionality, for example a phosphate group. The removal of dissolved calcium from the hydration process delays the critical saturation level to nucleate hydrate phases [181, 182]. Furthermore, depending on the solubility of the calcium complex or salt as well as the retarder dosage, a precipitate layer may form on the surfaces of clinker and hydrate phases. Similar to the precipitation of C–S–H and ettringite during early hydration described in chapter **2.2.2**, this can create a diffusion barrier against water access and poison active sites [180, 183, 184].

## 2.3 CHEMICAL ADMIXTURES IN CEMENT HYDRATION

Most retarding admixtures are either inorganic salts or organic compounds [24]. The former include sodium tetraborate (Borax,  $\text{Na}_2\text{B}_4\text{O}_7$ ), zinc oxide ( $\text{ZnO}$ ) as well as various phosphates and phosphonates [24] among others. Inorganic retarders are generally more expensive than organic ones [185] and are thus primarily used to meet certain demands in application. For example, zinc oxide specifically targets the hydration of the silicate phase [24] while phosphonates can cause an especially long-lasting retardation [186].

Organic retarders are mostly salts of some carboxylic acids (e.g., citric and tartaric acid) or certain sugars and their derivatives. Whether they possess retarding ability depends on their molecular structure. They adsorb via their carbonyl group(s) on both positively and negatively charged clinker surfaces, on the latter bridged by  $\text{Ca}^{2+}$  cations. The adsorption is stabilized by a hydroxy group in  $\alpha$ -position to the carbonyl group. This is why the sodium salt of the  $\alpha$ -hydroxycarboxylic tartaric acid (**Figure 19, A**) is an excellent retarder. Whereas sodium caprate, which has the same carbon backbone but carries no hydroxy groups (**Figure 19, B**), possesses no retarding ability.

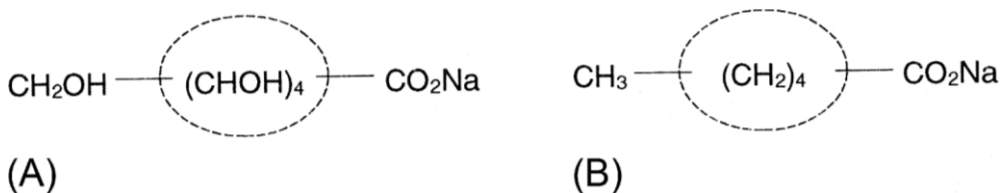


**Figure 19:** Sodium tartrate retarder (A) and non-retarding sodium caprate (B) [167].  
Reprinted with permission.

In the case of sugars, the retarding ability also depends on whether the sugar is reducing or not [176]. A sugar can act as a reducing agent if it possesses a ‘free’ carbonyl group, this means it has an aldehyde group in open form (**Figure 20**). This includes by definition all monosaccharides since ketoses can tautomerize to aldoses in solution. Di-, oligo- and polysaccharides can be reducing if the glycosidic bonds connecting the monosaccharide units allow for a ring opening. In open form, the aldehyde group can be oxidized to a carboxyl group. This reaction is catalyzed by an alkaline environment, which applies to cement pore solution [187, 188]. For this reason, reducing sugars such as glucose and maltose degrade during cement hydration while non-reducing sugars such as sucrose and raffinose do not [189–192]. However, this does not signify that non-reducing sugars always possess superior retarding ability. In pore solution, glucose reacts to gluconate salts which are better retarders than various non-reducing sugars because the anion gluconate possesses a very high affinity towards calcium which enhances both its adsorption on the surfaces and its capacity to bind free  $\text{Ca}^{2+}$  cations in the liquid [168, 187, 190, 191]. Still, the non-reducing sugar sucrose is currently the most effective retarder for Portland cement [24, 189, 191, 193].

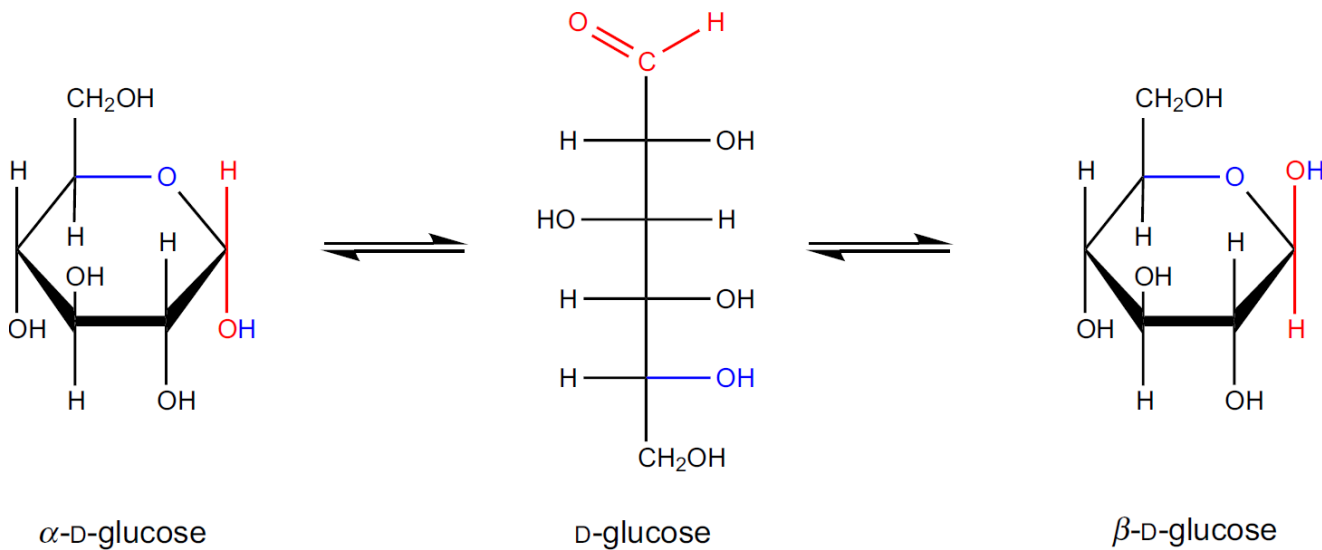


**Figure 20:** Transformation of D-glucose between  $\alpha$  and  $\beta$  ring form via the open intermediate [168].  
Reprinted with permission.

Many aliphatic sugars, both reducing and non-reducing, belong to a group known as “delayed accelerators” [193]. This unofficial term describes retarders that extend the dormant period, but subsequently increase the reaction rate during the acceleration period [180, 194].

The use of retarding admixtures, regardless of type, is often accompanied by an increase in final strength and / or durability. Retarders appear to strike a balance between the binder surfaces and the liquid phase with regards to the amount of nucleation and growth sites of hydrates [176], resulting in the development of a well-ordered atomic structure.

### 2.3.4 Dispersing agents

The main goal of using dispersing admixtures is to improve the rheological properties of the hydrating binder. Viscous concrete cannot be homogenized or pumped without the use of considerable mechanical force which might be impracticable in application. The simplest method to improve the concrete flowability is to raise the w/c ratio as this increases the interparticle space. However, it also reduces the durability and load-bearing capacity of the hardened concrete as explained in chapter 2.2.1. Furthermore, with increasing interparticle space the solids tend to segregate due to gravity if the hydrating binder is not continuously agitated. This is also referred to as ‘bleeding’ of the cement. For these reasons it is advisable to use a w/c ratio as high as necessary but as low as possible.

Dispersing admixtures help in this matter by enhancing the aqueous suspension of cement grains without having to increase the w/c ratio. As described in chapter 2.2.3, cement particles tend to flocculate (**Figure 21**, left) which entraps mixing water and increases the viscosity of the hydrating binder. The action of a dispersant is to preferentially adsorb either on the positively or the negatively charged particle surfaces [195, 196]. Covering a surface masks its charge while the unoccupied surfaces of the opposite charge electrostatically repulse each other. As a result, the particles disperse (**Figure 21**, right) instead of flocculating which enhances the flowability of the hydrating binder [196,

## 2.3 CHEMICAL ADMIXTURES IN CEMENT HYDRATION

197]. If the rheological properties remain within the limits of application demand, the use of dispersing agents can be combined with lowering the w/c ratio to increase strength and durability. Hence, they are alternatively referred to as ‘water reducers’ [166, 197, 198] (**Figure 22**).

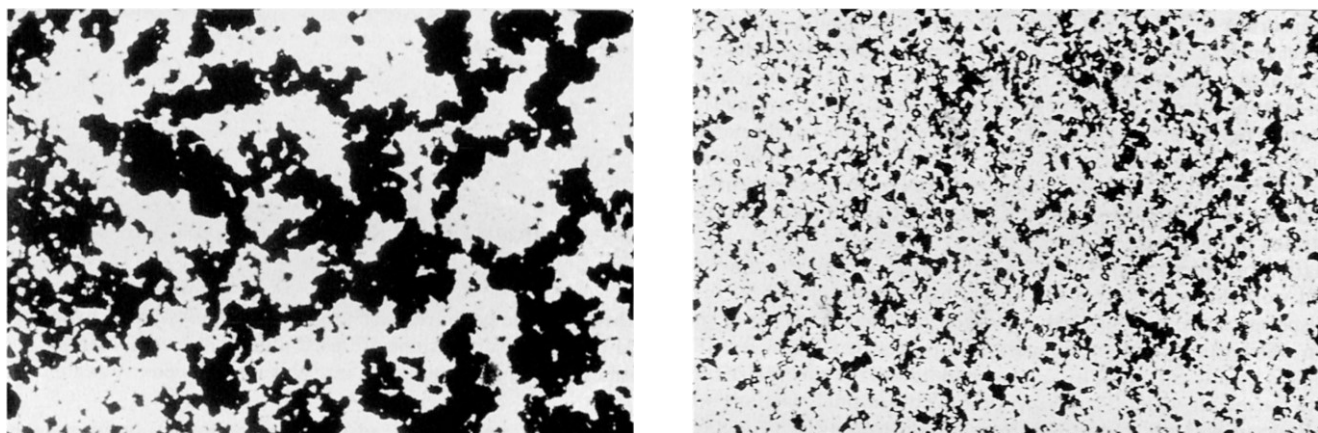


**Figure 21:** Photographs of suspended cement particles before (left) and after (right) superplasticizer addition [167]. Reprinted with permission.

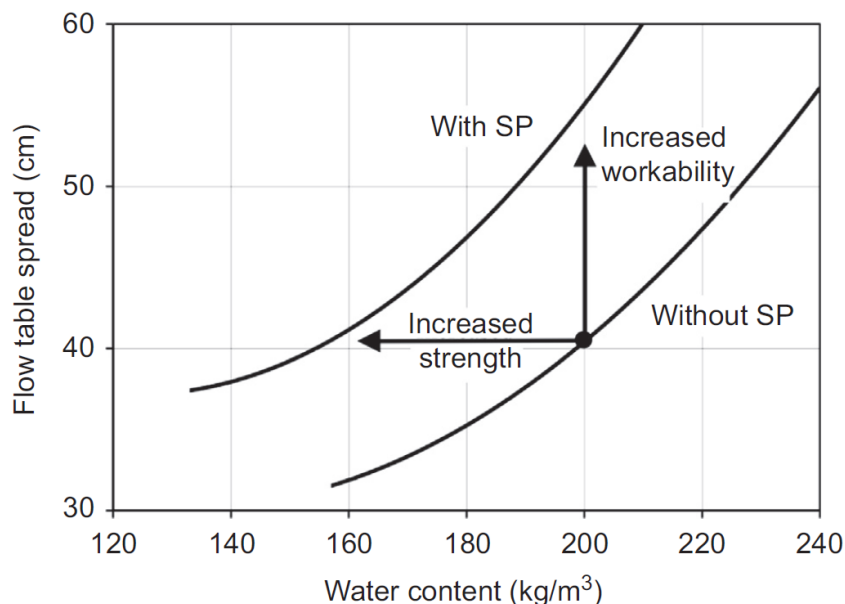


**Figure 22:** Effects of superplasticizer (SP) addition on rheological properties and water demand of cement [197]. Reprinted from [160] with permission.

Dispersing agents generally fall in one of two categories, they are either considered a plasticizer or a superplasticizer. Alternative designations are mid-range and high-range water reducers. This distinction is mainly based on performance. Superplasticizers generally display a superior performance at similar dosages and require a lower dosage for a comparable effect. Additionally, plasticizers have a lower ceiling in dispersing ability beyond which an increase in dosage is largely ineffective. In the following, only superplasticizers will be described in more detail as they are subject of this thesis.

To strongly adsorb on the charged surfaces, a dispersing agent needs to possess a so-called ‘backbone’ that carries functional groups of the opposite charge, for example carboxyl or sulfo groups (**Figure 23**, black). In the 1960s, polynaphthalene and polymelamine sulfonates were the first linear polymer superplasticizers used in cement [199, 200]. The dispersing effectiveness can be further enhanced by adding non-adsorbing side chains (**Figure 23**, blue) to the backbone, these will strongly increase the steric repulsion between dispersant molecules adsorbed on different cement grains [195, 201]. Such comb-shaped copolymers are the most efficient dispersing admixtures at the time of writing [202–204]. They are capable of reducing water demand by up to 40% [160] and provide an unrivalled increase in flowability. Depending on application, compacting or levelling the concrete after pouring might no longer be necessary [198, 205]. The use of such self-consolidating concretes reduces costs and construction downtime and enhances the production of prefabricated parts.

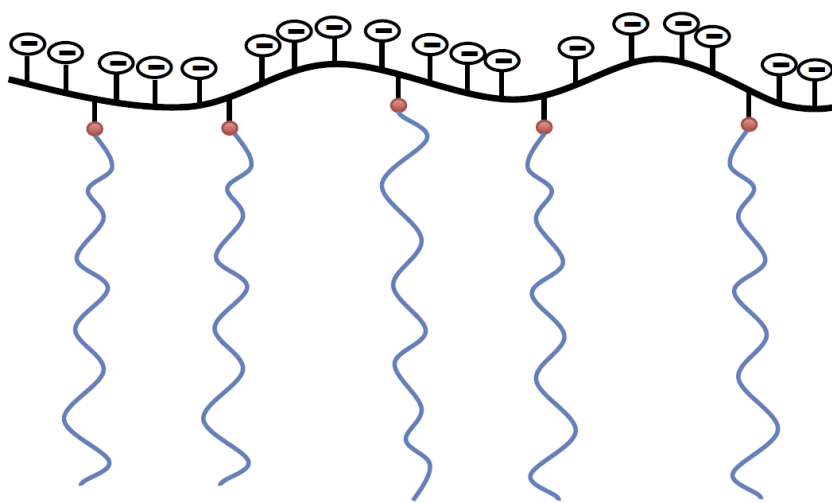


**Figure 23:** Structural elements of a comb-shaped copolymer superplasticizer [168].  
Reprinted with permission.

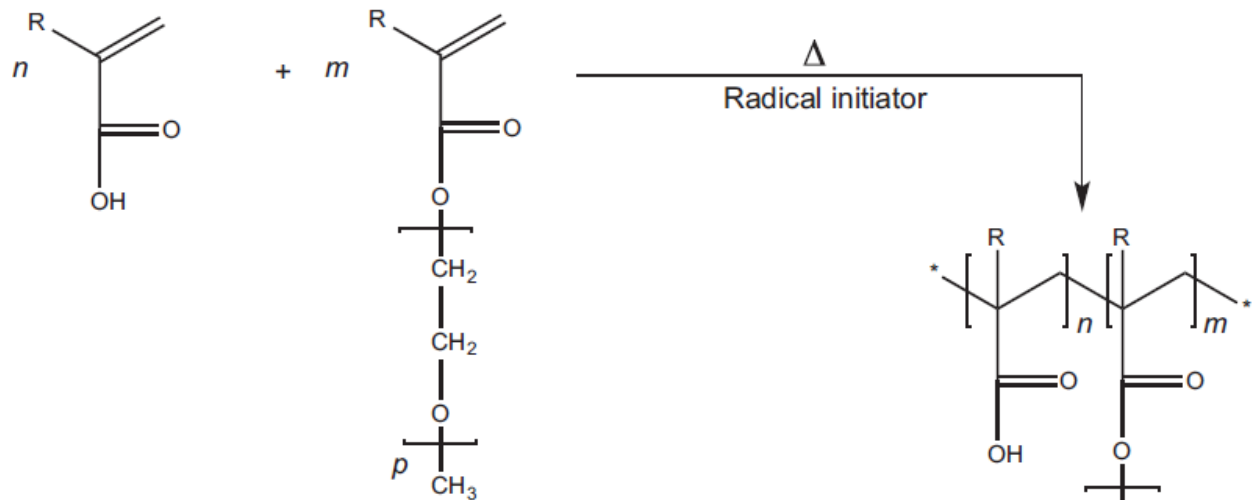
Comb-shaped superplasticizers were the result of Japanese efforts to increase the performance of linear dispersants in the 1980s [206]. First developed were polycarboxylate esters, with carboxylate referring to the charged backbone and ester denoting the type of chemical bond which attaches the side chains to the backbone. Since the ester bonds are prone to break up in the alkaline cement pore solution [207], they have been superseded by ethers and to a lesser degree amides and imides. For this reason, the common abbreviation ‘PCE’ today mostly refers to the ethers. Ester-based PCEs have largely been relegated to special applications where the detachment of the side chains during hydration, which has a similar effect as the delayed addition of a linear superplasticizer, can be utilized.

The PCE side chains consist of polyethylene glycol (PEG) in most cases, in some instances polypropylene oxide is used [208, 209]. The backbone charges usually comprise units of methacrylic, acrylic or maleic acid. In free radical copolymerization (**Figure 24**, top), these unsaturated acids react with other unsaturated groups that have been attached to the PEG chains via the aforementioned ester or ether (amid, imide) bonds. Examples are allyl-PEG ethers (APEG), vinyl-PEG ethers (VPEG), methallyl-PEG ethers (HPEG, MPEG refers to the ester bond with methacrylic acid) and isoprenyl-PEG ethers (IPEG) [210]. The polymerization of the unsaturated carbon atoms forms the backbone. Polymer analogous esterification (**Figure 24**, bottom) is an alternative synthesis pathway that uses preformed polyacid chains as the backbone to which pure PEG is grafted. The advantage of this method is that

## 2.3 CHEMICAL ADMIXTURES IN CEMENT HYDRATION

the PCEs have a lower polydispersity index (PDI, signifying a narrower molecular weight distribution) due to the more balanced distribution of the side chains along backbone polymers of uniform length. The free radical copolymerization is still the more common industrial production method since it is generally cheaper and compatible with a wide range of monomers. Additionally, it is possible to enforce conformity of the structure by using monomers that cannot homopolymerize such as maleic anhydride and APEG [211] which results in a strictly alternating pattern of charge-bearing units and sidechains.

Free radical copolymerization



Polymer analogous esterification

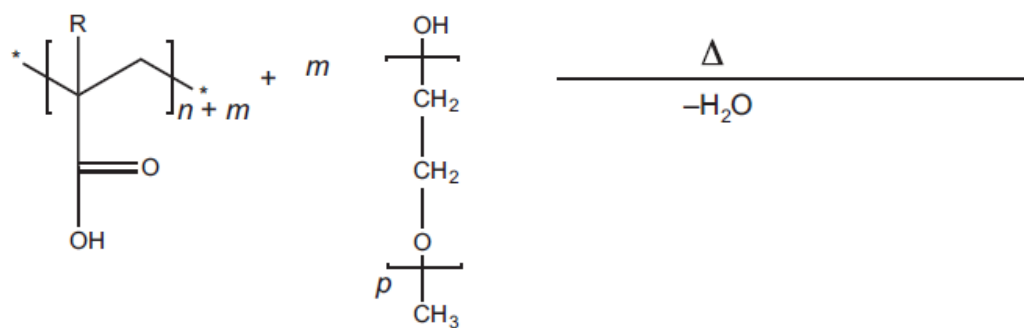


**Figure 24:** Major synthesis routes for PCE superplasticizers [168]. Reprinted with permission.

The greatest advantage of PCEs apart from their sheer efficiency is the ability to tailor them towards specific demands. Apart from the chemical nature and length of both backbone and side chains, PCE dispersing ability further depends on the distribution and the grafting density of the side chains in relation to the backbone. All of these parameters can be modified to provide suitable solutions for individual application demands [212]. The longer the side chains are, the greater is the steric repulsion which lowers the viscosity of the fresh concrete. The higher the side chain density is, the lower is the density of charged groups along the backbone which reduces the strength and speed of adsorption of

the PCE molecule on the charged surface [196, 201, 213, 214]. For example, an ideal PCE for precast concrete would have a low side chain density in order to provide a strong dispersing effect early in hydration when the concrete is poured into the mold. In ready-mix concrete, maximizing flowability is less important than keeping it over time which is called ‘slump retention’. This requires the PCE to have a higher side chain density, so that the molecules adsorb slower and provide a more sustained dispersing effect.

As a side effect, PCEs delay the acceleration period by prolonging the induction period (**Figure 25**). This retardation is stronger the higher the charge density and the lower the side chain length are, both of which increase the adsorption of the PCE on the cement grains [215–218]. The ability of PCEs to remove  $\text{Ca}^{2+}$  from pore solution by complexation as well as formation of calcium-bridged polymer clusters [167, 219–222] might also contribute to the retarding action. This has not been definitely proven yet since it is difficult to separate the impact of the PCEs’  $\text{Ca}^{2+}$  chelation ability on cement hydration from that on particle dispersion [176]. The retarding effect of PCEs on hydration is much smaller than that of the dedicated retarders described in the previous chapter 2.3.3.

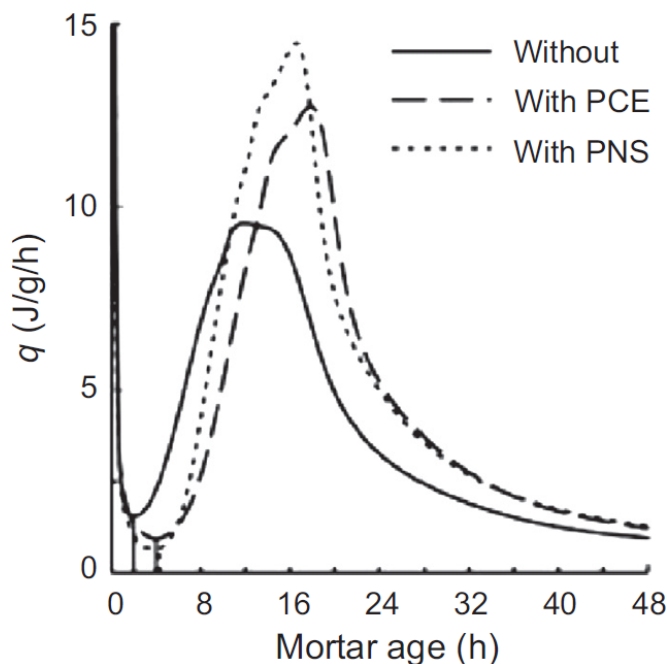


**Figure 25:** Impact of superplasticizers PNS and PCE on mortars containing OPC [223].

Reprinted from [176] with permission.

The major weakness of PCEs is their incompatibility with non-calcined clays contained in concrete aggregates and supplementary cementitious materials (SCMs). This issue is only getting more severe over time as clay-free deposits dwindle from continuous exploitation and the share of SCMs in modern cements increases to lower the carbon footprint. The PCE molecules intercalate into the sheet structure of clay minerals [224, 225] and are thus not available to adsorb on the charged surfaces. As a stop-gap measure, alongside the PCE a sacrificial agent can be added which preferably intercalates, such as polyvinyl alcohol or glycol [226]. Research towards a long-term solution includes the modification of PCE side chains [226], for example in the case of VPEG by creating terpolymers with hydroxy butyl vinyl ether (HBVE) and a maleate-based ester [227]. Another approach is to calcine the clay SCMs and identify the best-performing superplasticizers among conventional PCEs [228].

## 2.4 Impact of cement aging on hydration

### 2.4.1 Background information

In the previous chapters it has been presented that setting, hardening, and the durability of cementitious binders as well as the impact of admixtures are determined by the hydration process. Binders are geared towards high chemical reaction potential between cement and water by combining chemically and morphologically optimized clinker compositions with large active surfaces. While favorable at the point of use, this reaction potential is equally detrimental if the binder is exposed to moisture prior to the intended application. This premature contact of the cement particles with  $H_2O$  is called ‘prehydration’. During prehydration, a binder can also react with atmospheric  $CO_2$ . Both processes are summarized under the term ‘cement aging’. As explained in chapter 1.3, this can be misleading since aging in chemistry also describes environmental interactions *after* the main reaction. In this work, aging always refers to the exposure of binders *prior* to application and never to describe changes of the hardened cement post-hydration. Cement aging results in the formation of hydrate and carbonate phases, the so-called ‘aging products’, on the particle surfaces (**Figure 26**).

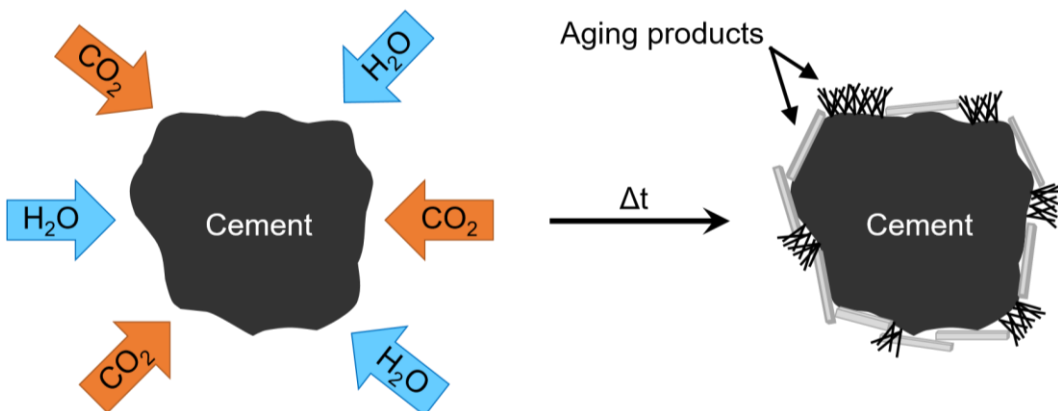


**Figure 26:** Schematic representation of the cement aging process.

Possible reasons for cement aging are manifold. The first image that comes to mind is that of cement bags lying around on a construction site under exposure to the elements. In fact, aging accompanies the cement from the moment the clinker leaves the kiln. Chapter 2.1.3.2 described that during clinker milling gypsum is interground as a set regulator and that it is partially dehydrated to hemihydrate. The crystal water released by the gypsum prehydrates the clinker [229]. It was also mentioned that the degree of gypsum dehydration depends on the mill design, which means cements can be more or less prehydrated based on the milling technology used by the manufacturer. Moreover, additional water is sometimes sprayed into the mill to reduce the temperature during grinding [230–232]. After passing the mill, if the cement powder is still hot when it is loaded into silos for storage, the dehydration of gypsum will continue, and the cement may take up additional moisture from condensation at the silo walls. The prehydration can become so severe that it causes a partial false set of the stored cement, aptly named a ‘silo set’ [233, 234].

Dry-mix products have a limited shelf life, usually several months to one year, for similar reasons. As blends and since they usually contain chemical admixtures in powder form, dry-mixes can possess

even higher reaction potential towards water than pure cements. Moreover, should any components contain bound H<sub>2</sub>O, combined with condensation this can lead to prehydration even if air- and water-tight packaging is used. In the following sections, an overview about the research into the aging impact on the cement hydration and the performance of chemical admixtures is given.

### 2.4.2 Aging impact on binders

Although the phenomenon of cement aging had been known long before, it was not scientifically investigated until the 1930s. At that time, the ongoing development of infrastructure throughout the United States received additional funding to combat the effects of the world economic crisis. Some of the building projects undertaken involved mass concreting, such as the Hoover Dam which was constructed from 1931 to 1936. As described in chapter 2.1.3.2, cracking is an issue in mass concrete structures due to the high amounts of heat released during hydration. Since retarder technology was still in its early stages, cements for mass concreting were usually calcined at lower temperatures and ground less intensely to limit the alite content and the active surface area. This came at the cost of lower load-bearing capacity and durability. Furthermore, the elimination of temperature spikes did not completely prevent the formation of cracks. The concrete was still prone to ‘sulfate attack’, the ingress of sulfate ions which would reform ettringite from monosulfoaluminate or react with unhydrated remnants of the aluminate phase. Since ettringite has a lower density than both monosulfoaluminate and clinker, this causes a volume expansion that results in cracking.

An alternative method to prevent heat cracking in use at the time was to pretreat a cement with small amounts of water which would also lead to a lower heat release during hydration [235–237]. It was discovered that prehydrated ‘regular’ cements displayed a higher average resistance to sulfate attack than the coarse low-alite cements [238]. Consequently, the prehydration of cement was more closely investigated to be better utilized. Apart from slowing the strength development [233, 235] prehydration was found to change setting times and rheological behavior [239–242]. These effects were primarily attributed to the agglomeration of cement particles and the formation of ettringite on their surfaces during the water pretreatment [243–246].

The moisture uptake of a cement was found to depend on the relative humidity (RH) applied, the exposure duration, the surrounding temperature and the particle size. Thereby it was realized that in bulk, cements prehydrated less the finer they were ground. Despite the larger active surface area, the narrow gaps between the small-sized grains impeded the penetration of moisture beyond the upper particle layers [247].

In subsequent investigations the focus changed from whole cements to individual clinker phases in order to isolate and identify the chemical reactions occurring during prehydration. It was found that the relative humidity has to exceed a certain threshold for the clinker phases to sorb water and that this threshold is different for each phase. At 20 °C, the monoclinic C<sub>3</sub>S and C<sub>2</sub>S only sorbed water above 63% and 64% RH respectively [248]. C<sub>3</sub>S reacts to C–S–H and portlandite during prehydration and the RH determines their relative distribution. Close to the 63% RH threshold, almost no portlandite is formed and the ratio of CaO to SiO<sub>2</sub> in C–S–H approximates 3. At maximum humidity (99%) the CaO to SiO<sub>2</sub> ratio ranges from 1.5 to 2.0, resembling C–S–H from regular silicate hydration and ample

## 2.4 IMPACT OF CEMENT AGING ON HYDRATION

---

amounts of portlandite are formed [249]. Orthorhombic  $C_4AF$  and cubic  $C_3A$  possess higher sorption thresholds than the silicate phases, at 78% and 80% RH, respectively. However, orthorhombic  $C_3A$  already starts to sorb water at 55% RH [248]. In prehydration, cubic  $C_3A$  first reacts to  $C_4AH_{13}$  which subsequently converts to  $C_3AH_6$  [250]. Orthorhombic  $C_3A$  forms the same prehydrates while the incorporated  $Na^+$  is leached out as  $NaOH$ . This presents a possible cause for its lower water sorption threshold [251]. If  $C_3A$  is exposed to atmospheric  $CO_2$  during prehydration, the final aging products are monocarboaluminate ( $3 CaO \cdot Al_2O_3 \cdot CaCO_3 \cdot 11 H_2O$ ) and for orthorhombic  $C_3A$  additionally sodium carbonate ( $Na_2CO_3$ ). Orthorhombic  $C_3A$  forms prehydrates and carbonates at a higher rate than cubic  $C_3A$  under comparable aging conditions [251]. This signifies that the order of reactivity between the two  $C_3A$  polymorphs is reversed as compared to regular hydration where cubic  $C_3A$  is more reactive towards water (chapter 2.2.2.3).

The aging of cement constituents other than the clinker phases was also investigated. Residual calcium oxide ('free lime') was identified as the component most sensitive towards water. It already starts prehydrating to portlandite at 14% RH [252]. In the presence of  $CO_2$ , portlandite subsequently reacts to calcium carbonate ( $CaCO_3$ ), whose morphology depends on the humidity level. At low RH, all three  $CaCO_3$  modifications (calcite, aragonite and vaterite) are formed while towards higher RH the calcite polymorph is increasingly preferred.

During aging, calcium sulfate hemihydrate re-hydrates to gypsum. There is no threshold for water sorption, but the moisture uptake does not increase linearly with RH. It starts to accelerate at 34% RH, decelerates again above 44% RH and accelerates a second time after passing 78% RH [253, 254]. Mixes of  $C_3A$  and calcium sulfate hemihydrate were aged to better simulate the situation in Portland cement where the clinker is interground with gypsum to control setting behavior. The sorption profile of the mix is essentially a combination of those of the two components: Moisture uptake is limited below 34% RH (first acceleration point of hemihydrate) and sharply increases around 72% (mix with cubic  $C_3A$ ) or 64% RH (mix with orthorhombic  $C_3A$ ) [253]. This increase also marks the onset of ettringite formation from the  $C_3A$  / hemihydrate mix [253, 255].

In prehydration, water is sorbed by the condensation of vapor on the binder particles. A liquid film is formed that starts to dissolve the grain surface. Once the ion saturation of the liquid reaches critical levels, the prehydrates nucleate and precipitate on the particle surface, similar to a regular hydration [253]. Apart from this chemical sorption, water can also be physically sorbed via van-der-Waals forces. The ratio between chemical and physical sorption during prehydration depends on the exposed material. Three cases can be distinguished [248]:

1. Water is predominantly chemically sorbed, making the sorption mostly irreversible when the RH is lowered. This is observed in free lime.
2. Both chemical and physical sorption occur quantitatively, the sorbed water is partially released by lowering the RH. Pure  $C_3A$  prehydrates this way.
3. Physical sorption prevails, the sorbed water is mostly released by lowering the RH. Calcium sulfate hemihydrate, anhydrite and the silicate phases display this prehydration behavior.

The more water is chemically sorbed, the higher is the total water uptake. By weight of solid, free lime sorbs more water than  $C_3A$ , which in turn sorbs more than  $C_3S$ . Even more impactful is the formation

## 2.4 IMPACT OF CEMENT AGING ON HYDRATION

---

of ettringite and gypsum during prehydration which incorporate large amounts of water into their crystal structure. The total water uptake of pure anhydrous calcium sulfate is very low in comparison to the hemihydrate despite starting to sorb moisture at 58% RH [248].

Raising the surrounding temperature during prehydration increases the rate of water sorption but does not significantly affect the ratio between chemically and physically sorbed water or the sorption thresholds [248]. Additionally, the higher the specific surface area of a sample, the more water is sorbed during prehydration [248, 253].

Recently, limestone addition was presented as a means to partially counteract the detrimental effects of prehydration [256]. Originally, fine limestone was used to increase the flowability of cements with a narrow particle size distribution as described in chapter 2.1.3.2. Depending on application, the limestone is also beneficial for the setting and hardening. Small limestone particles can act as a heterogeneous catalyst by providing a large surface for hydrate nucleation and growth which lowers the energy requirements associated with these processes. The downside of limestone addition is that it can decrease final strength because it does not form C–S–H as a pozzolanic additive would do. Setting time and compressive strength development of a Portland cement / limestone blend were less affected by aging than the pure cement. At low degrees of prehydration the blend behaved almost identical to unaged Portland cement [256].

### 2.4.3 Aging impact on admixtures

Cement aging also impacts the use of admixtures. The precipitation of prehydrates in combination with particle agglomeration during aging change the charge and area of the active surface which affects the performance of active and interactive admixtures whose working mechanisms rely on surface interaction. Aging can either compliment the admixture effect, lowering the required dosage for a certain performance, or impede it, raising the dosage requirement. Across multiple studies by different research groups, a variety of admixtures have been investigated with regards to their performance in aged cement. An overview of the results is given in the following:

The water retention agent methyl hydroxyethyl cellulose (MHEC) showed an increased performance in aged Portland cement [257]. In the same study the accelerators calcium formate ( $\text{Ca}(\text{HCO}_3)_2$ ) and amorphous aluminate ( $\text{Al}_2\text{O}_3$ ) were found to be less effective after aging the cement. However, an aluminum sulfate accelerator for shotcrete was more effective in decreasing the setting time if the binder had been aged [258]. The latter was attributed to a slower dissolution of the set regulator calcium sulfate hemihydrate after prehydration. This signifies that even within an admixture category such as accelerators the performance can benefit or suffer from cement aging.

A similar ambivalence was observed for superplasticizers. In one study it was reported that the performances of a PNS and a PCE (both commercial products) were negatively affected by cement aging, the linear polymer more severely than the comb-shaped copolymer [257]. These findings contradict a previous work [259], where the dispersing effects of PNS and PCE were stronger in aged cement.

## 2.4 IMPACT OF CEMENT AGING ON HYDRATION

---

In a mechanistic study [260] created as a follow-up to [257] the performances of MPEG- and APEG-PCEs synthesized in the laboratory also decreased in aged cement. The MPEG-PCEs possessed a higher charge density and displayed a stronger reduction in dispersing effectiveness than the APEG-PCEs [260]. In aged blends of  $C_3A$  and gypsum, the performances of the lab-synthesized PCEs were found to primarily depend on the  $C_3A$  morphology and the length of exposure. The PCEs initially rose in effectiveness with increasing aging duration of a cubic  $C_3A$  / gypsum blend. If the blend had been aged for more than 72 hours though, the PCE performance started to decrease again. In blends containing orthorhombic  $C_3A$  an inverse trend was observed. The authors conclude that the precipitation of prehydrates and the particle agglomeration occurring during aging have opposite effects on the PCE performance: The formation of ettringite is slow in blends with the (in prehydration) less reactive cubic  $C_3A$  and is initially outweighed by the particle agglomeration. As a result, during early prehydration the total active surface area gets reduced. Less superplasticizer is required to cover this surface, which was confirmed by measuring the saturated adsorbed amount of polymer. This explains why at the same dosage the PCEs displays a better performance after the cubic  $C_3A$  / gypsum blend has been aged for short and medium durations. The longer the exposure, the more ettringite is formed which provides additional surface for superplasticizer adsorption. Thus, the PCE effectiveness starts to decrease towards long aging periods. In the (in prehydration) more reactive orthorhombic  $C_3A$ , the rate of ettringite formation during aging is higher, thus the total active surface area increases from the beginning of the exposure. After the surface is largely covered by prehydrates the water uptake decelerates. Due to the ongoing particle agglomeration, the total active surface area starts to shrink towards long aging periods. For this reason, the orthorhombic  $C_3A$  / gypsum mix is more effectively dispersed by the PCEs after long exposure which is the exact opposite of the cubic polymorph.

This conclusion might serve as an explanation as to why the two previous studies obtained contradicting results for the performance of commercial superplasticizers in aged cement [257, 259]. While in both investigations the Portland cement was exposed to 90% RH, the surrounding temperatures differed. The positive impact on superplasticizer dispersing effectiveness was observed at 20 °C [259] whereas the performance drop was noted at 35 °C [257]. As mentioned in the previous chapter **2.4.2**, the rate of water sorption increases with the temperature, which indicates that in [257] prehydration was more severe than in [259]. Since Portland cement is even less reactive than a blend of cubic  $C_3A$  and gypsum, this means that in [259] particle agglomeration might have played a greater role than prehydrate formation, thus enhancing superplasticizer performance while in [257] it was the other way around.

Up to this point, only results have been presented where the binder was aged while fresh admixtures were introduced at the start of hydration. On the other hand, the admixtures in powder form contained in dry-mix products are already present during exposure. For this reason, investigators have started to include admixtures in aging experiments to determine the direct effects of exposure on them and whether their presence also affects the aging of the binder.

An example for a dry-mix product that might suffer from a limited shelf-life due to aging are self-leveling underlays (SLUs). In one study, the effect of aging on a model formulation consisting of a ternary binder system dry-mixed with a lithium carbonate accelerator and a superplasticizer was investigated [261]. It was observed that aging significantly damaged the formulation. Its water demand doubled, signifying that the dispersing effect of the superplasticizer was much reduced after it had been present

## 2.4 IMPACT OF CEMENT AGING ON HYDRATION

---

during exposure. Furthermore, as a result of aging the compressive strength of the model formulation 1 day after the start of hydration was decreased by up to 40%. The authors attribute the aging effects to the massive ettringite formation from aluminate cement and anhydrite in the presence of lithium carbonate during exposure.

### 3 Scope of the present thesis

#### 3.1 Research objectives

From the studies on cement aging presented in chapter 2.4, [248, 251–254, 257, 261] were conducted at the Chair for Construction Chemistry of the Technical University of Munich (Prof. Dr. Johann Plank). Funding was provided by the *Nanocem* research network (grant *Core project #7*) and the *Deutsche Forschungsgemeinschaft* ‘German research society’ (grant *PL 472/9-1*). From the results of these works two follow-up topics for further research on cement aging were identified, which provide the basis for the present thesis:

1. The impact of aging on the performance of retarders in Portland cement. This had only been investigated to a very limited extent when compared to accelerators or dispersing agents. The main result so far had been that due to the lower heat release after aging cement, less retarder might be required in application [262]. Moreover, preliminary investigations at the Chair suggested that the aging impact on retarder performance is connected to the working mechanism: Strongly adsorbing sodium gluconate (NaGluc) was affected differently by aging than potassium pyrophosphate (KPPhos) which is a powerful precipitation agent for dissolved  $\text{Ca}^{2+}$ . To elucidate this, the impact of these retarders on the hydration of the individual clinker phases  $\text{C}_3\text{S}$  and  $\text{C}_3\text{A}$  (with sulfate) after aging was to be examined in addition to Portland cement. Additionally, the effect on the (pre)hydration product ettringite was to be isolated by having the two retarders interact with lab-synthesized ettringite. Since the previous study on superplasticizers [260] had revealed a strong influence of the  $\text{C}_3\text{A}$  morphology, both monoclinic and triclinic  $\text{C}_3\text{S}$  as well as cubic and orthorhombic  $\text{C}_3\text{A}$  were to be investigated.
2. An in-depth analysis of the aging of a model self-leveling underlayment (SLU) as an example for a dry-mix product. As described earlier, these are multi-component binder systems geared towards high reactivity in hydration which makes them particularly susceptible to aging. Previously, individual clinker phases were investigated to gain more insight into the aging of Portland cement. In similar fashion, dry-mix components were to be aged alone and in various combinations to study individual vulnerabilities towards exposure and identify interactions between components during aging. Expanding on previous investigations [261], the model SLU was to be based on a ternary binder system (TBS) consisting of ordinary Portland cement (OPC), calcium aluminate cement (CAC) and calcium sulfate anhydrite (AH). Three admixtures were to be used, an accelerator for the CAC (lithium carbonate), a retarder (sodium potassium tartrate) and a superplasticizer (commercial PCE).

A research proposal covering these two topics was accepted by the *Deutsche Forschungsgemeinschaft* (DFG) under the grant *PL 472/9-2 “Influence of aging of binder systems on the performance of additives”* [263]. A summary of the main experimental work carried out in the course of the project is provided in **Figure 27**. It is based on the schedule suggested in the proposal and includes modifications as well as additions made during the project runtime.

### 3.1 RESEARCH OBJECTIVES

↓

Synthesis	Aging	Investigations
C <sub>3</sub> A cub	OPC 3 + 14 days	
C <sub>3</sub> A orth	C <sub>3</sub> A cub + gypsum 3 + 14 days	Characterization of fresh and aged OPC (XRD, FT-IR, TG-MS, ESEM)
	C <sub>3</sub> A orth + gypsum 3 + 14 days	Hydration of fresh and aged OPC w/ or w/o NaGI or KPPhos (calorimetry, <i>in situ</i> XRD, TOC, UV-Vis, ICP-OES)
C <sub>3</sub> S tric		Characterization of fresh and aged C <sub>3</sub> A + gypsum (XRD, FT-IR, TG-MS, ESEM)
C <sub>3</sub> S mono	C <sub>3</sub> S tric 3 + 14 days	Hydration of fresh and aged C <sub>3</sub> A + gypsum w/ or w/o NaGI or KPPhos (calorimetry, <i>in situ</i> XRD, TOC, UV-Vis, ICP-OES)
Synthetic ettringite	C <sub>3</sub> S mono 3 + 14 days	Rheology and compressive strength tests of fresh and aged OPC w/ or w/o NaGI or KPPhos
TBS	Synthetic ettringite 3 + 14 days	Characterization of fresh and aged C <sub>3</sub> S (XRD, FT-IR, TG-MS, ESEM)
	TBS w/o admixtures 1 + 7 days	Hydration of fresh and aged C <sub>3</sub> S w/ or w/o NaGI or KPPhos (calorimetry, <i>in situ</i> XRD, TOC, UV-Vis, ICP-OES)
Model SLU w/ aged TBS	TBS + lithium 1 + 7 days	Interaction of gluconate and phosphate with synthetic ettringite (TOC, UV-Vis)
Model SLU w/ aged TBS + lithium	TBS + tartrate 1 + 7 days	Characterization of fresh and aged TBS w/ or w/o admixtures (XRD, FT-IR, TG-MS, ESEM)
Model SLU w/ aged TBS + tartrate	TBS + PCE 1 + 7 days	
Model SLU w/ aged TBS + PCE	TBS + all admixtures 1 + 7 days	
	OPC 1 + 7 days	Rheology and compressive strength tests of model SLUs with different aged admixtures
Model SLU w/ aged OPC	CAC 1 + 7 days	Characterization of fresh and aged OPC / CAC / AH (XRD, FT-IR, TG-MS, ESEM)
Model SLU w/ aged CAC	AH 1 + 7 days	
Model SLU w/ aged AH		
		Hydration of model SLUs with aged OPC / CAC / AH (calorimetry, <i>in situ</i> XRD, ICP-OES)
		Rheology and compressive strength tests of model SLUs with aged OPC / CAC / AH
<b>Final report for German Research Association</b>		

**Figure 27:** Main experimental work carried out over the course of the DFG project PL 472/9-2  
“Influence of aging of binder systems on the performance of additives”.

### 3.1 RESEARCH OBJECTIVES

---

**Figure 27** assigns a color to each investigated “system”. Both project topics were divided into separate systems designed to be compared with each other, they differ by a variable that is expected to change the aging and / or hydration behavior. Examples are different clinker phase morphologies or model SLUs with different aged components. The experimental work for each investigated system consists of three consecutive steps, “Synthesis”, “Aging” and “Investigations”. The experimental methods applied in each step are discussed in the following chapter **3**. The results for each investigated system and comparisons between them are provided in chapter **4**. Chapter **5** summarizes the findings for both topics and also provides the official project report submitted to the DFG.

## 3.2 Experimental work

This chapter provides information about the experimental methods used in the synthesis, aging and investigation parts of the project. Procedures comprising multiple steps are introduced by a flowchart for better overview that is followed by a description of each step. Specific indications such as quantities and measurement inputs can be found in the scientific publications associated with the project which are enclosed with this thesis.

### 3.2.1 Synthesis procedures

In the “Synthesis” step, the clinker phases  $C_3S$  and  $C_3A$  as well as synthetic ettringite are produced in the laboratory. The OPC as well as the other binders CAC and AH were acquired from commercial producers. Both the TBS and the SLU were formulated in the laboratory from fresh and aged components.

#### 3.2.1.1 Clinker phases $C_3A$ and $C_3S$

The synthesis procedure of the clinker phases  $C_3A$  and  $C_3S$  consists of 4 steps (**Figure 28**).

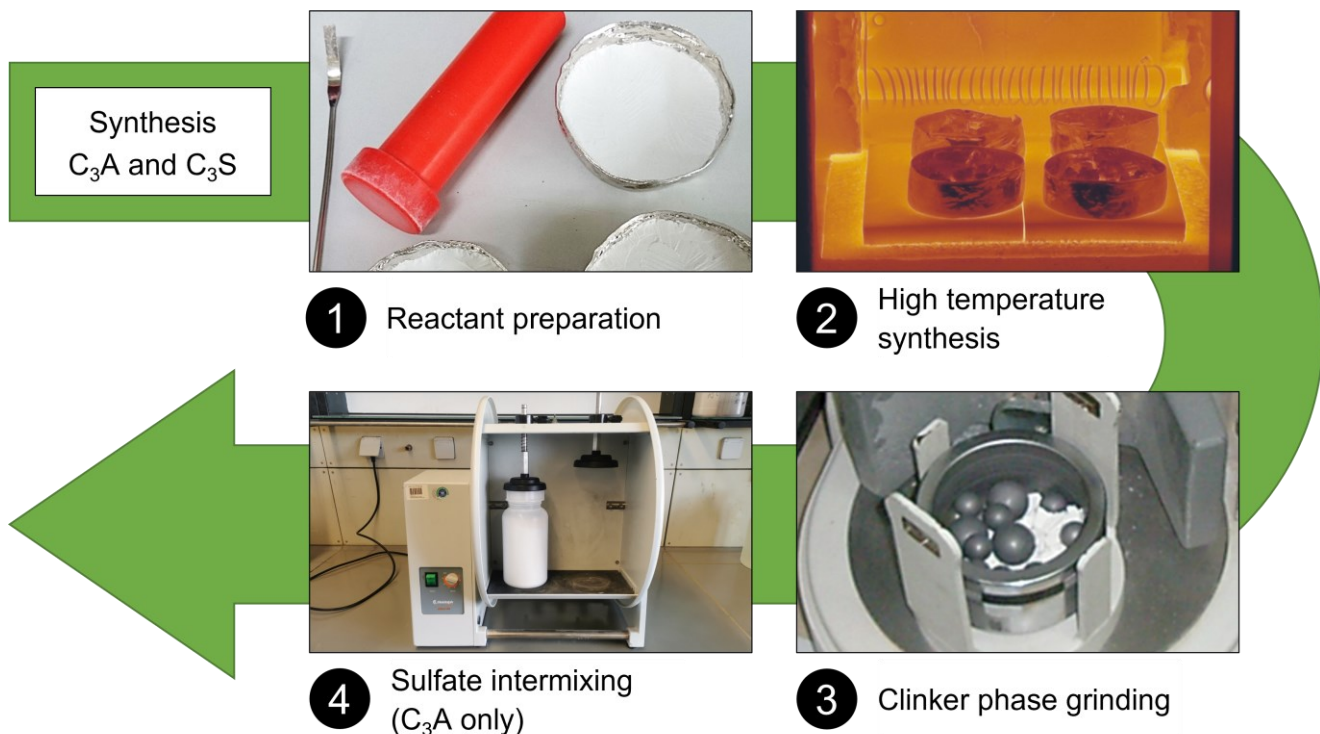


**Figure 28:** Overview of the preparation of the clinker phases  $C_3A$  and  $C_3S$ .

- 1** The clinker phases were synthesized from  $CaCO_3$  and  $Al_2O_3$  ( $C_3A$ ) or  $CaCO_3$  and  $SiO_2$  ( $C_3S$ ), respectively. Initially, quarried  $CaCO_3$  was utilized, however this led to a reddish discoloration of the otherwise bright white  $C_3A$  while the normally off-white  $C_3S$  displayed a solid green color (**Figure 29**). For this reason, only clinker phases synthesized from precipitated  $CaCO_3$  were used in the retarder investigations.

### 3.2 EXPERIMENTAL WORK

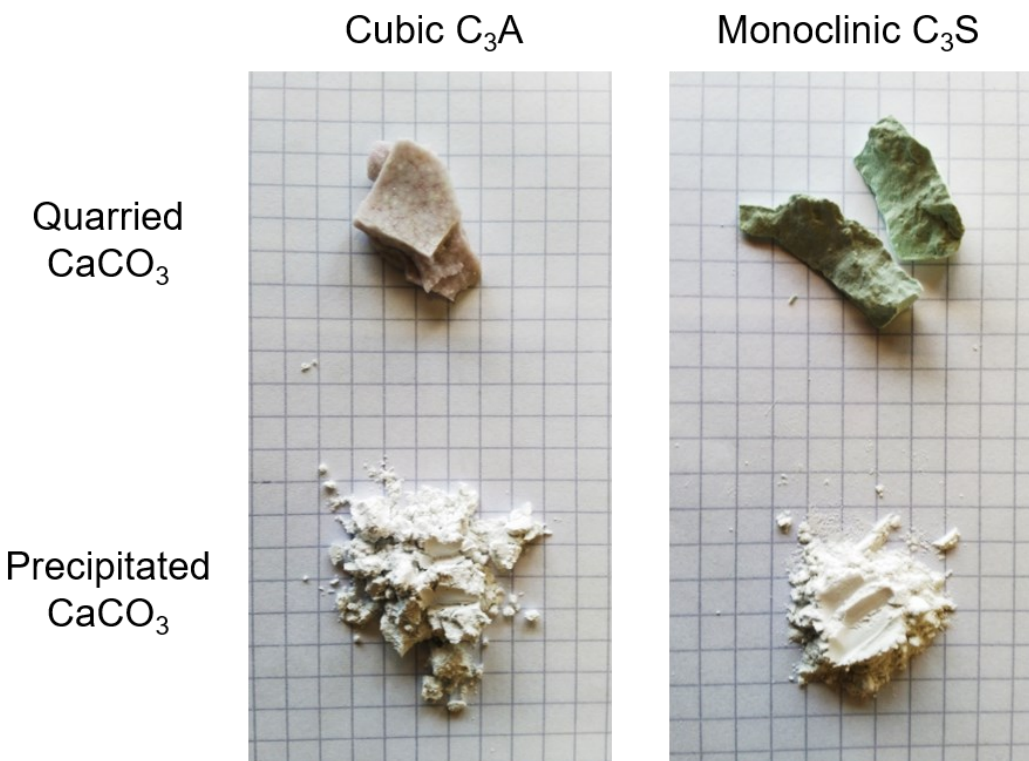


**Figure 29:** Visual comparison between clinker phases synthesized from quarried or precipitated  $\text{CaCO}_3$ .

- ② The high temperature clinker synthesis was carried out in laboratory chamber furnaces, Nabertherm *LH 15/14* and *LHT 08/16*, loosely based on a procedure described in [38]. The reactants were homogenized and filled into crucibles made from a platinum alloy containing 10% rhodium for increased temperature stability. The powder was compacted by hand to promote the solid-state reaction. Excessive contact pressure was avoided to prevent an explosive liberation of  $\text{CO}_2$  during calcination. To synthesize cubic  $\text{C}_3\text{A}$ , stoichiometric blends of  $\text{CaCO}_3$  and  $\text{Al}_2\text{O}_3$  were repeatedly fired at 1400 °C. After each run the product composition was determined by powder X-ray diffraction. Phase purity was declared after the intermediate products  $\text{C}_{12}\text{A}_7$  (mayenite) and  $\text{CaO}$  (lime) had disappeared. To obtain  $\text{Na}^+$  substituted orthorhombic  $\text{C}_3\text{A}$ , the  $\text{CaCO}_3 / \text{Al}_2\text{O}_3$  blend was modified to contain 10.6 wt.%  $\text{NaNO}_3$  and the crucibles were covered with platinum lids to reduce losses from  $\text{Na}_2\text{O}$  sublimation. Alternatively, the  $\text{NaNO}_3$  content can be reduced to 7.0 wt.% when maximum firing temperature is lowered to 1300 °C.  $\text{C}_3\text{S}$  was similarly synthesized from  $\text{CaCO}_3$  and  $\text{SiO}_2$  at 1450–1600 °C. The substituted monoclinic polymorph was stabilized with 1.1 wt.%  $\text{MgO}$  and 0.7 wt.%  $\text{Al}_2\text{O}_3$ .
- ③ The pure clinker phases were finely ground to a particle size distribution (PSD) similar to that of the CEM I 52.5 N sample ( $d_{50} = 15 \mu\text{m}$ ,  $d_{90} = 46 \mu\text{m}$ ) using a Fritsch *Pulverisette 6* planetary mono mill and metal sifters. Particle size was monitored with a laser granulometer (Cilas 1064) using isopropyl alcohol as the dispersion medium and ultrasound to disperse particle agglomerates.

Maintaining a consistent PSD across different clinker phases is important since the active surface area determines the degree of aging and the subsequent hydration behavior / admixture interaction as described in chapter 2.4. The hardness grade of the individual phases was found to decrease in the order  $\text{C}_3\text{S}$ , cubic  $\text{C}_3\text{A}$ , orthorhombic  $\text{C}_3\text{A}$ . The softer a material is, the more difficult it is to

### 3.2 EXPERIMENTAL WORK

obtain a narrow particle size distribution and the higher is the share of overly fine particles which have to be recycled by firing them again. The hardness was increased by raising the synthesis temperature. Both triclinic and monoclinic C<sub>3</sub>S are innately hard enough that maximum temperatures between 1450 °C to 1600 °C yielded clinker which was comparatively easily ground to the target PSD. For C<sub>3</sub>A, the best results were obtained at 1300–1400 °C, which posed a challenge for orthorhombic C<sub>3</sub>A since Na<sup>+</sup> is partially lost due to Na<sub>2</sub>O sublimation above 1275 °C [38]. As specified above, over 10 wt.% of NaNO<sub>3</sub> had to be applied at 1400 °C which is in significant excess of the 3.7–4.6 wt.% Na<sub>2</sub>O required to stabilize the orthorhombic modification (chapter 2.1.1.3).

The change from quarried to precipitated CaCO<sub>3</sub> also increased the softness of the clinker phases. In comparison, precipitated CaCO<sub>3</sub> particles are larger, more regularly shaped and possess smoother surfaces, all of which lowers the reactivity in the solid-state reaction. As a countermeasure, the precipitated CaCO<sub>3</sub> was ground in the planetary mono mill prior to firing. After this pretreatment, the ‘rugged’ CaCO<sub>3</sub> particles yielded harder C<sub>3</sub>A phases. This improved the grinding to narrower particle size distributions considerably (**Figure 30**).

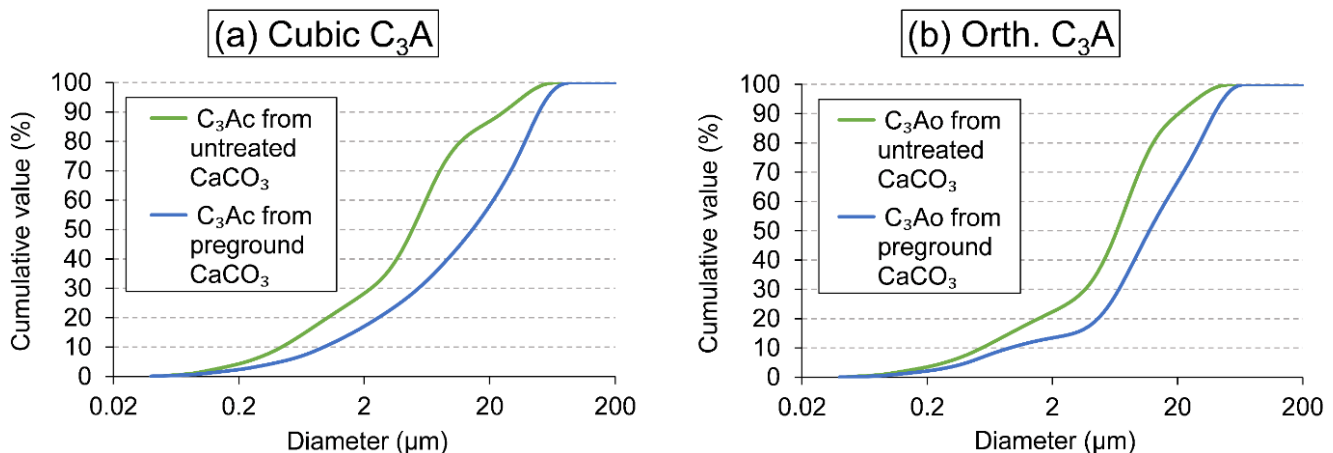


**Figure 30:** Effects of pregrinding CaCO<sub>3</sub> on the particle size distributions of the C<sub>3</sub>A polymorphs.

- ④ Prior to aging, the cubic and orthorhombic C<sub>3</sub>A were intermixed with calcium sulfate to simulate the conditions in Portland cement which forms ettringite in prehydration. As in [260], gypsum was chosen as the sulfate source. In this previous work it was found that gypsum reacted to ettringite with both C<sub>3</sub>A polymorphs at prehydration conditions of 35 °C and 90% RH while the presence of hemihydrate to avoid formation of aluminum hydrates was not required. The absence of hemihydrate signifies that the reproduction of C<sub>3</sub>A hydration in Portland cement is not perfectly accurate. However, it also eliminates the re-hydration of hemihydrate as a side reaction from the mechanistical study. The selected gypsum had a particle size distribution close to that of the CEM I 52.5 N and the clinker phases. Using a Heidolph REAX 20/4 overhead shaker, the gypsum was dry-blended with C<sub>3</sub>A at a 1 : 1 ratio by weight which corresponds to a molar ratio of C<sub>3</sub>A to gypsum of 1 : 1.57.

## 3.2 EXPERIMENTAL WORK

### 3.2.1.2 Binders, ternary binder system and self-levelling underlayment

The formulation of TBS and SLU were separated (**Figure 31**). This way, the TBS or one of its components could be aged before the admixtures were added. It allows to distinguish between the aging impact on the TBS alone from that on the SLU (TBS + admixtures).

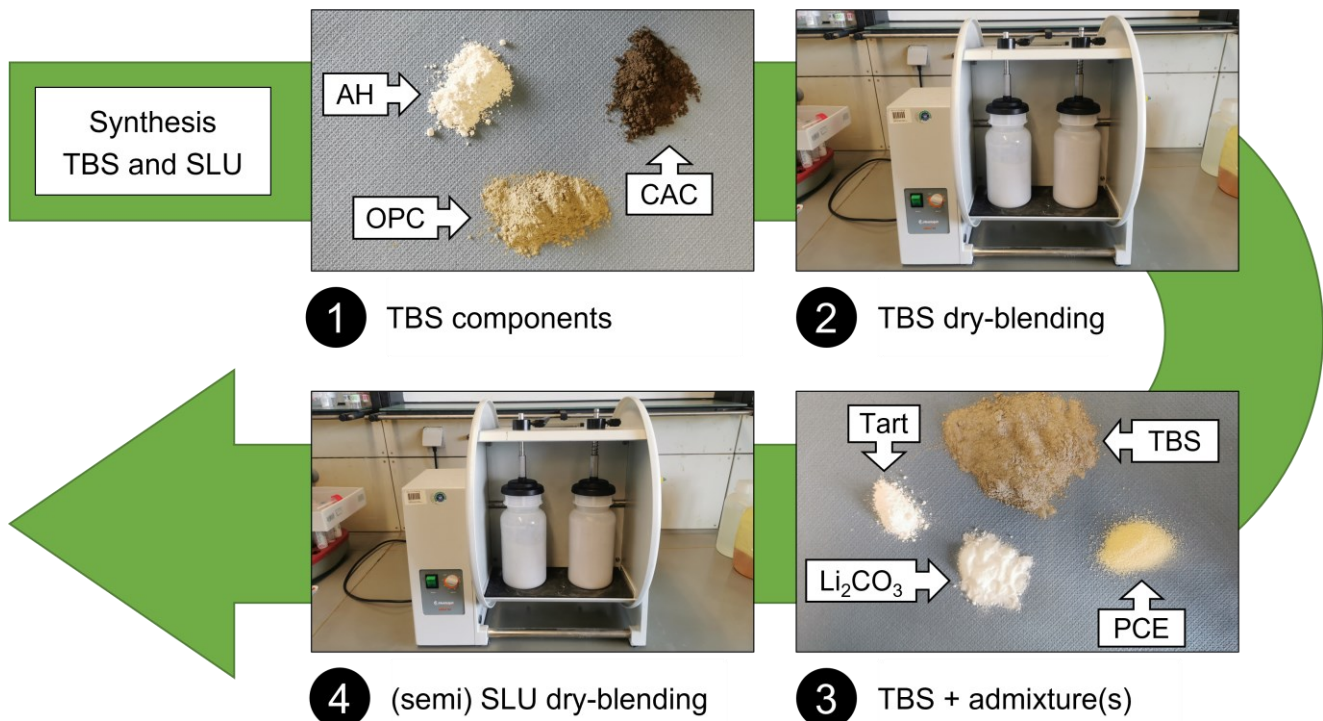


**Figure 31:** Overview of the preparation of the TBS and the SLU.

- ①+② The TBS consisted of OPC, CAC and AH. Regarding the OPC, one CEM I 52.5 N (*Milke®* brand) sample provided by HeidelbergCement was used for both the retarder investigations and the TBS. The CAC was a *Ciment Fondu®* produced by Kerneos. Both cements were selected with regards to their application in commercial dry-mix products. AH (from hydrogen fluoride production) was provided by Solvay. The particle size of the TBS components was cut off at 90 µm by sieving before they were blended together in the overhead shaker.
- ③+④ To create the model SLU, the TBS was admixed with an accelerator (lithium carbonate), a retarder (sodium potassium tartrate) and a superplasticizer (commercial PCE). The blend of TBS and all three admixtures was called a ‘fully formulated’ model SLU. If the aging impact on a single admixture was to be examined, only this admixture was blended with the TBS prior to aging as a so-called ‘semi-formulated’ SLU. The other two (non-aged) admixtures were added prior to the hydration experiments. The admixture dosages in the model SLU were developed from [261]. As mentioned in chapter 2.4.3, in that study the water demand of the model SLU doubled after aging, specifically from a w/f ratio of 0.25 to 0.50 in order to obtain measurable engineering properties. The use of different w/f ratios for fresh and aged SLU samples would make a direct comparison between their hydration behaviors fundamentally unsound since this ratio is the main parameter governing hydration as explained in chapter 2.2.1. It was found that if the admixture dosages were tuned to result in a demand of 0.50 w/f for the fresh SLU, then it could be properly hydrated after aging without having to increase the w/f further. A w/f ratio

## 3.2 EXPERIMENTAL WORK

of 0.50 is considerably higher than what would be used for a commercial SLU in application, but the more conclusive determination of the aging impact on the TBS and the admixtures outweighs this deviation of the model SLU.

### 3.2.1.3 Synthetic ettringite

Synthetic ettringite was precipitated from aluminum sulfate ( $\text{Al}_2(\text{SO}_4)_3$ ), calcium chloride ( $\text{CaCl}_2$ ) and sodium hydroxide ( $\text{NaOH}$ ) in deionized and degassed water. The precipitate was centrifuged and redispersed in water repeatedly to remove the dissolved by-product sodium chloride ( $\text{NaCl}$ ). The wet ettringite was stored in a drying chamber at 40 °C for 2 days. Afterwards it was ground to a particle size distribution similar to that of the CEM I 52.5 N and the clinker phases.

### 3.2.2 Aging procedure

In the “Aging” step, clinker phases, binders, binder systems with admixtures and other systems were exposed to water vapor and  $\text{CO}_2$  in the laboratory. The aging procedure comprises 4 steps (Figure 32).

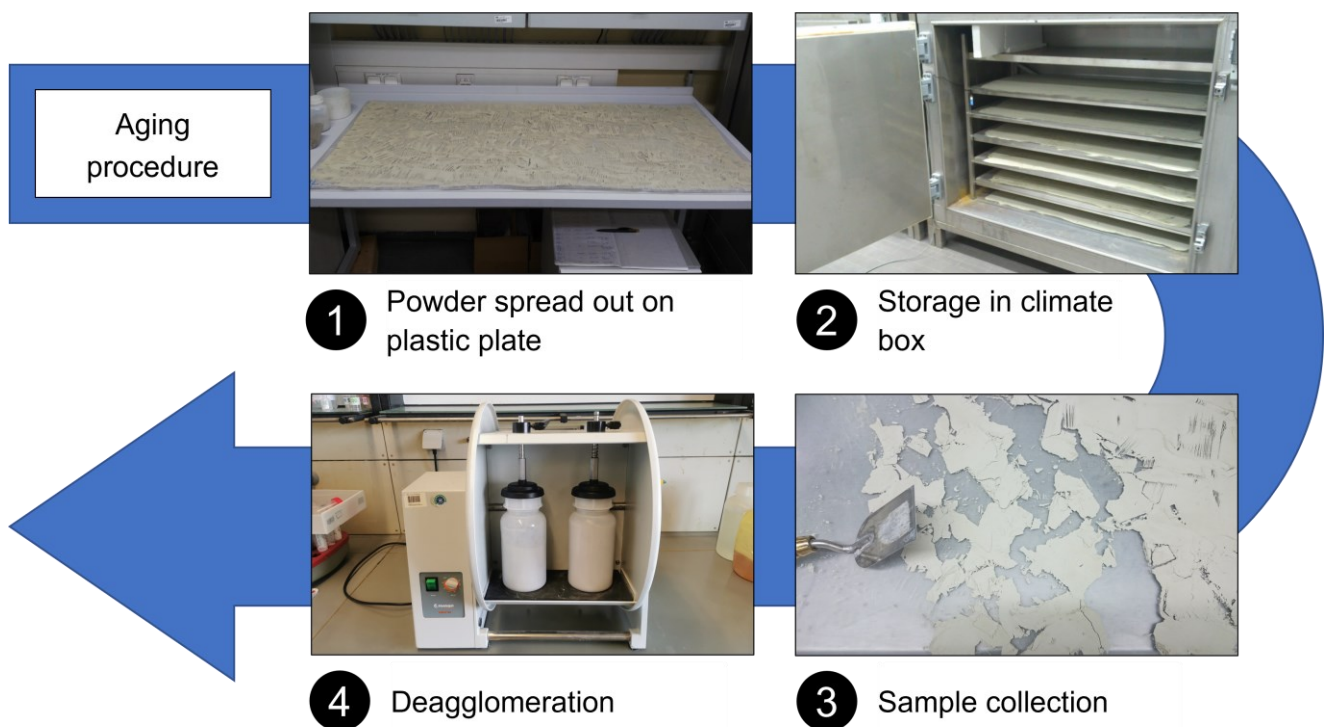


**Figure 32:** Overview of the preparation of the aged samples.

- 1 Samples were spread out evenly on 135 × 60 cm Plexiglas® plates using a small trowel, with each plate holding exactly 50.0 g of material. The small sample size was chosen to keep the amount of stacked particle layers on the plate as low as possible. This was to avoid a ‘bulk-effect’ as described

## 3.2 EXPERIMENTAL WORK

---

in chapter **2.4.2** whereby narrow gaps between small particles limit the penetration of water vapor to deeper layers during prehydration [247].

- ② The filled plates were exposed to water vapor and atmospheric CO<sub>2</sub> at 35 °C ( $\pm 2$  °C accuracy) and 90% RH ( $\pm 5\%$  accuracy) in a custom climate box. The same as in [257, 260, 261], these conditions were chosen to guarantee water sorption by all clinker phases based on the sorption thresholds determined in [248]. The previous studies on superplasticizers [257, 259, 260] had proven that the exposure duration is a crucial factor in the hydration of aged binders and the admixture performance. Thus, the exposure duration was varied from 1 to 14 days depending on project topic and investigated system.
- ③ After the allotted exposure duration, the plates were removed from the climate box and the aged samples were collected with the trowel. The thinly spread powders had agglomerating in the humid environment, forming a delicate sheet which broke into platelets during removal from the plates.
- ④ The aged samples were stored in airtight containers and churned in the overhead shaker. This deagglomerated the platelets and converted them back into powders.

### 3.2.3 Investigation of the aging impact

The “Investigations” step consists of two parts: At first, aged samples were characterized and compared to fresh ones in order to determine changes in the chemical composition resulting from exposure. Subsequently, fresh and aged samples were hydrated to elucidate the aging impact on the hydration behavior of binders.

#### 3.2.3.1 Sample characterization

The chemical compositions of fresh and aged samples were compared via powder X-ray diffractometry (XRD), Fourier-transformed infrared (FT-IR) spectroscopy, thermogravimetric analysis (TGA), in instances coupled with mass spectrometry (TG-MS) and (environmental) scanning electron microscopy ((E)SEM) (**Figure 33**).

### 3.2 EXPERIMENTAL WORK

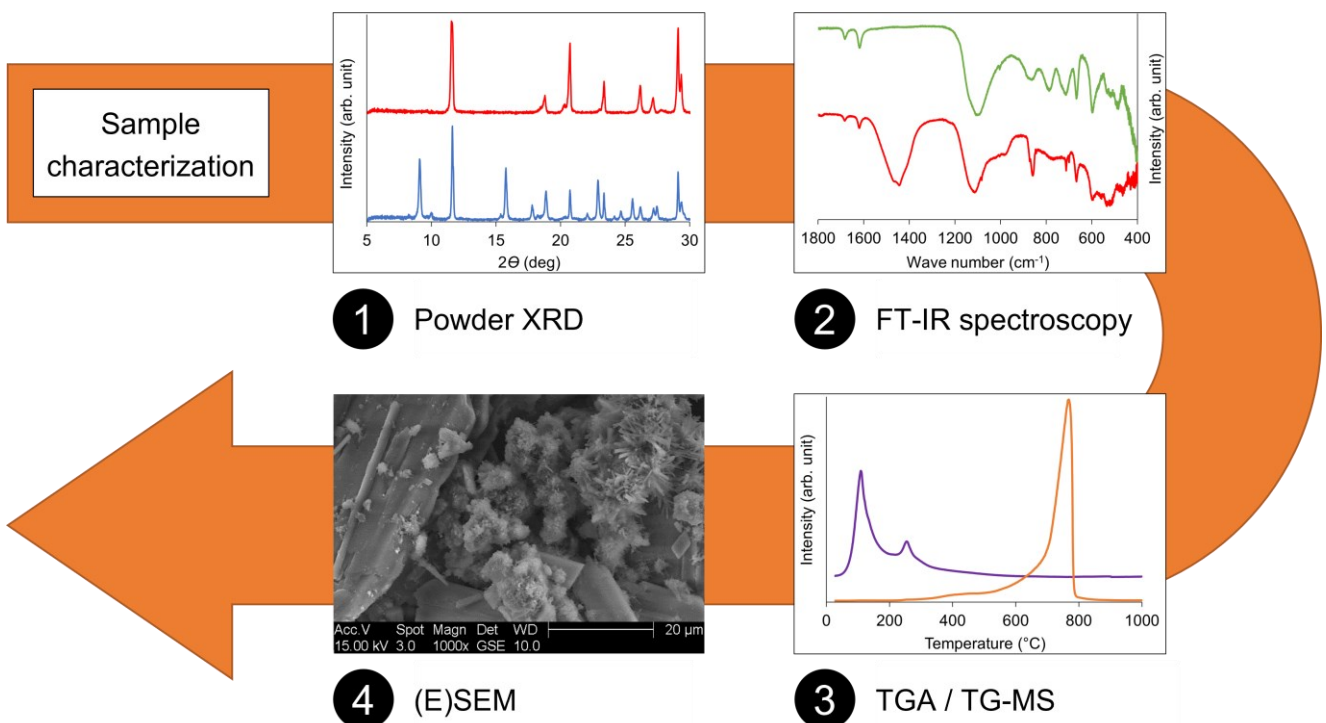


**Figure 33:** Overview of the methods used to characterize fresh and aged samples.

- ① Powder XRD is used to identify crystalline phases on the particle surface. Experiments were carried out using a Bruker AXS *D8 Advance*<sup>®</sup> instrument with Bragg-Brentano geometry. This device is fed with plastic specimen holders which creates an advantage for aging investigations. Instead of filling the holders with aged samples collected from the Plexiglas<sup>®</sup> plates, powder can be aged in the holders and measured without additional preparation. Changes of the surface composition can be more accurately determined with such an undisturbed sample. Whereas the crystalline prehydrates formed during aging on the plates could potentially sustain damage during collection and deagglomeration of the samples. The only downside to the preparation-free approach is that it does not allow for a quantitative determination the surface composition via Rietveld refinement.
- ② FT-IR spectroscopy was performed at a Bruker Optics *Vertex*<sup>®</sup> 70 instrument equipped with an attenuated total reflectance (ATR) diamond crystal. This setup is geared towards the investigation of the sample surface rather than the bulk composition. Compared to powder XRD the surface analysis is less precise, but X-ray amorphous phases can be detected. Quantitative infrared spectroscopy was discarded since the setup did not permit an exact reproduction of the contact pressure between the sample and the diamond crystal which factors into the band intensity.
- ③ TGA data were obtained from a simultaneous thermal analyzer (STA), for TG-MS experiments it was coupled with a quadrupole mass spectrometer (QMS). Thermogravimetry allows to quantitatively determine the uptake of water and carbon dioxide during aging. As the sample is slowly heated up the sorbed H<sub>2</sub>O is released and CO<sub>2</sub> is liberated from the calcination of carbonates. TGA only accounts for the total weight loss over a certain temperature range which can make it difficult to differentiate between water and CO<sub>2</sub> uptake. Coupling the TGA with mass spectrometry enables a clear distinction between H<sub>2</sub>O and CO<sub>2</sub> release by molecular weight. Furthermore, H<sub>2</sub>O and CO<sub>2</sub> releases are marked by peaks in the intensity of the ion currents

## 3.2 EXPERIMENTAL WORK

---

recorded over the course of the TG-MS measurement. This allows for the identification and quantification of individual prehydration products that release H<sub>2</sub>O at different temperatures. However, a quantitative TG-MS analysis is not possible when the decomposition temperatures are close to each other, say for ettringite and gypsum. This results in an overlap of the ion current peaks and the integration of the peak area does not yield conclusive results.

- ④ By providing images of the sample surfaces, (environmental) scanning electron microscopy (E)SEM allow for a qualitative analysis through visual identification of characteristic morphologies. Both SEM and ESEM were carried out at a *XL 30 FEG* microscope by FEI. In ESEM mode, the regular secondary electron (SE) detector was replaced with a Peltier cooling stage and a gaseous SE detector which is able to operate at low H<sub>2</sub>O pressure instead of vacuum. This helps preserving aging products that contain large amounts of water and would quickly decompose in vacuum, such as ettringite. However, since the measurement chamber is filled with water vapor, the resolution of ESEM is lower than that of SEM.

### 3.2.3.2 Examining the hydration behavior

After the characterization part, the hydration behaviors of fresh and aged samples were compared. The experiments were divided between four investigative approaches (**Figure 34**): First, the aging impact on the reactivity of binders and admixtures was determined by a time-resolved analysis of the hydration process via isothermal heat-flow calorimetry and *in situ* XRD. Second, the depletion of chemical admixtures from the liquid phase during hydration due to adsorption or precipitation was measured via total organic carbon (TOC) analysis and ultraviolet-visible (UV / Vis) spectrophotometry. Third, the concentration of free Ca<sup>2+</sup> cations in the pore solution, which is an indicator both for the dissolution of the binder and the formation of hydrates, was determined via inductively coupled plasma optical emission spectroscopy (ICP-OES). Finally, the aging impact on engineering properties of the binders was quantified by measuring the spread flow, the setting time and the compressive strength.

All samples containing cements were hydrated with deionized water obtained from a Barnstead Nanopure Diamond® water purification plant. The clinker phases were instead mixed with a solution containing 50 mmol L<sup>-1</sup> Na<sub>2</sub>SO<sub>4</sub>, 27.5 mmol L<sup>-1</sup> K<sub>2</sub>SO<sub>4</sub> and 12.5 mmol L<sup>-1</sup> KOH to simulate the alkaline environment of cement pore solution. In all experiments, samples were homogenized with a VWR VWT® 1419 vortex mixer at the start of hydration.

Regarding the time of admixture addition during hydration, in the first topic on retarders, the investigated retarders sodium gluconate and potassium pyrophosphate were dissolved in the mixing water (or in the alkali solution in case of the clinker phases). A delayed addition during hydration was not considered. The time of addition does not apply in the second topic on SLU aging, where all admixtures were dry-mixed with the TBS prior to hydration.

## 3.2 EXPERIMENTAL WORK

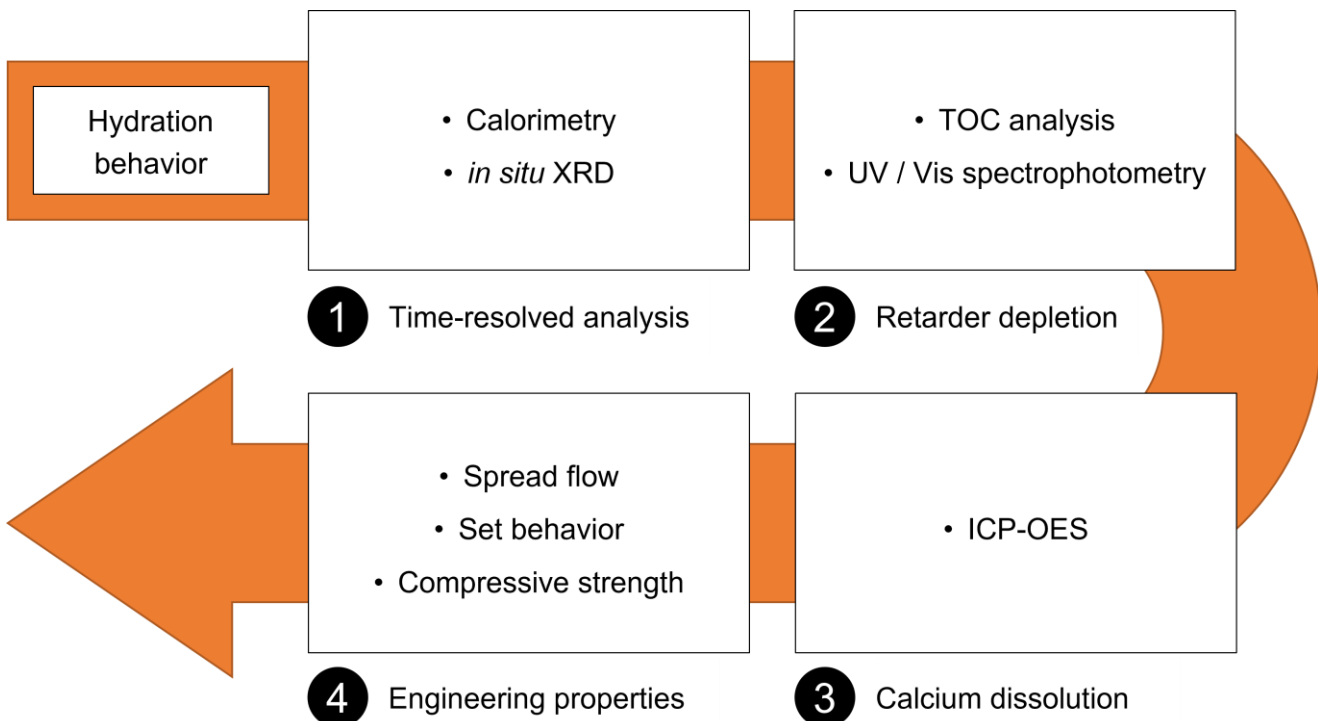


**Figure 34:** Overview of the methods used to analyze the hydration of fresh and aged samples.

- ① Isothermal heat flow calorimetry was performed using a Thermometric AB *TAM Air® 3114* device. Experiments were carried out according to DIN EN 196-11 [264] unless otherwise specified in the results. Heat flow was recorded until the measured value fell below 0.5 mW. For selected samples, a second round of measurements was performed where the hydration was terminated directly after a prominent heat flow peak. The nature of the associated hydration reaction was then determined by identifying the hydration products (except C–S–H) via powder XRD. The hydration process was also analyzed *in situ* via XRD. At the start of hydration, the sample is poured into a special specimen holder and covered with an X-ray transmittant polyimide film (Kapton®) to prevent water evaporation (**Figure 35**, right). The hydrating sample is then repeatedly scanned at a fixed time interval and the individual diffraction patterns are combined into a time-resolved measurement.

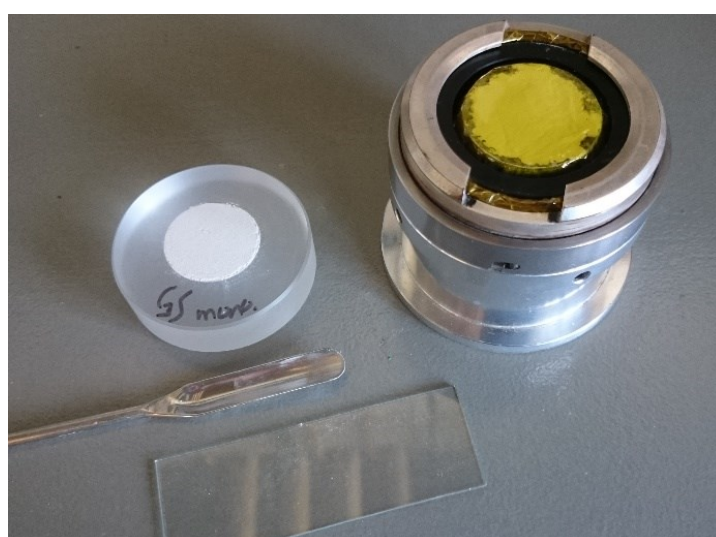


**Figure 35:** Preparation of powder XRD (left) and *in situ* XRD (right) samples.

### 3.2 EXPERIMENTAL WORK

- ② The depletion of admixtures from the liquid phase was only investigated if they had been dissolved in the mixing water / alkaline solution. These experiments were thus only performed for the first topic on the aging impact on the retarders sodium gluconate and potassium pyrophosphate. To separate the liquid phase hydrating samples were centrifuged and the supernatants passed through a polyethersulfone (PES) filter.

Liquids from samples admixed with sodium gluconate retarder were fed into an Elementar *liquiTOC*<sup>®</sup> analyzer. This instrument determines the total organic carbon (TOC) content of the sample in several steps (**Figure 36**). The liberation of purgeable organic carbon (POC) by heating the sample to 70 °C can be ignored since the retarder samples contain no volatile carbon compounds. Inorganic carbon (IC) is removed from the samples via acid catalyzed oxidation to CO<sub>2</sub>. The sample is then heated to 850 °C which results in the oxidation of the non-purgeable organic carbon (NPOC). The CO<sub>2</sub> releases associated with IC and NPOC are separately quantified with an infrared gas detector. The NPOC value of a sample containing sodium gluconate minus the NPOC of pure pore solution yields the amount of gluconate remaining in the liquid phase.

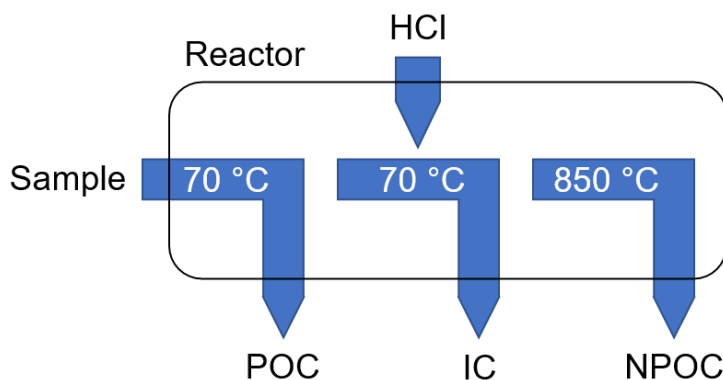
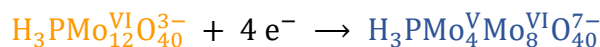
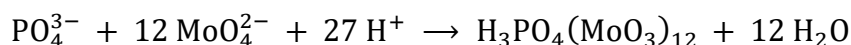


**Figure 36:** Schematic representation of the operating principle of a TOC analyzer.

Liquids from samples admixed with potassium pyrophosphate retarder first had the pyrophosphate converted to orthophosphate via acid hydrolysis. Subsequently, an ammonium molybdate solution with potassium antimony(III) oxide tartrate was added as well as L-(+)-ascorbic acid. Molybdic acid is released from ammonium heptamolybdate tetrahydrate in the presence of the potassium antimony(III) oxide tartrate and forms phosphomolybdic acid with the orthophosphate. In the presence of the reducing agent L-(+)-ascorbic acid the phosphomolybdic acid changes from a weak yellow color to a strong blue one, the so-called 'molybdenum blue' [265].



The intensity of the blue color is proportional to the amount of orthophosphate / pyrophosphate in the sample. The amount of the retarder remaining in the liquid phase can thus be photometrically determined. Corresponding measurements were carried out at a wavelength of 880 nm using an Agilent *Cary*<sup>®</sup> 50 UV / Vis spectrophotometer.

### 3.2 EXPERIMENTAL WORK

---

- ③ Inductively coupled plasma optical emission spectrometry (ICP-OES) was used to determine the concentration of free  $\text{Ca}^{2+}$  cations in pore solution. Liquid was again obtained by centrifugation of hydrating samples and filtration of the supernatants. Measurements were carried out at an Agilent 725 device. There, the liquid samples are sprayed into ionized argon plasma produced by a strong electromagnetic field. The hot plasma atomizes the sample contents and causes the atoms to repeatedly lose and recombine with electrons. The radiation hereby emitted is measured by a charge-coupled detector. The radiation wavelength is different for each chemical element, allowing for a precise analysis of the sample composition. ICP-OES is not as widespread in the analytical chemistry of construction and building materials as atomic absorption spectroscopy (AAS). The use of AAS was also specified in the original research proposal for this project. The switch to ICP-OES was made since the AAS is prone to interference between  $\text{Ca}^{2+}$  and  $\text{Al}^{3+}$  [266]. This is not a significant issue in Portland cement where the  $\text{Al}_2\text{O}_3$  to  $\text{CaO}$  ratio is comparatively small. However, when the  $\text{C}_3\text{A}$  clinker phase or the CAC are examined, the results for free  $\text{Ca}^{2+}$  concentrations would be inconclusive if AAS was used.
- ④ The aging impact on the engineering properties of binders was investigated by comparing the spread flow, setting time and compressive strength development of fresh and aged samples. Respective measurements are usually carried out in strict adherence to the standards laid out by the European Committee for Standardization, ASTM International and others. For this project, the experimental setups as prescribed by the standards had to be modified for smaller sample sizes. This was necessary due to the limiting factors in the supply of aged material: The Plexiglas® plates were filled with just 50.0 g of powder at once, only six plates could be simultaneously stored in the climate box and the exposure lasted for up to 14 days.

Another bottleneck concerns the clinker phases  $\text{C}_3\text{A}$  and  $\text{C}_3\text{S}$  whose availability was further reduced by the necessity to obtain a narrow particle size distribution which matches that of the OPC. As a result, the clinker phases were not included in the investigation of the engineering properties. For the OPC and SLU samples the experimental setups were modified as described in the following:

Spread flow tests were conducted based on DIN EN 12706-12 [267]. This standard stipulates that a smooth-bore metal tube is filled with the binder paste. After the tube is lifted and the paste has flown out, the diameter of the spread-out paste is measured. In DIN EN 12706-12 the tube is specified to have an inner diameter of 30 mm and a height of 50 mm. In this project a smaller tube with an inner diameter of 14 mm and a height of 25 mm was used. This reduced the required amount of binder at a w/b ratio of 0.50 to 6.5 g per measurement.

The investigation of the setting process followed DIN EN 196-3 [268] which prescribes the use of a Vicat apparatus (**Figure 37**). A steel load tipped by a needle is repeatedly lowered into a rubber Vicat ring filled with the binder paste. During setting the penetration depth of the needle decreases as the hydrating binder increasingly supports the weight of the load. The Vicat ring, a cone with an upper inner diameter of 70 mm, a lower inner diameter of 80 mm and a height of 40 mm, was replaced by a cylindrical glass vessel with an inner diameter of 15 mm and a height of 20 mm. At w/b ratios between 0.50 and 0.60, the required amount of binder per measurement could thus be lowered from 400 g to 15 g. To compensate for the smaller sample size, the steel load was replaced with an aluminum one, reducing the weight of the load from 300 g to 100 g.

### 3.2 EXPERIMENTAL WORK



**Figure 37:** Vicat apparatus with glass vessel holding the hydrating sample.

The strength of hardened binders was tested based DIN EN 196-1 [269]. This standard describes compressive and tensile strength measurements of prismatic specimens cast from mortar (at a weight ratio of 1 : 3 between binder and aggregate). The mold specified in DIN EN 196-1 yields three specimens, each of which are 160 mm in length, 40 mm in width and 40 mm in height. In this project a custom mold (**Figure 38**) was used which produces three prisms 40 mm long, 15 mm wide and 15 mm high. To compensate for the reduced strength of the smaller prisms they were cast from pure binder instead of mortar. Even so, the amount of binder required for three prisms fell from 450 g to 45 g at w/b ratios of 0.50 and 0.55. Only the compressive strength was determined, the small prisms are not compatible with the tensile strength measurement equipment.

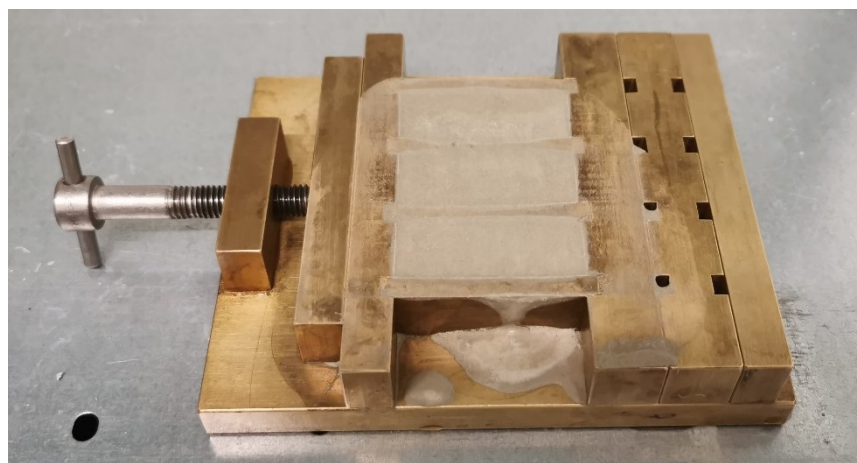


**Figure 38:** Preparation of prisms from hydrated paste for compressive strength tests.



## 4 Results and discussion

### 4.1 Outline

The presentation of the project results in this thesis follows the associated scientific publications (**Figure 39**). The results of the investigative work were published in three articles in scientific journals (all peer-reviewed) and three contributions to scientific conferences (two peer-reviewed). The first project topic on the aging impact on retarder performance produced two journal articles, one about clinker phases and the other about Portland cement. The second topic on the aging of dry-mixes was published in a single journal article. Part of the project results presented at the conferences found no room in the journal articles. For this reason, the conference contributions (as published in the proceedings) are presented alongside the journal articles in this thesis. From the three contributions, two belong to the first topic on retarder performance and include results for both the clinker phases and Portland cement. They have similar contents and differ only in language, one is in German, the other in English. The last contribution is about the topic on dry-mix aging.

In the following, each of these six publications is reprinted as published in the conference proceedings or scientific journal. They are sorted by project topic. An overview of the contents is prepended to each journal article. Both topics follow with a section on further investigations which contains the conference contributions among other additional results and findings related to the project.

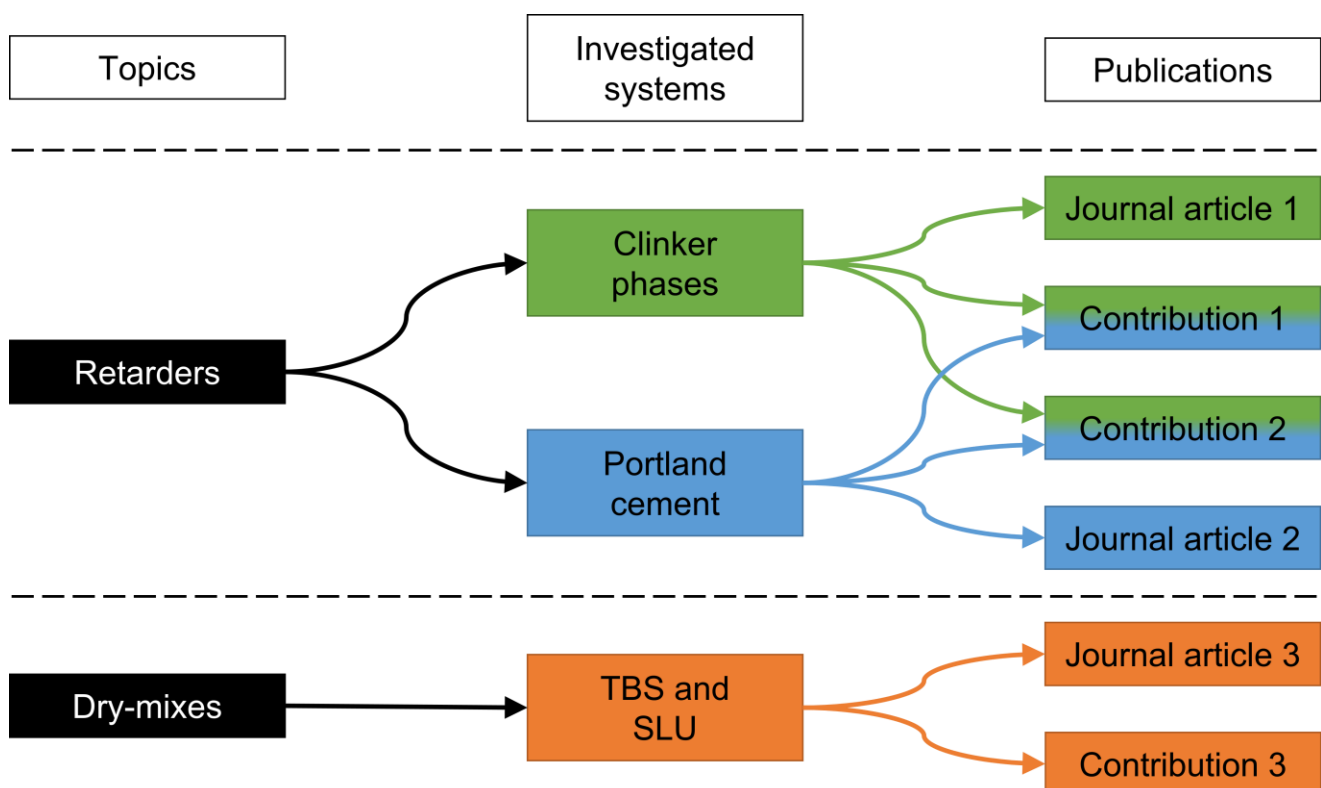


**Figure 39:** Overview of the scientific publications associated with each project topic.

## 4.2 Topic 1: Impact of aging on retarder performance in clinker phases and Portland cement

### 4.2.1 Journal article 1: Clinker phase $C_3A$

#### 4.2.1.1 Content overview for journal article 1

The first journal article solely contains results on the  $C_3A$  clinker phase while the  $C_3S$  investigations were omitted from this publication. The main reason for this decision was that the two aluminate polymorphs investigated in the project, cubic and orthorhombic  $C_3A$ , were found to display vastly different hydration behaviors after aging with gypsum. As described in chapter 2.4, earlier studies [248, 252, 253, 260] had discovered that orthorhombic  $C_3A$  sorbs  $H_2O$  faster and at lower humidities than cubic  $C_3A$  and that the formation of ettringite during prehydration causes deviations in setting time and flowability of Portland cement [243–246]. However, the hydration behavior of the aged  $C_3A$  polymorphs had not been systematically investigated yet. For this reason, a part of the first journal article was dedicated to the mechanisms of aged  $C_3A$  hydration before the aging impact on sodium gluconate and potassium pyrophosphate was discussed. The following overview of the article's contents is divided into 4 parts for a better understanding (**Figure 40**).

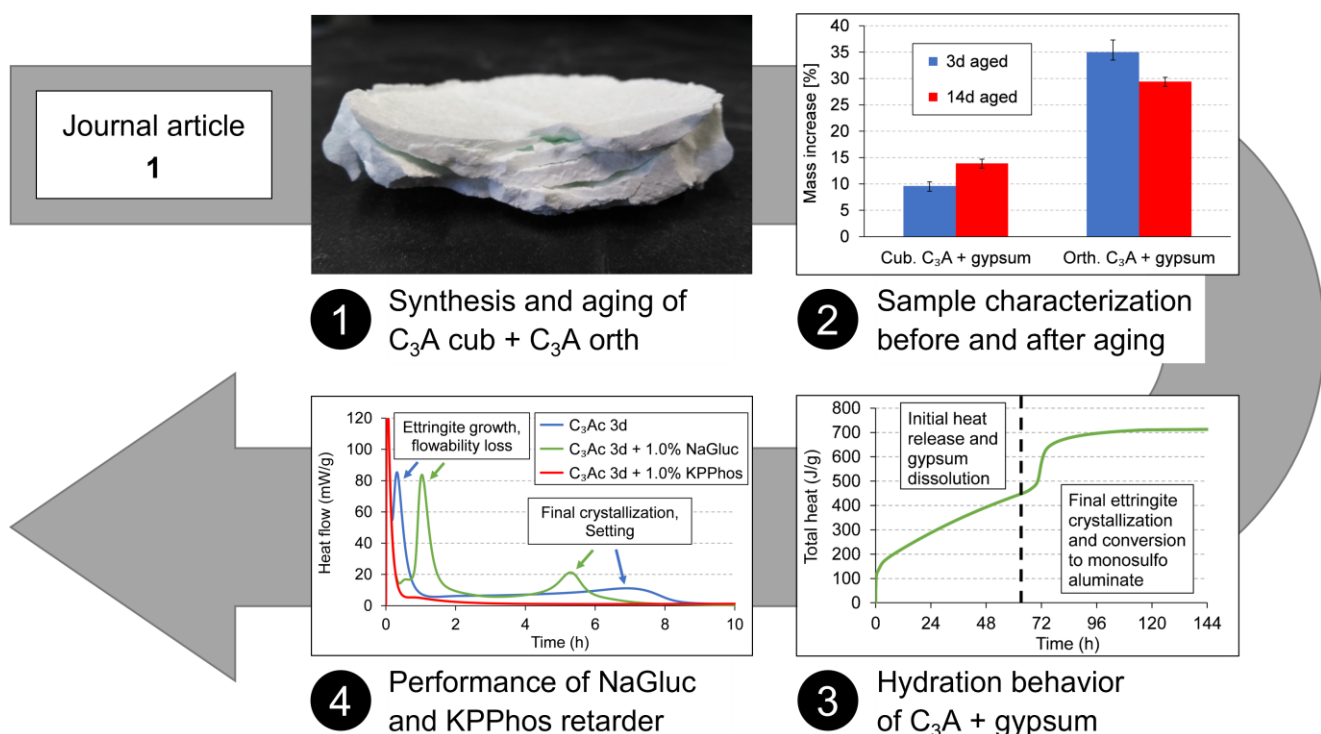


**Figure 40:** Overview of journal article 1 on the aging of the  $C_3A$  clinker phase.

- ① The  $C_3A$  polymorphs were successfully synthesized as described in chapter 3.2.1.1. Cubic and orthorhombic  $C_3A$  were each mixed with gypsum at a 1: 1 ratio by weight and exposed to water vapor and atmospheric  $CO_2$  at 35 °C and 90% RH. The exposure duration was either 3 days (designated 'short-term' aging) or 14 days (designated 'long-term' aging).

- ② After aging, C<sub>3</sub>A / gypsum blends were weighed. As expected based on previous studies, all samples had increased in weight due to H<sub>2</sub>O and CO<sub>2</sub> uptake. For cubic C<sub>3</sub>A, the weight gain over 14 days was found to be only ~40% higher than that over 3 days, signifying that the strongest increase occurs early in aging. Also as anticipated, samples with orthorhombic C<sub>3</sub>A had taken up more H<sub>2</sub>O and CO<sub>2</sub> than those with cubic C<sub>3</sub>A both after 3 and after 14 days of aging. However, the total mass increase of the orthorhombic C<sub>3</sub>A / gypsum blend over 14 days was lower than that over 3 days, meaning that part of the gained weight is lost again over the course of long-term aging.

These observations could be elucidated by sample characterization via powder XRD, FT-IR, ESEM and TG-MS. In accordance with [260], when aged with gypsum both cubic and orthorhombic C<sub>3</sub>A formed ettringite as the sole initial aging product. The ettringite then decomposed due to the atmospheric CO<sub>2</sub>, the decomposition products could be identified as CaCO<sub>3</sub>, Al(OH)<sub>3</sub> and gypsum. It was discovered that orthorhombic C<sub>3</sub>A not only forms ettringite faster during aging than cubic C<sub>3</sub>A, but that the ettringite decomposition was further advanced as well, especially after long-term aging. Ettringite incorporates large amounts of H<sub>2</sub>O into its crystal structure which is released during the decomposition. This is why the total weight increase of orthorhombic C<sub>3</sub>A with gypsum over 3 days is higher than that over 14 days. The ettringite decomposition also explains why the weight growth of cubic C<sub>3</sub>A with gypsum – albeit continuous – becomes much slower towards long-term aging.

- ③ The hydration behaviors of fresh and aged C<sub>3</sub>A / gypsum blends were compared with calorimetry and XRD. The fresh samples first hydrated to ettringite which was then partially converted to monosulfoaluminate. A mix of trisulfate and monosulfoaluminate as the final hydration product was to be anticipated since the 1 : 1 ratio of C<sub>3</sub>A and gypsum by weight corresponds to a 1 : 1.57 molar ratio of aluminate and sulfate. As expected, the ettringite formation proceeded at a stable rate until the sulfate had been depleted, at this point a peak in heat release marked the final ettringite crystallization and the onset of the conversion to monosulfoaluminate.

Aging significantly accelerated the hydration of C<sub>3</sub>A / gypsum blends, revealing a much higher initial hydration rate. This is attributed to a seeding effect of the ettringite crystallites formed on the C<sub>3</sub>A / gypsum surfaces during aging. In contrast to the fresh samples, during hydration the sulfate dissolution phase and the final ettringite crystallization were not clearly separated after aging. In aged cubic C<sub>3</sub>A / gypsum blends the heat release associated with these reactions partially overlapped. In aged orthorhombic C<sub>3</sub>A / gypsum blends they occurred almost simultaneously. This signifies that after aging the final crystallization and conversion of ettringite to monosulfoaluminate is less (cubic C<sub>3</sub>A) or essentially no longer (orthorhombic C<sub>3</sub>A) dependent on the ion saturation of the pore solution. Rather, ettringite crystallites formed during aging can immediately continue to grow on contact with the mixing water.

- ④ The accelerating effect of aging on the hydration of C<sub>3</sub>A / gypsum made the investigation of its impact on retarder performance all the more relevant. The impact of 1.0% bwob (by weight of binder, here C<sub>3</sub>A with gypsum) sodium gluconate (NaGluc) or potassium pyrophosphate (KPPhos) dissolved in the mixing water was studied with calorimetry, XRD and depletion experiments (TOC and UV / Vis spectrophotometry).

## 4.2 TOPIC 1: AGING IMPACT ON RETARDER PERFORMANCE

---

The addition of NaGluc to the hydration of aged cubic C<sub>3</sub>A / gypsum reduced the seeding effect and resulted in a more pronounced separation of the gypsum dissolution and the final ettringite crystallization. However, it also shortened the dissolution phase overall, leading to an even earlier final crystallization. This signifies that the retarder NaGluc actually acts as an accelerator in this specific regard. As described in chapter **2.2.2.3** on C<sub>3</sub>A hydration in the presence of sulfate, ettringite precipitation at the start of the hydration has a decelerating effect, most likely due to the formation of a diffusion barrier against water access to the clinker and / or the poisoning of C<sub>3</sub>A dissolution sites. After aging, the seeding effect substantially increases the early ettringite formation. Based on the depletion of the retarder from the liquid phase it is assumed that the NaGluc adsorption competes with the ettringite precipitation in covering the particle surfaces. While it slows the dissolution initially (reduction of the seeding effect), NaGluc adsorption also weakens the diffusion barrier / poisoning and leads to an overall earlier sulfate depletion / final ettringite crystallization. The effect is similar to that of a “delayed accelerator” as mentioned in chapter **2.3.3**.

KPPhos had a much greater impact on the hydration of aged C<sub>3</sub>A / gypsum than NaGluc. The seeding effect was effectively suppressed, and the hydration progressed very slowly. This behavior is attributed to the strong ability of KPPhos to precipitate free Ca<sup>2+</sup> (solutions of calcium became turbid after the addition of KPPhos which was not observed for NaGluc). Thus, after dissolving the Ca<sup>2+</sup> is immediately removed by the pyrophosphate which stalls the growth of the ettringite seeds due to the lack of calcium and the poisoning of growth sites by the calcium phosphate precipitates.

**4.2.1.2 Reprint of journal article 1**

**Impact of aging on the hydration of tricalcium aluminate ( $C_3A$ ) / gypsum blends and  
the effectiveness of retarding admixtures**

F. A. Hartmann, J. Plank

*Zeitschrift für Naturforschung B*, 75 (8), 2020, 739–753

<https://doi.org/10.1515/znb-2020-0087>

Reprinted with permission from De Gruyter

Florian Andreas Hartmann and Johann Plank\*

# Impact of aging on the hydration of tricalcium aluminate ( $C_3A$ )/gypsum blends and the effectiveness of retarding admixtures

<https://doi.org/10.1515/znb-2020-0087>

Received May 19, 2020; accepted July 4, 2020; published online August 22, 2020

**Abstract:** In the production of concrete from cement powder and water, setting behavior of the slurry is determined by the formation of ettringite ( $Ca_6Al_2(OH)_{12} \cdot (SO_4)_3 \cdot 26 H_2O$ ) from tricalcium aluminate ( $Ca_9Al_6O_{18}$ , abbreviated  $C_3A$ ) and gypsum ( $CaSO_4 \cdot 2 H_2O$ ). Due to the high reaction potential of cement and water, premature hydration can occur after unintentional exposure to moisture. Model binary mixtures of  $C_3A$  and gypsum stored at 90% relative humidity and 35 °C produced ample amounts of ettringite, which subsequently reacted with atmospheric  $CO_2$  to  $CaCO_3$ ,  $Al(OH)_3$  and gypsum. Investigated were the two main polymorphs of tricalcium aluminate encountered in cement, pure, cubic  $C_3A$  and orthorhombic  $C_3A$  in which calcium is partially substituted by sodium or potassium. Alkali substituted  $C_3A$  converted to ettringite faster and more completely than pure  $C_3A$ . Ettringite from prehydration caused a seeding effect, which promotes crystal growth and accelerates bulk hydration of the  $C_3A$ /gypsum mixtures. Set retarders commonly applied in cement were dissolved in the mixing water prior to hydration to investigate their ability to counteract this acceleration. Sodium gluconate merely delayed the crystal growth but does not prolong the hydration process overall. Potassium pyrophosphate retarded much more effectively by suppressing the seeding effect via removal of calcium ions from the hydration reaction.

**Keywords:** calcium aluminates; calcium silicates; cement aging; hydration; prehydration; retarder.

\*Corresponding author: Johann Plank, Chair for Construction Chemistry, Technische Universität München, Lichtenbergstraße 4, 85748 Garching bei München, Germany,  
E-mail: sekretariat@bauchemie.ch.tum.de. <https://orcid.org/0000-0002-4129-4784>

Florian Andreas Hartmann, Chair for Construction Chemistry, Technische Universität München, Lichtenbergstraße 4, 85748 Garching bei München, Germany,  
E-mail: florian.a.hartmann@tum.de. <https://orcid.org/0000-0002-0056-5242>

## 1 Introduction

Cementitious building materials are not inert during the period between manufacture and application at the job site. Their chemical reaction potential toward atmospheric moisture and carbon dioxide in combination with strong hygroscopicity may lead to aging of the cement. Premature water uptake results in an overgrowth of the cement particles with hydration products such as ettringite and calcium silicate hydrates. Such “prehydration” can negatively affect workability, set behavior and strength development of the cementitious material [1–6]. Furthermore, the interactions between cement and admixtures such as superplasticizers, accelerators and water retention agents were reported to change significantly after aging, ranging from variations of dosages required to actual inversion of the intended effect [7–10].

Improper storage and handling of cementitious materials at high temperature and high humidity conditions are commonly known causes for prehydration. But cement aging can occur already as early as during manufacturing. Firstly, during the clinker milling water is released from the interground set control agent gypsum due to the elevated temperature. Even worse, water is often injected into the mill to control the temperature increase. Secondly, during cement storage in silos temperatures of ~80 °C can occur which results in additional water release from the gypsum [11].

Cement hydration is not a single process, and neither is prehydration. Cement is comprised of various constituents, with the main components being the clinker phases. These include the calcium silicates, namely alite ( $Ca_3OSiO_4$ ,  $C_3S$ ) and belite ( $Ca_2SiO_4$ ,  $C_2S$ ), the tricalcium aluminate ( $Ca_9Al_6O_{18}$ ,  $C_3A$ ) and the ferrite phase ( $Ca_4Al_{4-x}Fe_xO_{10}$ ,  $\sim C_4AF$ ). All these phases exhibit different reactivities in water [12]. Thus, to assess and understand cement aging and prehydration, it is necessary to investigate the clinker phases individually.

Previous studies demonstrated that individual cement constituents react differently toward atmospheric moisture. Generally, the clinker phases containing aluminate absorb water faster and at lower relative humidities (RH) than the silicates [13, 14]. Using a sorption balance, Dubina

et al. [15] determined the threshold RH values at which the clinker phases begin to absorb water for C<sub>3</sub>S at 63%, C<sub>2</sub>S at 64%, cubic C<sub>3</sub>A (C<sub>3</sub>A<sub>c</sub>) at 80%, orthorhombic C<sub>3</sub>A (C<sub>3</sub>A<sub>o</sub>) at 55%, and C<sub>4</sub>AF at 78%. These results confirm an earlier report that C<sub>3</sub>A<sub>o</sub> is much more prone to prehydration than C<sub>3</sub>A<sub>c</sub> [16]. The higher water uptake of C<sub>3</sub>A<sub>o</sub> was found out to be predominantly owed to physisorption while C<sub>3</sub>A<sub>c</sub> mainly reacted chemically with moisture to form ettringite [17].

The distinction between the two C<sub>3</sub>A polymorphs is important since both are commonly encountered in cement. During the calcination of industrial clinkers, C<sub>3</sub>A may have incorporated various foreign ions [12, 18–20]. The most significant ones are K<sup>+</sup> and Na<sup>+</sup>, due to their ability to change the C<sub>3</sub>A crystal structure by substitution. For example, at a sodium oxide content of 3.7–4.6 wt%, the orthorhombic polymorph is preferred while below this value, cubic C<sub>3</sub>A is formed [21]. C<sub>3</sub>A<sub>o</sub> is frequently referred to as “substituted” C<sub>3</sub>A, and the cubic polymorph as “pure” C<sub>3</sub>A, although in industrial cements even C<sub>3</sub>A<sub>c</sub> always contains minor amounts of K<sub>2</sub>O/Na<sub>2</sub>O (0–3.7 wt%). Mixtures of both polymorphs are common, with their relative shares depending on the alkali content in the feed.

Due to the presence of set control agents (CaSO<sub>4</sub> · n H<sub>2</sub>O), the main hydration product of C<sub>3</sub>A in cement is ettringite (Ca<sub>6</sub>Al<sub>2</sub>(OH)<sub>12</sub> · (SO<sub>4</sub>)<sub>3</sub> · 26 H<sub>2</sub>O). Thus, to simulate the conditions in actual cement when studying C<sub>3</sub>A prehydration a source of sulfate needs to be present. Earlier studies have revealed that in the presence of sulfates both C<sub>3</sub>A polymorphs are more reactive toward moisture than in the absence of sulfate, and that C<sub>3</sub>A<sub>o</sub> absorbed more water than C<sub>3</sub>A<sub>c</sub> [17, 22]. Furthermore, it was demonstrated that a binary mixture of C<sub>3</sub>A and β-CaSO<sub>4</sub> · 0.5 H<sub>2</sub>O produces ettringite as the sole reaction product, and that such ettringite formation occurs via capillary condensation and the formation of liquid water films in which both phases dissolve and then react to ettringite [17].

In a subsequent study, the dispersing effectiveness of various kinds of superplasticizers (naphthalene sulfonate and several polycarboxylates) on prehydrated C<sub>3</sub>A/gypsum mixtures was investigated [10]. There, an increased fluidizing effect was found which became weaker at prolonged exposure times, and after 14 days of aging none of the superplasticizers were able to disperse the binary mixture anymore.

However, so far none of the previous studies has elucidated the differences between the individual C<sub>3</sub>A polymorphs (cubic or orthorhombic) relative to their hydration behavior before and after aging with calcium sulfate. Therefore, here we report on C<sub>3</sub>A<sub>c</sub> and C<sub>3</sub>A<sub>o</sub> mixtures with gypsum exposed to high atmospheric moisture at elevated temperature for specific periods of time. After

aging, the C<sub>3</sub>A/gypsum mixtures were characterized using powder X-ray diffraction (XRD), Fourier-transform infrared spectroscopy (FT-IR), mass spectrometry-coupled thermogravimetry (TG-MS) and ESEM imaging. The hydration behavior of the fresh and aged mixtures was investigated via isothermal heat flow calorimetry and *in situ* XRD.

In the second part of the study, the effectiveness of two different retarders in the hydration of prehydrated binary mixtures was investigated. Sodium gluconate (NaC<sub>6</sub>H<sub>11</sub>O<sub>7</sub>) and potassium pyrophosphate (K<sub>4</sub>P<sub>2</sub>O<sub>7</sub>) were chosen as retarders because of their quite different working mechanisms. Gluconate retards by adsorbing onto the clinker phases and hydrates, thereby hindering both dissolution and crystal growth [23]. Pyrophosphate chelates calcium ions and forms a layer of calcium pyrophosphate on the particle surface. This acts as a barrier for the access of water and the dissolution of ions from the clinker surface, while already dissolved calcium is precipitated and thus not available for the formation of hydration products [24, 25]. The consideration behind using retarders that rely on different working mechanisms was to elucidate which one proved more effective in aged C<sub>3</sub>A/gypsum mixtures and whether retarders could offset the negative impact of prehydration. Such knowledge may help to select the most appropriate retarder for applications in which prehydration during storage or transport is experienced. The retarders were dissolved in the liquid phase prior to mixing with the prehydrated C<sub>3</sub>A/gypsum blends. Retarder depletion from solution during hydration was verified via total organic carbon (TOC) determination (gluconate) and UV-vis spectrophotometry (pyrophosphate).

## 2 Experimental section

### 2.1 Preparation of C<sub>3</sub>A<sub>c</sub> and C<sub>3</sub>A<sub>o</sub>

C<sub>3</sub>A was synthesized from precipitated CaCO<sub>3</sub> (Merck EMSURE®, 98.5+%) and Al<sub>2</sub>O<sub>3</sub> (Nabaltec NABALOX® NO 784, 99.7%) via high temperature solid state reaction based on a literature report [26]. Initial usage of natural CaCO<sub>3</sub> had led to a reddish color of the otherwise bright white C<sub>3</sub>A product probably caused by impurities. This was avoided by using the precipitated CaCO<sub>3</sub>, however due to its larger and more spherical particles, the synthesized C<sub>3</sub>A had a comparatively soft texture, thus exhibiting a rather broad particle size distribution (Figure 1) after cooling to ambient and milling. Therefore, prior to synthesis, the precipitated CaCO<sub>3</sub> was ground in a planetary mono mill (Fritsch Pulverisette 6) twice for 30 min at 300 rpm to obtain harder C<sub>3</sub>A during sintering. The high temperature synthesis was

carried out in chamber furnaces (Nabertherm LH 15/14 and LHT 08/16) using crucibles (Heraeus, Ø 70 mm, height 40 mm) made from a platinum alloy containing 10% rhodium.

To synthesize pure, cubic C<sub>3</sub>A, stoichiometric quantities of CaCO<sub>3</sub> and Al<sub>2</sub>O<sub>3</sub> were sintered at 1400 °C for 6 h, then cooled to ambient temperature. The clinker was then ground in the planetary mono mill. After a second firing at 1400 °C for 6 h the intermediary products mayenite and free lime had disappeared as evidenced by the powder XRD patterns (Figure 2), and pure C<sub>3</sub>A<sub>c</sub> was obtained.

Alkali substituted, orthorhombic C<sub>3</sub>A was prepared by introducing Na<sup>+</sup> into the structure via addition of NaNO<sub>3</sub> (Merck EMSURE®, 99.5+%) before sintering. Significant evaporation of Na<sub>2</sub>O was observed from 1250 °C upwards, resulting in a mixture of cubic and orthorhombic C<sub>3</sub>A. When synthesized below this temperature, C<sub>3</sub>A<sub>o</sub> again exhibited a soft texture which resulted in a higher share of

smaller particles and a broader particle distribution after milling compared to C<sub>3</sub>A<sub>c</sub>. This would have made comparisons of the two polymorphs impossible regarding hydration behavior and interaction with the retarders. To avoid this, CaCO<sub>3</sub>, Al<sub>2</sub>O<sub>3</sub> and NaNO<sub>3</sub> were first calcined at 1000 °C, then finely ground ( $d_{50} < 5 \mu\text{m}$ ) at ambient temperature before sintering to yield C<sub>3</sub>A<sub>o</sub> of a harder texture. Maximum temperature was limited to 1300 °C, the crucibles were covered with platinum lids and NaNO<sub>3</sub> quantities were increased to a theoretical content of 7.0 wt% Na<sub>2</sub>O before loss in order to account for evaporation. By doing so, pure C<sub>3</sub>A<sub>o</sub> was obtained when the excess of NaNO<sub>3</sub> was exhausted after sintering twice at 1300 °C for 6 h as confirmed by powder XRD (Figure 2).

After sintering, both C<sub>3</sub>A<sub>c</sub> and C<sub>3</sub>A<sub>o</sub> polymorphs were ground in the planetary mono mill to a particle size ( $d_{50} = 16 \mu\text{m}$ ,  $d_{90} = 46 \mu\text{m}$ ) similar to that of a commercial cement sample which was used in parallel aging studies (HeidelbergCement CEM I 52.5 N Milke®). Particle sizes

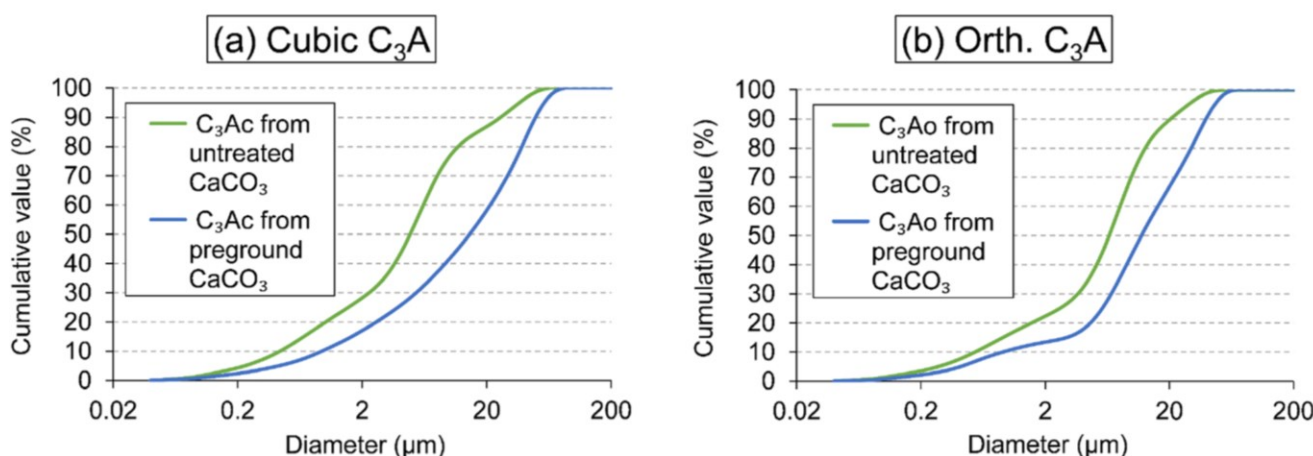


Figure 1: Comparison between particle size distributions of the C<sub>3</sub>A polymorphs with and without grinding CaCO<sub>3</sub> before synthesis.

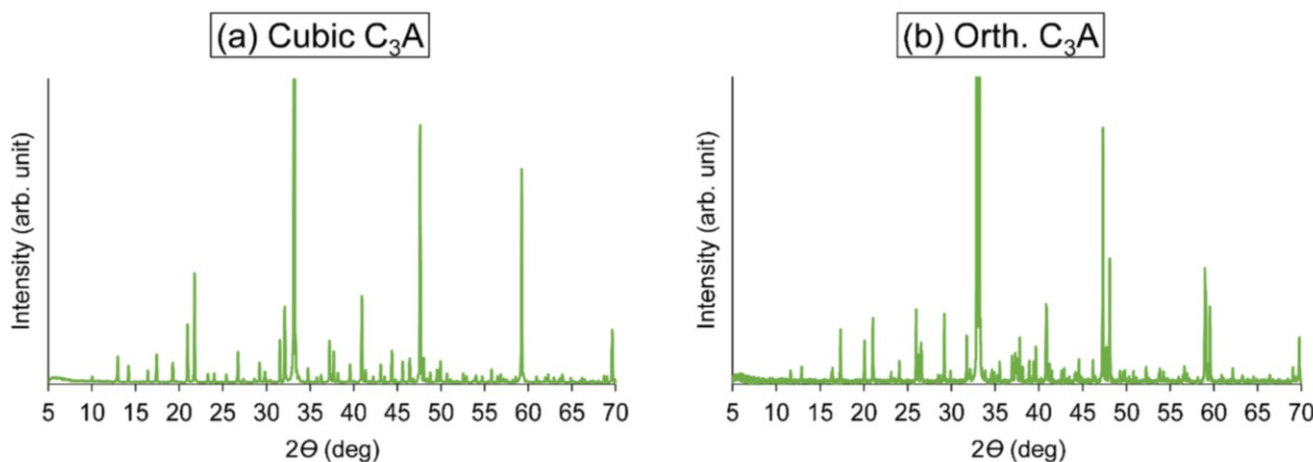


Figure 2: X-ray diffraction patterns of cubic (left) and orthorhombic (right) C<sub>3</sub>A phases as prepared, shown in the 2θ range of 5–70°.

were determined by laser granulometry (Cilas 1064) using isopropyl alcohol as dispersion medium and ultrasound to disperse particle agglomerates.

## 2.2 Aging of C<sub>3</sub>A polymorphs with gypsum

Gypsum (Merck EMSURE®, 99.0+%) was added to each of the two C<sub>3</sub>A polymorphs at a 1 : 1 ratio by weight following earlier investigations [10]. Dry intermixing was performed for 2 h in a Heidolph Reax® 20/4 overhead shaker. The fresh mixtures were spread out in 50.0 g portions on 135 × 60 cm Plexiglas® plates to expose as much surface as possible at a similar layer thickness (~0.2 mm) for all samples during aging. The mixtures were then aged in a custom-built climate box for 3 or 14 days at 90 ± 5% RH, passing the threshold for both C<sub>3</sub>A<sub>c</sub> and C<sub>3</sub>A<sub>o</sub> to sorb water, and 35 ± 2 °C. After exposure, the samples were collected and weighed with a Sartorius CP 423 S laboratory scale to monitor changes in sample mass resulting from aging.

## 2.3 Characterization of aged samples

The formation of prehydration products during the aging process was monitored with powder XRD. For this purpose, plastic XRD holders were filled with the fresh mixtures and aged together with the plates. After storage for 3 and 14 days in the climate box, the samples could thus be measured without any additional preparation. By doing so, damage to the particle surfaces prior to XRD analysis was prevented. All XRD measurements in this study were performed on a Bruker AXS D8 Advance® instrument with Bragg–Brentano geometry and a CuK $\alpha$  source. For characterization of the aging products, measurements were made in the 2 $\theta$  range of 5–70° in steps of 0.008° at 30 kV accelerating voltage and 35 mA irradiation intensity with an exposure time of 0.5 s per step.

FT-IR analysis was carried out on a Bruker Optics Vertex® 70 instrument equipped with an attenuated total reflection (ATR) diamond crystal. During each measurement, the sample was scanned 15 times from 400 to 4000 cm<sup>-1</sup> at a resolution of 0.24 cm<sup>-1</sup>.

TG-MS data were collected from a Netzsch simultaneous thermal analyzer (STA) 409 PC Luxx® coupled with a Netzsch quadrupole mass spectrometer (QMS) 403 Aëlos® Quadro. The samples were heated from 20 to 900 °C at a constant rate of 10 K/min.

Environmental scanning electron microscopy (ESEM) was performed on a FEI XL 30 FEG instrument using a Peltier

cooling stage and a gaseous secondary electron (GSE) detector. Images of uncoated aged samples were taken at 1 mbar H<sub>2</sub>O pressure and an accelerating voltage of 15 kV.

## 2.4 Hydration of C<sub>3</sub>A/gypsum

### 2.4.1 Heat flow calorimetry

The heat flow during hydration of fresh and aged C<sub>3</sub>A/gypsum mixtures at 20.0 °C was recorded by heat flow calorimetry using a Thermometric AB TAM Air® 3114 isothermal calorimeter. In each experiment, 2.00 g of powder were weighed into a 10 mL glass vial. To simulate the alkaline and ionic environment existing in cement pore solution, hydration was performed in a solution containing 50 mmol L<sup>-1</sup> Na<sub>2</sub>SO<sub>4</sub> (VWR Analar NORMAPUR®, 98.5+%), 27.5 mmol L<sup>-1</sup> K<sub>2</sub>SO<sub>4</sub> (Merck EMSURE®, 99.0+%) and 12.5 mmol L<sup>-1</sup> KOH (VWR Analar NORMAPUR®, 85.0+%) based on a recipe for synthetic cement pore solution (SCPS) [27], but without adding CaSO<sub>4</sub>. The alkali salts were dissolved in deionized water obtained from a Barnstead Nanopure Diamond® water purification system. The alkaline solution was added at a ratio of water to binder (w:b) of 1.0 before the vial was sealed with a crimped aluminum cap. The sample was then homogenized at maximum speed for 120 s using a VWR VWT® 1419 vortex mixer and subsequently placed into the measurement chamber. The hydration reaction was usually recorded until the heat flow reached zero. Samples were also removed from the calorimeter at earlier stages in order to characterize the products of individual stages of the hydration process by XRD analysis (2 $\theta$  range 5–50°, 0.034°/step, 0.4 s/step, 30 kV, 35 mA).

### 2.4.2 Retarders

The sodium gluconate (Merck EMSURE®, 98.0+%) and potassium pyrophosphate (Sigma-Aldrich, 97%) retarders were dissolved in the alkaline solution prior to conducting the hydration experiment. CaSO<sub>4</sub> had to be omitted from the SCPS recipe since it led to turbidity when preparing the pyrophosphate solution due to premature precipitation of calcium pyrophosphate. No such turbidity occurred when dissolving gluconate, underlining the differences in retarder working mechanisms. The retarders were applied at dosages of 1.0% by weight of binder (bwob). This high dosage is necessary since the investigated model binder system consists wholly of the highly reactive combination of C<sub>3</sub>A phase and sulfate whereas in Portland cement these components in most cases account only for up to ~20 wt% of the binder.

### 2.4.3 *In situ* XRD

About 2.20 g of C<sub>3</sub>A/gypsum in alkaline solution (with or without retarder) at a w : b ratio of 1.0 were homogenized for 120 s in 10 mL glass vials at maximum speed using the vortex mixer. The paste was then poured into a metal *in situ* sample holder and covered with an X-ray transmittant polyimide (Kapton®) film to prevent water evaporation. Scans were recorded every 30 min using the same measurement parameters as for the characterization of the hydration products ( $2\theta$  range 5–50°, 0.034°/step, 0.4 s/step, 30 kV, 35 mA).

### 2.4.4 TOC and UV-vis

Eight gram of C<sub>3</sub>A/gypsum in alkaline solution with retarder (w : b ratio = 2.0) were homogenized for 120 s at maximum speed using the vortex mixer and then centrifuged for 10 min at 8500 rpm and 20 °C. The supernatant was separated using a polyethersulfone (PES) syringe filter with a mesh size of 0.2 µm. Supernatants from samples containing gluconate were measured using an Elementar liquiTOC® TOC analyzer at a pH of 2. Supernatants from samples with pyrophosphate were subjected to acidic hydrolysis for 45 min at 90 °C and a pH of 1 to convert the pyrophosphate to orthophosphate. The pH was then increased to three before a commercially acquired ammonium molybdate solution with potassium antimony(III) oxide tartrate (Bernd Kraft) for photometric determination of phosphate and L-(+)-ascorbic acid (Alfa Aesar, 99+) were added as described in a previous study [28]. If the supernatant had still contained phosphate the solution exhibited a blue color from the complex formed with the molybdate solution (“Mo blue method”) [29]. The phosphate content was quantified by determining the intensity of the blue color via UV-vis spectrophotometry at 880 nm using a Cary WinUV® 50 device.

## 3 Results and discussion

At first, the effects of prehydration on the C<sub>3</sub>A/gypsum mixtures were studied with respect to changes in sample mass and formation of hydration products on the particle surfaces during aging. Secondly, the hydration behavior of fresh and aged samples was monitored via heat flow calorimetry and *in situ* XRD. Finally, retarders were added to the liquid phase to investigate their effect on prehydrated samples during hydration.

### 3.1 Impact of aging on C<sub>3</sub>A/gypsum mixtures

#### 3.1.1 Changes in sample mass

The mass of both C<sub>3</sub>A<sub>c</sub> and C<sub>3</sub>A<sub>o</sub> samples mixed with gypsum increased during aging (Figure 3). The mass of the C<sub>3</sub>A<sub>c</sub> mixture increased by ~10% after 3 days and by ~14% after 14 days of aging, thus indicating that most of the water uptake occurred within the first 3 days. Apparently, initial prehydration is rapid and results in significant formation of early hydration products.

This effect was even stronger for the mixture containing C<sub>3</sub>A<sub>o</sub>. There, an increase of no less than 35 wt% occurred within 3 days. Unlike C<sub>3</sub>A<sub>c</sub> however, after 14 days of exposure the mass increase had decreased again slightly too ~29%. We attribute this to the carbonation of ettringite under prolonged exposure to atmospheric CO<sub>2</sub>, as demonstrated for synthetic ettringite in an earlier study [30]. With the formation of CaCO<sub>3</sub> and gypsum a large part of the crystal water incorporated into the ettringite structure is released thus reducing sample mass.

#### 3.1.2 Characterization of aging products via XRD

The aging process occurring on the particles’ surfaces was tracked via powder XRD (Figure 4). In addition to reflections for ettringite, also lines for CaCO<sub>3</sub> (calcite polymorph) and Al(OH)<sub>3</sub> (gibbsite polymorph) could be detected after 3 days (C<sub>3</sub>A<sub>o</sub>) and 14 days (C<sub>3</sub>A<sub>c</sub> + C<sub>3</sub>A<sub>o</sub>) of aging, thus signifying the degradation of ettringite at extended exposure. Furthermore, the surface reaction of C<sub>3</sub>A<sub>o</sub>/gypsum progressed significantly faster than that of C<sub>3</sub>A<sub>c</sub>/gypsum. On the surface of C<sub>3</sub>A<sub>o</sub>, all ettringite had already decomposed after 14 days of aging whereas C<sub>3</sub>A<sub>c</sub> still exhibited a mixture of ettringite, CaCO<sub>3</sub> and Al(OH)<sub>3</sub>. We attribute this to the different relative reactivities of the two polymorphs which produce ettringite at different rates.

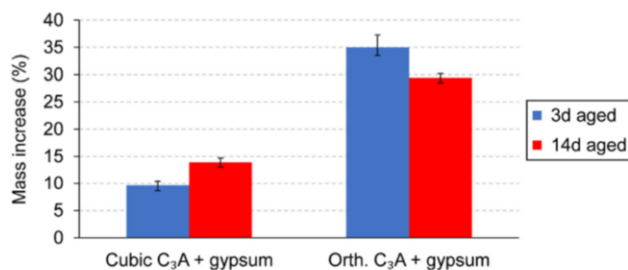


**Figure 3:** Mass increase of binary C<sub>3</sub>A/gypsum mixtures resulting from aging at 90% relative humidity (RH) and 35 °C.

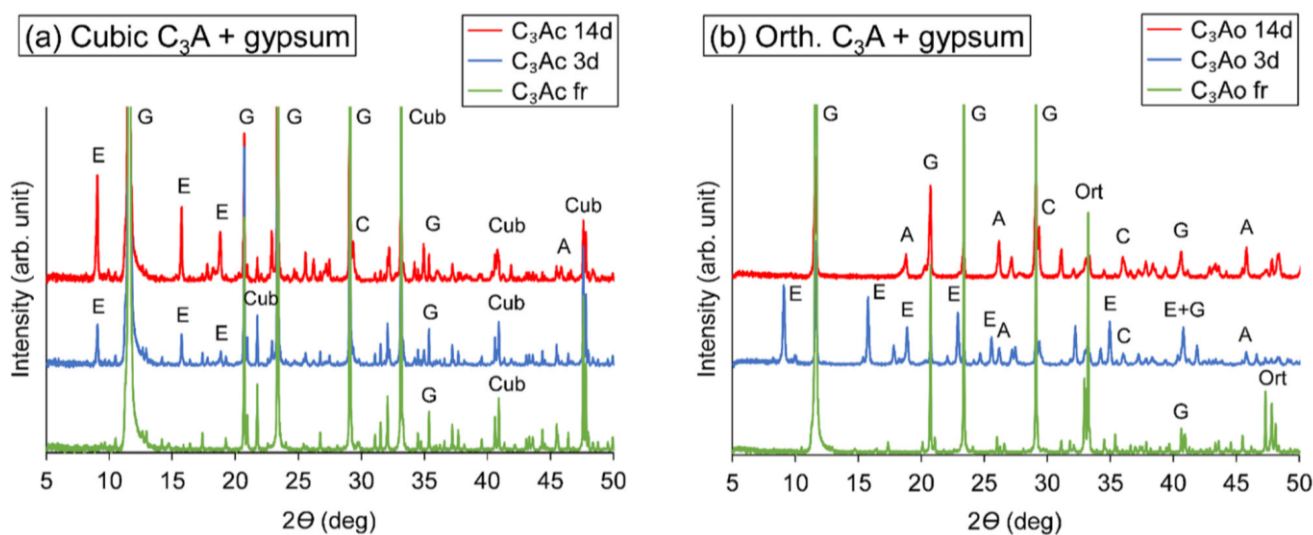


**Figure 4:** Powder XRD analysis of C<sub>3</sub>A<sub>c</sub>/gypsum (a) and C<sub>3</sub>A<sub>o</sub>/gypsum (b) blends before and after aging at 90% RH / 35 °C. The following phases were identified: C<sub>3</sub>A<sub>c</sub> (Cub), C<sub>3</sub>A<sub>o</sub> (Ort), gypsum (G), ettringite (E), calcite (C) and gibbsite (A).

### 3.1.3 Tracking the aging via FT-IR analysis

FT-IR analysis was employed to uncover whether aging products had formed on the particle surface that were not detected by XRD. The IR spectra of the C<sub>3</sub>A/gypsum blends are displayed in Figure 5. All infrared bands could be assigned either to C<sub>3</sub>A and gypsum or to the previously identified prehydration and carbonation products ettringite, CaCO<sub>3</sub> (calcite) and Al(OH)<sub>3</sub> (gibbsite). Thus, these are the only products formed on the particle surface during aging. Continued carbonation ( $\nu_{C-O}$  at 1400 cm<sup>-1</sup>) over 14 days was observed for both C<sub>3</sub>A modifications. The largest amounts of H<sub>2</sub>O (3400 cm<sup>-1</sup>) and OH<sup>-</sup> (3650 cm<sup>-1</sup>) originating from ettringite were found for the C<sub>3</sub>A<sub>o</sub>/gypsum mixture after 3 days of aging, thus confirming that C<sub>3</sub>A<sub>o</sub> undergoes prehydration much faster than C<sub>3</sub>A<sub>c</sub>, and that in the C<sub>3</sub>A<sub>o</sub>/gypsum system ettringite formation peaks after a shorter aging period. The sulfate content in the samples remained constant as would be expected. In comparison, the Al–O bands (650–900 cm<sup>-1</sup>) first decreased after 3 days of aging and after 14 days developed a different pattern which we attribute to the change from tetrahedral environment for Al in C<sub>3</sub>A to the octahedral coordination first in ettringite and then in Al(OH)<sub>3</sub> [31].

### 3.1.4 ESEM imaging of prehydration products

To track the nature of the products of the aging processes on the surface, ESEM images of C<sub>3</sub>A/gypsum mixtures were taken after 3 and 14 days of exposure (Figure 6). Remarkably, ettringite formation in C<sub>3</sub>A<sub>c</sub> was confined to specific

parts of the surface while other areas exhibited no sign of prehydration. The C<sub>3</sub>A<sub>c</sub> used in this study was synthesized without any foreign ion content which implies that the surface possesses less defects and therefore less nucleation sites than C<sub>3</sub>A<sub>o</sub>. In comparison, C<sub>3</sub>A<sub>o</sub> produced ample amounts of ettringite across its entire surface, which confirms its generally higher reactivity as compared to its cubic counterpart and is in line with the previous observations obtained after 3 days of aging via mass increase and surface analysis (Figures 3–5).

After 14 days of exposure, for the sample containing C<sub>3</sub>A<sub>c</sub> a mixture of ettringite crystals and carbonation products was detected whereas ettringite had largely disappeared from the C<sub>3</sub>A<sub>o</sub> blend (Figure 6). This is in line with the observation from powder XRD, where after 14 days of aging, ettringite was only detected on the C<sub>3</sub>A<sub>c</sub>/gypsum surface. However, in the C<sub>3</sub>A<sub>o</sub> mixture an ettringite remnant deeply embedded in the surrounding carbonation products was discovered (enlarged section in Figure 6, bottom right). This raised the question whether in C<sub>3</sub>A<sub>o</sub> after 14 days of exposure a part of the ettringite had not decomposed but was instead overgrown by a layer of CaCO<sub>3</sub> and Al(OH)<sub>3</sub> which obscured it from detection via powder XRD.

### 3.1.5 Investigation of the aging process via TG-MS

To clarify the presence of aging products below the surface TG-MS was employed. Here, the sample composition is determined by measuring the mass loss originating from the release of H<sub>2</sub>O and CO<sub>2</sub>. H<sub>2</sub>O is liberated from gypsum and

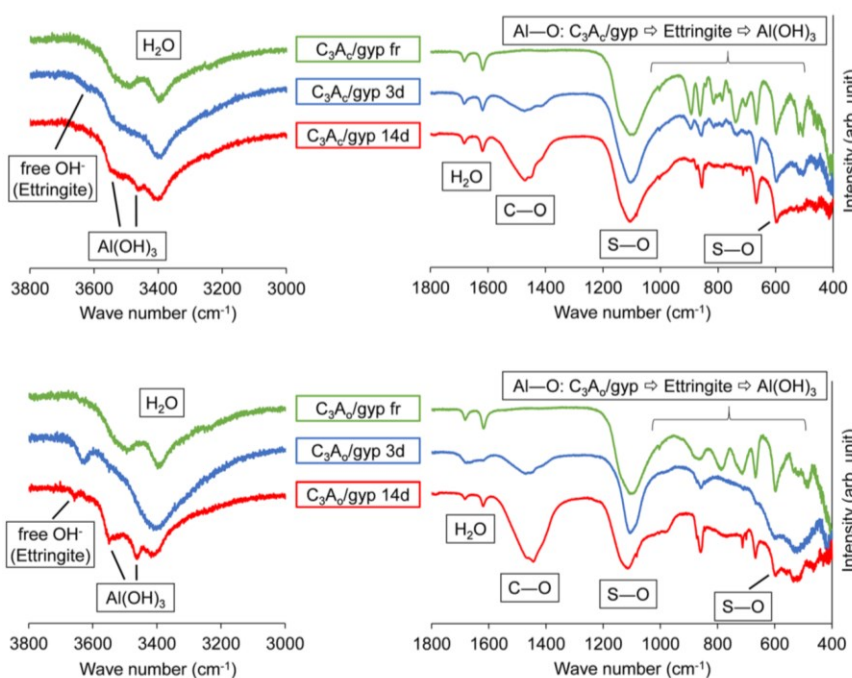


**Figure 5:** FT-IR analysis of binary  $\text{C}_3\text{A}/\text{gypsum}$  (top) and  $\text{C}_3\text{A}/\text{gyp}$  (bottom) mixtures before and after aging at 90% RH / 35 °C.

the aging products ettringite and  $\text{Al}(\text{OH})_3$  at characteristic temperatures. This is exemplified in Figure 7 (left) for the  $\text{C}_3\text{A}_c/\text{gypsum}$  mixture aged for 3 days. The percentual mass losses calculated via peak integration are tabularly presented in Figure 7 (right) as well.

The results confirm that after 3 days of exposure, ettringite had formed from both  $\text{C}_3\text{A}$  polymorphs, which is

supported by a corresponding decrease of the amount of gypsum. Also, as presented before in Sections 3.1.1–3.1.4,  $\text{C}_3\text{A}_o$  produces considerably more ettringite than  $\text{C}_3\text{A}_c$  (Figures 3–6). Moreover, the release of  $\text{CO}_2$  from  $\text{CaCO}_3$  and of  $\text{H}_2\text{O}$  from  $\text{Al}(\text{OH})_3$  clearly confirm that already after 3 days of aging some of the ettringite had decomposed to  $\text{CaCO}_3$  and  $\text{Al}(\text{OH})_3$ , respectively.

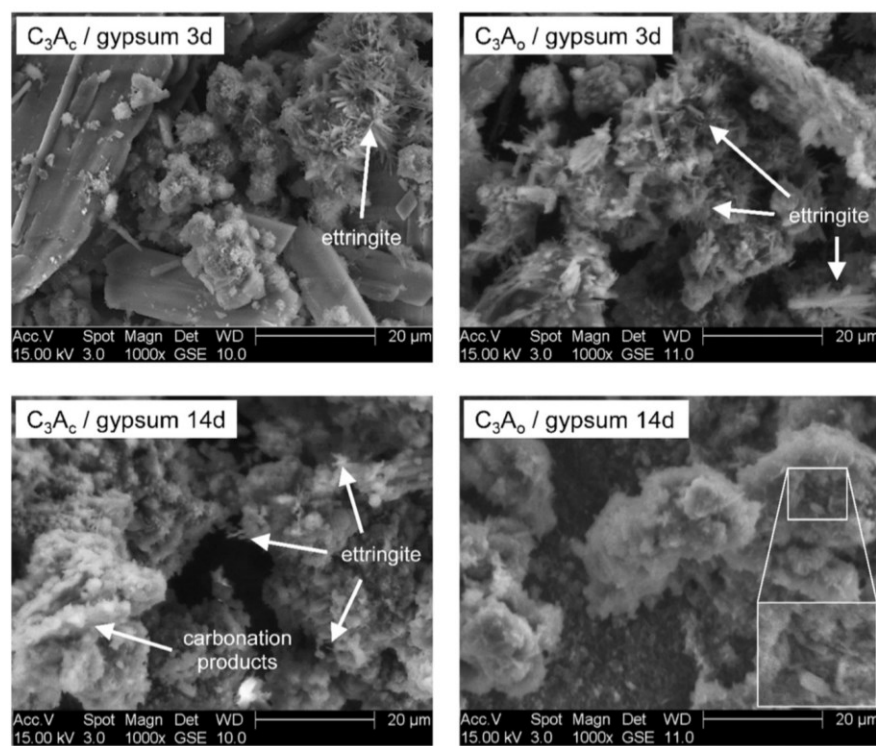


**Figure 6:** ESEM images of binary  $\text{C}_3\text{A}/\text{gypsum}$  mixtures before and after aging at 90% RH / 35 °C.

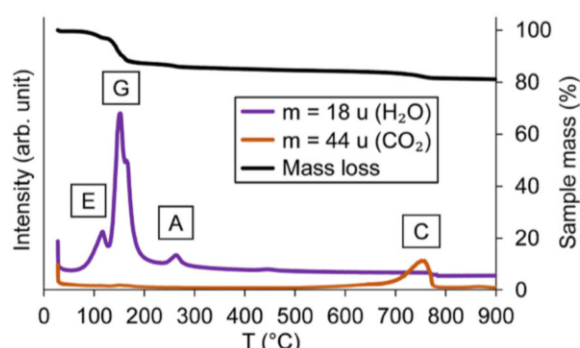


**Figure 7:** TG-MS analysis of binary C<sub>3</sub>A/gypsum mixtures before and after aging at 90% RH / 35 °C, and corresponding mass losses attributed to the decomposition processes of ettringite (E), gypsum (G), Al(OH)<sub>3</sub> (A) and CaCO<sub>3</sub> (C).

After 14 days of exposure, ettringite was detected via TG-MS in the C<sub>3</sub>A<sub>o</sub>/gypsum sample which confirmed that below its surface ettringite was present which had not been captured via powder XRD (Figure 4). However, the associated H<sub>2</sub>O mass loss was relatively low at < 1% (Figure 7). Also, no discernible peak for ettringite in the C<sub>3</sub>A<sub>c</sub>/gypsum mixture aged for 14 days could be detected although its presence had been clearly confirmed via powder XRD (Figure 4) and ESEM (Figure 6).

We attribute these discrepancies to the partial overlapping of the peak signifying ettringite with the double peak attributable to gypsum in the TG-MS spectrum (Figure 7). Thus, the mass loss calculated from peak integration is not precise, especially when the amount is already low such as for ettringite after 14 days of aging.

### 3.2 Hydration behavior of fresh and aged binary C<sub>3</sub>A/gypsum mixtures

#### 3.2.1 Time-dependent hydration analysis of the C<sub>3</sub>A/gypsum system

Figure 8 (top left) displays as an example the heat flow calorimetric analysis of the fresh C<sub>3</sub>A<sub>o</sub>/gypsum mixture hydrated at a w : b ratio of 1.0. After a strong initial heat release (exceeding 200 mW g<sup>-1</sup>) due to the dissolution of C<sub>3</sub>A<sub>o</sub> and instant ettringite formation [32], the heat flow fell to ~2 mW g<sup>-1</sup> within 6 h. Thereafter, ettringite formation progressed continuously as gypsum dissolved. Over the next 60 h, the heat flow slowly decreased to 1 mW g<sup>-1</sup>.

At that point, all gypsum has been consumed and the delicate balance between gypsum dissolution and ettringite precipitation is disturbed. The remaining dissolved C<sub>3</sub>A and gypsum then react in a final ettringite crystallization which is marked by a peak in heat flow occurring

Sample	Mass loss (%)			
	H <sub>2</sub> O from ettringite	H <sub>2</sub> O from gypsum	H <sub>2</sub> O from Al(OH) <sub>3</sub>	CO <sub>2</sub> from CaCO <sub>3</sub>
C <sub>3</sub> A <sub>c</sub> fr	—	9.9	—	—
C <sub>3</sub> A <sub>c</sub> 3d	2.5	8.6	0.9	2.1
C <sub>3</sub> A <sub>c</sub> 14d	n/a	8.9	1.4	5.4
C <sub>3</sub> A <sub>o</sub> fr	—	10.0	—	—
C <sub>3</sub> A <sub>o</sub> 3d	10.5	4.9	2.5	4.6
C <sub>3</sub> A <sub>o</sub> 14d	0.8	6.3	4.0	12.5

72 h after the start of hydration (Figure 8). When the sulfate concentration in the pore solution drops below 2.4 mg L<sup>-1</sup>, the ettringite structure comprising three equivalents of sulfate for every equivalent of aluminate (“trisulfo aluminate”, Ca<sub>6</sub>Al<sub>2</sub>(OH)<sub>12</sub> · (SO<sub>4</sub>)<sub>3</sub> · 26 H<sub>2</sub>O) becomes increasingly unstable and a partial conversion of ettringite to “monosulfo aluminate” (Ca<sub>4</sub>Al<sub>2</sub>(OH)<sub>12</sub> · SO<sub>4</sub> · 12 H<sub>2</sub>O) occurs [12]. The binary-by-weight mixtures of C<sub>3</sub>A/gypsum mixtures investigated here correspond to a molar ratio of C<sub>3</sub>A to gypsum of 1 : 1.57. This produces a mixture of ettringite and monosulfo aluminate as the final hydration product. The hydration process was completed approximately 120 h after the start of the experiment. In comparison, the hydration of the C<sub>3</sub>A<sub>c</sub>/gypsum mixture was slower, but otherwise similar (Figure 8, top right).

This sequence of reactions was established by XRD analysis of the hydrated C<sub>3</sub>A/gypsum at different stages of the hydration process. For this purpose, the calorimetric experiments were repeated with additional samples, which were removed from the calorimeter before or after heat flow peaks. The hydrated mixtures were mounted onto sample holders and investigated without additional preparation. Thereby, from shortly after the start of hydration until before the peak at 72 h, a mixture of C<sub>3</sub>A, gypsum and ettringite could be detected (Figure 9). After this peak, at the end of the hydration process (120 h), the educts C<sub>3</sub>A and gypsum had completely disappeared and monosulfo aluminate was detected alongside ettringite.

The total heat of hydration (Figure 8, bottom) was calculated by integration of the heat flow over time. The hydration process can be separated into two distinct periods as indicated by the dotted line. While gypsum was still dissolving, the total heat increased nearly linearly, only slightly tapering off due to the slow decrease in heat flow. In the second step, the total heat at first grew exponentially due to the heat flow peak before leveling off

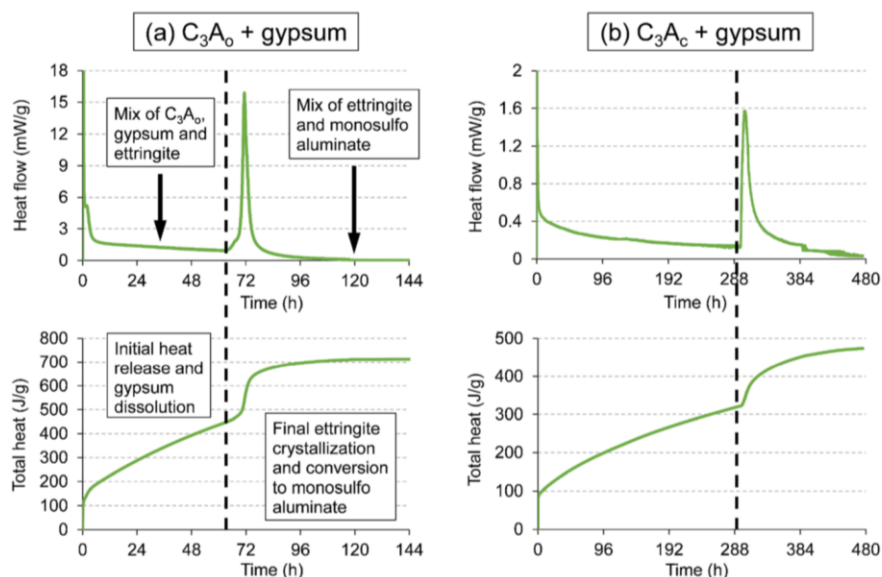


**Figure 8:** Heat flow calorimetric analysis of the fresh binary  $\text{C}_3\text{A}_0/\text{gypsum}$  (left) and  $\text{C}_3\text{A}_c/\text{gypsum}$  (right) mixtures ( $w:b$  ratio = 1.0).

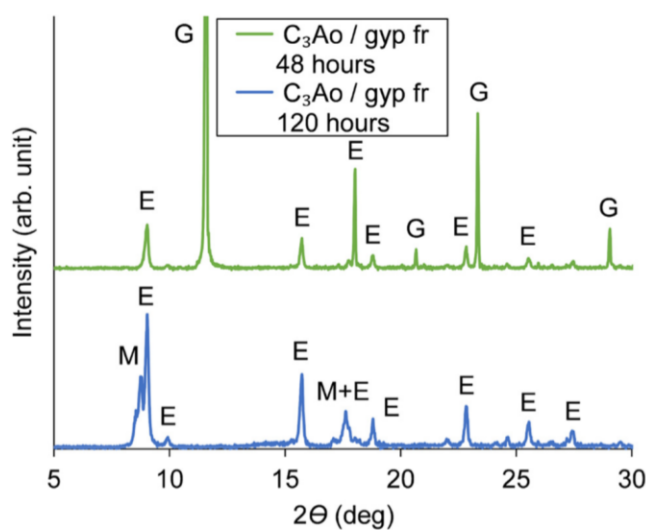


**Figure 9:** Powder XRD analysis of the fresh  $\text{C}_3\text{A}_0/\text{gypsum}$  mix before and after final ettringite crystallization, shown in the  $2\theta$  range of 5–30°.

during the final ettringite crystallization and subsequent partial conversion to monosulfo aluminate.

### 3.2.2 Impact of aging on mixtures containing cubic $\text{C}_3\text{A}$

Figure 10 (left) displays the total heat released from fresh and aged  $\text{C}_3\text{A}_c/\text{gypsum}$  mixtures over the first 24 h of hydration. During this time, the fresh sample was in the gypsum dissolution phase with the total heat increasing nearly linearly. In comparison, both aged samples produced an immediate and strong heat release which after 24 h leveled off at  $\sim 410 \text{ J g}^{-1}$  as opposed to the fresh, non-prehydrated mixture which reached  $\sim 130 \text{ J g}^{-1}$  by this time. Apparently, prehydration greatly accelerates hydration of the  $\text{C}_3\text{A}_c/\text{gypsum}$  system.

We attribute this strongly accelerated hydration process to a seeding effect of ettringite formed during aging. This assumption is supported by the two periods, gypsum

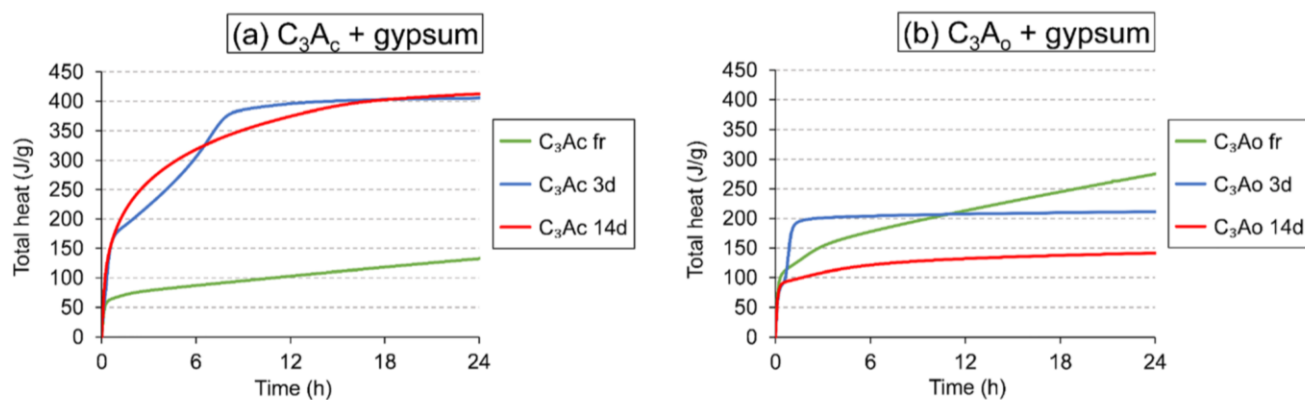


**Figure 10:** Heat flow calorimetric analysis of the fresh and aged binary  $\text{C}_3\text{A}_c/\text{gypsum}$  (a) and  $\text{C}_3\text{A}_0/\text{gypsum}$  (b) blends ( $w:b$  ratio = 1.0).

dissolution and final ettringite crystallization/conversion to monosulfo aluminate, clearly overlapping in the hydration of the aged samples. This indicates that the ettringite formation is no longer dependent on ion oversaturation of the pore solution. Rather, ettringite nuclei formed during aging can grow immediately when water is added, and no energy barrier needs to be overcome any more as a condition for their growth [33].

Among the aged samples, the results for the hydration after 3 days of exposure slightly differed from that after 14 days. After 3 days, total heat developed more slowly after the initial heat release with a slight, but distinct increase toward the end of the hydration process. This signifies that after the shorter aging period the overlap between the two periods during hydration is only partial with an, albeit weak, final ettringite crystallization still occurring. After 14 days of exposure, heat increases logarithmically during hydration, indicating a full temporal overlap of the two periods.

### 3.2.3 Impact of aging on mixtures containing orthorhombic C<sub>3</sub>A

The conversion of C<sub>3</sub>A<sub>o</sub> to ettringite during aging was more complete than that of C<sub>3</sub>A<sub>c</sub> with the total heat released decreasing from ~410 J g<sup>-1</sup> (C<sub>3</sub>A<sub>c</sub> 3, 14 days) to ~220 J g<sup>-1</sup> (C<sub>3</sub>A<sub>o</sub> 3 days) and ~150 J g<sup>-1</sup> (C<sub>3</sub>A<sub>o</sub> 14 days) as shown in Figure 10 (right). These values are significantly lower than those for the fresh C<sub>3</sub>A<sub>o</sub> mixture (~700 J g<sup>-1</sup>, Figure 8), signifying that the major part of the hydration process had taken place during aging already. The hydration curve of the samples aged for 3 days resembles that of the C<sub>3</sub>A<sub>c</sub>/gypsum system, yet in greatly accelerated form because of an even stronger seeding effect due to the massive ettringite formation in C<sub>3</sub>A<sub>o</sub>/gypsum during aging (Figures 3–7). The hydration reaction is thus complete within ~1.5 h after the start of the experiment.

To verify these results from heat flow calorimetry, the course of hydration was tracked via *in situ* XRD. This allows for monitoring the hydration process continuously as opposed to taking snapshots at a specific moment during hydration as when performing XRD analysis on the calorimetry samples. The first 8 h of hydration for the C<sub>3</sub>A<sub>o</sub>/gypsum blend before and after aging are displayed in Figure 11. There, compared to the fresh sample a much earlier and stronger ettringite formation was apparent after 3 days of exposure, and a corresponding instantaneous decrease of gypsum was detected. From the sample aged for 14 days, ettringite formed more slowly in the beginning and much gypsum was released again due to the carbonation of ettringite

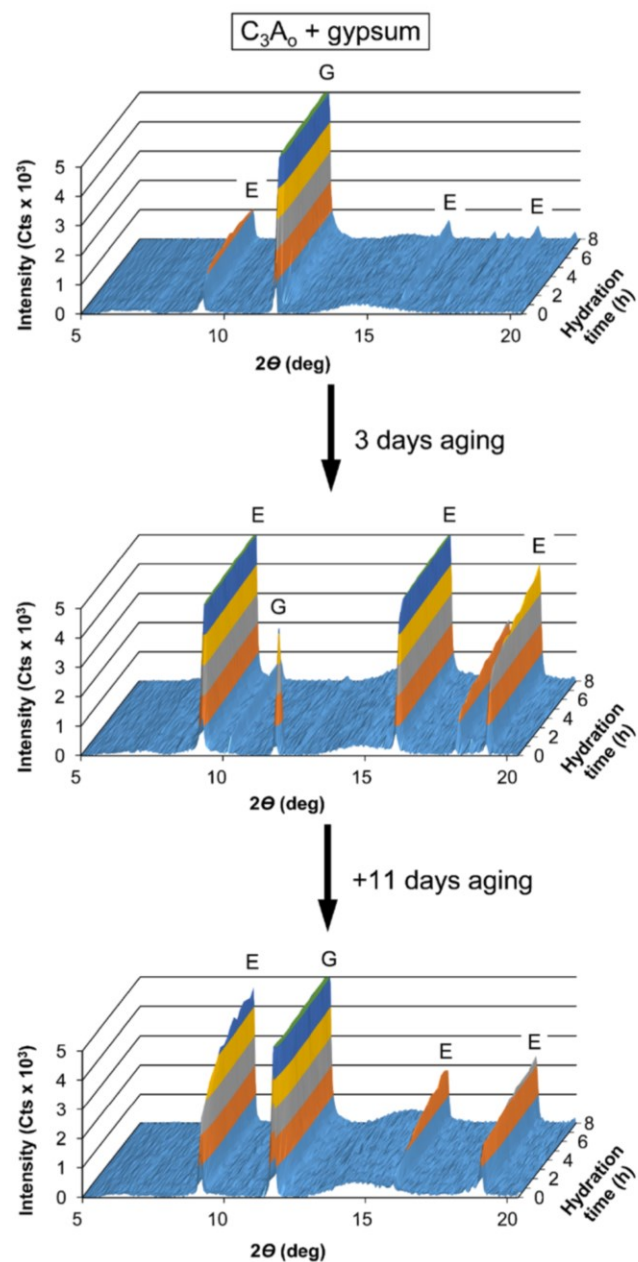


**Figure 11:** *In situ* XRD analysis of the binary C<sub>3</sub>A<sub>o</sub>/gypsum mixture (w:b ratio = 1.0) upon hydration, before and after aging at 90% RH / 35 °C.

formed during aging. The *in situ* XRD investigations thus confirm the results from heat flow calorimetry as presented in Figures 8 and 10.

### 3.3 Impact of retarders on the hydration of aged C<sub>3</sub>A

If a cementitious binder is exposed to atmospheric moisture and prehydrated, the accelerated ettringite formation

**Table 1:** Amounts of sodium gluconate (NaGluc) or potassium pyrophosphate (KPPhos) depleted from the liquid phase after mixing with C<sub>3</sub>A/gypsum blends ( $w:b$  ratio = 2.0, retarder dosage = 1.0% bwob) and centrifugation.

Retarder	C <sub>3</sub> A <sub>c</sub> /gypsum			C <sub>3</sub> A <sub>o</sub> /gypsum		
	Fresh	3 days	14 days	Fresh	3 days	14 days
NaGluc	99%	77%	89%	99%	78%	80%
KPPhos	>99%	>99%	>99%	>99%	>99%	>99%

results in a significantly decreased workability during application. To gain an understanding whether this effect can be counteracted by the use of admixtures, the hydration experiments from Section 3.2 were repeated with 1.0% bwob of either sodium gluconate or potassium pyrophosphate retarder dissolved in the alkaline solution prior to mixing with the aged C<sub>3</sub>A/gypsum blends.

### 3.3.1 Depletion of retarders from the liquid phase by C<sub>3</sub>A/gypsum

Prior to the hydration experiments, the depletion of the retarders in the applied dosage of 1.0% bwob from the liquid phase via adsorption and/or precipitation during mixing with aged C<sub>3</sub>A/gypsum blends was investigated. For this purpose, TOC analysis (gluconate) or UV-vis spectrophotometry (pyrophosphate) was carried out on supernatants that had been separated from the binder after mixing at an elevated  $w:b$  ratio of 2.0 to account for fluid uptake by the C<sub>3</sub>A/gypsum. For comparison, fresh, unaged C<sub>3</sub>A/gypsum was also investigated.

For both fresh and aged blends of either C<sub>3</sub>A polymorph, no pyrophosphate was detected in the supernatants. This signifies full removal of the retarder from the liquid phase (Table 1). Also, gluconate was almost completely depleted from the liquid phase by fresh C<sub>3</sub>A/gypsum, while ~20% of the gluconate remained in solution after mixing with the aged blends, except for the cubic polymorph after 14 days of exposure where the residual concentration was only ~10%. These results signify that strong interaction of both retarders with the C<sub>3</sub>A/gypsum blends is retained after aging.

### 3.3.2 Impact of retarders on aged cubic C<sub>3</sub>A

The heat flow curves of the C<sub>3</sub>A<sub>c</sub>/gypsum mixtures aged for 3 days hydrated with and without retarder admixture are shown in Figure 12. Compared to the neat mix, the addition of gluconate to the liquid phase delayed the onset of the

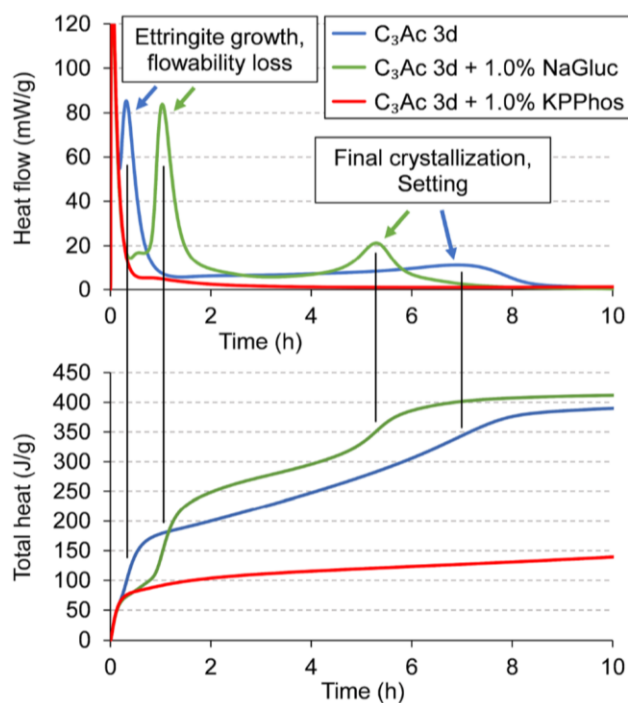


**Figure 12:** Heat flow calorimetric analysis of the three binary C<sub>3</sub>A<sub>c</sub>/gypsum mixture ( $w:b$  ratio = 1.0) aged for 3 days, admixed with either sodium gluconate (NaGluc) or potassium pyrophosphate (KPPhos) retarders.

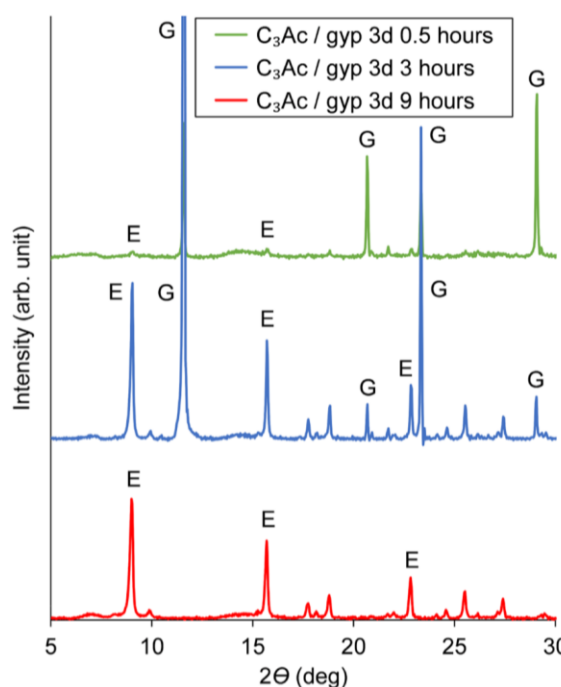


**Figure 13:** Powder XRD analysis of the 3 days aged C<sub>3</sub>A<sub>c</sub>/gypsum mix before initial ettringite formation (top) and before (middle) and after (bottom) final ettringite crystallization, shown in the  $2\theta$  range of 5–30°.

first heat flow peak by ~1 h. Samples were removed from the calorimeter before and after this peak and analyzed by XRD (Figure 13). A sample with gluconate taken out 0.5 h after the start of hydration was still liquid and exhibited comparatively small amounts of ettringite, likely formed during aging. A second sample taken out 3 h into hydration did not flow anymore and contained significant amounts of ettringite (Figure 13). The first heat flow peak can thus be attributed to the crystal growth of ettringite formed during prehydration as a direct result of the seeding effect and leads to a stiffening of the sample.

This is followed by a second heat flow peak between 4 and 6 h after the start of hydration (Figure 12). Finally, a third sample was taken out from the calorimeter after 8 h and investigated by XRD. It did no longer contain gypsum (Figure 13) and had hardened significantly. The second heat flow peak thus denotes the final ettringite crystallization after gypsum dissolution is completed. Interestingly, the admixture of gluconate, while retarding the initial ettringite growth, resulted in an earlier (by ~1.5 h) and more distinct final ettringite crystallization as compared to that occurring in the hydration of the mixture aged for 3 days without retarder, which has already been described in Section 3.2.2 as weak and partially overlapping with the gypsum dissolution. We assume that in the absence of retarders, the seeding effect leads to a rapid growth of the isolated ettringite clusters on the surface of C<sub>3</sub>A<sub>c</sub> aged for 3 days as observed via ESEM (Figure 6). This quickly covers the particle surfaces with ettringite. As a

result, the hydration process is shifted early on from dissolution limitation toward diffusion limitation, thus prolonging the reaction. Gluconate, which is known to effectively adsorb on hydrate phases such as ettringite due to its slump-retaining properties in cement [34], delays this overgrowth so much that C<sub>3</sub>A/gypsum can dissolve before it occurs. This reduces the overall duration of the hydration process and increases the prominence of the final ettringite crystallization. Thus remarkably, the gluconate retarder actually shortens the period during which the C<sub>3</sub>A<sub>c</sub>/gypsum mixture aged for 3 days retains some degree of workability.

The addition of 1.0% bwob pyrophosphate had a much stronger effect than gluconate on the hydration of C<sub>3</sub>A<sub>c</sub>/gypsum aged for 3 days, effectively suppressing the seeding effect of ettringite from prehydration (Figure 12). Sample hardness and total heat of hydration increased nearly linearly over a much prolonged hydration period of ~50 h. We attribute this to the different working mechanism of the pyrophosphate retarder which forms a layer of calcium pyrophosphate on the particle surface and captures calcium ions from the pore solution. This poisons the nucleation sites on the ettringite crystals precluding prehydration while at the same time slowing down the formation of new ettringite crystal nuclei in the pore solution during hydration by the removal of calcium ions.

The results of the heat flow calorimetry experiments with retarders were also verified via *in situ* XRD (Figure 14). Gluconate admixture showed that gypsum consumption

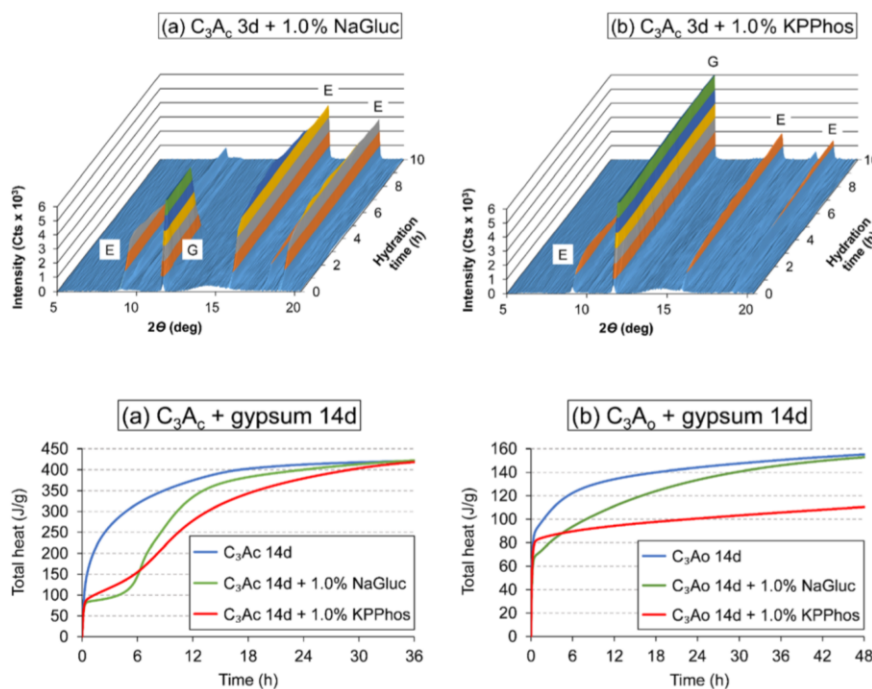


**Figure 14:** *In situ* XRD analysis of the hydrating process of binary C<sub>3</sub>A<sub>c</sub>/gypsum mixture aged for 3 days, admixed with either sodium gluconate (NaGluc, a) or potassium pyrophosphate (KPPhos, b) retarders.

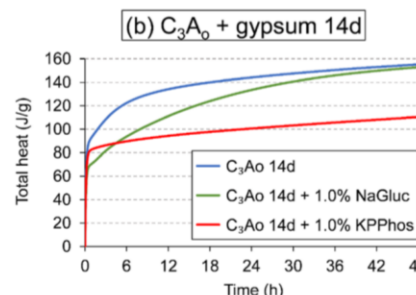


**Figure 15:** Heat flow calorimetric analysis of the binary mixtures of C<sub>3</sub>A<sub>c</sub>/gypsum (a) and C<sub>3</sub>A<sub>o</sub>/gypsum (b) aged for 14 days, admixed with either sodium gluconate (NaGluc) or potassium pyrophosphate (KPPhos) retarders (w : b ratio = 1.0).

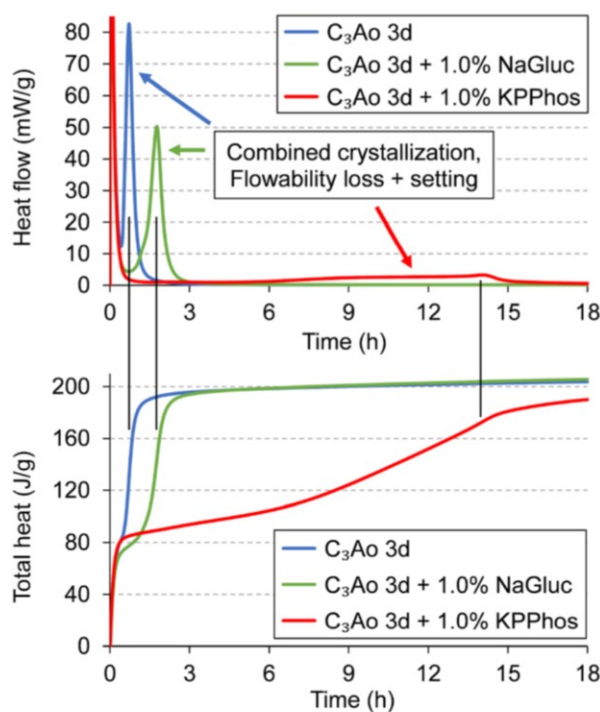


**Figure 16:** Heat flow calorimetric analysis of the binary C<sub>3</sub>A<sub>o</sub>/gypsum mixture ( $w:b$  ratio = 1.0) aged for 3 days, admixed with either sodium gluconate (NaGluc) or potassium pyrophosphate (KPPhos) retarders.

was completed ~4 h after the start of hydration which is in line with the onset of the final ettringite crystallization observed in heat flow calorimetry. Hydration with pyrophosphate yielded only a comparatively small amount of ettringite over 10 h with ample amounts of gypsum remaining.

The effect of gluconate on samples aged for 14 days was stronger than after 3 days of exposure. Massive ettringite growth started only after 6 h of hydration (Figure 15, left). This is in line with the higher depletion of gluconate from the liquid phase after 14 days of exposure as compared to that after 3 days of aging (Table 1). On the other hand, pyrophosphate was less

effective with increased aging duration. Its initial retardation effect was slightly weaker than that of gluconate and the overall hydration was not as significantly prolonged compared to the other samples as observed after 3 days of exposure.

### 3.3.3 Impact of retarders on aged orthorhombic C<sub>3</sub>A

The hydration of C<sub>3</sub>A<sub>o</sub>/gypsum after 3 days of exposure shows only a single heat flow peak (Figure 16). Unlike C<sub>3</sub>A<sub>c</sub>, there is apparently no time wise separation of initial ettringite growth and final crystallization. This can be attributed to the even stronger seeding effect of the orthorhombic polymorph due to massive ettringite formation during aging as discussed in 3.2.3 which completes the hydration reaction in ~1.5 h. Gluconate admixture leads to a retardation of ~1 h on this “combined” ettringite crystallization.

As for the cubic polymorph, pyrophosphate is the superior retarder for C<sub>3</sub>A<sub>o</sub>/gypsum after 3 days of exposure. However, the impact of pyrophosphate on the more reactive C<sub>3</sub>A<sub>o</sub> mixture is significantly smaller than on its cubic counterpart, with the hydration reaction nearing completion after ~24 h compared to ~50 h for C<sub>3</sub>A<sub>c</sub>. *In situ* XRD of C<sub>3</sub>A<sub>o</sub>/gypsum aged for 3 days (Figure 17) showed complete gypsum consumption after ~6 h for pyrophosphate and after ~1 h for gluconate which matches the onsets of the combined ettringite crystallization observed in heat flow calorimetry (Figure 16).

Over 14 days of exposure, the C<sub>3</sub>A<sub>o</sub>/gypsum mixture was largely hydrated already as discussed in Section 3.2.3. Thus, in the hydration process the heat flow after the release of dissolution heat during the first few minutes (~80 J g<sup>-1</sup>) was small in comparison to that of the C<sub>3</sub>A<sub>c</sub> blends after 14 days of exposure. However, C<sub>3</sub>A<sub>o</sub> and C<sub>3</sub>A<sub>c</sub> were affected similarly by the retarders after 14 days of aging (Figure 15) with gluconate being more effective initially but having less impact on hydration than pyrophosphate after ~6 h.

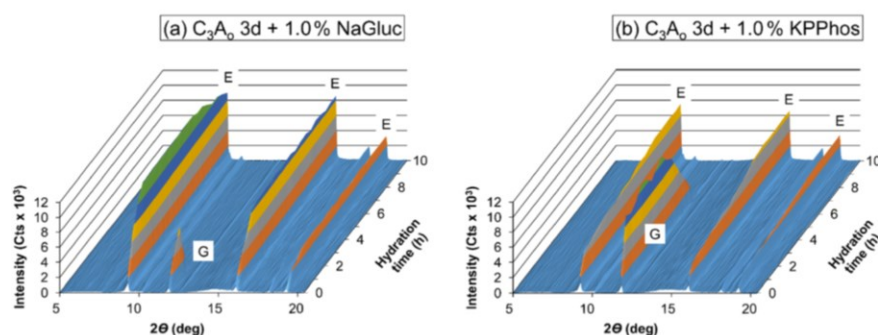


**Figure 17:** *In situ* XRD analysis of the hydrating binary C<sub>3</sub>A<sub>o</sub>/gypsum mixture aged for 3 days, admixed with either sodium gluconate (NaGluc, a) or potassium pyrophosphate (KPPhos, b) retarders.

## 4 Conclusions

This study aimed at investigating the impact of the C<sub>3</sub>A polymorph on the hydration behavior of C<sub>3</sub>A/gypsum mixtures which were exposed to 90% RH at 35 °C for time periods of 3 and 14 days. The changes in the material properties and the composition of the aged samples were monitored with powder XRD, FT-IR, ESEM imaging and TG-MS. Ettringite was confirmed as the only initial aging product of blends from cubic or orthorhombic C<sub>3</sub>A polymorphs and gypsum. During this prehydration period, the conversion of alkali substituted C<sub>3</sub>A<sub>0</sub> to ettringite was faster and more complete compared to that of pure C<sub>3</sub>A<sub>c</sub>. Under the applied aging conditions, the ettringite subsequently reacted with atmospheric CO<sub>2</sub> and decomposed into CaCO<sub>3</sub>, Al(OH)<sub>3</sub> and gypsum.

Heat flow calorimetric and *in situ* XRD analyses revealed that the ettringite crystals formed during aging act as a seeding material which greatly accelerates the hydration process as compared to that for fresh C<sub>3</sub>A/gypsum mixtures. Thus, in applications aged cements can exhibit much reduced initial and final setting times and reduced workability.

The performance of retarders in mitigating this seeding and accelerating effect was found to be dependent on the kind of retarder and its working mechanism. Sodium gluconate and potassium pyrophosphate were tested at elevated dosages of 1.0% by weight due to the increased demand in such a model binder system consisting only of the highly reactive combination of C<sub>3</sub>A phase and sulfate. In aged cubic C<sub>3</sub>A/gypsum, gluconate, which works via adsorption on particle surfaces, retarded the initial growth of ettringite formed during prehydration, thus slowing the spread of ettringite on the particle surfaces. This however reduced the diffusion limitation of the hydration process thus accelerating the gypsum dissolution and resulting in an earlier final ettringite crystallization. Therefore, the period during which the sample retained some degree of workability was actually shortened by gluconate admixture. Potassium pyrophosphate was more effective in prolonging the hydration and setting process by suppressing the seeding effect of ettringite crystals formed during prehydration. Deposition of a layer of calcium pyrophosphate on the particle surfaces poisons the nucleation sites of the ettringite crystals precluding prehydration. Simultaneously, formation of new ettringite crystal nuclei in the pore solution during hydration is slowed by the precipitation of dissolved calcium ions by the phosphate.

The results signify that the hydration behavior of the C<sub>3</sub>A phase in cement can be severely impacted by exposure to atmospheric moisture and CO<sub>2</sub>. These findings are particularly important for the application of dry-mix mortars, as such mixtures are geared toward high reactivity in hydration. Applicators are advised to pay careful attention to the relative shares of the C<sub>3</sub>A polymorphs and the choice of retarding agent.

**Author contribution:** All the authors have accepted responsibility for the entire content of this submitted manuscript and approved submission.

**Research funding:** The authors are most grateful to Deutsche Forschungsgemeinschaft, Bonn, Germany (DFG) for financing this project under the grant PL-472/9-2 “Influence of aging of binder systems on the performance of additives”.

**Conflict of interest statement:** The authors declare no conflicts of interest regarding this article.

## References

1. Stoian J., Oey T., Bullard J. W., Huang J., Kumar A., Balonis M., Terrill J., Neithalath N., Sant G. *Cem. Concr. Res.* 2015, **70**, 94–103.
2. Maltese C., Pistolesi C., Bravo A., Celli F., Cerulli T., Salvione D. *Cem. Concr. Res.* 2007, **37**, 856–865.
3. Sprung S. *ZKG Int.* 1978, **31**, 305–309.
4. Schmid G., Bier T. A., Wutz K., Maier M. *ZKG Int.* 2007, **60**, 94–103.
5. Barbic L., Tinta V., Lozar B., Marincovic V. *J. Am. Ceram. Soc.* 1991, **74**, 954–949.
6. Whittaker M., Dubina E., Al-Mutawa F., Arkless L., Plank J., Black L. *Adv. Cem. Res.* 2013, **25**, 12–20.
7. Winnefeld F. *ZKG Int.* 2008, **61**, 68–77.
8. Dubina E. *Plank J. ZKG Int.* 2012, **65**, 60–68.
9. Theisen K., Johansen V. *J. Am. Ceram. Soc. Bull.* 1975, **54**, 787–791.
10. Meier M. R., Napharatsamee T., Plank J. *Construct. Build. Mater.* 2017, **139**, 232–240.
11. Mould A. E., Williams D. W. *Build. Sci.* 1974, **9**, 243–245.
12. Taylor H. F. W. *Cement Chemistry*, 2nd ed.; Academic Press: London, 1997.
13. Jensen O. M., Hansen P., Lachowski E. E., Glasser F. P. *Cem. Concr. Res.* 1999, **29**, 1505–1512.
14. Dubina E., Plank J., Black L. *Cem. Concr. Res.* 2015, **73**, 36–41.
15. Dubina E., Wadsö L., Plank J. *Cem. Concr. Res.* 2011, **41**, 1196–1204.
16. Dubina E., Black L., Sieber R., Plank J. *Adv. Appl. Ceram.* 2010, **109**, 260–268.
17. Dubina E., Plank J., Black L., Wadsö L. *Adv. Cem. Res.* 2014, **26**, 29–40.
18. Boikova A. I., Domansky A. I., Paramonova V. A., Stavitskaja G. P., Nikuschenko V. M. *Cem. Concr. Res.* 1977, **7**, 483–492.
19. Gobbo L., Sant'Agostino L., Garcez L. *Cem. Concr. Res.* 2004, **34**, 657–664.
20. Lee F. C., Banda H. M., Glasser F. P. *Cem. Concr. Res.* 1982, **12**, 237–246.

21. Takeuchi Y., Nishi F., Maki I. *Zeit. Krist.* 1980, **152**, 259–307.
22. Kirchheim A. P., Fernández-Altable V., Monteiro P. J. M., Dal Molin D. C. C., Casanova I. *J. Mater. Sci.* 2009, **44**, 2038–2045.
23. Singh N. B. *Cem. Concr. Res.* 1976, **6**, 455–460.
24. Rickert J., Thielen G. *Cem. Concr. Aggr. J.* 2004, **26**, 1–10.
25. Bishop M., Bott S. G., Barron A. R. *Chem. Mater.* 2003, **15**, 3074–3088.
26. Wesselsky A., Jensen O. M. *Cem. Concr. Res.* 2009, **39**, 973–980.
27. Kelzenberg A. L., Tracy S. L., Christiansen B. J., Thomas J. J., Clarage M. E., Hodson S., Jennings H. M. *J. Am. Ceram. Soc.* 1998, **81**, 2349–2359.
28. Nilles V., Plank J. *Cem. Concr. Res.* 2012, **42**, 736–744.
29. Nagul E. A., McKelvie I. D., Worsfold P., Kolev S. D. *Anal. Chim. Acta* 2015, **890**, 60–82.
30. Plank J., Zhang-Preße M., Ivleva N. P., Niessner R. *Construct. Build. Mater.* 2016, **122**, 426–434.
31. Fernández-Carrasco L., Torrens-Martín D., Morales L. M., Martínez-Ramírez S. Infrared Spectroscopy—Materials Science, Engineering and Technology. In *Infrared Spectroscopy—Materials Science, Engineering and Technology*; Theophanides T., Ed. IntechOpen Limited: London, 2012; pp. 369–382, <https://doi.org/10.5772/36186>.
32. Meier M. R., Sarigaphuti M., Sainamthip P., Plank J. *Construct. Build. Mater.* 2015, **93**, 877–883.
33. Sear R. P. *J. Phys. Condens. Matter.* 2007, **19**, 033101.
34. Jeknavorian A. A., Koyata H., McGuire D. B., Jovanovic I. Slump retention in cementitious compositions. US Patent 8070875, 2011.

### 4.2.2 Journal article 2: Portland cement

#### 4.2.2.1 Content overview for journal article 2

The second journal article expands on the results of the first one. The investigative methods used to determine the aging impact on retarder performance in C<sub>3</sub>A / gypsum were applied to Portland cement. As the OPC had not to be synthesized in the laboratory, enough material was available to perform additional experiments on the engineering properties at the end of the investigation (**Figure 41**).

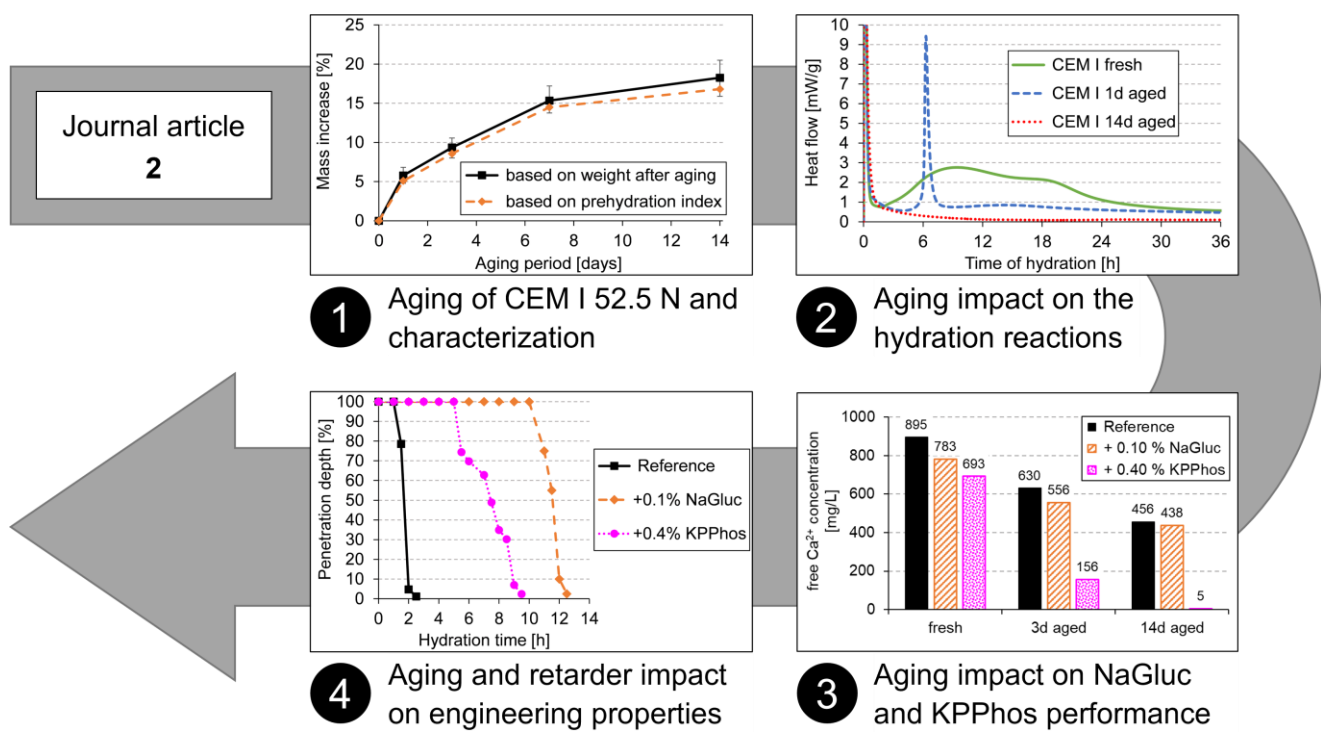


**Figure 41:** Overview of journal article 2 on the retarder performance in aged CEM I 52.5 N.

- ① Samples of CEM I 52.5 N were exposed to water vapor and atmospheric CO<sub>2</sub> at 35 °C and 90% RH for periods of 1, 3, 7 or 14 days.

The aged cement samples were characterized with powder XRD and TGA. Ettringite formed from the aluminate clinker phases and interground sulfate. Its amount in the aged samples depended on the exposure duration. The longer the aging period, the more ettringite would form but at the same time more of this ettringite would decompose to CaCO<sub>3</sub>, Al(OH)<sub>3</sub> and gypsum due to the exposure to atmospheric CO<sub>2</sub>. As a result, the highest amount of ettringite is reached after an intermediate exposure duration, between 3 and 7 days of aging.

The occurrence of portlandite and the decrease of C<sub>3</sub>S peak intensities in powder XRD verified the prehydration of the silicate phase. The amount of portlandite in the aged samples was very low regardless of exposure duration. Portlandite was found to be more reactive with atmospheric CO<sub>2</sub> than ettringite which meant it converted to CaCO<sub>3</sub> quickly after formation.

The amount of  $\text{H}_2\text{O}$  in the aged samples did not increase significantly anymore between 7 and 14 days of exposure. At this point, the rates of prehydrate formation under water uptake and their decomposition under water release are balanced.

- ② The hydration behaviors of fresh and aged cement samples were compared via calorimetry, *in situ* XRD and (E)SEM imaging. In calorimetry, fresh CEM I 52.5 N displayed a broad double peak, which is common for Portland cement. It marks both the reaction of the silicate phase (first peak) and the sulfate depletion / final ettringite crystallization (second peak). After aging, this double peak was largely replaced by a narrow single peak. With increasing exposure duration this single peak occurred earlier in hydration. After 14 days of aging, it merged with the heat released at the start of hydration. This signifies that aging accelerates the hydration of Portland cement and that this effect is proportional to the exposure duration. Via *in situ* XRD it was discovered that the single peak corresponds to the sulfate depletion / final ettringite crystallization. The ettringite formation during hydration is promoted by the seeding effect of the ettringite formed during aging. On the other hand, it was found that the hydration of the silicate phase is strongly decelerated after aging. (E)SEM imaging revealed that the enhanced ettringite formation after aging results in a dense overgrowth of the cement particles which slows the water access to the silicate phase.

Two of the observations made so far appeared to contradict each other: The accelerating effect of aging on ettringite formation kept increasing with exposure duration although the amount of ettringite seeds in the sample decreased due to decomposition. Particle size measurements revealed a fraction of nanosized particles in samples that had been aged for 14 days. These particles are assumed to result from the decomposition of the prehydrates, which means they are primarily  $\text{CaCO}_3$ . They would heterogeneously catalyze the hydration process similar to a limestone addition as described in chapter **2.4.2** and gradually replace the decomposing ettringite seeds as the cause for the acceleration effect.

- ③ To determine the impact of cement aging on retarders, the hydration experiments were repeated with 0.1% bwoc NaGluc or 0.4% bwoc KPPhos dissolved in the mixing water. At these dosages, the two retarders display a comparable performance in fresh CEM I 52.5 N. After aging, the retarders were found to primarily compete with the seeding effect on ettringite formation: After intermediate exposure of 3 and 7 days, when the amount of ettringite seeds was the highest, the retarders had only a weak impact on hydration. In turn, after long aging periods, when a significant part of the ettringite seeds had decomposed, the retarders had the strongest impact, which was even higher than on fresh CEM I 52.5 N. This also signifies that the accelerating effect of the nanosized decomposition products gets overridden by the retarding ability of both NaGluc and KPPhos. Regarding the individual performance of the retarders, calorimetry showed that KPPhos performed equally to or worse than NaGluc had the cement been aged for 1 or 3 days. After an exposure of 7 or 14 days however, KPPhos retarded the hydration much stronger than NaGluc.

The reason for this performance shift was determined by examining the retarder depletion from the liquid phase and analyzing the concentration of free  $\text{Ca}^{2+}$  in the pore solution. Unlike 0.1% bwoc NaGluc, 0.4% bwoc KPPhos is always fully depleted from the liquid after short or intermediate exposure. Only after 14 days of aging did a measurable amount remain dissolved after the hydration start. At the same time, the amount of free  $\text{Ca}^{2+}$  in the pore solution was found to decrease with increasing exposure duration. As a result, after 14 days of aging 0.4% KPPhos were

## 4.2 TOPIC 1: AGING IMPACT ON RETARDER PERFORMANCE

---

sufficient to precipitate the free  $\text{Ca}^{2+}$  entirely. This is confirmed by the KPPHos not getting fully depleted in this case. As described in the overview of journal article 1, the removal of  $\text{Ca}^{2+}$  strongly retards the hydration of aged cement or  $\text{C}_3\text{A}$  since the growth of ettringite seeds is impeded by the lack of calcium and the poisoning effect of calcium phosphate precipitates. It explains the strong performance of KPPHos at long aging periods. Whereas after short and intermediate exposure more ettringite seeds are present and calcium is released into the pore solution faster which means a KPPHos dosage of 0.4% bwoc is no longer sufficient to stall the hydration as effectively.

- ④ The transferability of this mechanistical study on hydration behavior to actual cement application was tested by comparing the results to experiments on setting behavior and compressive strength development. The setting times of aged cements matched the occurrence of the single peaks in calorimetry, verifying that these peaks are primarily caused by ettringite formation. The strong retarding effect of KPPHos after long aging periods as observed in calorimetry could only partially be reproduced since the samples tended to dry out before properly setting. The compressive strength of aged CEM I 52.5 N developed much slower than that of fresh cement, confirming that the hydration of the silicate phases is significantly impeded after aging. Overall, no discrepancies between the mechanistical investigations and the engineering properties of aged cement were found.

**4.2.2.2 Reprint of journal article 2**

**New insights into the effects of aging on Portland cement hydration and on retarder performance**

F. A. Hartmann, J. Plank

*Construction and Building Materials*, 274, 2020, 122104.

<https://doi.org/10.1016/j.conbuildmat.2020.122104>

Reprinted with permission from Elsevier



## New insights into the effects of aging on Portland cement hydration and on retarder performance



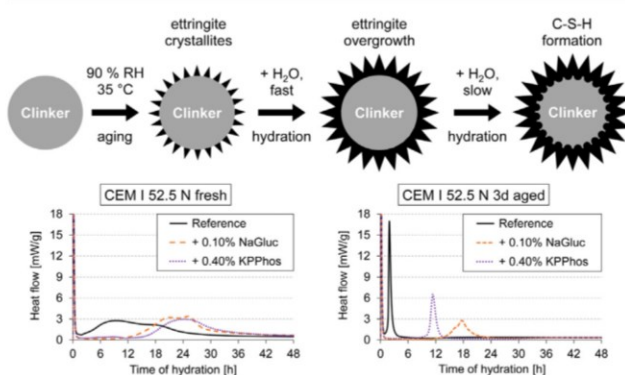
Florian A. Hartmann, Johann Plank\*

Technische Universität München, Chair for Construction Chemistry, Lichtenbergstr. 4, 85748 Garching, Germany

### HIGHLIGHTS

- Effect of aging a CEM I 52.5 N at 90 % RH/35 °C on hydration was investigated.
- Nanoscale ettringite from aging acts as seeding material which accelerates setting.
- Resulting ettringite overgrowth slows C-S-H formation and strength development.
- Impact of retarders lower after aging, increases with carbonation of ettringite.

### GRAPHICAL ABSTRACT



### ARTICLE INFO

#### Article history:

Received 28 September 2020

Received in revised form 9 December 2020

Accepted 17 December 2020

#### Keywords:

Portland cement  
Cement aging  
Prehydration  
Admixture  
Retarder  
Ettringite  
Setting behavior  
Compressive strength

### ABSTRACT

To gain a better understanding of the aging impact on the mechanisms of cement hydration, a Portland cement was intentionally exposed to moist air under controlled conditions. This resulted in the formation of nanoscale ettringite needles on the particle surfaces which act as seeding materials, thereby accelerating setting. The subsequent ettringite overgrowth of cement particles slows water access to the silicate phases, thus retarding strength development. The effectiveness of gluconate and pyrophosphate retarders against this accelerated hydration is limited at short aging periods, but sharply increases towards prolonged aging times when the ettringite seeds are carbonated by atmospheric CO<sub>2</sub>.

© 2020 Elsevier Ltd. All rights reserved.

### 1. Introduction

Cements possess a high inherent reactivity towards water. Although this is advantageous in application, it also leads to

premature hydration when unintentionally exposed to moist air. While improper storage and handling of cementitious materials at high humidities are commonly known to cause such "prehydration", this can occur already in the manufacturing of cement. During clinker milling, gypsum is interground to act as a set control agent in cement hydration. With the temperature in the mill reaching ~ 110–120 °C, crystal water from gypsum is released and reacts with the clinker. Even worse, often additional water is injected into

\* Corresponding author.

E-mail address: sekretariat@bauchemie.ch.tum.de (J. Plank).

the mill for cooling purposes. Moreover, the elevated temperatures occurring in cement silos may trigger further release of water [1].

Earlier studies reported that individual cement constituents can react differently when exposed to moisture. The aluminate clinker phases were found to sorb water faster than the silicate phases [2,3]. Using a sorption balance, Dubina et al. [4] determined the threshold relative humidity (RH) values at which the clinker phases begin to sorb water. The results were as follows: C<sub>3</sub>S 63 %, C<sub>2</sub>S 64 %, cubic C<sub>3</sub>A 80 %, orthorhombic C<sub>3</sub>A 55 % and C<sub>4</sub>AF 78 %.

Cement prehydration results in the premature formation of hydration products on the particle surfaces including ettringite and calcium silicate hydrates. This was shown to have adverse effects on rheological properties, setting times and strength development of cementitious building materials [5–10]. Furthermore, the interactions between cement and admixtures which are intricately linked to particle surface properties were reported to change significantly and often inconsistently after aging. Dubina et al. [11] presented that aged cement, while exhibiting a higher water demand, required lower amounts of methylcellulose to achieve a comparable water retention capacity. They also observed a sharp decline in the accelerating performance of calcium formate and amorphous Al<sub>2</sub>O<sub>3</sub> with increasing aging duration. Most remarkably, the accelerating effect even turned into a retarding effect after the Portland cement had been exposed to moisture for more than 3 days. In contrast, for aged cement Maltese et al. [12] reported a setting time reduction from aluminum sulphate used as a shot-crete accelerator.

Further studies presented that cement aging can both positively and negatively affect the interaction with superplasticizers. Winnefeld [13] observed an increasing performance of both polycaprolactone and polycarboxylate based superplasticizers in aged cement while Dubina et al. reported the opposite [11]. Meier et al. [14] suggested that the impact of cement aging on superplasticizers depends on the composition of the cement in use, especially on the amount and polymorphism of the C<sub>3</sub>A clinker phase.

Against this background, we aim to expand both on the hydration behavior of aged cement and the interaction with admixtures. For this purpose, a CEM I 52.5 N was exposed to moist air at 90 % RH and 35 °C for up to 14 days. After aging, the samples were characterized using thermogravimetric analysis (TGA) and powder X-ray diffraction (XRD) and their hydration behavior was compared to a fresh CEM I 52.5 N sample via heat flow calorimetry and *in situ* XRD.

So far, none of the previous studies has elucidated the impact of retarders based on different working mechanisms on the hydration of aged cement. Therefore, the hydration of prehydrated cement in the presence of sodium gluconate (NaC<sub>6</sub>H<sub>11</sub>O<sub>7</sub>) or potassium pyrophosphate (K<sub>4</sub>P<sub>2</sub>O<sub>7</sub>) dissolved in the mixing water was investigated. The working mechanism of gluconate relies on hindrance of the dissolution of the clinker phases and the crystal growth of hydrates by surface adsorption of the retarder [15,16]. Pyrophosphate is known to chelate calcium ions and forms a layer of calcium pyrophosphate around the cement particles. This acts as a barrier against water access to the clinker, while at the same time already dissolved calcium is removed from the pore solution which restricts the formation of hydration products [17,18]. Our goal was to determine which retarder was more effective and reliable in aged CEM I 52.5 N and possibly counteracted undesired effects from prehydration such as changes in the setting behavior. Mechanistically, the uptake of retarder during hydration resulting from adsorption on cement was quantified via total organic carbon (TOC, gluconate) determination or spectrophotometric (pyrophosphate) analysis. Furthermore, the impact of retarder addition on the calcium ion concentration in the pore solution of aged cement was examined via inductively coupled plasma optical emission spectrometry (ICP-OES).

Finally, the behaviors of both retarders in actual application of an aged CM I 52.5 N with respect to setting behavior and early compressive strength development were assessed.

## 2. Experimental Section

### 2.1. Materials

The CEM I 52.5 N sample (Milke® brand) was provided by HeidelbergCement. Its mineralogical composition as was determined (unless stated otherwise) by Rietveld refined powder XRD [19] using a Bruker AXS D8 Advance® instrument with Bragg-Brentano geometry and a CuK $\alpha$  ( $\lambda = 1.5406 \text{ \AA}$ ) source is presented in Table 1.

Sodium gluconate (Merck EMSURE®, purity 98.0+ %) and potassium pyrophosphate (Sigma-Aldrich, 97 %) retarders were commercially acquired and used as-is. In all experiments with retarders present, they were dissolved in the mixing water prior to hydration. As mixing water, deionized H<sub>2</sub>O produced with a Barnstead Nanopure Diamond® water purification system was used.

### 2.2. Aging procedure

The fresh CEM I 52.5 N powder was spread out on 135 × 60 cm Plexiglas® plates in portions of 50.0 g (layer thickness only ~0.2 mm), thus maximizing the exposure of particle surfaces to water vapor. The samples were then aged at 90 ± 5 % relative humidity and 35 ± 2 °C in a climate box for 1; 3; 7 or 14 days. After exposure, the aged cement powder was collected, weighed with a Sartorius CP 423 S laboratory scale, and stored in airtight containers.

### 2.3. Characterization of aged cement

#### 2.3.1. Thermogravimetric analysis

Compositional changes of the cement samples resulting from aging were determined via thermogravimetric analysis (TGA) using a Netzsch simultaneous thermal analyzer (STA) 409 PC Luxx®. In measurement, the samples were heated from 20 to 900 °C at a constant rate of 10 °C per minute.

#### 2.3.2. Powder XRD

The formation of early hydration products on the particle surfaces during the aging process was investigated with powder XRD. A fresh CEM I 52.5 N sample was filled into a plastic XRD holder and aged alongside the spread-out samples on the Plexiglas® plates. After aging, the sample placed on the XRD holder

**Table 1**  
Phase composition and minor constituents of the CEM I 52.5 N sample.

Phase	Content [mass %]
C <sub>3</sub> S	52.7
C <sub>2</sub> S	26.1
C <sub>3</sub> A cub.	7.7
C <sub>3</sub> A orth.	1.2
C <sub>4</sub> AF	3.2
Free lime (Franke)	0.1
Anhydrite	2.5
Hemihydrate*	0.3
Dihydrate*	0.6
Calcite	4.4
Quartz	0.9
Arcanite	0.2
Dolomite	0.1
Sum	100.0

\* determined via thermogravimetry

was measured without any additional preparation. This method avoids potential damage to the crystallite hydrates when the aged cements were collected from the plates. Powder XRD measurements were taken at a range of 5–70° 2θ in steps of 0.008°, with an exposure time of 0.5 s per step at 30 kV accelerating voltage and 35 mA irradiation intensity.

### 2.3.3. SEM and ESEM imaging

Scanning electron microscopy (SEM) of the aged CEM I 52.5 N was carried out on a FEI XL 30 FEG device with a secondary electron (SE) detector. Images of uncoated samples were taken at an accelerating voltage of 10 kV. Environmental SEM (ESEM) of hydrated samples of the aged cement was performed on the same instrument after their hydration had been stopped with isopropyl alcohol. Here, a Peltier cooling stage and a gaseous secondary electron (GSE) detector were used to take images of uncoated samples at 1 mbar H<sub>2</sub>O pressure and an accelerating voltage of 15 kV.

### 2.3.4. Particle size distribution

The particle size distributions of fresh and aged CEM I 52.5 N samples were determined via laser granulometry on a Cilas model 1064 instrument. Prior to measurement, the samples were subjected to ultrasound in isopropyl alcohol to disperse agglomerates.

## 2.4. Hydration experiments

### 2.4.1. Isothermal heat flow calorimetry

Heat flow during hydration of the fresh and aged cement in the absence and presence of retarders was recorded using a Thermo-metric AB TAM Air® 3114 isothermal calorimeter at 20 °C following DIN EN 196-11 [20]. For each measurement, 4.00 g powder were weighed into a 10 mL glass vial. Pure deionized water or retarder solution tempered to 20 °C was added to the cement at a water-to-cement (w/c) ratio of 0.55 before the vial was sealed with a crimped aluminum cap. The sample was then homogenized for 120 s using a VWR VWT® 1419 vortex mixer at maximum speed and subsequently placed into the measurement chamber. The hydration reaction was recorded until the heat flow fell below 0.5 mW/g.

### 2.4.2. *in situ* XRD

3.20 g of fresh or aged cement in pure water or retarder solution (w/c ratio = 0.55) were homogenized for 120 s in 10 mL glass vials at maximum speed using the vortex mixer. The paste was then poured into a metal *in situ* sample holder and covered with an X-ray transmittant polyimide (Kapton®) film to prevent water evaporation. Scans were recorded every 30 min at 5–50° 2θ, 0.034°/step, 0.4 sec/step, 30 kV and 35 mA.

## 2.5. Pore solution analysis

Depletion of the retarders from the mixing water by fresh or aged cement was investigated via TOC analysis (samples containing NaGluc) or UV-Vis spectrophotometry (samples containing KPPPhos). Furthermore, ICP-OES was employed to determine the impact of aging and retarder addition on the free Ca<sup>2+</sup> concentration in the pore solution. Preparation of the pore solution was similar for all three methods: 8.00 g of fresh or aged cement were added to pure water or retarder solution at an increased w/c ratio of 2.0 to account for fluid uptake by the cement. The slurries were homogenized for 120 s using the vortex mixer set to maximum speed before centrifugation at 8500 rpm and 20 °C for 10 min utilizing a Stratos Biofuge®. The supernatants were decanted, and small solid particles were removed using a polyethersulfone (PES) syringe filter with a mesh size of 0.2 μm.

### 2.5.1. TOC and UV-Vis spectrophotometry

Supernatants from samples containing gluconate were measured using an Elementar *liquiTOC*® total organic carbon (TOC) analyzer after adjusting the pH to 2. Supernatants from samples holding pyrophosphate were subjected to acidic hydrolysis for 45 min at 90 °C and a pH of 1 to convert the pyrophosphate to orthophosphate. The pH was then increased to 3 before an ammonium molybdate solution containing potassium antimony(III) oxide tartrate (Bernd Kraft) for photometric determination of phosphate was added alongside L-(+)-ascorbic acid (Alfa Aesar, 99+ %) as described in a previous study [21]. Presence of phosphate in the supernatant was indicated by a blue color resulting from the complex formed with the molybdate solution ("Mo blue method") [22]. The phosphate content was quantified by determining the intensity of the blue color via UV-Vis spectrophotometry at 880 nm using a Cary WinUV® 50 device.

### 2.5.2. ICP-OES

Inductively coupled plasma optical emission spectrometry (ICP-OES) was performed on an Agilent 700 Series device equipped with a SPS 3 autosampler. The supernatants were diluted at 1: 30 (vol./vol.) with 1 M HNO<sub>3</sub> before measurement. Calibration was carried out at concentrations of 0.1; 1; 10 and 100 mg/L using a commercial standard (Merck ICP multi-element standard solution IV).

## 2.6. Properties of paste produced from fresh and aged cement

Investigations into the setting behavior and compressive strength development were performed according to standard test methods which were modified for the smaller quantities of aged cement available.

### 2.6.1. Setting behavior

Setting behavior was determined based on a modified DIN EN 196-3 standard [23]. The experiment was scaled down according to an earlier study [24]. Hence, the steel load of the Vicat apparatus was replaced with aluminum, reducing its weight from 300 g to 100 g. Cylindrical glass vessels with an inner diameter of 15 mm and a height of 20 mm substituted the Vicat cone. For sample preparation, pure water or retarder solution at w/c ratios of 0.50, 0.55 and 0.60 were added to 15.00 g of fresh or aged cement placed in the glass vessel. The vessel was sealed with a snap-on lid before mixing for 120 s using a vortex mixer. Subsequently, the lid was removed, the glass vessel placed under the aluminum load and the test was performed at 60 % RH and 20 °C. The needle was lowered into the paste every 30 min until the initial set occurred and then every 15 min. The achievement of final set was verified by replacement of the needle with a Vicat ring as prescribed in the norm. In between measurements, the vessel was sealed again to mitigate water evaporation.

### 2.6.2. Compressive strength

Determination of compressive strength was performed according to a modified DIN EN 196-1 [25]. Test specimens were prepared from cement paste and not mortar as specified in the norm. 45.00 g of fresh or aged cement divided between two 40 mL glass vessels were mixed with pure water or retarder solution at a w/c ratio of 0.55, placed into two vortex mixers and homogenized for 120 s. The slurry was poured into a custom-made brass mold yielding three prisms with dimensions of 40 × 15 × 15 mm each. The mold was then placed on a Toni Technik ToniVib vibrating table set to 50 Hz for a further 120 s before excess paste was removed. After 24 h of storage at 20 °C above water (> 85 % RH), the specimens were demolded. Using a Toni Technik ToniNORM test plant, compressive strengths of the prisms were determined after demolding or after 2 or 6 days of additional storage under water.

### 3. Results and discussion

#### 3.1. Impact of aging on CEM I 52.5 N

##### 3.1.1. Mass changes resulting from the aging process

The first step in the analysis of the aged CEM I 52.5 N sample was to weigh the samples after removal from the climate box to capture the time-dependent mass change resulting from exposure to humid atmosphere. As displayed on the right in Fig. 1 (solid line plot), the mass of the sample increases continuously over the 14 days aging period, most strongly in the first 3 days which presents about 50 % of the total weight increase recorded after 2 weeks of exposure. This result demonstrates that even relatively short exposure times induce a significant uptake of moisture by cement.

The uptake of atmospheric moisture was more thoroughly investigated by thermogravimetric analysis (TGA). The total percentual mass losses recorded for the cement samples from 60 to 900 °C were split as shown in the table on the left of Fig. 1. Mass losses occurring below 550 °C can be primarily attributed to the release of H<sub>2</sub>O while above 550 °C mainly CO<sub>2</sub> is liberated by the decomposition of CaCO<sub>3</sub> [26,27]. In the fresh CEM I 52.5 N, H<sub>2</sub>O and CO<sub>2</sub> are released from the interground gypsum and limestone, while after aging the liberated water and CO<sub>2</sub> mainly derive from early hydration and carbonation products.

According to the individual mass losses recorded in Fig. 1, it is apparent that the uptake of water and the resulting hydrate formation contribute most to the mass increase occurring at early aging periods. This water sorption decelerates at extended exposure periods and reaches a plateau after 14 days. A similar trend can be observed for the uptake of CO<sub>2</sub>, yet the total amount of CO<sub>2</sub> sorbed is considerably higher than that of H<sub>2</sub>O.

It has to be stated that precise distinction between hydrate and carbonate decomposition from the aged samples is difficult, and some inaccuracy is involved. MgCO<sub>3</sub> resulting from the carbonation of periclase decomposes below 550 °C while the dehydration of calcium silicate hydrates (C-S-H) overlaps with the CO<sub>2</sub> release of carbonates and carbonated hydrates in TG-MS above 550 °C [10]. To differentiate the aging products from the interground materials, Stoian et al. [10] introduced the "prehydration index" (PI). The PI of an aged cement is calculated by subtracting from its total percentual mass loss  $\Delta m_t$  that of a fresh sample from the same batch  $\Delta m_0$ :

$$PI = \Delta m_t - \Delta m_0$$

We adopted this approach and converted the PI obtained for the individual aging periods into corresponding percentual mass increases, as is shown on the right in Fig. 1 (dashed line plot). They closely matched the percentual mass increases obtained from weighing the aged samples.

##### 3.1.2. Characterization of aging products

Powder XRD analysis was employed to identify the hydrates and carbonates formed during aging on the cement particles' sur-

faces. The XRD patterns of the fresh, 3 days and 14 days aged CEM I 52.5 N samples are displayed in Fig. 2.

There, ettringite was identified as the main hydration product resulting from aging at 90 % RH and 35 °C. Beyond 3 days of exposure the ettringite signal decreased, signifying carbonation and decomposition of this phase into calcite, aluminum hydroxide and gypsum as we have observed in previous studies [28,29] as well. Furthermore, despite a continuous decline of the C<sub>3</sub>S reflections, portlandite as by-product of the silicate hydration could only be detected after 3 days of aging (Fig. 2, right), signifying rapid conversion of portlandite to calcite [30,31]. Correspondingly, the reflections signifying calcite which already are present in the diffractogram of fresh CEM I 52.5 N as a result of limestone addition increased significantly in intensity over the 14-day exposure period.

#### 3.2. Hydration behavior of fresh and aged cement

##### 3.2.1. Calorimetric analysis

Following the characterization of cement samples exposed to moist air, their hydration behavior was investigated via heat flow calorimetry and compared to that of the fresh CEM I 52.5 N. In all tests, a w/c ratio of 0.55 was applied. As is presented in Fig. 3, the unaged sample displays a hydration behavior which is characteristic for Portland cements. Following the dormant period, the main hydration reaction occurs over an extended period of time (2–24 h) with the heat flow curve showing two peaks signifying the maximum of the silicate reaction at ~ 9 h of hydration time, and the sulfate depletion peak (conversion of ettringite to monosulfo aluminate) at ~ 20 h.

For the aged samples, a radically different hydration behavior was observed. Already after 24 h of exposure, the two peaks were replaced by a very prominent spike of heat release approximately 6.5 h after the start of hydration (Fig. 3). This peak occurs earlier with increasing aging time (3 and 7 days, ref. Table 2 in Section 3.3) until after 14 days (Fig. 3, dotted line) of exposure it completely merges with the dissolution heat released during the first contact of cement with water. Thus, aging appears to greatly accelerate the hydration process.

##### 3.2.2. *in situ* XRD analysis

To verify this observation, the first 16 h of hydration of the fresh and aged CEM I 52.5 N were monitored via *in situ* XRD. Fig. 4 displays the peak intensities of ettringite (measured at  $2\theta = 9.0^\circ$ ), portlandite ( $2\theta = 17.8^\circ$ ) and alite ( $2\theta = 34.2^\circ$ ) over the first 16 h of hydration. After aging, a significant increase in ettringite formation was observed. On the other hand, the formation of portlandite as a side-product of silicate hydration was strongly reduced. Correspondingly, there was no sign of alite consumption as a result of C-S-H formation after aging (X-ray intensities of clinker phases are low at the start of hydration when the sample surface is most wet). The acceleration after aging observed via calorimetry

Aging period	Mass loss [%] 60–550 °C (prim. H <sub>2</sub> O)	Mass loss [%] 550–900 °C (prim. CO <sub>2</sub> )	Prehydration index (PI) [%]
fresh	1.0	2.4	0
1 day	2.5	5.7	4.8
3 days	3.6	7.6	7.9
7 days	5.0	11.0	12.7
14 days	5.3	12.4	14.4

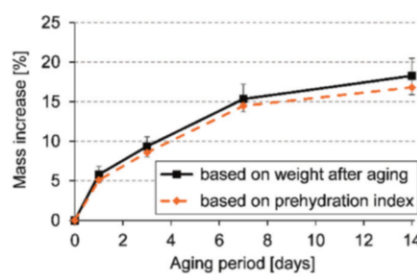
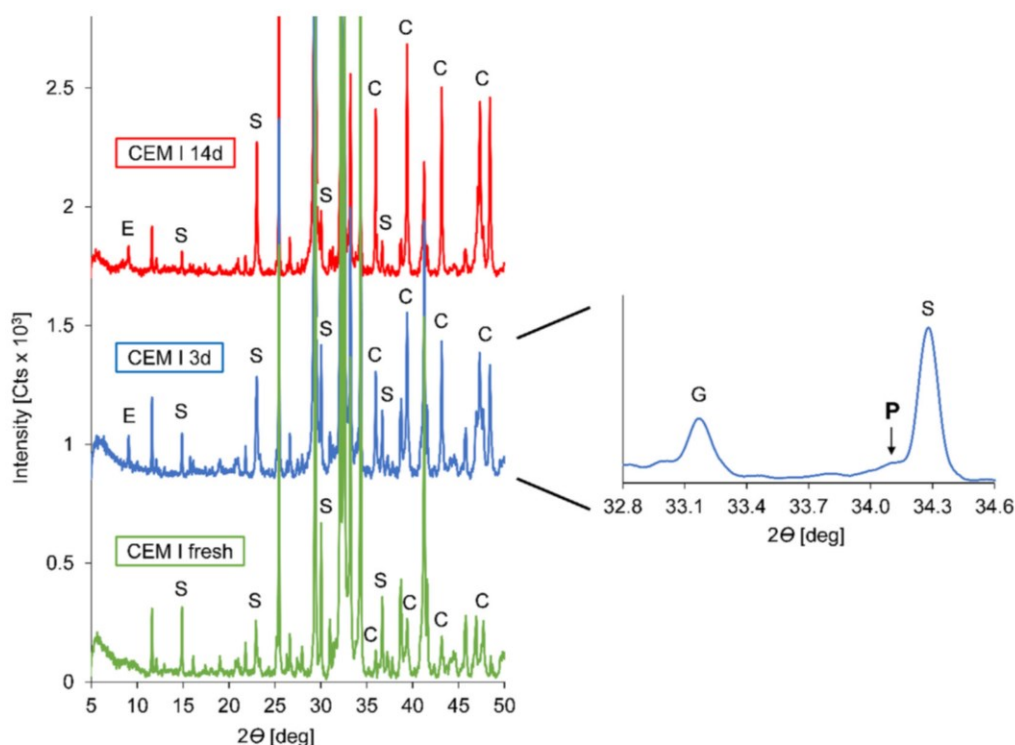
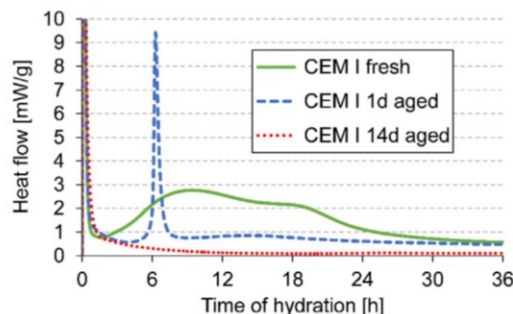


Fig. 1. Thermogravimetric analysis of the CEM I 52.5 N sample before and after aging for 1–14 days at 90 % RH/35 °C.



**Fig. 2.** Powder XRD analysis of the CEM I 52.5 N sample, before and after aging at 90 % RH / 35 °C. C = calcite; E = ettringite; S =  $\text{C}_3\text{S}$ ; P = portlandite.



**Fig. 3.** Heat flow calorimetric analysis of fresh and aged CEM I 52.5 N samples ( $w/ratio = 0.55$ ).

primarily applies to ettringite formation while the hydration of the silicates appears to be retarded by the aging process.

### 3.2.3. SEM / ESEM imaging

To probe into the mechanism underlying the hydration behavior, SEM images of fresh (Fig. 5, left) and 1-day aged cement (Fig. 5, center) were taken. As can be seen there, the aged cement sample is covered with nanoscale ettringite needles which are absent in the fresh cement sample. Apparently, the submicron ettringite crystals act as a seeding material which trigger rapid ettringite formation in aged cement as recorded in calorimetry and *in situ* XRD. In consequence, the cement particles hydrated e.g. for 8 h exhibit a dense overgrowth of ettringite on their surface, as observed via ESEM imaging (Fig. 5, right).

Apparently, this overgrowth slows the access of mixing water to the yet unreacted part of the clinker which mostly consists of silicate phases. This way, the silicate reaction is strongly retarded, resulting in a much-reduced heat flow after the early hydration

period (Fig. 3), and in decreased portlandite formation (Fig. 4). A schematic representation of the process underlying the mechanism proposed for the hydration of an aged Portland cement is shown in Fig. 6.

As is evidenced from the powder XRD investigations on aged cement (see Section 3.1.2), at extended exposure periods to moist air, ettringite present on the particle surfaces deteriorates due to carbonation. Hence, at longer aging times a reduced seeding effect and consequently lower acceleration of early cement hydration should be expected. However, when the aging time was prolonged to 14 days, hydration of the aged cement occurred earlier than after shorter aging periods. We assume that hydration is further accelerated by a fine particle fraction identified in 14 days aged cement via lasergranulometric determination of the particle size as is displayed in Fig. 7. Compared to fresh CEM I 52.5 N, after 3 days of aging the average particle size increased due to ettringite overgrowth of the particles and agglomeration while the small particle fraction as represented by the  $d_{10}$  value (maximum diameter of the smallest 10 % of the particle distribution) decreased. However, after 14 days of aging a noticeable fraction of fine particles (~ 400 nm) appeared, which we attribute to nanoscale calcite resulting from the carbonation of ettringite.  $\text{CaCO}_3$  was proven to contribute to cement hydration by hemicarboaluminate and monocarboaluminate formation [32]. At a small enough particle size, it can provide additional nucleation sites [33] which we assume to provide an accelerator replacement for the decomposed ettringite.

### 3.3. Performance of retarders in fresh and aged cement

So far, the investigations demonstrated that aging much accelerates the hydration of CEM I 52.5 N as a result of the seeding effect of nanoscale ettringite and calcite. This gives reason to study the effectiveness of set retarders in aged cement.

## 4.2 TOPIC 1: AGING IMPACT ON RETARDER PERFORMANCE

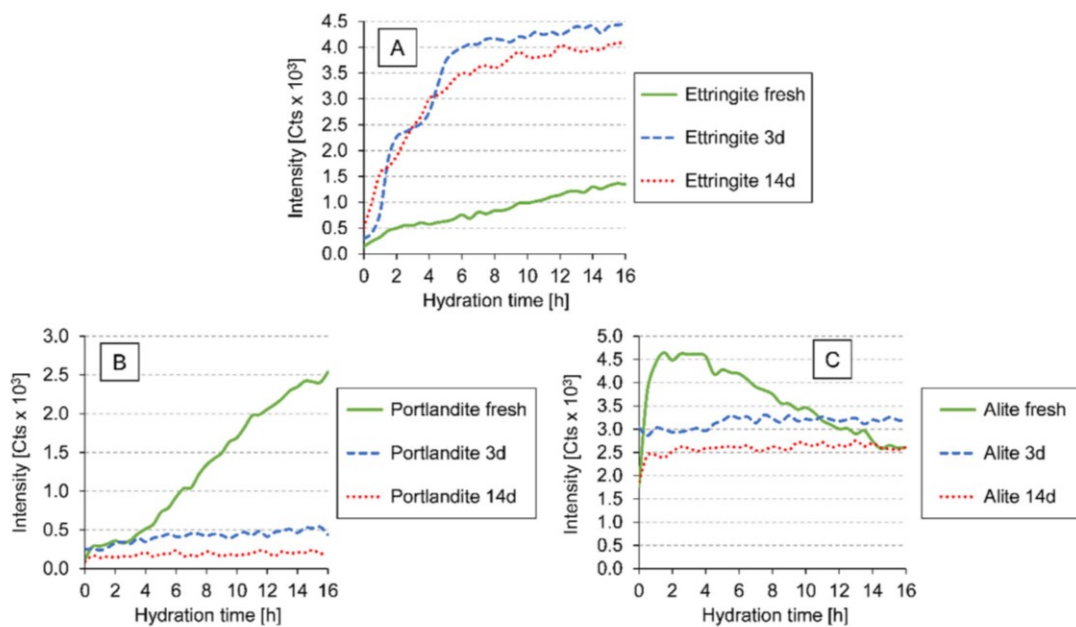


**Fig. 4.** *In situ* XRD analysis of the hydrating CEM I 52.5 N ( $w/c$  ratio = 0.55), before and after aging for 3 days at 90 % RH / 35 °C; displayed are peak intensities of ettringite (A, measured at  $2\theta = 9.0^\circ$ ), portlandite (B,  $2\theta = 17.8^\circ$ ) and alite (C,  $2\theta = 34.2^\circ$ ).

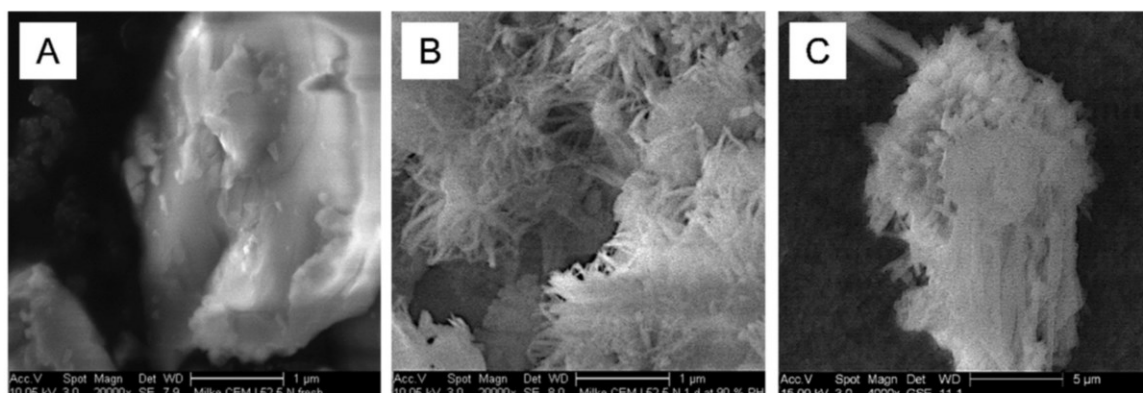


**Fig. 5.** SEM images of CEM I 52.5 N sample before (A) and after (B) aging for 1 day at 90 % RH / 35 °C. ESEM image of 1-day aged CEM I 52.5 N particle (C) after 8 h of hydration at  $w/c = 0.55$ , magnification: 20000 (SEM); 4000 (ESEM).

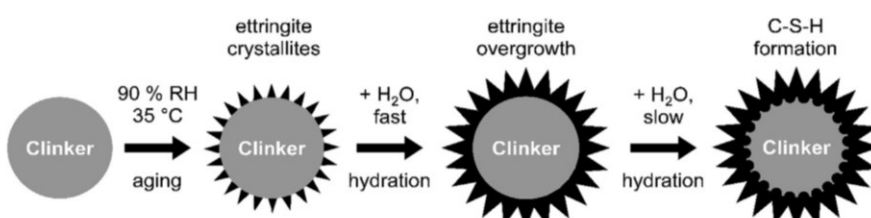


**Fig. 6.** Mechanism proposed to explain the hydration pathways of aged Portland cement.

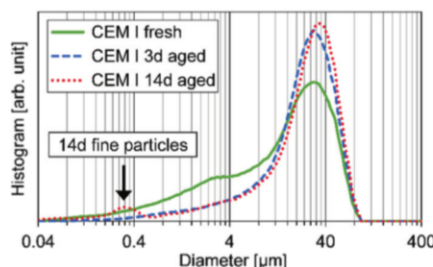
Here, the performances of a retarder which works via adsorption on cement, sodium gluconate (NaGluc), and potassium pyrophosphate (KPPhos) which achieves retardation via chelation and precipitation of calcium ions, were compared.

0.10 % by weight of cement (bwoc) of NaGluc and 0.40 % bwoc KPPhos possess a similar retardation capability in fresh CEM I 52.5 N (Fig. 8). Interestingly, after 3 days of aging, the difference

in dose-effect relation between the two retarders is even further exacerbated, with 0.10 % NaGluc retarding hydration significantly more than 0.40 % KPPhos (Fig. 8).

The results on the retarding effectiveness of the two admixtures in fresh and aged cement samples as evidenced by heat flow calorimetry are summarized in Table 2. The times listed correspond to the heat flow maxima as exemplarily marked by

## 4.2 TOPIC 1: AGING IMPACT ON RETARDER PERFORMANCE



Sample	Particle size [μm]		
	d <sub>10</sub>	d <sub>50</sub>	d <sub>90</sub>
fresh	1.1	15.6	45.4
3 d aged	4.0	23.9	49.7
14 d aged	2.4	25.2	51.4

Fig. 7. Particle size distribution of fresh and aged CEM I 52.5 N samples as measured by laser granulometry.

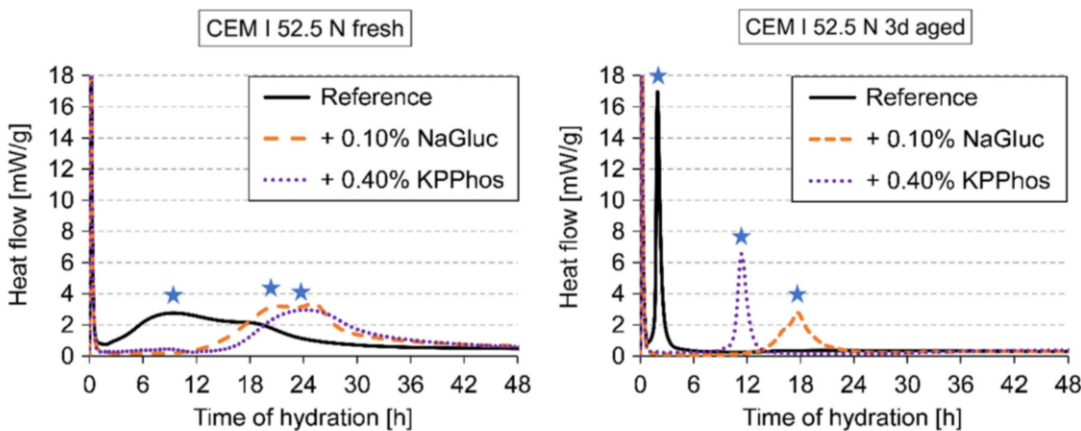


Fig. 8. Heat flow calorimetric analysis of fresh (left) and 3 days aged (right) CEM I 52.5 N sample hydrating in the presence or absence of NaGluc or KPPhos retarder (w/c ratio = 0.55); stars indicate the first maximum of heat flow.

five-point stars in Fig. 8. Since a double peak occurs in fresh CEM I 52.5 N, the time of the first peak is given.

It is observed that in the presence of both retarders hydration is still accelerated when the cement sample is aged up to 3 days (KPPhos) or 7 days (NaGluc). However, at further increased aging periods the acceleration switched completely to retardation and became particularly strong for KPPhos which retarded the 14 days aged cement sample for no less than 293 h.

Table 2

Occurrences of first heat flow maxima during the hydration of fresh and aged CEM I 52.5 N in the presence or absence of NaGluc or KPPhos retarder (w/c ratio = 0.55).

Sample	Time [h] of first heat flow peak		
	Reference	+ 0.10 % NaGluc	+ 0.40 % KPPhos
fresh	9.0	21.0	24.0
1 d aged	6.5	16.0	17.0
3 d aged	2.0	17.0	11.5
7 d aged	3.0	15.0	57.0
14 d aged	< 1*	28.5	293.0

\*no distinct peak observed, as described in Section 3.2.1.

The experiments suggest that both admixtures present effective retarders in fresh as well as aged cement, and that their performance decreases at short to medium aging times as they have to counteract the seeding effect of nanoscale ettringite produced during prehydration. However, once the seeding effect of nanoscale ettringite weakens due to carbonation, the retarder effectiveness increases drastically. KPPhos is apparently more sensitive than NaGluc to the changing amount of nanoscale ettringite present due to formation and degradation during aging. At the same time, it becomes evident that for a cement sample which has been unintentionally aged for an unknown period, its behavior in combination with retarders might prove quite unpredictable.

In two preceding studies [14,29] on the aging of binary C<sub>3</sub>A / gypsum blends at similar conditions of 90 % RH / 35 °C, the peak amount of ettringite in an aged sample was reached between 3 and 7 days of exposure, which fits the retarders' behavior in the present work. It also serves as an explanation to why the pure CEM I 52.5 N reference hydrates slightly later after 7 days aging (3 h) than after 3 days (2 h). After 7 days the amount of nanoscale calcite is apparently not yet high enough to offset the loss of nanoscale ettringite due to carbonation.

### 3.4. Pore solution analysis of fresh and aged cement samples

#### 3.4.1. Depletion of retarders from pore solution

To mechanically understand the behavior of the retarders during the hydration process, the interaction of NaGluc and KPPhos with aged cement particles was assessed via adsorption measurements employing TOC (NaGluc) or UV-Vis spectrophotometry (KPPhos).

Fig. 9 displays the depletion for different dosages of NaGluc and KPPhos from the pore solution as calculated from the amounts remaining in the liquid phase. Pastes holding 0.10 % NaGluc or 0.40 % KPPhos as applied in the hydration experiments were studied. It was found that depletion via adsorption of gluconate decreases substantially with aging time, especially at increased dosages. For example, at 0.1 % addition to cement NaGluc adsorption decreased from 92 % in the fresh cement to 73 % in the 14 days aged cement. As such, increased aging durations appear to have a similar effect as delayed addition of gluconate to the paste which benefits its retarding capability due to the presence of fresh, not yet adsorbed retarder. This explains the consistent performance of gluconate in aged CEM I 52.5 N observed via heat flow calorimetry (Table 2).

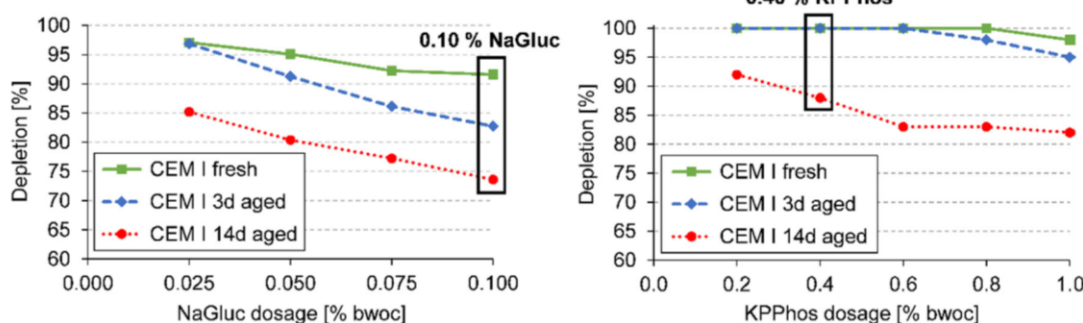


**Fig. 9.** Depleted amounts of sodium gluconate (NaGluc, left) or potassium pyrophosphate (KPPhos, right) from the pore solution of fresh and aged CEM I 52.5 N pastes (w/c ratio = 2.0).

In contrast, 0.40 % KPPhos are completely depleted from the pore solution in both the fresh and the 3 days aged cement. This elucidates the poor performance of KPPhos compared to NaGluc in heat flow calorimetry after 3 days aging. Only in the paste of the 14 days exposed CEM I 52.5 N the pyrophosphate had not been completely precipitated, there still 18 % had remained in solution. With regards to the vastly superior retardation of KPPhos after 14 days (Table 2), it appears when both retarders remain partially dissolved that pyrophosphate can retard the hydration much longer than gluconate.

#### 3.4.2. Impact of retarders on $\text{Ca}^{2+}$ concentration in the pore solution

The depletion methods were supplemented by examining the effect of NaGluc or KPPhos addition on the  $\text{Ca}^{2+}$  concentration present in the pore solution of hydrating cement.

Fig. 10 displays the results obtained via ICP-OES for fresh and aged CEM I 52.5 N. As is determined by the reference samples, the  $\text{Ca}^{2+}$  concentration decreases with increasing aging period, signifying slower dissolution of the cement resulting from the ettringite overgrowth as illustrated in Fig. 6. Addition of 0.10 % NaGluc consistently results in slightly lower values as compared to the reference. The difference diminishes with increasing aging time, indicating that the adsorption of gluconate on cement particles hindering  $\text{Ca}^{2+}$  dissolution lessens, which mirrors the observations made before on depletion (Fig. 9).

When 0.40 % KPPhos are admixed to the fresh CEM I 52.5 N paste, the  $\text{Ca}^{2+}$  concentration is just ~ 20 % lower than in the reference which signifies that only part of the amount of calcium dissolving from fresh cement can be chelated at this KPPhos dosage. However, after 3 days of aging, the amount of  $\text{Ca}^{2+}$  in the pore solu-

tion decreases drastically by ~ 75 %, indicating that most of the dissolved calcium is getting precipitated. Finally, after 14 days of exposure practically all  $\text{Ca}^{2+}$  is removed from the pore solution by KPPhos. Thus, the rate of calcium dissolution sharply decreases with increasing aging time and it can be assumed that an excess of KPPhos remains in the pore solution of 14 days aged cement which matches the results from spectrophotometry (Fig. 9).

#### 3.5. Impact of retarders on engineering properties of fresh and aged cement

##### 3.5.1. Investigation of setting behavior

In the final part of the present study, the effect of the retarders on application-related properties of aged cement samples, namely setting behavior and compressive strength development was investigated.

The results for the setting behavior are displayed in Fig. 11. At the top, the penetration depth of the Vicat needle during hydration of a 3 days aged CEM I 52.5 N sample is plotted as an example. Below a value of 5 %, penetration depth did not change significantly anymore. This indicates achievement of final set, which was verified with the Vicat ring.

The final setting times for the individual mixtures are summarized in the table part of Fig. 11. Apart from the w/c ratio of 0.55 first used in heat flow calorimetry and *in situ* XRD, 0.50 for fresh and 0.60 for 14 days aged cement were tested as well, since water demand progressively increases with aging time. While 0.55 w/c ratio almost results in bleeding when applied to fresh CEM I 52.5 N, after 14 days of exposure it just barely enables homogenization.

The setting times of non-admixed fresh and aged CEM I 52.5 N correspond very well to the heat flow curves presented before in Fig. 8 and tabulated in Table 2. They confirm that the heat release primarily is owed to accelerated ettringite formation. The superior set retarding ability of NaGluc in 3 days aged cement shown in Fig. 11 (top) also matches the heat flow calorimetry. However, in the setting of 14 days aged cement the vastly superior retardation of KPPhos as observed in heat flow calorimetry is not apparent. Also, the effectiveness of KPPhos appears to strongly depend on the w/c ratio of the paste even for the fresh CEM I 52.5 N. Unlike heat flow calorimetry, the samples are not sealed throughout the setting process. For the duration of each penetration depth measurement, the snap-on lids are removed which results in water evaporation. Since an airtight sealing during setting on the job site is unrealistic, the high retardation capability of KPPhos towards long aging times as suggested by heat flow calorimetry does not directly translate to actual application.

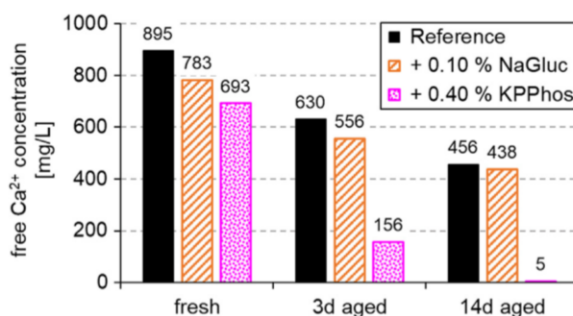
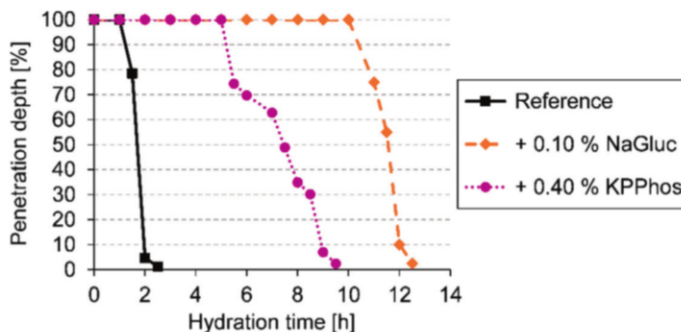


**Fig. 10.** Concentration of freely dissolved  $\text{Ca}^{2+}$  present in the pore solution of fresh and aged CEM I 52.5 N pastes admixed with NaGluc or KPPhos retarder (w/c ratio = 2.0).

## 4.2 TOPIC 1: AGING IMPACT ON RETARDER PERFORMANCE



w/c ratio	Setting time [h]				
	fresh		3 d aged		14 d aged
	0.50	0.55	0.55	0.55	0.60
Reference	6.0	6.5	2.0	1.0	1.0
0.10 % NaGluc	17.5	18.5	12.5	9.0	23.5
0.40 % KPPhos	16.0	21.5	9.0	7.5	24.0

**Fig. 11.** Final setting times of fresh and aged CEM I 52.5 N samples, in the presence and absence of NaGluc or KPPhos retarder. At the top, the setting behavior of 3 days aged CEM I 52.5 N is shown as an example.

### 3.5.2. Determination of early compressive strength

While set retardation presents the primary reason for admixing retarders such as NaGluc and KPPhos to cement, further investigations were carried out to elucidate their impact on compressive strength development of the fresh and aged cement samples. Table 3 shows the compressive strength development over 1 week for pastes produced from fresh or aged CEM I 52.5 N samples admixed with retarder.

As expected, in the fresh cement the retarders decrease the compressive strength mainly during the first 24 h. However, between 3 days and 1 week of curing, KPPhos approximately matched the strength of the reference sample while NaGluc significantly exceeded those values. Strength gains from retarding admixtures [34] result from a more ordered controlled crystallization of cement hydrates.

Unlike setting, which was observed to accelerate after aging (Fig. 11), compressive strength development was slower as a result of exposure (Table 3). Even after 1 week of curing the 14 days aged CEM I 52.5 N had not developed any measurable strength, independent of whether a retarder had been added or not. This is in line with calorimetry where heat release after the ettringite formation

was negligible (Figs. 3 and 8). It confirms the mechanism proposed in Fig. 6 where C-S-H formation is impeded by the ettringite overgrowth of the cement particles.

## 4. Conclusions

The present study aimed at investigating the hydration behavior of a CEM I 52.5 N sample after exposure to 90 % RH / 35 °C for time periods between 1 and 14 days. Changes in the material composition caused by the aging process were examined via thermogravimetric analysis and powder XRD. Under these conditions, the aluminate as well as the silicate phases sorb water, with ettringite and portlandite being the primary prehydration products. In aged CEM I 52.5 N the amount of ettringite is highest between 3 and 7 days of aging, and later decreases as a result of ettringite carbonation into calcite, aluminum hydroxide and gypsum.

The hydration of aged CEM I 52.5 N samples was monitored via heat flow calorimetry, *in situ* XRD and (E)SEM imaging. Exposure to moist air results in the formation of nanoscale ettringite needles on the cement surface. During hydration, these crystals act as seeding materials, thereby greatly accelerating the reaction of the

**Table 3**

Compressive strength development of fresh and aged CEM I 52.5 N samples, hydrated in the presence or absence of NaGluc or KPPhos retarder (w/c ratio = 0.55).

Sample	Addition	Compressive strength [N/mm <sup>2</sup> ]		
		24 h	3 days	1 week
fresh	Reference	4.4	15.2	21.3
	+ 0.1 % NaGluc	< 3	19.9	29.4
	+ 0.4 % KPPhos	< 3	13.4	22.3
3 d aged	Reference	< 3	6.6	13.7
	+ 0.1 % NaGluc	< 3	4.5	14.7
	+ 0.4 % KPPhos	< 3	< 3	9.5
14 d aged	Reference	< 3	< 3	< 3
	+ 0.1 % NaGluc	< 3	< 3	< 3
	+ 0.4 % KPPhos	< 3	< 3	< 3

aluminates to ettringite. The ettringite overgrowth of the cement particles' surfaces strongly impedes the hydration of the calcium silicates.

Addition of set retarders sodium gluconate (0.1 % bwoc) and potassium pyrophosphate (0.4 % bwoc) respectively decelerates ettringite formation, as was observed via heat flow calorimetry. However, at short to medium aging times, the effectiveness of both retarders is limited by the strong seeding effect of the nanoscale ettringite. Only at prolonged aging times when the ettringite is gradually decomposed by atmospheric CO<sub>2</sub>, then both retarders develop strong effects which much exceed those in the fresh cement sample.

A mechanistic study on the retarders' depletion from the mixing water via adsorption (NaGluc) or Ca<sup>2+</sup> precipitation (KPPhos) revealed that the longer the CEM I 52.5 N had been exposed to moist air, the higher was the retarder concentration initially remaining in the pore solution during hydration. Thus, increased aging durations act similar to a delayed addition of the admixtures, which benefits their performance due to the presence of not yet consumed retarder after the start of hydration.

Finally, the effect of aging on setting behavior and early compressive strength development of the cements was investigated. The setting times of non-admixed fresh and aged CEM I 52.5 N corresponded to the results from heat flow calorimetry. The addition of retarders revealed a strong dependency of their effectiveness on the w/c ratio, more so for KPPhos than NaGluc, making the latter the more reliable choice.

Compressive strength of fresh and briefly aged CEM I 52.5 N was only initially reduced by the retarders, with the addition of sodium gluconate even resulting in a considerable gain as compared to the reference after 1 week of curing. However, after long aging periods the cement did not produce measurable strength during this timeframe regardless if retarders were present or not.

The results signify that the engineering properties of a cement sample and the effectiveness of chemical admixtures can be significantly affected by aging to the point of becoming unpredictable. Our results underline that careful handling and storage of cement samples or blends, especially when used in dry-mix mortar compounds, must be given high attention.

#### CRediT authorship contribution statement

**Florian A. Hartmann:** Conceptualization, Data curation, Investigation, Project administration, Validation, Visualization, Writing - original draft. **Johann Plank:** Funding acquisition, Resources, Supervision, Writing - review & editing.

#### Declaration of Competing Interest

The authors declare that they have no known competing financial interests or personal relationships that could have appeared to influence the work reported in this paper.

#### Acknowledgements

The authors are most grateful to Deutsche Forschungsgemeinschaft, Bonn, Germany (DFG) for financing this project under the grant PL-472 / 9-2 "Influence of aging of binder systems on the performance of additives". We would also like to express our thanks to HeidelbergCement company for providing the cement sample and to chair alumni Dr. Elina Dubina and Dr. Markus Meier for conducting preliminary investigations on the project.

#### References

- [1] A.E. Mould, D.W. Williams, The effects of high ambient temperatures on gypsum plasters, *Build. Sci.* 9 (3) (1974) 243–245, [https://doi.org/10.1016/0007-3628\(74\)90023-1](https://doi.org/10.1016/0007-3628(74)90023-1).
- [2] E. Dubina, J. Plank, L. Black, Impact of water vapor and carbon dioxide on surface composition of C<sub>3</sub>A polymorphs studied by X-ray photoelectron spectroscopy, *Cem. Concr. Res.* 73 (2015) 36–41, <https://doi.org/10.1016/j.cemconres.2015.02.026>.
- [3] O.M. Jensen, P.F. Hansen, E.E. Lachowski, F.P. Glasser, Clinker mineral hydration at reduced relative humidities, *Cem. Concr. Res.* 29 (9) (1999) 1505–1512, [https://doi.org/10.1016/S0008-8846\(99\)00132-5](https://doi.org/10.1016/S0008-8846(99)00132-5).
- [4] E. Dubina, L. Wadsö, J. Plank, A sorption balance study of water vapor sorption on anhydrous cement minerals and cement constituents, *Cem. Concr. Res.* 41 (2011) 1196–1204, <https://doi.org/10.1016/j.cemconres.2011.07.009>.
- [5] S. Sprung, Effect of storage conditions on the properties of cement, *ZKG Int.* 31 (1978) 305–309.
- [6] G. Schmid, T.A. Bier, K. Wutz, M. Maier, Characterization of the aging behavior of premixed dry mortars and its effect on their workability properties, *ZKG Int.* 60 (2007) 94–103.
- [7] K. Theisen, V. Johansen, Prehydration and strength development of Portland cement, *J. Am. Ceram. Soc. Bull.* 54 (9) (1975) 787–791.
- [8] L. Barbic, V. Tinta, B. Lozar, V. Marincovic, Effect of storage time on the rheological behavior of oil well slurries, *J. Am. Ceram. Soc.* 74 (1991) 954–1949, <https://doi.org/10.1111/j.151-2916.1991.tb04326.x>.
- [9] F.B. Nonnenbrock, G.L. Kalousek, C.H. Junper, Effects of partial prehydration and different curing temperatures on some of the properties of cement and concrete, *J. Res. Natl. Bur. Stan.* 16 (5) (1936) 487, <https://doi.org/10.6028/jres.016.029>.
- [10] J. Stoian, T. Oey, J.W. Bullard, J. Huang, A. Kumar, M. Balonis, J. Terrill, N. Neithalath, G. Sant, New insights into the prehydration of cement and its mitigation, *Cem. Concr. Res.* 70 (2015) 94–103, <https://doi.org/10.1016/j.cemconres.2015.01.012>.
- [11] E. Dubina, J. Plank, Influence of moisture- and CO<sub>2</sub>-induced aging in cement on the performance of admixtures used in construction chemistry, *ZKG Int.* 65 (2012) 60–68.
- [12] C. Maltese, C. Pistolesi, A. Bravo, F. Celli, T. Cerulli, D. Salvione, A case history: Effect of moisture on the setting behavior of a Portland cement reacting with an alkali-free accelerator, *Cem. Concr. Res.* 37 (2007) 856–865, <https://doi.org/10.1016/j.cemconres.2007.02.020>.
- [13] F. Winnefeld, Influence of cement aging and addition time on the performance of superplasticizers, *ZKG Int.* 61 (2008) 68–77.
- [14] M.R. Meier, T. Napharatsamee, J. Plank, Dispersing performance of superplasticizers admixed to aged cement, *Constr. Build. Mater.* 139 (2017) 232–240, <https://doi.org/10.1016/j.conbuildmat.2016.12.126>.
- [15] N.B. Singh, Effect of gluconates on the hydration of cement, *Cem. Concr. Res.* 6 (4) (1976) 455–460, [https://doi.org/10.1016/0008-8846\(76\)90074-0](https://doi.org/10.1016/0008-8846(76)90074-0).
- [16] C. Nalet, A. Nonat, Effects of functionality and stereochemistry of small organic molecules on the hydration of tricalcium silicate, *Cem. Concr. Res.* 87 (2016) 97–104, <https://doi.org/10.1016/j.cemconres.2016.06.002>.
- [17] J. Rickert, G. Thielen, Influence of a long-term retarder on the hydration of clinker and cement, *Cem. Concr. Aggreg.* 26 (2) (2004) 1–10, <https://doi.org/10.1520/CCA12315>.
- [18] M. Bishop, S.G. Bott, A.R. Barron, A new mechanism for cement hydration inhibition: Solid-state chemistry of calcium nitrilotri(methylene) triphosphonate, *Chem. Mater.* 15 (2003) 3074–3088, <https://doi.org/10.1021/cm0302431>.
- [19] G. Le Saout, V. Kocabi, K. Scrivener, Application of the Rietveld method to the analysis of anhydrous cement, *Cem. Concr. Res.* 41 (2) (2011) 133–148, <https://doi.org/10.1016/j.cemconres.2010.10.003>.
- [20] DIN EN 196-11 (2019). Methods of testing cement – Part 11: Heat of hydration – Isothermal Conduction Calorimetry method. German version EN 196-11.
- [21] V. Nilles, J. Plank, Study of the retarding mechanism of linear sodium polyphosphates on  $\alpha$ -calcium sulfate hemihydrate, *Cem. Concr. Res.* 42 (5) (2012) 736–744, <https://doi.org/10.1016/j.cemconres.2012.02.008>.
- [22] E.A. Nagul, I.D. McKelvie, P. Worsfold, S.D. Kolev, The molybdenum blue reaction for the determination of orthophosphate revisited: Opening the black box, *Anal. Chim. Acta* 890 (2015) 60–82, <https://doi.org/10.1016/j.aca.2015.07.030>.
- [23] IN EN 196-3 (2017). Methods of testing cement – Part 3: Determination of setting times and soundness. German version EN 196-1.
- [24] D. Stephan, J. Plank, Einfluss von Verzögerern auf Alit und Zemente mit unterschiedlichem Gehalt an Klinkerphasen, in: J. Plank (Ed.), *Bauchemie von der Forschung bis zur Praxis: 5. Tagung Bauchemie in München [9.10.2003]*, Gesellschaft Dt. Chemiker, Frankfurt am Main, 2003, pp. 31–38.
- [25] DIN EN 196-1 (2016). Methods of testing cement – Part 1: Determination of strength. German version EN 196-1.
- [26] P. Mounanga, A. Khelidj, A. Loukili, V. Baroghel-Bouny, Predicting Ca(OH)<sub>2</sub> content and chemical shrinkage of hydrating cement pastes using analytical approach, *Cem. Concr. Res.* 34 (2) (2004) 255–265, <https://doi.org/10.1016/j.cemconres.2003.07.006>.
- [27] H.F.W. Taylor, *Cement Chemistry*, Vol. 2, Thomas Telford, London, 1997.
- [28] J. Plank, M. Zhang-Preßé, N.P. Ivleva, R. Niessner, Stability of single phase C<sub>3</sub>A hydrates against pressurized CO<sub>2</sub>, *Constr. Build. Mater.* 122 (2016) 426–434, <https://doi.org/10.1016/j.conbuildmat.2016.06.042>.

## 4.2 TOPIC 1: AGING IMPACT ON RETARDER PERFORMANCE

---

- [29] F.A. Hartmann, J. Plank, Impact of aging on the hydration of tricalcium aluminate ( $C_3A$ )/gypsum blends and the effectiveness of retarding admixtures, *Z. Naturforsch. B* 75 (8) (2020) 739–753, <https://doi.org/10.1515/znb-2020-0087>.
- [30] E. Ruiz-Agudo, K. Kudłacz, C.V. Putnis, A. Putnis, C. Rodriguez-Navarro, Dissolution and carbonation of portlandite  $[Ca(OH)_2]$  single crystals, *Environ. Sci. Technol.* 47 (19) (2013) 11342–11349, <https://doi.org/10.1021/es402061c>.
- [31] D.T. Beruto, F. Barberis, R. Botter, Calcium carbonate binding mechanisms in the setting of calcium and calcium–magnesium putty-limes, *J. Cult. Heritage* 6 (3) (2005) 253–260, <https://doi.org/10.1016/j.culher.2005.06.003>.
- [32] Y. Jeong, C.W. Hargis, S. Chun, J. Moon, Effect of calcium carbonate fineness on calcium sulfoaluminate-belite cement, *Materials* 10 (8) (2017) 900–917, <https://doi.org/10.3390/ma10080900>.
- [33] J. Camiletti, A.M. Soliman, M.L. Nehdi, Effect of nano-calcium carbonate on early-age properties of ultra-high-performance concrete, *Mag. Concr. Res.* 65 (5) (2013) 297–307, <https://doi.org/10.1680/macr.12.00015>.
- [34] V.S. Ramachandran, Concrete admixtures handbook: properties, science and technology. William Andrew, 1996.

### 4.2.3 Further investigations on topic 1

#### 4.2.3.1 Compilation of the results

This section comprises the results of the retarder topic that were not published in journal articles. With the exception of the retarder interactions with synthetic ettringite they have been presented at two scientific conferences. The contributions to the conferences' proceedings are provided following an overview of their contents.

#### Synthetic ettringite investigation

The research proposal for this project included additional depletion experiments (TOC, UV / Vis spectrophotometry) with the retarders NaGluc and KPPhos. The hydrating clinker phases or Portland cement were to be replaced with pure ettringite synthesized beforehand. This was to isolate and analyze the depletion of the retarders from the liquid phase by the ettringite formed both during aging and in hydration. The aim of this experiment was to contribute to elucidating the findings of the preliminary investigation, which suggested that the aging impact on retarder performance is connected to the working mechanism of the retarder (see chapter 3.1).

Aging the synthetic ettringite had not been envisaged by the research proposal, this was added during the course of the project after the importance of the balance between formation and decomposition of ettringite seeds became clear. Synthetic ettringite was prepared as described in chapter 3.2.1.3. Aging the ettringite for up to 14 days at 35 °C and 90% RH caused it to decompose to CaCO<sub>3</sub>, Al(OH)<sub>3</sub> and gypsum, similar to what had been previously observed in C<sub>3</sub>A / gypsum blends and OPC. For the depletion experiments, fresh and aged ettringite samples were dispersed in the alkaline solution that had also been used for the C<sub>3</sub>A / gypsum blends to simulate the alkaline environment in cement pore solution. In the alkaline solution, up to 1.0% bwoe (by weight of ettringite) NaGluc or KPPhos were dissolved. The dispersions were agitated using a vortex mixer. Afterwards the liquid phase was separated via centrifugation and filtering. The liquid samples were prepared for TOC or UV / Vis spectrophotometry as described in chapter 3.2.3.2.

The results for the depletion of NaGluc from the liquid phase by fresh and aged synthetic ettringite are displayed in **Figure 42**. The depletion decreases with increasing retarder dosage for fresh and 3 days aged ettringite. After long-term aging for 14 days however, the depletion remains at a value of ~90% from 0.1 to 1.0% bwoe NaGluc, indicating a strong adsorption of the retarder on the ettringite decomposition products. This matches the results of journal article 2 where NaGluc displayed a stark increase in effectiveness towards long-term aging of OPC, even surpassing its performance in the fresh CEM I 52.5 N. It also reinforces the assumption in journal article 1 that NaGluc and ettringite compete for the covering of the particle surface after short-term aging the C<sub>3</sub>A / gypsum blend as opposed to the retarder just adsorbing on ettringite.

A comparable correlation between the exposure duration of ettringite and the depletion of KPPhos retarder could not be obtained. The KPPhos was always 100% depleted from the liquid. This signifies that even after 14 days of aging, synthetic ettringite dissolves calcium fast enough to completely consume up to 1.0% bwoe (by weight of ettringite) KPPhos.

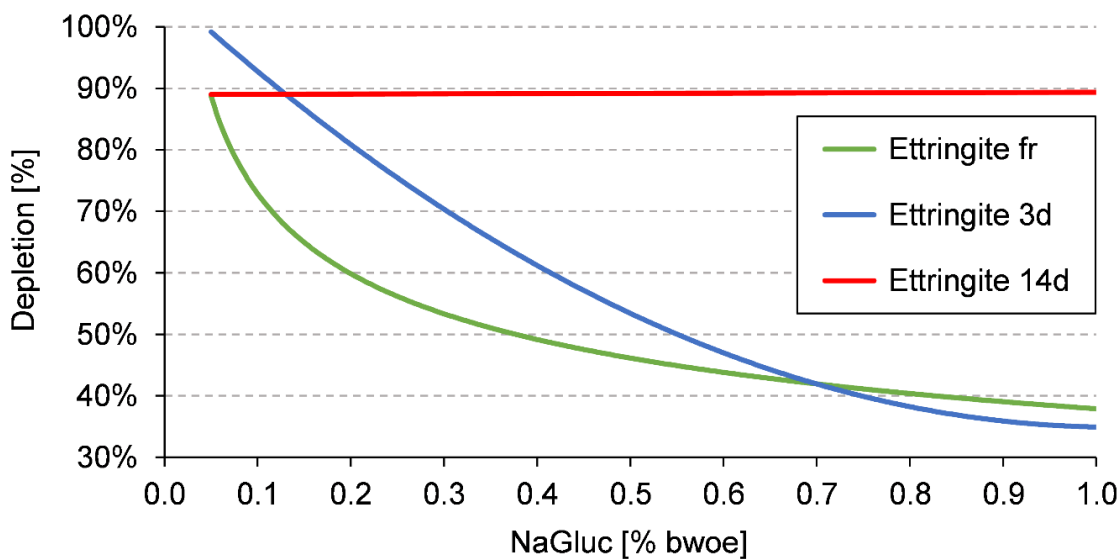


**Figure 42:** Depletion of NaGluc retarder from the liquid phase by fresh and aged synthetic ettringite.

### Conference contributions 1 and 2

The two contributions have similar contents, #1 is in German, #2 in English. The results cover the aging impact on the performance of NaGluc and KPPhos in the hydration of both clinker phases, C<sub>3</sub>A (with gypsum) and C<sub>3</sub>S. The experimental preparation for the heat-flow calorimetry of C<sub>3</sub>A / gypsum differed between the journal articles and the conference contributions. Early in the experimental work of the retarder topic, fresh and aged C<sub>3</sub>A / gypsum samples were mixed with the alkaline solution *inside* the calorimeter using so-called ‘admix ampoules’ (**Figure 43**). The alkaline solution is filled into two syringes connected to the vial holding the C<sub>3</sub>A / gypsum sample. After the mount has been lowered into the calorimeter, the solution is injected into the vial and the mix is homogenized by revolving a shaft reaching from outside the calorimeter into the vial. An L-shaped stirrer blade is attached to the shaft. This setup allows to record the heat release from the moment the alkaline solution comes into contact with the C<sub>3</sub>A / gypsum as opposed to homogenizing the sample after the start of the hydration outside the calorimeter with a vortex mixer. Thus, the admix ampoules are suited to investigate reactions occurring very early in hydration such as the formation of ettringite. However, it was found that the L-shaped stirrer is inferior to the vortex mixer in properly homogenizing the samples, especially if they contained aged C<sub>3</sub>A / gypsum. As a result, heat release peaks were broader, had lower maximum intensities and sometimes appeared at different times when the admix ampoule was used instead of the vortex mixer. For this reason, the application of admix ampoules was discontinued and only the vortex mixer was used in obtaining the results published in the journal articles. This is why the heat flow calorimetry results of C<sub>3</sub>A / gypsum differ between the journal articles and the conference contributions. Still, the accelerating effect of NaGluc on the final crystallization of aged cubic C<sub>3</sub>A / gypsum described in journal article 1 was already observed while still using the admix ampoules, as it is mentioned in contribution 2.

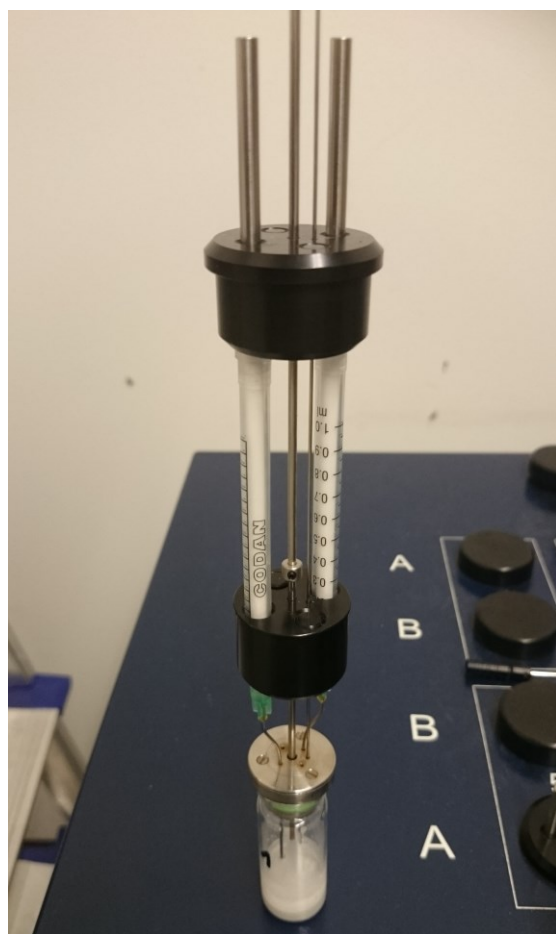


**Figure 43:** Admix ampoule with emptied syringes and hydrated samples after removal from the calorimeter.

As for the other clinker phase,  $\text{C}_3\text{S}$ , it displayed a very different aging behavior as compared to that of  $\text{C}_3\text{A}$  / gypsum. The water uptake during up to 14 days of aging was lower than for both  $\text{C}_3\text{A}$  / gypsum and CEM I 52.5 N. Furthermore, there was no significant difference between non-doped triclinic  $\text{C}_3\text{S}$  and doped monoclinic  $\text{C}_3\text{S}$ . Similar to the OPC, the amount of portlandite in the aged  $\text{C}_3\text{S}$  samples was comparatively low, it readily reacted with atmospheric  $\text{CO}_2$  to  $\text{CaCO}_3$  during aging.

With regards to the retarder impact on hydration behavior, NaGluc displayed an exceptional effectiveness in fresh  $\text{C}_3\text{S}$ . At 0.10% bwob, the same dosage as in the OPC in journal article 2, the hydration of monoclinic  $\text{C}_3\text{S}$  at room temperature was effectively suppressed for at least 7 days. In calorimetry, no measurable heat release was recorded after the start of hydration before the experiment was terminated after 144 hours (6 days). Triclinic  $\text{C}_3\text{S}$  was also very strongly retarded by NaGluc, but the onset of a low-rate hydration reaction was observed ~41 hours after the start of the experiment. These observations match the results of a study from 1979 [180] which relates the extreme retardation of  $\text{C}_3\text{S}$  to the poisoning of hydrate nucleation sites by NaGluc.

After aging the  $\text{C}_3\text{S}$ , the NaGluc impact on hydration was reduced. Halving the dosage from 0.10% to 0.05% bwob further reduced its performance, revealing a dose-effect relation of NaGluc in aged  $\text{C}_3\text{S}$ . In comparison, halving the KPPhos dosage from 0.40% to 0.20% bwob did not reduce its effect nearly as significantly. It is assumed that the solution of calcium from aged  $\text{C}_3\text{S}$  is slow enough that 0.20% bwob KPPhos is a sufficient dosage to remove most of the free  $\text{Ca}^{2+}$  from the pore solution.

**4.2.3.2 Reprint of conference contribution 1**

**Wirksamkeit von Verzögerern in gealtertem Zement und reinen Klinkerphasen**

F. A. Hartmann, M. R. Meier, J. Plank

*20. Internationale Baustofftagung (ibausil)*

Weimar, Germany, 12–14 September 2018

in:

H.-M. Ludwig (pub.), Proceedings, volume 1, 590–597

Reprinted with permission from

F.A. Finger-Institut für Baustoffkunde, Bauhaus-Universität Weimar

Hartmann, F. A., Meier, M. R., Plank, J.

## Wirksamkeit von Verzögerern in gealtertem Zement und reinen Klinkerphasen

### 1. Einleitung

Zement ist bei Lagerung kein inerter Baustoff, sondern weist ein hohes chemisches Reaktionspotential auf. Die sogenannte Zementalterung beschreibt die vorzeitige Hydratation des Zements (engl. „prehydration“, kurz für preliminary hydration) durch Aufnahme von Luftfeuchtigkeit und CO<sub>2</sub>. Erstere wird durch Sorption von gasförmigem Wasser aus der atmosphärischen Luft verursacht und durch die hygrokopische Eigenschaft des Zements begünstigt. Dieser Prozess kann bereits bei der Herstellung von Zement eintreten. Während des Mahlens kommt der Klinker häufig mit Wasser in Kontakt, sowohl zur Temperaturregulierung als auch durch Freisetzung aus zugemahlenem Gips. Weiterhin kann eine Alterung durch unsachgemäße Lagerung des Zements, oftmals in Kombination mit Witterungseinflüssen und unzureichendem Schutz vor hoher Luftfeuchtigkeit, hervorgerufen werden. Die Folgen sind schlecht einzuschätzende Verarbeitbarkeit und gestörtes Abbindeverhalten des Zements, eine für die jeweilige Verwendung ungeeignete Festigkeitsentwicklung [1-3] sowie signifikante Unterschiede in der Wechselwirkung mit Zusatzmitteln [4, 5].

Diese Veränderungen der Zementeigenschaften sind auf die Bildung von Alterungsprodukten auf den Klinkeroberflächen durch Kontakt mit Feuchtigkeit und CO<sub>2</sub> zurückzuführen. Die einzelnen Klinkerphasen weisen dabei verschiedene Reaktionspotentiale auf, beispielsweise sorbieren Aluminate schneller und mehr Wasser als Silikate [6]. Somit sind für Zemente unterschiedlicher Klinkerzusammensetzung Abweichungen in der Alterung zu erwarten. Daher ist es entscheidend, neben den Zementen auch die reinen Klinkerphasen auf ihr Alterungsverhalten zu untersuchen.

In dieser Studie liegt der Fokus auf der Alterung von Tricalciumsilikat Ca<sub>3</sub>(SiO<sub>4</sub>)O / C<sub>3</sub>S und Tricalciumaluminat Ca<sub>9</sub>Al<sub>6</sub>O<sub>18</sub> / C<sub>3</sub>A im Vergleich zu einem Portlandzement CEM I 52,5 N. Ferner werden die Auswirkungen der Alterung auf die Wechselwirkung von Zement und Klinkerphasen mit Verzögerern untersucht. Als Verzögerer wurden neben dem im Transportbeton weit verbreiteten [7] Natriumgluconat (Na<sup>+</sup> C<sub>6</sub>H<sub>11</sub>O<sub>7</sub><sup>-</sup>) noch Kaliumpyrophosphat (K<sub>4</sub>P<sub>2</sub>O<sub>7</sub>) verwendet. Der Einsatz von chemisch unterschiedlich aufgebauten Verzögerern soll zur Aufklärung der Mechanismen der verzögernden Wirkung in gealtertem Zement beitragen.

## 2. Versuchsdurchführung

Die Klinkerphasen  $C_3S$  und  $C_3A$  wurden jeweils in reiner und in dotierter Form synthetisiert. Aus den Naturprodukten Kalkstein und Ton hergestellter Klinker enthält Alkali- und Erdalkalimetalle, welche Einfluss auf die Kristallmodifikation haben. In industriellem Klinker kristallisiert  $C_3S$  überwiegend in monokliner Struktur ( $C_3S_m$ ), welche durch den Einbau von Calcium-, Aluminium- und Eisenionen stabilisiert wird. Gleichermassen führt ein ausreichend hoher Gehalt von Natrium zur Bildung von orthorhombischem  $C_3A_o$  [8]. Bei der Laborsynthese aus Reinstoffen werden dagegen triklines  $C_3S_t$  und je nach  $Na_2O$ -Zugabe reines kubisches oder ein Gemisch aus  $C_3A_c$  und  $C_3A_o$  erhalten.

$C_3S_m$  und  $C_3S_t$  wurden aus  $CaCO_3$  und  $SiO_2$ ,  $C_3A_c$  und  $C_3A_o$  aus  $CaCO_3$  und  $Al_2O_3$  jeweils im Molverhältnis 3 : 1 hergestellt. Die Hochtemperatur-Festkörperreaktion wurde in Platin/Rhodium-Tiegeln bei 1450 °C für  $C_3S$  und 1300 °C für  $C_3A$  durchgeführt. Zur Synthese von monoklinem  $C_3S$  wurde mit 1,1 Gew.%  $MgO$  und 0,7 Gew.%  $Al_2O_3$  dotiert. Des Weiteren wurden  $C_3A_c$  und  $C_3A_o$  synthetisiert. Bei  $C_3A_o$  muss ein Überschuss an  $Na_2O$  zugesetzt werden, um Verluste durch Sublimation während des Sinterns auszugleichen. Der  $Na_2O$ -Gehalt im Endprodukt beträgt 3,7 – 4,6 Gew.% [8]. Die Klinkerphasen wurden in einer Planetenkugelmühle aufgemahlen und die Reinheit durch Pulver-XRD (D8 advance, Bruker AXS, Karlsruhe) bestätigt.

Proben von CEM I 52,5 N und den reinen Klinkerphasen wurden für 3 und 14 Tage bei einer Temperatur von  $35 \pm 2$  °C und  $90 \pm 5$  % relativer Luftfeuchtigkeit gealtert. Durch diese extremen Bedingungen wird sichergestellt, dass Wasser auch auf den geringer reaktiven Oberflächen der undotierten Phasen sorbiert [6]. Außerdem kann dadurch eine mehrmonatige Exposition bei gemäßigten Klimaverhältnissen in einem vergleichsweise kurzen Zeitraum simuliert werden.  $C_3A_c$  und  $C_3A_o$  wurden im Verhältnis 1 : 1 mit Gips ( $CaSO_4 \cdot 2 H_2O$ ) vermischt, um die Bildung von Ettringit ( $C_3A \cdot 3 CaSO_4 \cdot 32 H_2O$ ) aus Aluminaten und Sulfatträgern während der Zementhydratation abzubilden. Um eine möglichst große aktive Oberfläche während der Alterung zu erzeugen, wurden die pulverförmigen Proben in Portionen von 50 g in sehr dünner Schicht auf 135 x 60 cm Plexiglas®-Platten verteilt.

Zur Untersuchung der Hydratation des gealterten Zements und der Klinkerphasen wurde die Wärmefreisetzung während der Abbindereaktion im isothermen Kalorimeter (TAM Air, Thermometric AB, Schweden) gemessen. Die Verzögerer Natriumgluconat und Kaliumpyrophosphat wurden im Anmachwasser gelöst. Aufgrund der hohen Reaktivität des Aluminats setzt die durch die Ettringitbildung ausgelöste Wärmeentwicklung unmittelbar nach Kontakt der  $C_3A$ /Gips-Mischung mit Wasser ein. Das Anmischen muss in diesem Fall *in situ*, also in der Messkammer des Kalorimeters, erfolgen. Die Zugabe des Anmachwassers erfolgt dabei über *admix ampoules*, einer Halterung mit zwei 1 mL-Spritzen sowie einer handbetriebenen Rührwelle mit L-förmigem Rührblatt, an der ein 10 mL-Rollrandglas luftdicht befestigt wird, welches die Probe enthält. Der gesamte Aufbau wird anschließend im Kalorimeter vor Reaktionsstart auf 20 °C equilibriert. Die Zement- und  $C_3S$ -Proben wurden außerhalb des Kalorimeters angemischt.

### 3. Ergebnisse und Diskussion

#### 3.1 Alterung von CEM I 52,5 N und Klinkerphasen

Vor dem Einbringen in die Klimaboxen wurden von allen Bindemitteln Proben entnommen, diese röntgenographisch charakterisiert, anschließend auf den XRD-Objekträgern mitgealtert und nach 3 sowie 14 Tagen erneut gemessen. Auf der Oberfläche von CEM I 52,5 N konnten dabei als Alterungsprodukte Ettringit sowie die CaCO<sub>3</sub>-Polymorphe Calcit und Aragonit identifiziert werden, während der relative Anteil an unreagiertem C<sub>3</sub>S abnahm.

Bei den Aluminatphasen zeigte C<sub>3</sub>A<sub>o</sub> innerhalb der ersten 3 Tage eine sehr starke Ettringitbildung, wie in **Abbildung 1** zu erkennen ist. Nach 14 Tagen war dieser Oberflächenettringit komplett zu Aragonit, Calcit sowie dem Al(OH)<sub>3</sub>-Polymorph Bayerit zerfallen und der Gipsanteil hatte entsprechend wieder zugenommen. Bei C<sub>3</sub>A<sub>c</sub> war über den gesamten Alterungszeitraum eine langsamere, aber kontinuierliche Bildung von Ettringit und Aragonit zu beobachten. Die unterschiedlichen Reaktivitäten der C<sub>3</sub>A-Modifikationen decken sich mit früheren Beobachtungen [9].

Sowohl für C<sub>3</sub>S<sub>t</sub> als auch C<sub>3</sub>S<sub>m</sub> war nach 3 Tagen Alterung praktisch keine Veränderung im XRD zu erkennen. Erst nach 14 Tagen konnte die Bildung von Aragonit und Calcit sowie ein korrespondierender Rückgang des unreagierten C<sub>3</sub>S beobachtet werden.

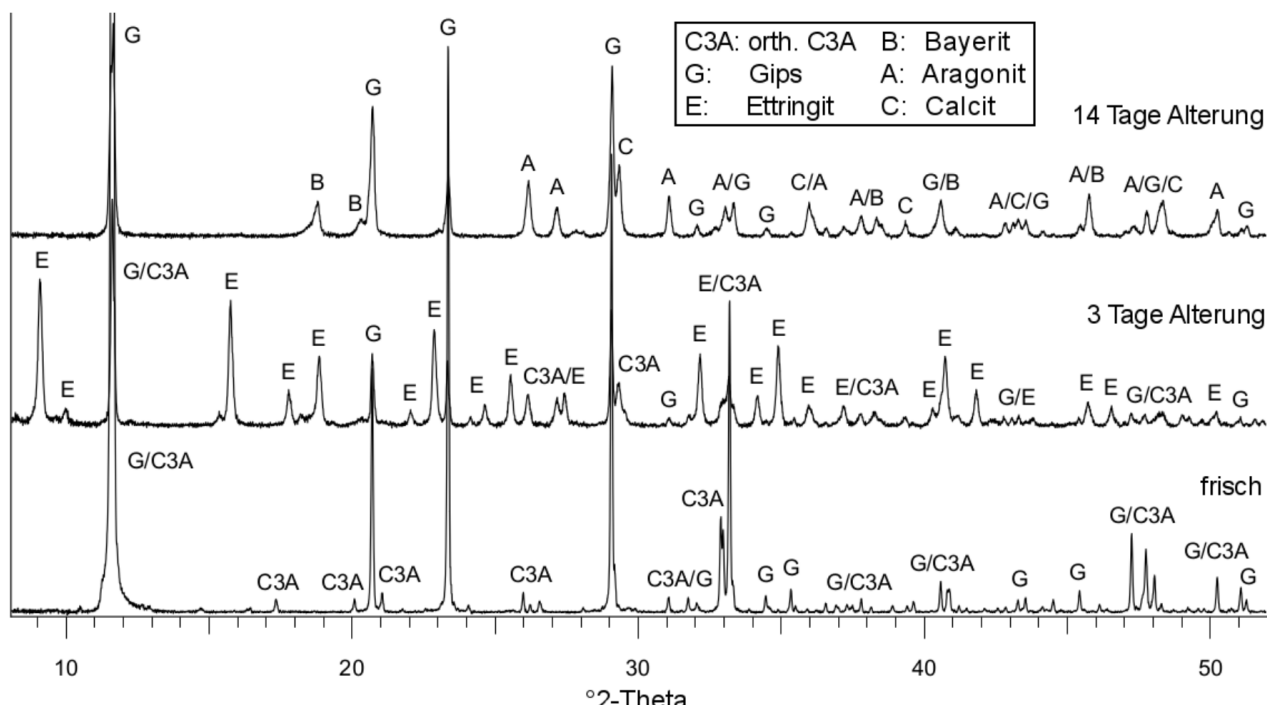


**Abb. 1:** Röntgendiffraktogramme einer frischen binären Mischung aus C<sub>3</sub>A<sub>o</sub> und Gips sowie nach 3 beziehungsweise 14 Tagen Alterung dieser Mischung.

Die gealterten Ansätze wurden gewogen und die prozentuale Massenzunahme gegenüber den jeweiligen Einwaagen bestimmt (**Abb. 2**). Die Zunahme verlief nicht linear, sondern war in den ersten Tagen der Alterung besonders stark und zwischen 3 und 14 Tagen vergleichsweise geringer. Bei der binären Mischung aus C<sub>3</sub>A<sub>o</sub> und Gips nahm die Masse zwischen 3 und 14 Tagen sogar wieder ab. Grund dafür ist der Zerfall

von Ettringit (**Abb. 1**) und die resultierende Freisetzung von Kristallwasser. Nach 3 Tagen Alterung betrug die Gewichtszunahme beim Zement und den C<sub>3</sub>S-Phasen 9-16 Gew.% wohingegen bei C<sub>3</sub>A<sub>0</sub>/Gips eine Zunahme von nicht weniger als 47 Gew.% eintrat.

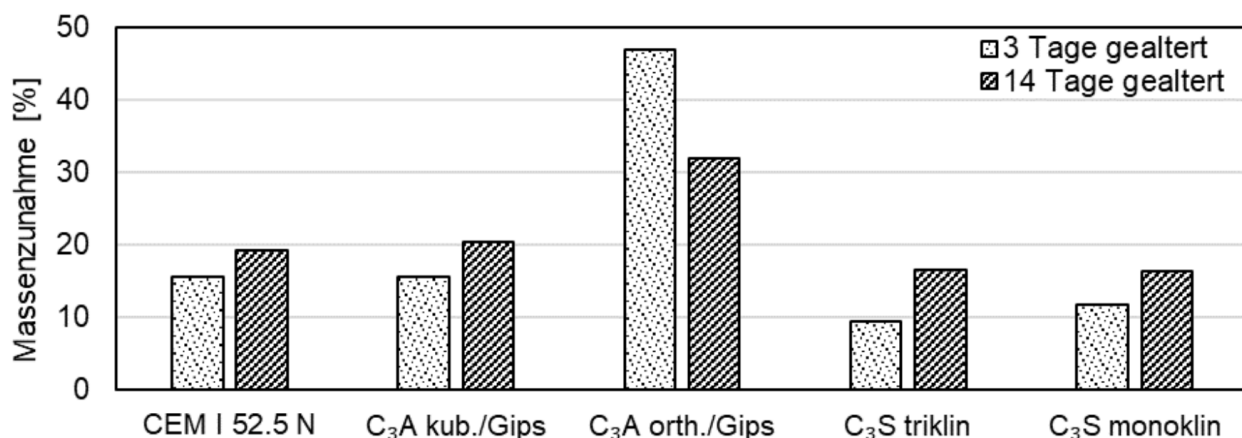


**Abb. 2:** Prozentuale Massenzunahme von CEM I 52,5 N und Klinkerphasen nach 3 beziehungsweise 14 d Alterung bei 35 °C und 90 % RH.

### 3.2 Hydrationsuntersuchungen

Ein Vergleich von frischem und gealtertem CEM I 52,5 N zeigte, dass die Alterung grundsätzlich zu einer wesentlich verzögerten Ettringitbildung führt, die vor allem während der ersten Tagen ausgeprägt ist (**Tab. 1**).

Der Zusatz von Natriumgluconat und Kaliumpyrophosphat hatte unterschiedliche Auswirkungen auf die einzelnen Phasen der Hydrationsreaktion.

Die Verzögerer beeinflussten die Ettringitbildung in gealtertem Zement stark. Gluconat verzögerte dabei stärker als Pyrophosphat. Darüber hinaus nahm die verzögernde Wirkung von Gluconat bei längeren Alterungszeiten stark zu, dieser Effekt konnte für Pyrophosphat nicht beobachtet werden.

**Tab. 1:** Zeitpunkt der maximalen Wärmefreisetzung für Ettringitbildung und silikatische Hauptreaktion von CEM I 52,5 N (w/z = 0,5) mit und ohne Verzögerer, frisch und 3 d beziehungsweise 14 d gealtert, in Stunden nach dem Anmischen.

CEM I 52,5 N	Ettringitbildung			Silikatische Hauptreaktion		
	frisch	3 d	14 d	frisch	3 d	14 d
ohne Verz.	sofort	1,8 h	2,5 h	9,9 h	nicht nachweisbar	
0,05 % NaGluc		6,3 h	15,5 h	14,3 h		
0,10 % NaGluc		<b>18,8 h</b>	<b>40,5 h</b>	19,6 h		
0,20 % K <sub>4</sub> P <sub>2</sub> O <sub>7</sub>		7,2 h	8,5 h	22,7 h		
0,40 % K <sub>4</sub> P <sub>2</sub> O <sub>7</sub>		14,3 h	16,8 h	<b>38,7 h</b>		

Bezüglich der silikatischen Reaktion des frischen Zements war hingegen Pyrophosphat der stärkere Verzögerer. Die sehr geringe Wärmefreisetzung der Silikatreaktion von gealtertem Zement machte eine Quantifizierung der verzögernden Wirkung unmöglich, da sich die Signale kaum vom Messuntergrund abhoben.

Die unterschiedliche Wirksamkeit der Verzögerer bezüglich Ettringitbildung und Silikatreaktion wurde im Folgenden näher betrachtet. Bei  $C_3S_m$  und  $C_3S_t$  ohne Verzögerer zeigte eine dreitägige Alterung keine nennenswerte Verzögerung der silikatischen Reaktion, wie dem Vergleich der **Abbildungen 3 und 4** zu entnehmen ist. Die maximale Wärmefreisetzung tritt sowohl in der frischen als auch der gealterten Phase nach etwa 12 h ein.

Gluconat verzögert frisches  $C_3S$  deutlich stärker als Zement. Während in frischem CEM I 52.5 N bei Zusatz von 0,05 % bwob (*by weight of binder*) die silikatische Hauptreaktion nach 14 h und bei Zugabe 0,1 % nach etwa 20 h auftrat (**Tab. 1**), konnte diese Reaktion in  $C_3S_t$  mit 0,05 % erst nach knapp 24 h und mit 0,1 % innerhalb von 6 Tagen überhaupt nicht beobachtet werden (**Abb. 3**). Die entsprechende Probe blieb unverändert im Anmachwasser und zeigte optisch keinerlei Reaktion.

Pyrophosphat hingegen verzögert frisches  $C_3S$  ähnlich wie Zement (**Abb. 3, Tab. 1**). Damit ist Gluconat, welches hinsichtlich der Verzögerung der Silikatreaktion in frischem CEM I 52.5 N Pyrophosphat unterlegen war, der effektivere Verzögerer für reines  $C_3S$ .

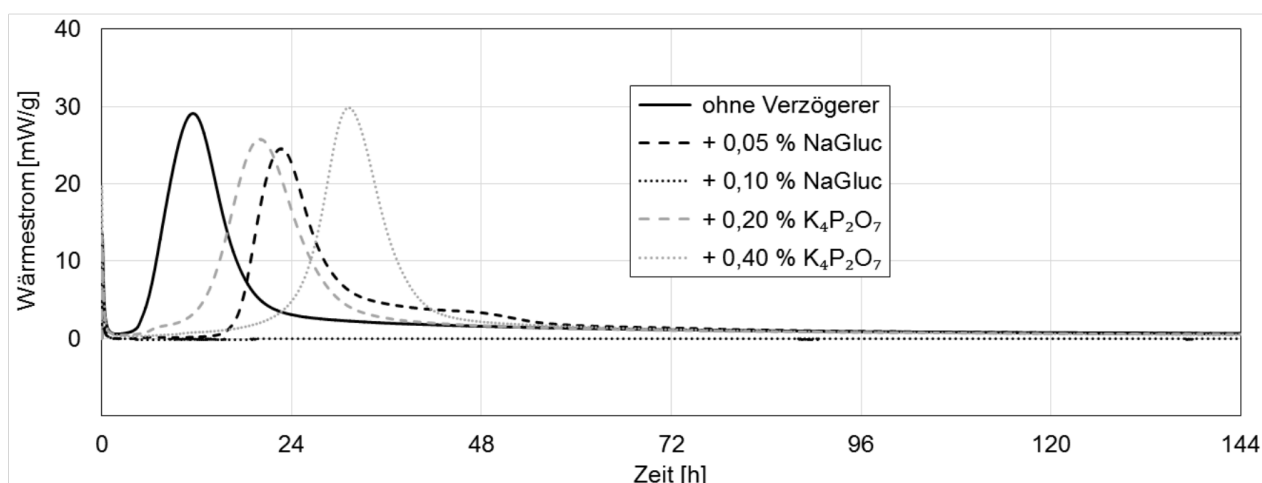


**Abb. 3:** Vergleich der verzögernden Wirkung von Natriumgluconat und Kaliumpyrophosphat in frischem trikalinem  $C_3S_t$  (w/b = 0,5).

Bei der Hydratation von gealtertem  $C_3S$  ging im Gegensatz zur frischen Phase die Wärmefreisetzung nach dem Lösungsprozess (~ 2 h) nicht auf null zurück (**Abb. 4**). Grund dafür sind die Alterungsprodukte, die als Nukleationskeime für die C-S-H-Bildung wirken. Der während dieser „semi-dormanten“ Periode gemessene Wärmefluss ist stark von der Verzögererzugabe abhängig. Für Gluconat konnte dabei und beim Zeitpunkt der maximalen Wärmefreisetzung eine Dosis-Wirkungs-Beziehung beobachtet werden (**Abb. 4 links**). Daher ist davon auszugehen, dass der Wirkmechanismus von Gluconat auf einer Adsorption des Verzögerers sowohl auf  $C_3S$  als auch auf den Alterungsprodukten beruht, wobei eine höhere Dosierung zu einer stärkeren Bedeckung der Oberfläche und damit geringeren Zahl an gleichzeitig aktiven Hydratationszentren führt.

Bei Zusatz von Pyrophosphat sind der Wärmestrom während der „semi-dormanten“ Periode sowie der Zeitpunkt der maximalen Wärmefreisetzung weniger von der Dosierung abhängig (**Abb. 4** rechts). Als Ursache dafür wird das hohe Calciumbindevermögen von Pyrophosphat angenommen. Analog zu den als Langzeitverzögerern genutzten Phosphonaten [10] kann Pyrophosphat gelöste  $\text{Ca}^{2+}$ -Ionen komplexieren und damit den Aufbau der C-S-H-Phasen verlangsamen. Dieser Prozess ist neben der Verzögererdosierung auch von der Freisetzungsrates der  $\text{Ca}^{2+}$ -Ionen abhängig. Durch die kontinuierliche Ca-Bindung wird die „semi-dormante“ Periode im Vergleich zum schnell adsorbierenden [11] Gluconat zeitlich stärker verlängert. Die gebildeten Ca-Phosphat-Komplexe präzipitieren nach Überschreiten einer Konzentrationsschwelle. Bei einer geringen Pyrophosphat-Dosis führen lokale Konzentrationsunterschiede in der Probe dazu, dass dieser Zeitpunkt unterschiedlich schnell erreicht wird. Die C-S-H-Bildung setzt dadurch später ein, der Hydratationsverlauf wird zeitlich gestreckt und die Wärmefreisetzung ist geringer als bei höherer Dosis.

Wie bei den Aluminatphasen war auch in  $\text{C}_3\text{S}_t$  und  $\text{C}_3\text{S}_m$  die Bildung der Alterungsprodukte nach 14 Tagen so weit fortgeschritten, dass keine quantifizierbare Wärmeentwicklung während der Hydratation mehr verzeichnet wurde.

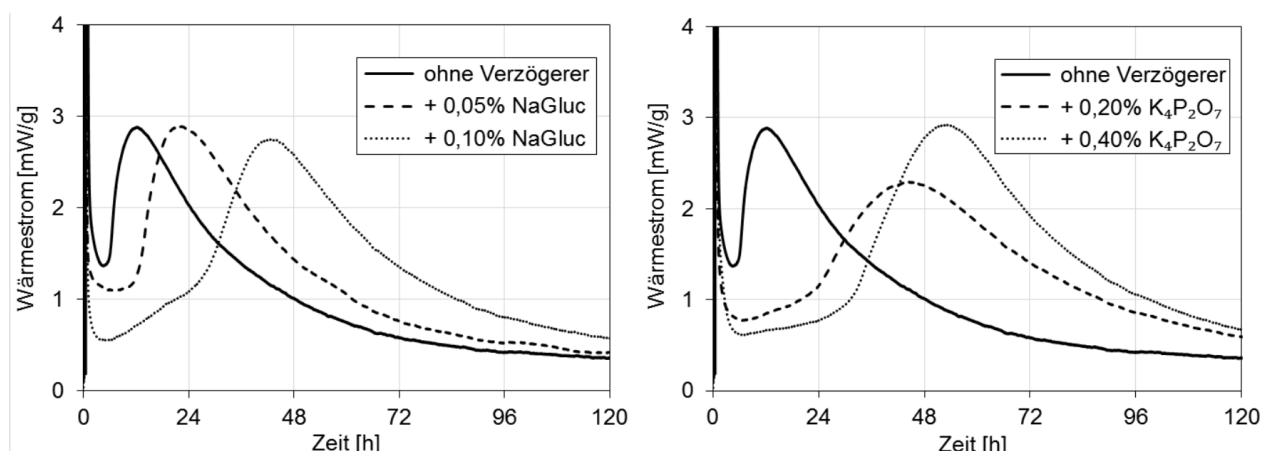


**Abb. 4:** Vergleich der verzögernden Wirkung von Natriumgluconat (links) und Kaliumpyrophosphat (rechts) in 3 d gealtertem  $\text{C}_3\text{S}_m$  (w/b = 0,6).

In  $\text{C}_3\text{A}_c$  mit Gips und ohne Verzögerer war wie bei Zement eine signifikant verlangsamte Ettringitbildung infolge Alterung zu beobachten (**Abb. 5**). Zusatz von Pyrophosphat führte zu einer zusätzlichen Verzögerung, Gluconat hingegen zeigte keine Wirkung.

Neben der Ettringitbildung wurden weitere Wärmefreisetzungsbereiche beobachtet und die zugehörigen Phasenbildungen mittels XRD identifiziert. In 3 d gealtertem  $\text{C}_3\text{A}_c$  reagierte innerhalb der ersten 24 h nach Beginn der Hydratation das Alterungsprodukt Aragonit zu Monocarbonat ( $\text{C}_3\text{A} \cdot \text{CaCO}_3 \cdot 11 \text{ H}_2\text{O}$ ) und Hemicarbonat ( $\text{C}_3\text{A} \cdot 0,5 \text{ Ca(OH)}_2 \cdot 0,5 \text{ CaCO}_3 \cdot 11,5 \text{ H}_2\text{O}$ ). In frischem  $\text{C}_3\text{A}_c$  und  $\text{C}_3\text{A}_o$  konnte die Umwandlung von Ettringit zu Monosulfat ( $\text{C}_3\text{A} \cdot \text{CaSO}_4 \cdot 12 \text{ H}_2\text{O}$ ) nach ca. 96 h Stunden beobachtet werden. Beide Prozesse wurden ebenfalls ausschließlich durch Pyrophosphat verzögert.

Aufgrund der bereits während der Alterung fortgeschrittenen Ettringitbildung konnte in  $\text{C}_3\text{A}_c$  nach 14 Tagen und im reaktiveren  $\text{C}_3\text{A}_o$  nach 3 beziehungsweise 14 Tagen keine signifikante Wärmefreisetzung mehr während der Hydratation beobachtet werden.

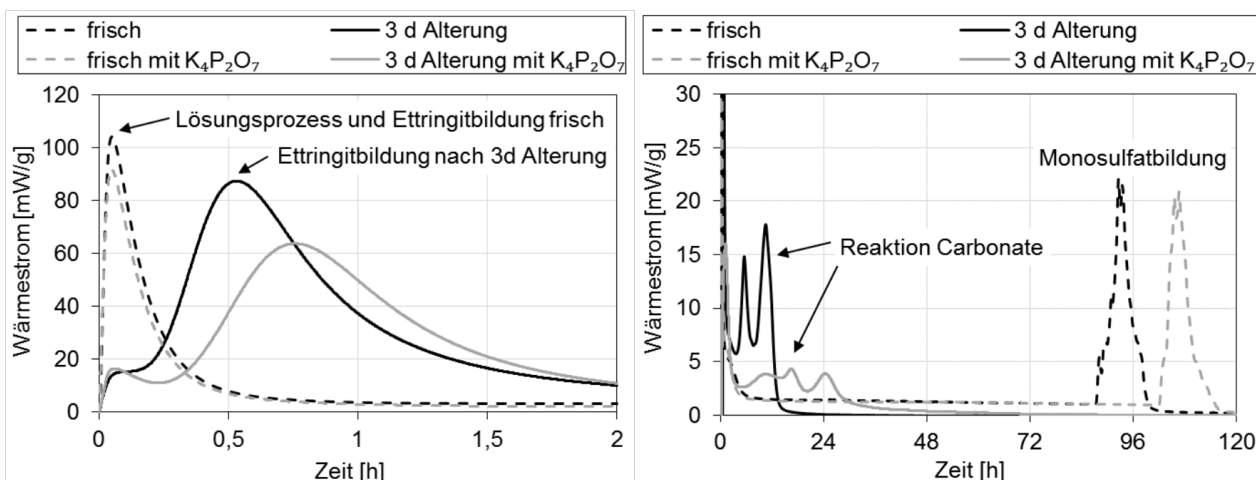


**Abb. 5:** Auswirkung der Zugabe von 0,4 % bwob  $K_4P_2O_7$  auf die Hydratation einer 3 d gealterten binären Mischung von  $C_3A_c$  und Gips ( $w/b = 2,0$ ) zu Beginn der Reaktion (links) und nach 5 Tagen (rechts).

#### 4. Zusammenfassung

In der vorliegenden Studie wurde die Wirksamkeit der Verzögerer Natriumgluconat und Kaliumpyrophosphat in frischem und gealtertem CEM I 52,5 N,  $C_3S_{t/m}$  sowie  $C_3A_{c/o}$  / Gips untersucht. Ziel der Untersuchungen mit Klinkerphasen war es, das Verhalten des gealterten Zements und die Wirkung der Verzögerer besser zu verstehen.

Gluconat verzögerte in gealtertem CEM I 52,5 N die Ettringitbildung effektiver als Pyrophosphat, welches jedoch in frischem Zement die silikatische Reaktion stärker verzögerte. Gleichzeitig wurde eine starke Zunahme der Wirkung von Gluconat mit der Alterungsdauer beobachtet. Darüber hinaus konnte festgestellt werden, dass der Alterungsprozess alleine bereits die Hydrationsreaktion verlangsamt, wobei dieser Effekt primär in den ersten Tagen der Alterung auftrat. Damit ist bei der Hydratation von kurzzeitig gealtertem Zement der relative Einfluss des Verzögerers am geringsten und der der Alterung am größten. Durch das schlecht kalkulierbare Abbindeverhalten stellt der Einsatz eines solchen Zements für den Anwender ein Problem dar.

Die Hydratation von frischem  $C_3S$  wurde durch Natriumgluconat besonders effektiv verzögert, bei einer Dosis von 0,1 % bwob war sie mindestens 6 Tage komplett unterbunden. Dieses Verhalten weicht stark von dem in frischem Zement ab. Im Gegensatz dazu zeigte Pyrophosphat bei der Hydratation beider Bindemittel eine vergleichbare Wirkung. Nach dreitägiger Alterung entsprach die Verzögerung durch Gluconat eher einer linearen Beziehung zwischen Dosis und Wirkung, als Folge eines adsorptiven Wirkmechanismus. Bei Pyrophosphat war die Komplexierung gelöster  $Ca^{2+}$ -Ionen und der dadurch langsamere Aufbau der C-S-H-Phasen entscheidend.

In  $C_3A$  / Gips trat durch den Alterungsprozess ebenfalls eine signifikante Verlangsamung der Ettringitbildung ein. Einzig die Zugabe von Pyrophosphat führte zu einer zusätzlichen Verzögerung dieses Prozesses.

### Literatur

- [1] Schmid, G.; Bier, T. A.; Wutz, K.; Maier, M.: *Characterization of the aging behaviour of premixed dry mortars and its effect on their workability properties*, ZKG International 60 (2007), S. 94-103.
- [2] Barbic, L.; Tinta, V.; Lozar, B.; Marincovic, V.: *Effect of storage time on the rheological behavior of oil well slurries*, Journal of the American Ceramic Society 74 (1991), S. 954-949.
- [3] Whittaker, M.; Dubina, E.; Plank, J.; Black, L.: *The Effects of Cement Prehydration on Engineering Properties*, Cement and Concrete Science, Birmingham, 2010, S. 101-104.
- [4] Winnefeld, F.: *Influence of cement ageing and addition time on the performance of superplasticizers*, ZKG International 61 (2008), S. 68-77.
- [5] Dubina, E.; Plank, J.: *Influence of moisture- and CO<sub>2</sub>-induced ageing in cement on the performance of admixtures used in construction chemistry*, ZKG International 65 (2012), S. 60-68.
- [6] Dubina, E.; Wadsö, L.; Plank, J.: *A sorption balance study of water vapor sorption on anhydrous cement minerals and cement constituents*, Cement and Concrete Research 41 (2011), S. 1196-1204.
- [7] Plank, J.: *Applications of biopolymers and other biotechnological products in building materials*, Applied Microbiology and Biotechnology 66 (2004), S. 1-9.
- [8] Wesselsky, A.; Jensen, O. M.: *Synthesis of pure Portland cement phases*, Cement and Concrete Research 39 (2009), S. 973-980.
- [9] Dubina, E.; Plank, J.; Black, L.; Wadsö, L.: *Impact of environmental moisture on C<sub>3</sub>A polymorphs in the absence and presence of CaSO<sub>4</sub> · 0.5 H<sub>2</sub>O*, Advances in Cement Research 26 (2014), S. 29-40.
- [10] Bishop, M.; Bott, S. G.; Barron, A. R.: *A new mechanism for cement hydration inhibition: Solid-state chemistry of Calcium Nitrilotris(methylene)triposphonate*, Chemistry of Materials 15 (2003), S. 3074-3088.
- [11] Tan, H.; Zou, F.; Ma, B.; Guo, Y.; Li, X.; Mei, J.: *Effect of competitive adsorption between sodium gluconate and polycarboxylate superplasticizer on rheology of cement paste*, Construction and Building Materials 144 (2017), S. 338-346.

### Ansprechpartner:

Prof. Dr. Johann Plank, M. Sc. Florian Hartmann, Dr. Markus Meier  
sekretariat@bauchemie.ch.tum.de  
Technische Universität München  
Lichtenbergstr. 4  
85747 Garching b. München

**4.2.3.3 Reprint of conference contribution 2**

**The impact of cement and clinker prehydration on retarder performance**

F. A. Hartmann, M. R. Meier, J. Plank

*15<sup>th</sup> International Congress on the Chemistry of Cement (ICCC)*

Prague, Czech Republic, September 16–20, 2019

in:

J. Gemrich (ed.), Papers and posters proceedings, 1–8

Reprinted with permission from

Research Institute of Binding Materials Prague



## The impact of cement and clinker prehydration on retarder performance

Florian Hartmann<sup>a</sup>, Markus Meier<sup>b</sup>, Johann Plank<sup>c</sup>

Chemistry, Technical University of Munich, Garching, Germany

<sup>a</sup>florian.hartmann@bauchemie.ch.tum.de

<sup>b</sup>markus.meier@bauchemie.ch.tum.de

<sup>c</sup>sekretariat@bauchemie.ch.tum.de

### ABSTRACT

Cement aging comprises unwanted reactions with water vapor and CO<sub>2</sub> before the intended hydration at the job site. The main causes are water injection during clinker grinding and exposure to moisture and atmospheric air. Aging negatively impacts flowability, set behavior and strength development of binders and changes their interaction with admixtures.

Investigations on retarder performance in fresh and aged CEM I 52.5 N using heat flow calorimetry revealed that sodium gluconate and potassium pyrophosphate influence different stages of cement hydration. Ettringite formation in aged cement was more strongly retarded by gluconate, whereas pyrophosphate proved superior in retarding C-S-H formation of fresh cement.

To gain a mechanistic understanding of these observations, the clinker phases C3S and C3A, the latter as a binary mixture with gypsum, were investigated individually with heat flow calorimetry.

Ettringite formation in aged CEM I 52.5 N and C3A was significantly delayed compared to fresh material. This effect essentially developed within the first 3 days of aging. By contrast, C-S-H formation from pure C3S was unaffected by aging. We conclude from these findings that aging has greatest effect on early-hydration properties like processing periods and stiffening time.

Regarding retarder performance in aged clinker, pyrophosphate effectiveness in C3A was greatly enhanced by aging, while gluconate accelerated both fresh and aged C3A instead of retarding. In C3S, retardation of C-S-H formation was also generally increased after aging. However, an exceptionally strong retarding effect of 0.1 % bwob gluconate in fresh C3S did not carry over to the aged samples.



## 1. INTRODUCTION

Cementitious building materials are not inert during the period between manufacture and application at the job site. They possess significant hygroscopy and chemical reaction potential with moisture and air. Partial preliminary hydration, often referred to as prehydration, comprises unwanted reactions of cementitious materials with water prior to application. It can occur as early as during clinker grinding whereby water is injected into the mill for cooling. Furthermore, added setting regulators gypsum and hemihydrate release H<sub>2</sub>O due to the elevated temperature and pressure in the mill.

Humidity from the Earth's atmosphere is another source of H<sub>2</sub>O. Interactions of cementitious materials with atmospheric components such as H<sub>2</sub>O and CO<sub>2</sub> are collectively called "cement aging". The aging process is owed to the cement's hygroscopic properties and often the result of improper storage and handling of building materials. High temperature and high humidity conditions prevalent in tropical and subtropical climate zones further facilitate aging.

The negative effects of prehydration and cement aging are unpredictable workability, set behavior and strength development of the binder [1-3], as well as significant changes in the interaction with admixtures, compared to fresh cement. Studies on superplasticizers [4-6] revealed that their performance can be affected positively or negatively, depending on the duration of aging and chemical composition of the admixture. Moreover, it has been reported [5] that in aged cement accelerators calcium formate and amorphous alumina almost lost their accelerating effect, suggesting they may even turn into retarders with increasing aging time.

These different performances in fresh and aged binder are caused by the formation of aging products on the surface of cement particles resulting from exposure to moisture and CO<sub>2</sub>. In prehydration, the various clinker phases exhibit different reactivities, water sorption by aluminates is significantly higher than by silicates [7]. This means that aging behavior of a cement depends on its clinker composition. Thus, in order to assess prehydration of a cement it is useful to investigate its clinker phases individually.

This study deals with aging of tricalcium silicate Ca<sub>3</sub>SiO<sub>5</sub> / C<sub>3</sub>S, also known as alite, and of tricalcium aluminate Ca<sub>3</sub>Al<sub>2</sub>O<sub>6</sub> / C<sub>3</sub>A. The results will be compared to those of Portland cement CEM I 52.5 N. Furthermore, the effect of aging on the interaction between these compounds and retarders sodium gluconate (Na<sup>+</sup> C<sub>6</sub>H<sub>11</sub>O<sub>7</sub><sup>-</sup>) and potassium pyrophosphate (K<sub>4</sub>P<sub>2</sub>O<sub>7</sub>) was investigated. Gluconate is known to adsorb on clinker phases, thus slowing down their dissolution, and also to adsorb on hydration products, which inhibits their crystal growth. Pyrophosphate on the other hand removes calcium ions from the pore solution and thus prevents the formation of hydration products. The overall goal of this study was to elucidate the performance of retarders in cement hydration and to uncover the mechanisms underlying the differences in their effectiveness.

## 2. EXPERIMENTAL PROCEDURES

### 2.1 Preparation of Clinker Phases

C<sub>3</sub>S was produced from CaCO<sub>3</sub> (Merck EMSURE<sup>®</sup>, Germany) and SiO<sub>2</sub> (Quarzwerke Millisil W12<sup>®</sup>, Germany), C<sub>3</sub>A from CaCO<sub>3</sub> und Al<sub>2</sub>O<sub>3</sub> (Nabaltec NABALOX NO 325<sup>®</sup>, Germany) at 3 to 1 molar ratios. Synthesis was carried out via high temperature solid state reaction in chamber furnaces Nabertherm LH 15/14 and LHT 08/16 using crucibles made from a platinum alloy containing 10 % rhodium. Reaction temperatures were 1600 °C for C<sub>3</sub>S and 1400 °C for C<sub>3</sub>A.

Apart from pure, triclinic C<sub>3</sub>S, doped, monoclinic C<sub>3</sub>S containing 1.1 wt.% MgO and 0.7 wt.% Al<sub>2</sub>O<sub>3</sub> was also prepared. Likewise, orthorhombic C<sub>3</sub>A doped with 10.6 wt.% Na<sub>2</sub>O was synthesized next to undoped, cubic C<sub>3</sub>A. It is necessary to use an excess of doping agent to account for Na<sub>2</sub>O losses during sintering due to partial sublimation above 1275 °C. Final Na<sub>2</sub>O content in C<sub>3</sub>A<sub>d</sub> ranges from 3.7 to 4.6 wt.% [8].

The clinker phases were ground in a planetary ball mill (Fritsch Pulverisette 6, Germany) to a particle size similar to that of reference CEM I 52.5 N Milke<sup>®</sup> (d<sub>50</sub> = 16 µm, d<sub>90</sub> = 46 µm) provided by HeidelbergCement. Phase purity was confirmed by powder XRD using a D8 Advance<sup>®</sup> instrument by Bruker AXS, Germany.



### 2.2 Aging Conditions

CEM I and clinker phases were aged for 3 and 14 days in a custom built climate box at  $35 \pm 2$  °C and  $90 \pm 5$  % relative humidity (RH). These conditions allow the simulation of long-term exposure to less harsh climate conditions and provide results on moisture / CO<sub>2</sub> uptake. C<sub>3</sub>A<sub>c</sub> and C<sub>3</sub>A<sub>o</sub> were drymixed with gypsum at a 1 : 1 weight ratio to enable the formation of ettringite (C<sub>3</sub>A · 3 CaSO<sub>4</sub> · 32 H<sub>2</sub>O). The fresh samples were thinly spread out (layer thickness < 1 mm) on 135 x 60 cm Plexiglas® plates in portions of 50 g to maximize the exposed surface area. Additionally, filled XRD sample holders were similarly aged and subjected to measurement after 3 and 14 days to monitor the aging process.

### 2.3 Heat Flow Calorimetry

Hydration behavior of aged cement and clinker phases was investigated with heat flow calorimetry using TAM Air® 3114/3236 and 3116-2/3239 isothermal calorimeters (Thermometric AB, Sweden). In all measurements the retarders sodium gluconate and potassium pyrophosphate were dissolved in the mixing water. Due to the high reactivity of C<sub>3</sub>A, ettringite formation starts immediately after adding water. For this reason, water addition and mixing had to be performed *in situ* with the powder samples being put inside the measuring chambers of the calorimeter first. Water was then added via an *Admix Ampoule*, a mount with two 1 mL syringes and a hand-operated stirring mechanism with a L-shaped blade. Cement and the C<sub>3</sub>S samples were always mixed with water outside the calorimeter.

## 3. RESULTS OF AGING CEM I 52.5 N AND CLINKER PHASES

### 3.1 Formation of Aging Products

XRD analysis of the CEM I 52.5 N sample after 3 days of aging revealed formation of calcite (trigonal CaCO<sub>3</sub>), which increased quantitatively over 14 days.

C<sub>3</sub>S<sub>m</sub> behaved similar to the CEM I sample, whereas C<sub>3</sub>S<sub>t</sub> remained largely unchanged during the first 3 days of aging. However, after 14 days strong calcite and, to a much lesser degree, aragonite (orthorhombic CaCO<sub>3</sub>) formation were observed.

The mixture of C<sub>3</sub>A<sub>o</sub> and gypsum was by far the most reactive compound during aging. The sample showed significant ettringite formation after 3 days of aging. (Figure 1). After 14 days however, the ettringite completely disappeared, having decomposed to calcite, aragonite and bayerite (monoclinic Al(OH)<sub>3</sub>). This is owed to the reaction of ettringite with atmospheric CO<sub>2</sub> [9]. Ettringite decomposition involves release of gypsum which is marked by an increase in the latter's signal intensities. In comparison, the mixture of C<sub>3</sub>A<sub>c</sub> and gypsum (not shown) only displayed minor ettringite and aragonite formation over the same period of time, thus indicating its lower reactivity as has been shown in earlier investigations [10].

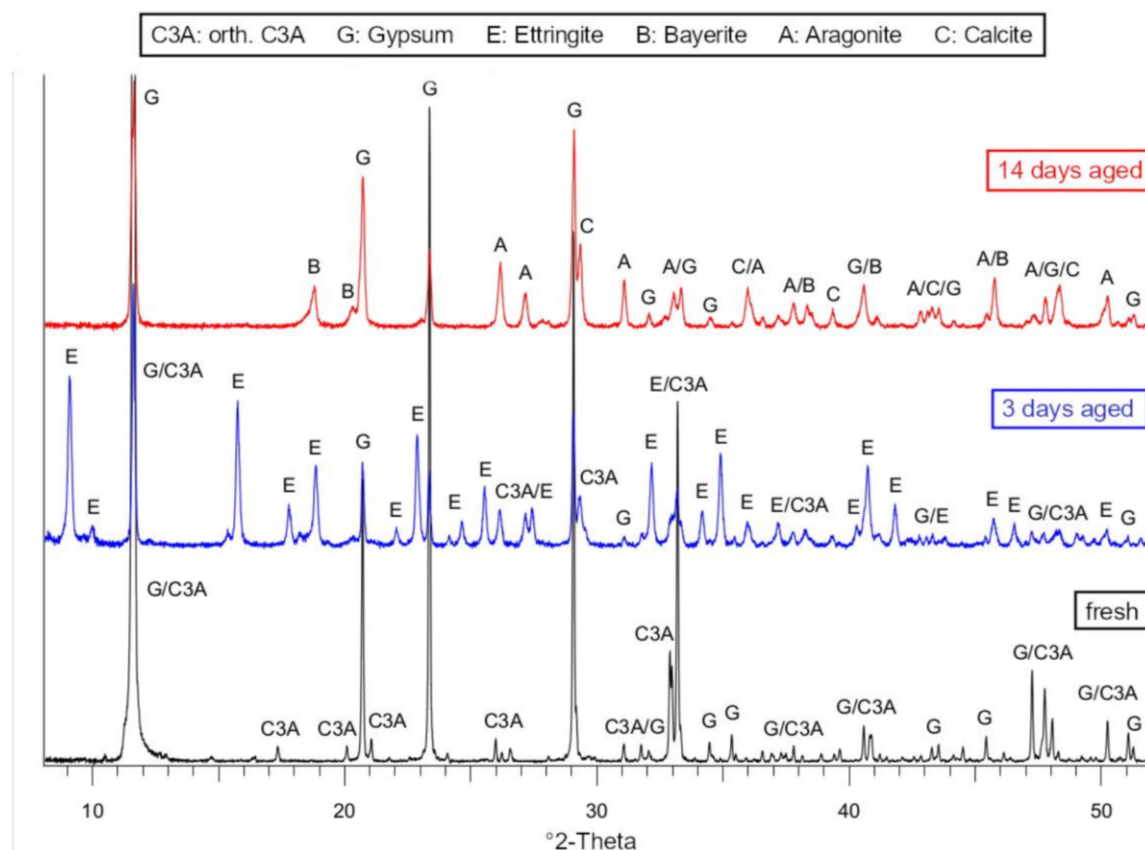


**Figure 1.** X-ray diffraction diagrams of a freshly prepared binary mixture of  $\text{C}_3\text{A}_o$  and gypsum (black), after 3 days aging (blue) and after 14 days aging (red) at 35 °C and 90 % RH

### 3.2 Moisture and $\text{CO}_2$ Uptake

The aged samples were weighed and the percentage weight change against the initial 50 g determined. All samples underwent a weight increase during aging (Figure 2) which was not linear. Apparently, most of the water and  $\text{CO}_2$  uptake occurred within the first 3 days. For example, aging of  $\text{C}_3\text{S}_m$  resulted in a weight increase of almost 12 % after 3 days, but after 14 days it was just over 16 %.  $\text{C}_3\text{S}_t$ , CEM I 52.5 N and  $\text{C}_3\text{A}_c$  mixed with gypsum showed a similar trend. Owing to its exceptionally high reactivity to form ettringite,  $\text{C}_3\text{A}_o$  mixed with gypsum had a weight increase of no less than 47 % after 3 days because ettringite incorporates large amounts of water into its crystal structure. However, between 3 and 14 days aging the sample weight decreased. This is caused by the degradation of ettringite whereby substantial amounts of crystal water are released again.

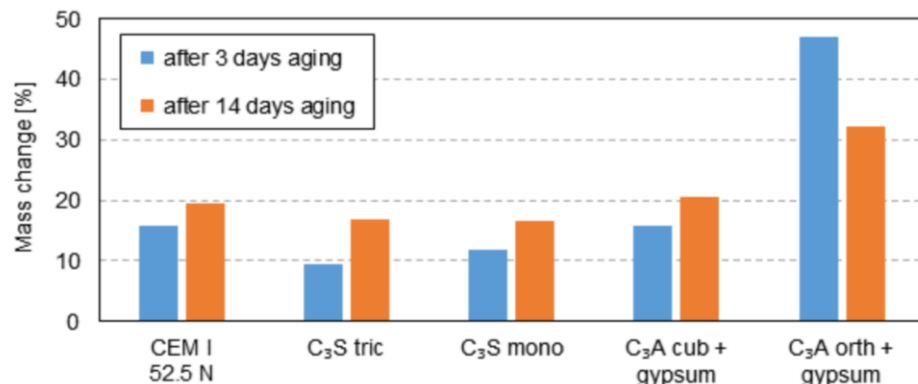


**Figure 2.** Mass change (in percent) of CEM I 52.5 N and individual clinker phases after 3 and 14 days of aging at 35 °C and 90 % RH



#### 4. ANALYSIS OF HYDRATION PROCESSES

##### 4.1 Hydration of CEM I 52.5 N

In fresh cement, the ettringite formation starts immediately after adding water and before the sample has fully dissolved. The heat released from ettringite formation therefore overlaps with the heat of dissolution which renders the two processes indistinguishable in a time-resolved heat flow diagram.

In 3 days aged CEM I 52.5 N however, the aging was found to cause a retarding effect on ettringite formation. It did not start until 2 hours after the addition of water, thus separating the heat of ettringite formation from the heat of dissolution in the heat flow diagram shown on the left in Figure 3. Following the addition of retarders to the mixing water, the ettringite formation was delayed by a further 12 hours with 0.40 % bwoc pyrophosphate and by 17 hours with 0.10 % gluconate.

In comparison to the 3 days aged cement on the left side of Figure 3, on the right a heat flow diagram of the hydration of fresh CEM I 52.5 N is shown. As stated earlier, ettringite formation in fresh cement occurs right after addition of water and is therefore not displayed in the diagram. The signals in the diagram instead show C-S-H formation, clearly identifiable from the characteristic twin peaks. Contrary to ettringite in aged cement, C-S-H formation in fresh cement is stronger retarded by 0.40 % pyrophosphate (26 hours) than 0.10 % gluconate (9 hours).

Unfortunately, it is not possible to make a direct comparison between ettringite and C-S-H formation in either the fresh or the aged cement. Apart from the ettringite formation in fresh cement overlapping with the dissolution heat, in aged cement the C-S-H formation does not appear in the heat flow diagram at all. It can be assumed that the overgrowth of the cement particles with aging products limits water access to the particle surfaces. This prolongs C-S-H crystal growth and therefore lowers its heat release maximum. Thus, in the heat flow diagram of aged cement on the left in Figure 3 C-S-H peaks cannot be observed since their signal intensity is too low to stand out against the background.

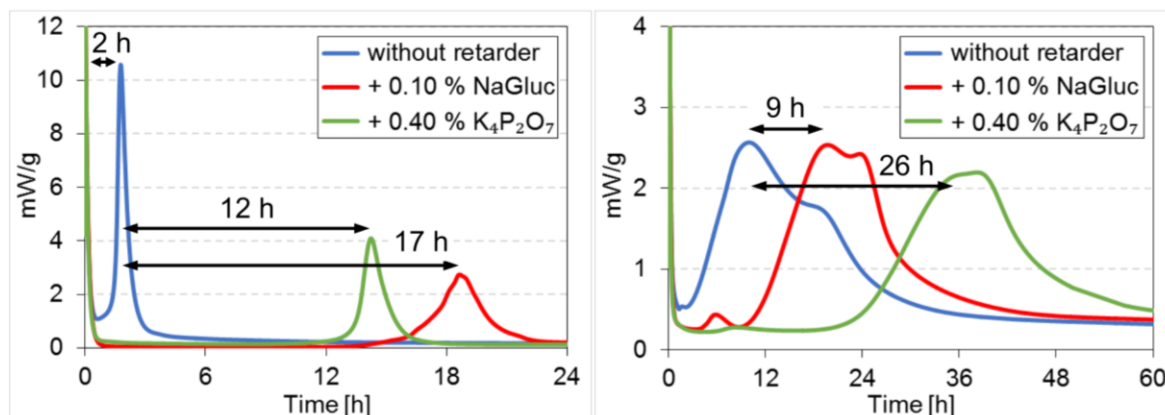


**Figure 3. Ettringite formation in 3 days aged (left) and C-S-H formation in fresh (right) CEM I 52.5 N (w/c ratio = 0.6) with retarders sodium gluconate and potassium pyrophosphate**

Aging for 14 days (not shown) lowered maximum heat release of ettringite formation but only increased retardation from 2 to 3 hours compared to 3 days aging. Therefore, a major part of the retardation effect of aging is already apparent after 3 days. This corresponds to the weight changes over time presented earlier in Figure 2, indicating that the retardation effect of aging is proportional to the formation of aging products on the particle surface. Furthermore, addition of retarders to the hydration of 14 days aged cement resulted in the absence of any measurable heat release during hydration. For this reason, 14 days aged samples of clinker phases were omitted from calorimetry investigations.

In conclusion, performance of sodium gluconate and potassium pyrophosphate varied between hydration stages. Gluconate was more effective in retarding the ettringite formation in aged cement, while pyrophosphate had a stronger effect on C-S-H formation in fresh cement. This raised the question whether the primary working mechanisms involved – adsorption for gluconate and removing calcium ions from pore solution for pyrophosphate – vary in effectiveness and importance throughout



the hydration process. To find out which mechanism has the biggest impact on ettringite and C-S-H formation respectively, focus was shifted from cement to the individual clinker phases. The hydration reactions of the essential clinker phases,  $\text{C}_3\text{A}$  for ettringite formation and  $\text{C}_3\text{S}$  for C-S-H formation, were investigated separately.

## 4.2 Hydration of Clinker Phase $\text{C}_3\text{A}$

### 4.2.1 Hydration of Cubic $\text{C}_3\text{A}$ with Potassium Pyrophosphate

Heat flow calorimetry of the 3 days aged mixture of cubic  $\text{C}_3\text{A}$  and gypsum showed a delay in ettringite formation of approximately 30 minutes compared to fresh  $\text{C}_3\text{A}_c$  (Figure 4). This is similar to CEM I 52.5 N, however the delay between fresh and aged cement was significantly higher at 2 hours (Figure 3).

Regarding retarders, pyrophosphate retarded ettringite formation in both fresh and aged mixtures of  $\text{C}_3\text{A}_c$  and gypsum. Its impact in fresh aluminate was limited to a slight decrease in maximum heat release, whereas aging increased the retarding effect of pyrophosphate significantly (Figure 4, left). Moreover, a second distinctive signal just under 96 hours after start of hydration (Figure 4, right) in fresh  $\text{C}_3\text{A}_c$  was also delayed by pyrophosphate. By comparison, in aged  $\text{C}_3\text{A}_c$  not one, but a pair of additional signals appeared within 24 hours after the start of hydration and thus far earlier than in fresh  $\text{C}_3\text{A}_c$ . This pair was also retarded by pyrophosphate. To identify the phase transitions behind the observed signals, the calorimeter samples were investigated with XRD 120 hours after the start of hydration.

In the samples prepared from fresh  $\text{C}_3\text{A}_c$ , only ettringite and monosulfate appeared in the X-ray diffractograms, which means the  $\text{C}_3\text{A}$  and the gypsum had fully dissolved. The late second signal observed in heat flow calorimetry could therefore originate from a late burst of ettringite formation due to sulfate depletion [11]. On the other hand, it could also mark the phase transformation from ettringite to monosulfate due to sulfate concentration in the pore solution falling below the threshold for ettringite stability.

XRD of aged  $\text{C}_3\text{A}_c$  samples revealed the presence of mono- and hemicarbonate next to ettringite and monosulfate. This indicates that part of the signal pair in heat flow calorimetry stems from the reaction of  $\text{C}_3\text{A}_c$  and the aging product aragonite to these carbonate phases.

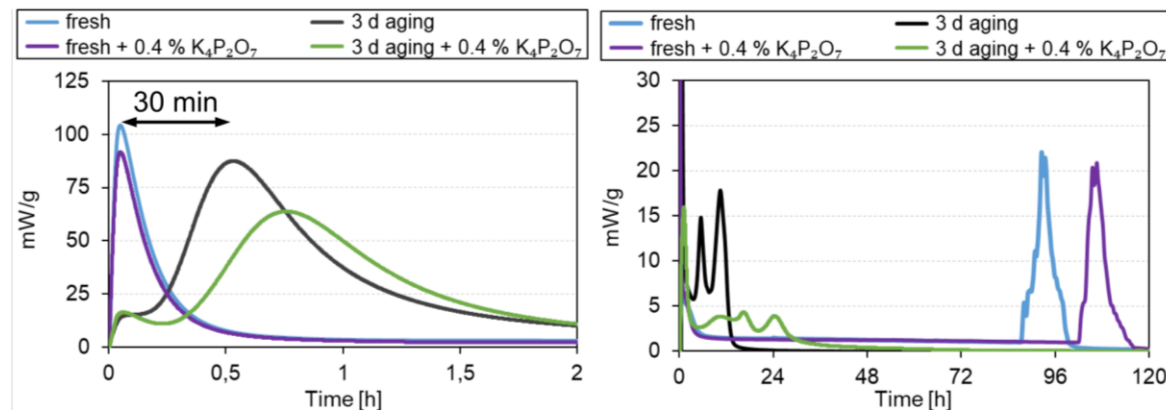


**Figure 4. Ettringite formation in fresh and 3 days aged  $\text{C}_3\text{A}_c + \text{gypsum}$  (w/b ratio = 2.0) with potassium pyrophosphate at the start of hydration (left) and over 5 days (right)**

### 4.2.2 Hydration of Cubic $\text{C}_3\text{A}$ with Sodium Gluconate

Addition of gluconate had the polar opposite effect on  $\text{C}_3\text{A}_c$  hydration compared to pyrophosphate. Ettringite formation was accelerated both in fresh and aged aluminate (Figure 5, left). The second signal in fresh was also affected, but the signal pair in aged  $\text{C}_3\text{A}_c$  was not (Figure 5, right). It is not uncommon that carboxylic acid-based retarders turn into accelerators. However the observed accelerating effect of gluconate stands in direct contrast to Cheung et al. [12], who showed that  $\text{C}_3\text{A}$ -hemihydrate mixtures can be effectively retarded with gluconate. Further investigations, particularly on the influence of the individual sulphate agents, are required.

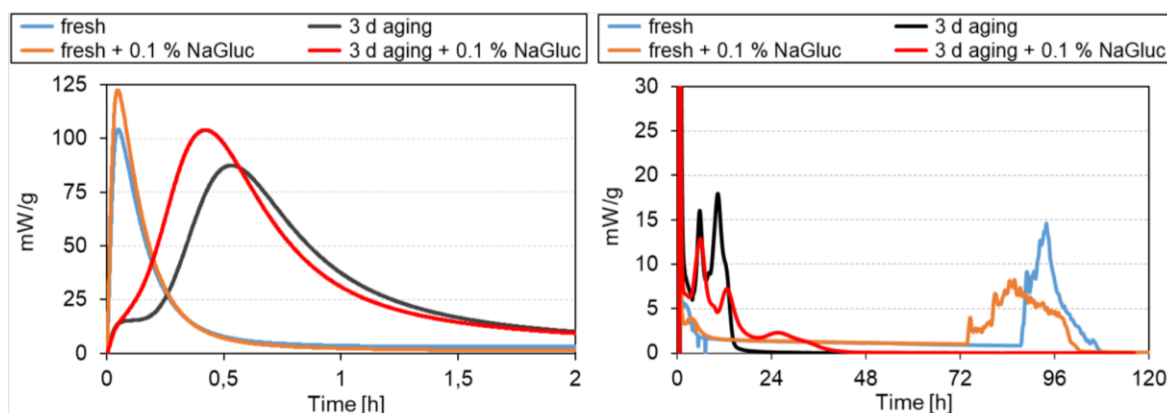


**Figure 5. Ettringite formation in fresh and 3 days aged  $\text{C}_3\text{A}_c$  + gypsum ( $w/b$  ratio = 2.0) with sodium gluconate at the start of hydration (left) and over 5 days (right)**

#### 4.2.3 Hydration of Orthorhombic $\text{C}_3\text{A}$

In fresh orthorhombic  $\text{C}_3\text{A}$  the accelerating effect of gluconate was observed as well, while pyrophosphate had little impact on hydration (Figure 6). Similar to cubic  $\text{C}_3\text{A}$ , a second signal appeared after 96 hours and was likewise retarded by pyrophosphate and accelerated by gluconate. No distinctive heat release was detected in the 3 days aged mixture of  $\text{C}_3\text{A}_o$  and gypsum. In this case, most of the hydration had already taken place during aging as evidenced in the X-ray diffractograms in Figure 1.

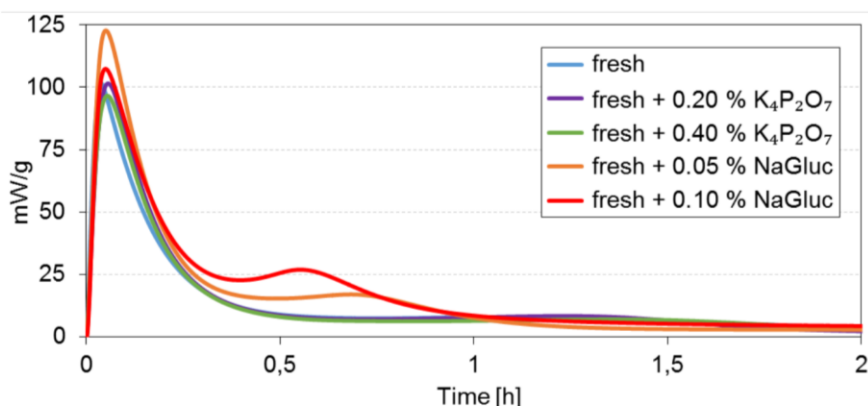


**Figure 6. Ettringite formation in fresh  $\text{C}_3\text{A}_o$  + gypsum ( $w/b$  ratio = 2.0) with sodium gluconate and potassium pyrophosphate**

### 4.3 Hydration of Clinker Phase $\text{C}_3\text{S}$

#### 4.3.1 Hydration of Fresh $\text{C}_3\text{S}$

In fresh triclinic  $\text{C}_3\text{S}$  the period from start of hydration to maximum heat release of C-S-H formation was 12 hours (Figure 7). This value corresponds well to fresh CEM I 52.5 N (Figure 3, left).

Dosages of 0.05 % bwob of gluconate and 0.20 % bwob of pyrophosphate had a similar retarding effect on fresh  $\text{C}_3\text{S}$ , both doubling the time to maximum heat release to 24 hours (Figure 7). This result confirms that using quadruple dosage of pyrophosphate to approximate gluconate performances in this study is appropriate.

Increasing pyrophosphate to 0.40 % only slightly shifted maximum heat release, whereas increasing gluconate to 0.10 % led to a very strong retarding effect compared to the other samples. In this case, the C-S-H formation was extremely protracted with small heat release maxima at on- and offset. Comparative measurements in fresh monoclinic  $\text{C}_3\text{S}$  (not shown) revealed an even stronger retarding effect. With 0.10 % gluconate no distinctive heat release could be detected for the whole measurement duration of 6 days, indicating that hydration had been completely inhibited. This



behavior is therefore not unique to the C<sub>3</sub>S<sub>t</sub> which, having none or very limited foreign ion content, is only found in small quantities in technical grade cement.

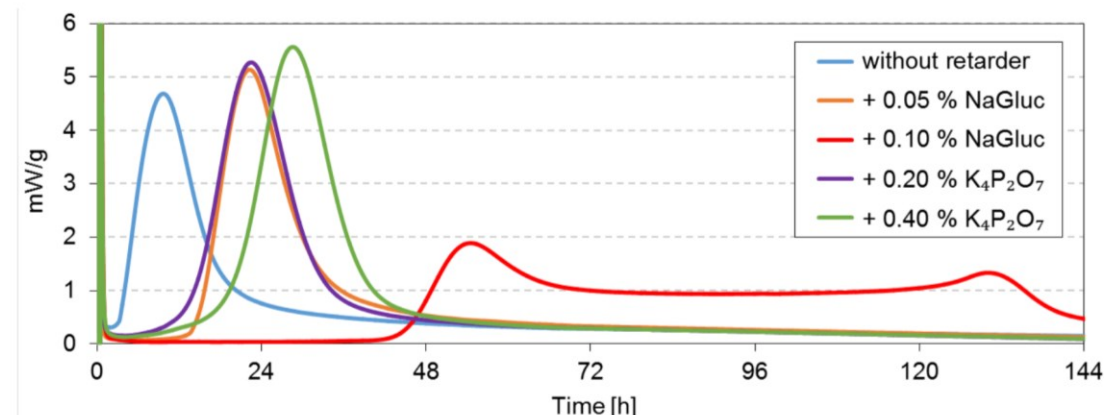


**Figure 7. C-S-H formation in fresh C<sub>3</sub>S<sub>t</sub> (w/b ratio = 0.6) with sodium gluconate and potassium pyrophosphate**

To rule out water demand of fresh C<sub>3</sub>S or insufficient mixing as causes for this protracted hydration, additional samples with increased water to binder ratio of 1.0 were left hydrating for one week at room temperature. As Figure 8 shows, fresh C<sub>3</sub>S without retarder and with 0.40 % K<sub>4</sub>P<sub>2</sub>O<sub>7</sub> visibly hydrated with only a small layer of surplus water remaining. On the other hand, the sample containing 0.10 % gluconate segregated without water consumption and the powder showed no caking at all. This confirmed the observations from heat flow calorimetry.

In conclusion, gluconate retarder performance significantly exceeded that of pyrophosphate at higher dosages in fresh C<sub>3</sub>S. This stands in direct contrast to fresh CEM I 52.5 N (Figure 3, left) where pyrophosphate had superior retarding effect on C-S-H formation.



**Figure 8. Hydration of fresh C<sub>3</sub>S<sub>m</sub> (w/b ratio = 1.0) without retarder (left), with 0.40 % bwob pyrophosphate (center) and with 0.10 % bwob gluconate (right)**

#### 4.3.2 Hydration of Aged C<sub>3</sub>S

After 3 days aging, maximum heat release of C-S-H formation in pure C<sub>3</sub>S was much lower than before aging, but still measurable (Figure 9). By comparison, aging of CEM I 52.5 N for 3 days had led to a complete disappearance of the respective signals in heat flow calorimetry. For C<sub>3</sub>S, this enabled direct comparison of the C-S-H formation between fresh (Figure 7) and aged clinker (Figure 9).

This comparison showed that, unlike ettringite formation, the aging process does not delay C-S-H formation. Both in fresh and aged C<sub>3</sub>S without retarders maximum heat release was reached approximately 12 hours after the start of hydration. Furthermore, heat flow calorimetry suggests that the onset of C-S-H formation in aged C<sub>3</sub>S actually occurs earlier than in fresh C<sub>3</sub>S. This is because



heat release of aged C<sub>3</sub>S does not reach zero during the induction period, signalling that C-S-H formation is already in progress. However, aging also extends the duration of C-S-H formation considerably, visible in the significant peak tailing all aged C<sub>3</sub>S samples displayed in the heat flow diagram. Apparently the aging products that overgrow the C<sub>3</sub>S surface act as seeding materials for C-S-H crystal growth, but also limit water access to the C<sub>3</sub>S below, therefore prolonging the hydration process.

Regarding retarder performance, 0.05 % bwob gluconate had a similar impact in fresh (Figure 7) and aged (Figure 9, left) C<sub>3</sub>S. The exceptionally strong retarding effect of 0.10 % gluconate in fresh C<sub>3</sub>S could not be observed in the aged clinker. Figure 9 shows that gluconate also affects the C-S-H formation during the induction period with heat release getting lower as gluconate dosage increases.

With pyrophosphate retarder there is less of a dose-effect relation (Figure 9, right), especially during the induction period. The retarding effect of pyrophosphate is based on removing calcium ions from pore solution. The overgrowth of particle surfaces with aging products slows calcium release from C<sub>3</sub>S, thus an increased pyrophosphate dosage does not enhance retardation as much as increasing dosage of the adsorbing gluconate.

Overall, in 3 days aged C<sub>3</sub>S pyrophosphate was more effective than gluconate, especially at the lower concentrations (Figure 9), which had displayed almost identical performance in fresh C<sub>3</sub>S (Figure 7).

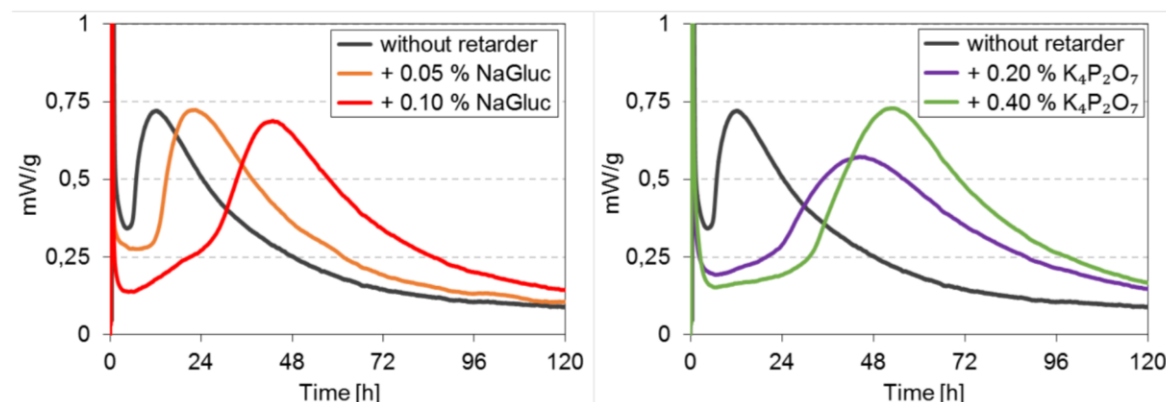


**Figure 9. C-S-H formation in 3 days aged C<sub>3</sub>S<sub>m</sub> (w/c ratio = 0.6) with sodium gluconate (left) and potassium pyrophosphate (right)**

## 5. CONCLUSION

In this study, performance of retarders sodium gluconate and potassium pyrophosphate was compared between fresh and aged CEM I 52.5 N, C<sub>3</sub>S and C<sub>3</sub>A. The aim of the research was to get a better understanding of the primary retarder mechanisms in the hydration process.

C<sub>3</sub>S and C<sub>3</sub>A were each synthesized in a pure and a doped modification. Along with CEM I, they were subjected to 35 °C / 90% relative humidity for 3 and 14 days. C<sub>3</sub>A samples had previously been drymixed with gypsum at a 1 : 1 weight ratio to account for ettringite formation during prehydration. Changes in the composition of particle surfaces during aging were monitored by XRD. Following these preparatory steps, hydration of fresh and aged samples was investigated with heat calorimetry, whereby gluconate and pyrophosphate were added to the mixing water.

Regarding CEM I, aging had a retarding effect on ettringite formation. This effect was strongest during the first days of aging, indicating that even short periods of prehydration during the job have a significant impact on binder properties. Addition of gluconate and pyrophosphate yielded different results in individual hydration stages. Ettringite formation in aged CEM I was more strongly retarded by gluconate, whereas pyrophosphate proved superior in retarding C-S-H formation of fresh cement. To find an explanation for this difference, the main clinker phases involved in the two hydration stages, C<sub>3</sub>A and C<sub>3</sub>S, were investigated individually.



Aging did retard ettringite formation of C<sub>3</sub>A with gypsum, albeit not as strongly as in CEM I. In fresh C<sub>3</sub>A a second distinctive heat release after 96 hours of hydration signalled either a late burst of ettringite formation or a phase transition from ettringite to monosulfate. Having partly taken place during aging already, hydration of aged C<sub>3</sub>A samples was completed much earlier, within approximately 24 hours. During this time, aging products reacted with remaining C<sub>3</sub>A to mono- and hemicarbonate.

Regarding retarders, pyrophosphate had a marginal effect on fresh C<sub>3</sub>A, but significantly delayed ettringite formation in aged C<sub>3</sub>A. Instead of retarding, gluconate accelerated both fresh and aged C<sub>3</sub>A.

In fresh C<sub>3</sub>S, retarding performance of pyrophosphate was comparable to fresh cement while gluconate was exceptionally effective at a dosage of 0.10 % bwob. It showed potential to completely block hydration for at least six days depending on C<sub>3</sub>S polymorph.

Aging the C<sub>3</sub>S did not delay the onset of C-S-H formation but significantly increased duration. Unlike fresh clinker and cement, C-S-H formation was observed as early as the induction period due to seeding effects of the aging products. The exceptional retardation effect of 0.10 % gluconate was not observed after aging, however retardation increased with dosage still. By contrast, increasing pyrophosphate dosage was less effective, indicating its retardation potential is limited by the slow calcium ion release of C<sub>3</sub>S particles overgrown with aging products.

## 6. ACKNOWLEDGEMENTS

The authors are most grateful to Deutsche Forschungsgemeinschaft, Bonn, Germany (DFG) for financing this project under the grant PL-472/9-2 and to HeidelbergCement company for providing cement.

## 7. REFERENCES

- [1] Schmid, G.; Bier, T. A.; Wutz, K.; Maier, M.: *Characterization of the aging behaviour of premixed dry mortars and its effect on their workability properties*, ZKG International 60 (2007), 94-103.
- [2] Barbic, L.; Tinta, V.; Lozar, B.; Marincovic, V.: *Effect of storage time on the rheological behavior of oil well slurries*, Journal of the American Ceramic Society 74 (1991), 954-949.
- [3] Whittaker, M.; Dubina, E.; Plank, J.; Black, L.: *The Effects of Cement Prehydration on Engineering Properties*, Cement and Concrete Science, Birmingham, 2010, 101-104.
- [4] Winnefeld, F.: *Influence of cement ageing and addition time on the performance of superplasticizers*, ZKG International 61 (2008), 68-77.
- [5] Dubina, E.; Plank, J.: *Influence of moisture- and CO<sub>2</sub>-induced ageing in cement on the performance of admixtures used in construction chemistry*, ZKG International 65 (2012), 60-68.
- [6] Meier, M. R.; Napharatsamee, T.; Plank, J. Dispersing performance of superplasticizers admixed to aged cement, Construction and Building Materials 139 (2017), 232-240.
- [7] Dubina, E.; Wadsö, L.; Plank, J.: *A sorption balance study of water vapor sorption on anhydrous cement minerals and cement constituents*, Cement and Concrete Research 41 (2011), 1196-1204.
- [8] Wesselsky, A.; Jensen, O. M.: *Synthesis of pure Portland cement phases*, Cement and Concrete Research 39 (2009), 973-980.
- [9] Plank, J.; Zhang-Preße, M.; Ivleva, N.P.; Niessner, R. *Stability of Single Phase C<sub>3</sub>A Hydrates Against Pressurized CO<sub>2</sub>*, Construction and Building Materials 122 (2016), 426-434.



- [10] Dubina, E.; Plank, J.; Black, L.; Wadsö, L.: *Impact of environmental moisture on C<sub>3</sub>A polymorphs in the absence and presence of CaSO<sub>4</sub> · 0.5 H<sub>2</sub>O*, Advances in Cement Research 26 (2014), 29-40.
- [11] Jansen, D.; Naber, C.; Ectors, D.; Lu, Z.; Kong, X.-M.; Goetz-Neunhoeffer, F.; Neubauer, J. *The early hydration of OPC investigated by in-situ XRD, heat flow calorimetry, pore water analysis and <sup>1</sup>H NMR: Learning about adsorbed ions from a complete mass balance approach*, Cement and Concrete Research 109 (2018), 230-242.
- [12] Cheung J., Jeknavorian A., Roberts L., Silva D.; *Impact of admixtures on the hydration kinetics of Portland cement*, Cement and Concrete Research 41 (2011), 1289-1309.



## 4.3 Topic 2: Impact of aging on the ternary binder system and chemical admixtures in self-levelling underlays

### 4.3.1 Journal article 3: Aging of various components of a model SLU

#### 4.3.1.1 Content overview for journal article 3

The third journal article deals with the aging of a model self-levelling underlayment (SLU) as an example for a dry-mix products with a limited shelf-life. The investigation was carried out in a step-by-step analysis (**Figure 44**). First, the aging impact on the components of a ternary binder system (TBS), which constitutes the basis of the SLU formulation, was studied. Second, fresh TBS containing one of three admixtures used in the model SLU (accelerator, retarder and superplasticizer) was aged to isolate the aging impact on an individual admixture. Finally, the hydration behavior of the fully formulated SLU containing all admixtures was analyzed before and after aging.

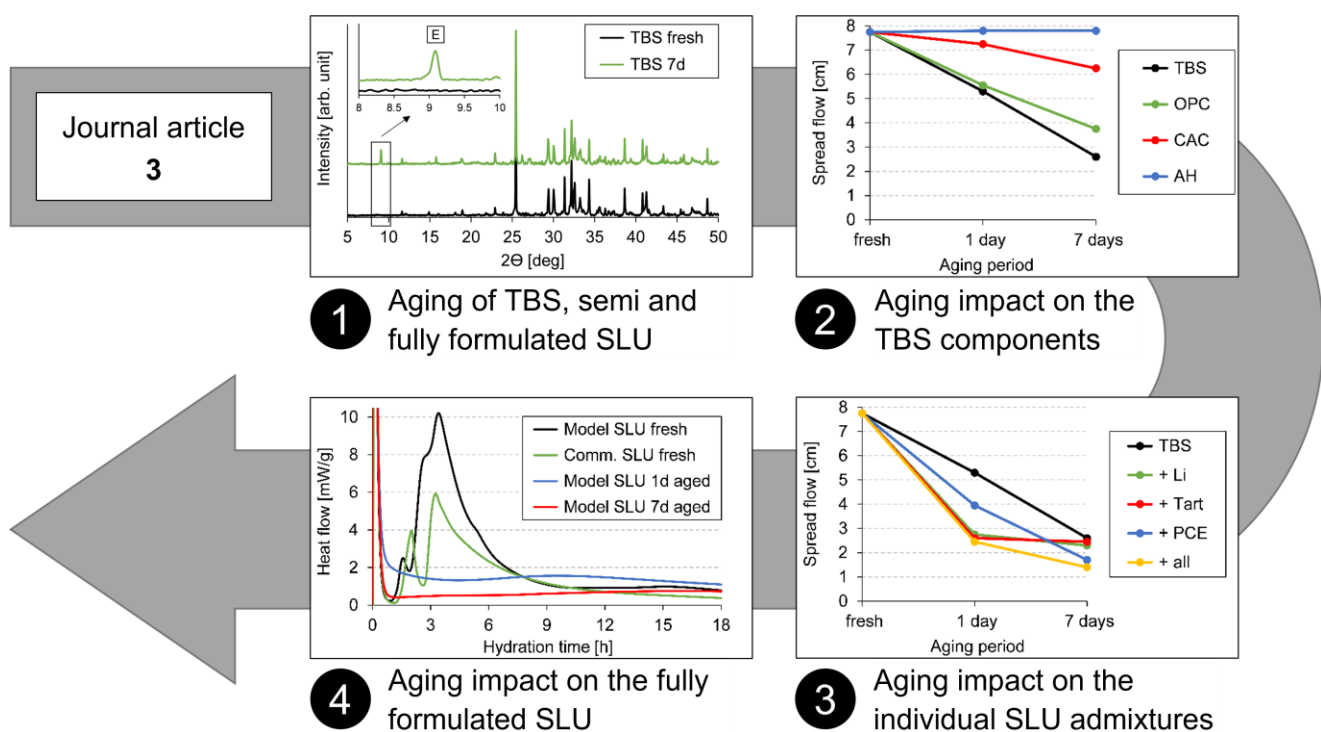


**Figure 44:** Overview of journal article 3 on the aging of TBS and SLU.

- 1 The TBS consists of ordinary Portland cement (OPC), calcium aluminate cement (CAC) and calcium sulfate anhydrite (AH). To formulate the SLU the TBS is admixed with lithium carbonate ( $\text{Li}_2\text{CO}_3$ ) as an accelerator for the CAC, sodium potassium tartrate as a retarder and the commercial BASF Melflux 2651 F (a PCE) as a superplasticizer.

A total of eight TBS batches were distinguished in the project: Five were prepared from fresh OPC, CAC and AH. One of these fresh TBS batches was aged without admixtures and three were admixed with one out of accelerator, retarder and superplasticizer. The fifth batch was admixed with all three admixtures, which constitutes the fully formulated model SLU. The three batches with one admixture each were called 'semi-formulated' SLUs. All fresh TBS batches were then aged at

35 °C and 90% RH. Exposure durations were 1 day (short-term aging) or 7 days (long-term aging). After exposure but prior to the experiments on hydration behavior, the missing two admixtures were added to the semi-formulated SLUs. This way, the aging impact on a single admixture in the model SLU can be isolated and investigated.

From the total of eight batches, the remaining three had one of OPC, CAC and AH aged for 1 or 7 days beforehand. This allows to investigate the impact of exposure of a single TBS component on hydration. These batches were not aged further and each immediately admixed with all three admixtures.

- ② First, model SLU samples where the whole TBS was aged were compared with samples where only one of the TBS components was aged. Samples with the whole TBS or the OPC aged displayed comparable hydration behaviors in most experiments. Samples containing aged CAC or aged AH also showed similarities in hydration. This is caused by differences in the aging behavior of the TBS and its individual components as revealed by powder XRD and TGA. It was found that the whole TBS and the OPC formed ettringite as a prehydration product. In OPC ettringite formed from the aluminate clinker phases and the sulfate set regulator, in the whole TBS additionally from CAC and AH. In contrast, even after 7 days of exposure no prehydrates were detected by powder XRD in both CAC and AH. Their water uptakes during after aging were much lower than those of OPC and the whole TBS. For the AH, this is consistent with the previously observed low water sorption of pure anhydrous  $\text{CaSO}_4$  as mentioned in chapter 2.4.2.

The ettringite formed during the aging of the whole TBS or the OPC caused a seeding effect in the hydration of the model SLU. The resulting rapid ettringite growth accelerated the setting process and impeded the compressive strength development as it had previously been observed for the hydration of pure OPC in journal article 2. Additionally, it caused a drastic flowability loss of the model SLU. The aging impact was generally more severe for samples which had the whole TBS exposed than for those that just contained aged OPC. This was due to the significantly higher water uptake of the whole TBS as a result of the additional ettringite formation from CAC and AH during prehydration.

- ③ Second, SLU samples where only the TBS was aged were compared with samples where the TBS was aged together with one of the three admixtures. It was discovered that all admixtures increased the prehydration degree of the TBS, among them the addition of  $\text{Li}_2\text{CO}_3$  caused the highest water uptake. At the same time, the admixtures completely lost their effect in the hydration process already after 1 day of aging ( $\text{Li}_2\text{CO}_3$  and tartrate) or after 7 days (PCE). As a result, the SLU sample consisting of aged TBS and  $\text{Li}_2\text{CO}_3$  in combination with unaged tartrate hydrated much slower and the sample with aged tartrate and unaged  $\text{Li}_2\text{CO}_3$  much faster than the reference. The presence of PCE during 1 day of aging did not change the hydration significantly. After 7 days however, not only did the PCE lose its dispersing ability, it also caused a significant retardation of the SLU's setting. The effect was much stronger than how a PCE would slightly retard Portland cement hydration as described in chapter 2.3.4.
- ④ The aging of the fully formulated model SLU revealed that the impacts on the individual admixtures stack if they are all present during exposure. For example, due to it containing the highest amount of admixtures the fully formulated SLU exhibited the highest water uptake of all investigated

#### 4.3 TOPIC 2: AGING IMPACT ON TBS AND MODEL SLU

---

samples during aging and the lowest spread flow. On the other hand, because accelerator and retarder both were aged and lost their effect, the compressive strength development was actually still better than that of the SLU sample containing aged accelerator and fresh retarder which slows the hydration.

Finally, the aging of the fully formulated model SLU was compared with that of a commercial product (*K 15* by Ardex). Their hydration behaviors were found to be comparable not only before but also after exposure.

**4.3.1.2 Reprint of journal article 3**

**Effects of exposure to atmospheric moisture and CO<sub>2</sub> on the performance of a ternary binder system and chemical admixtures in a self-levelling underlayment**

F. A. Hartmann, L. C. Mengel, J. Plank

Submitted to *Construction and Building Materials* on 15 May 2022

### **Declarations:**

Funding was provided by Deutsche Forschungsgemeinschaft, Bonn, Germany (DFG) under the grant PL-472/9-2 “Influence of aging of binder systems on the performance of additives”.

The authors wish to declare that no conflicts of interest or competing interests exist.

### **Abstract:**

The aging processes causing a limited shelf life of self-levelling underlays (SLUs) require a better understanding. Different components of a model formulation based on a ternary binder system (TBS) with accelerator, retarder and superplasticizer were exposed to atmospheric moisture and CO<sub>2</sub> at elevated temperatures and high humidity. Changes in the material composition, hydration behavior and engineering properties were investigated. The combined TBS possessed significantly higher hygroscopicity than its individual components, resulting in premature ettringite formation which exhibited a seeding effect that eliminates the dormant period. The presence of admixtures during exposure accelerated the TBS's aging and drastically lowered their performance in hydration. This negatively affected both setting and compressive strength development and unbalanced the hydration behavior of formulations with a mix of fresh and aged admixtures. The study highlights the importance of proper storage of dry-mixes to preserve their functionality over time.

### **Keywords:**

Admixture, Aging, Compressive strength, Prehydration, Self-levelling underlays, Setting behavior

### **Highlights:**

- Hydration of a model SLU formulation with different aged components was examined
- The combined TBS aged more severely than OPC, CAC and anhydrite individually
- Main exposure product of TBS was ettringite, exhibited seeding effect in hydration
- Aging TBS with admixtures lowered their performance compared to addition post-aging
- Negative impact of aging on TBS rheology / strength worsened by admixture presence

## 1. Introduction

High reactivity towards water is a key factor for the commercial success of cementitious building materials, though this results in a premature partial hydration upon unintentional contact with moisture. This process is known as “prehydration” or “aging” if carbonation by atmospheric CO<sub>2</sub> is also considered. There is a plethora of causes for aging, ranging from improper storage and handling of the building material prior to application back to cement manufacture. There, gypsum is interground with the clinker as a set control agent. The milling temperature reaches ~120 °C, at which crystal water is released from gypsum and can react with the clinker [1, 2]. This prehydration continues during storage of the ground material in silos where temperatures are still elevated [3, 4].

The exposure to moisture results in the premature formation of hydration products on the binder particles [5–9] which was proven to have adverse effects on rheological properties, setting times and strength development [10–14]. Furthermore, the interactions with admixtures which are intricately linked to particle surface properties were reported to change significantly and often inconsistently after aging [15–18]. This concerned both the adjustment of potentially aged binders to specified properties with fresh admixtures such as in ready-mix and precast applications as well as dry-mix compounds in which the admixture was present when exposure occurred during storage and transport. An example of the latter are self-leveling underlays (SLUs) which are applied to provide a level surface to uneven foundations [19–21]. In order to satisfy requirements for fast setting and strength development at minimum shrinkage to reduce construction downtime, commercial SLUs are frequently based on a ternary binder system (TBS) combining ordinary Portland cement (OPC), calcium aluminate cement (CAC) and anhydrite (AH) [22, 23]. This blend produces large amounts of fast forming expansive ettringite (Ca<sub>6</sub>[Al(OH)<sub>6</sub>]<sub>2</sub>(SO<sub>4</sub>)<sub>3</sub> · 26 H<sub>2</sub>O) during hydration. Retarders and superplasticizers to adjust workability, as well as accelerators for the CAC are common admixtures added to the TBS in fully formulated SLUs. With this highly reactive composition, the advantages in application come at the price of a limited shelf-life. Particularly in humid atmosphere, performance changes after prolonged storage have been reported [24]. With studies describing the aging impact on dry mortars having been published in recent years [25, 26], we aim to contribute further to this work by elucidating the effects of aging on the TBS and the chemical admixtures in SLUs.

Our investigations had two foci: First the aging of the combined system or one of its individual components OPC, CAC and AH and its impact on the TBS’s hydration behavior in the presence of unaged chemical admixtures were examined. Second, the TBS was admixed with one of accelerator, retarder or superplasticizer, aged and then hydrated together with the remaining two unaged admixtures to determine performance changes of individual admixtures after exposure in the presence of cementitious materials.

For these purposes, components of a self-developed model SLU were exposed to atmospheric moisture and CO<sub>2</sub> at 35 °C and 90 % relative humidity (RH) for 1 or 7 days. After aging, the powders were characterized using thermogravimetric analysis coupled with mass spectrometry (TG-MS) and powder X-ray diffraction (XRD) before being formulated into a full SLU mix. Hydration behavior was investigated both via heat flow calorimetry and the quantification of the free Ca<sup>2+</sup> contained in pore solution by inductively coupled plasma optical emission spectroscopy (ICP-OES). Finally, engineering properties of the SLUs with different aged components, namely rheological and setting behavior as well as compressive strength development, were compared. The ultimate goal of the study was to provide information as to which components of a common SLU formulation are particularly susceptible to aging and require close attention to limit exposure.

## 2. Experimental Section

### 2.1 Model SLU formulation

The composition of the model SLU formulation used in this study is given in **Table 1**. The recipe was fixed at an elevated water-to-formulation (w/f) ratio of 0.50 to account for higher water demand of dry-mix compounds after the aging process [26], thus the small dosage of superplasticizer. All components were passed through a sieve with a mesh size of 90 µm prior to formulation. The SLU was dry-mixed for 120 min using a Heidolph *REAX 20/4* overhead shaker at 15 rpm.

**Table 1:** Composition of the model SLU formulation used in this study.

Component	Manufacturer and product designation	Function	Content [wt.%]
OPC	HeidelbergCement CEM I 52.5 N Milke	Binder	47.23
CAC	Kerneos Ciment Fondu	Binder	32.75
AH	Solvay Fluoroanhydrite	Binder	19.06
Lithium carbonate	Chemetall	Accelerator	0.30
Sodium potassium tartrate	Jungbunzlauer	Retarder	0.60
PCE	BASF Melflux 2651 F	Superplasticizer	0.06

## 2.2 Aging procedure

The SLU components selected for aging were spread out in portions of 50.0 g on 135 x 60 cm Plexiglas plates (layer thickness ~0.2 mm), thus maximizing the exposed particle surface area to atmospheric moisture and CO<sub>2</sub>. They were then exposed to 90 ± 5 % relative humidity (RH) at 35 ± 2 °C in a custom-built climate box for 1 or 7 days. After aging, the powders were collected from the plates and SLUs with different aged components were formulated. The individual combinations that were examined in this study are listed in **Table 2**.

**Table 2:** Model SLUs with different aged components investigated in this study.

Designation	Aged components	Fresh components
TBS	TBS in pure form	accelerator, retarder, superplasticizer
TBS + Li	TBS with accelerator	retarder, superplasticizer
TBS + Tart	TBS with retarder	accelerator, superplasticizer
TBS + PCE	TBS with superplasticizer	accelerator, retarder
TBS + all	fully formulated SLU	none
OPC	OPC in pure form	CAC, AH, accelerator, retarder, superplasticizer
CAC	CAC in pure form	OPC, AH, accelerator, retarder, superplasticizer
AH	AH in pure form	OPC, CAC, accelerator, retarder, superplasticizer

### 2.3 Characterization of the aged SLU components

#### 2.3.1 TG-MS

Formation of hydration and carbonation products during aging was determined via thermogravimetric analysis coupled with mass spectroscopy (TG-MS) using a Netzsch simultaneous thermal analyzer (STA) 409 PC Luxx with a Netzsch quadrupole mass spectrometer (QMS) 403 Aëolos Quadro. The samples were heated from 20 to 1000 °C at a constant rate of 10 °C per minute.

#### 2.3.2 Powder XRD

Particle surface changes during exposure were investigated via powder XRD. Fresh SLU samples placed in plastic XRD holders were aged under the same conditions as the powders on the Plexiglas plates. That way, the samples can be directly measured after aging without requiring any preparation. This method prevents potential damage to the delicate crystalline aging products on the particle surfaces when the aged powders are collected from the plates. Powder XRD measurements were taken at a Bruker AXS D8 Advance instrument with Bragg-Brentano geometry and a CuK $\alpha$  ( $\lambda = 1.5406 \text{ \AA}$ ) source. Scans were recorded at a range of 5–70° 2 $\Theta$  in steps of 0.008° with an exposure time of 0.5 seconds per step at 30 kV accelerating voltage and 35 mA irradiation intensity.

## 2.4 Hydration behavior of fresh and aged samples

#### 2.4.1 Isothermal heat flow calorimetry

Comparative heat flow calorimetric analysis of the model SLU with different aged components was carried out at a Thermometric AB TAM Air 3114 isothermal calorimeter at 20 °C following DIN EN 196-11 [27]. For each measurement, 4.00 g of SLU powder were weighed into a 10 mL glass vial. Pure deionized water obtained from a Barnstead Nanopure Diamond water purification system and tempered to 20 °C was added to the sample at a w/f ratio of 0.50. The vial was sealed with a crimped aluminum cap and the slurry homogenized for 120 seconds using a VWR VWT 1419 vortex mixer at maximum speed. After placement into the measurement chamber, the heat flow was recorded until it dropped below 0.2 mW/g.

#### 2.4.2 ICP-OES

The impact of aging on the free Ca<sup>2+</sup> concentration in the pore solution was investigated via inductively coupled plasma optical emission spectrometry (ICP-OES). 12.0 g of SLU powder were mixed with deionized water (w/f ratio = 1.00) for 120 seconds at maximum vortex mixer speed. The samples were then centrifuged at 8500 rpm and 20 °C for 10 minutes using a Stratos Biofuge. The supernatants were decanted, and small solid particles removed using a polyethersulfone (PES) syringe filter with a mesh size of 0.2 µm. The filtrates were immediately acidified with 0.1 M HNO<sub>3</sub> at a 1 : 3 (vol./vol.) ratio and further diluted with deionized H<sub>2</sub>O 1 : 10 (vol./vol.) before the measurement, which was performed on an Agilent Technologies 725 device equipped with a SPS 3 autosampler. A multielement standard (Merck Standard IV) at concentrations of 0.1; 1; 10 and 100 mg/L was used for calibration.

### 2.5 Engineering properties of fresh and aged samples

Investigations into rheological and setting behavior as well as compressive strength development were gated by the limited quantities of aged SLU powder available (exposure in portions of only 50.0 g). Standardized test methods were thus modified for smaller sample sizes.

#### 2.5.1 Rheological behavior

Spread flow tests were performed based on DIN EN 12706-12 [28]. Deionized water at 0.50 w/f ratio was added to 6.5 g fresh or aged SLU powder in a 10 mL glass vial and homogenized for 120 seconds at maximum vortex mixer speed. A 14 x 25 mm brass cone placed on a glass plate was filled to the brim with the paste. The cone was lifted within two seconds and drained for ten seconds. After four minutes, the spread flow was measured with a caliper twice perpendicularly and the mean recorded.

#### 2.5.2 Setting behavior

Setting behavior was determined based on DIN EN 196-3 [29], scaled down according to a previous study [30]. The steel load of the Vicat apparatus was replaced with aluminum, reducing its weight from 300 g to 100 g. Cylindrical glass vessels with snap-on lids (inner diameter 15 mm, height 20 mm) substituted the Vicat cone. 15.00 g of fresh or aged SLU powder were placed in the glass vessel and mixed with deionized water (w/f ratio = 0.50) for 120 sec at maximum vortex mixer speed. The glass vessel was then placed under the aluminum load and the needle lowered into the paste every 30 minutes until initial set occurred and then every 15 minutes afterwards. The test was carried out in a walk-in climate chamber under stable environmental conditions of 20 °C and 60 % RH. Between measurements, the glass vessel remained sealed with the snap-on lid to limit water evaporation.

#### 2.5.3 Compressive strength

Compressive strength development was examined according to a modified DIN EN 196-1 standard [31]. Test specimens were prepared from SLU paste rather than mortar as specified in the norm. Deionized water (w/f ratio = 0.50) was added to 45.00 g of fresh or aged SLU powder equally divided between two 40 mL glass vessels and homogenized for 120 seconds using two vortex mixers set to maximum speed. The pastes were poured into a custom-made brass mold yielding three 40 x 15 x 15 mm prisms. The mold was then placed on a Toni Technik *ToniVib* vibrating table and compacted for a further 120 seconds at 50 Hz. Excess paste was removed, and the mold stored for 24 hours at 20 °C above water (> 85% RH) before the specimens were demolded. Compressive strength was determined directly after demolding as well as after 2 or 6 days of additional storage under water (3 or 7 days total) using a Toni Technik *ToniNORM* test plant.

### 3. Results and Discussion

#### 3.1 Impact of aging on SLU hydration behavior

##### 3.1.1 Deriving a model SLU formulation from a commercial product

The model SLU used in this study was formulated to match the hydration behavior of the commercial product Ardex *K15* as closely as possible when both are unaged. In a previous study [26] it was observed that after aging the water demand of SLUs increased from 0.25 w/f to 0.50. Using different w/f ratios for fresh and aged samples however would make comparisons of the hydration behavior less conclusive. We thus adjusted the formulation for a fixed w/f ratio of 0.50 in all cases by reducing superplasticizer dosage to avoid bleeding of the fresh sample.

Heat flow calorimetry of the fresh and aged model SLU samples at 0.50 w/f in comparison to fresh Ardex *K15* at 0.25 w/f is displayed in **Figure 1**. As shown on the left, we achieved roughly simultaneous occurrence of the heat flow maxima in the fresh model SLU and in the commercial product. The overall heat release of the model SLU was always higher due to the Ardex *K15* containing non-reactive filler materials in addition to the ternary binder system. Aging the model SLU revealed a severe impact on the hydration behavior already after 1 day of exposure. The heat flow over the first ~8 hours of hydration was much reduced compared to the fresh sample. Heat was being steadily released without prominent peaks but also without a distinctive dormant period shortly after the start of hydration, signifying a seeding effect that promoted early formation of hydrate phases. Total heat released (shown on the right in **Figure 1**) thus increased almost linearly after aging for 1 day and is expected to eventually match that of the fresh sample. The observed aging effects were exacerbated had the sample been aged for 7 days instead of one.

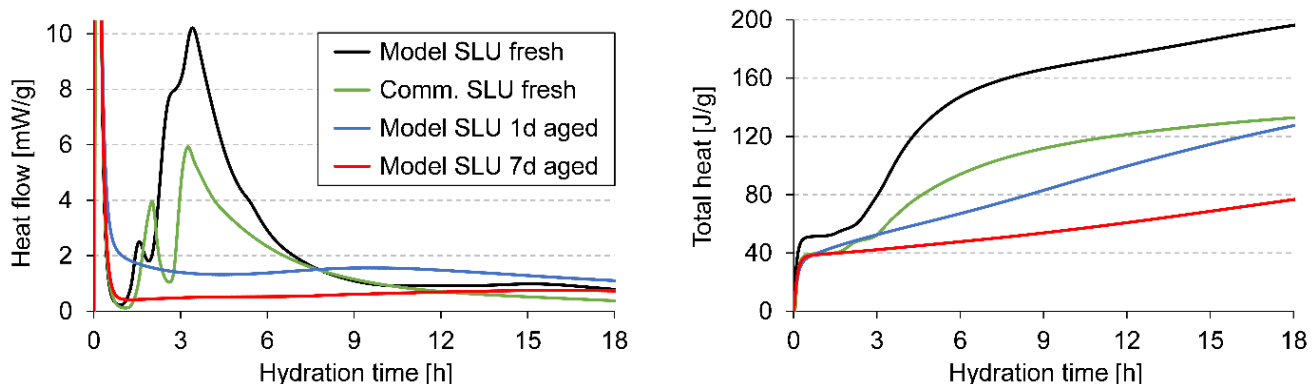


**Figure 1:** Heat flow calorimetric analysis of the fresh and aged model SLU (w/f ratio = 0.50), compared to commercial SLU Ardex *K15* (w/f ratio = 0.25).

To gain a better understanding of the aging effects impacting hydration to such a high degree, the SLU aging process was broken down into individual parts. Two investigation routes were selected: First, the aging of the combined TBS or one of its individual components (OPC, CAC and AH) before hydration in the presence of unaged chemical admixtures was examined. Second, the TBS was admixed with only one of accelerator, retarder or superplasticizer, aged and then hydrated together with the remaining two unaged admixtures. This aimed at investigating performance changes of individual admixtures after exposure to 35 °C / 90 % RH in the presence of the binders.

### 3.1.2 Calorimetric analysis of model SLUs with different aged components

**Figure 2** shows the heat flow calorimetry curves of model SLUs where either the combined TBS or one of its individual components OPC, CAC or AH were aged before hydration. After exposure for 1 day (top) the heat flow maxima of the TBS was delayed and occurred after ~7 hours compared to ~4 hours for the fresh SLU (**Figure 1**, left). Had only the OPC been aged, hydration was accelerated, and the heat flow showed a double peak already 4–5 hours after the start of hydration. With aged CAC or AH the heat flow peaked latest, at ~9 and ~11 hours after mixing, respectively. Moreover, these maxima were preceded by extensive dormant periods (~3 hours with aged CAC, ~6 hours with aged AH).

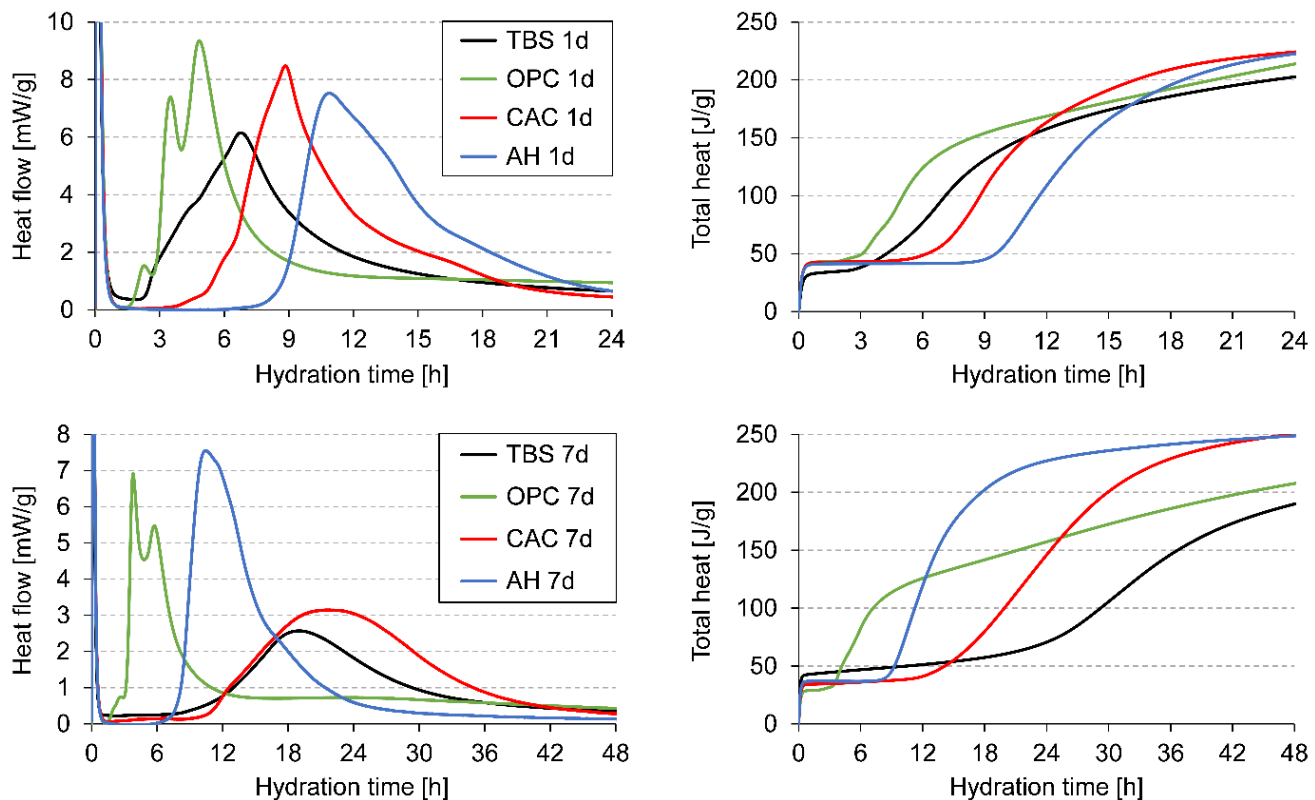


**Figure 2:** Heat flow calorimetric analysis of the model SLU (w/f ratio = 0.50) after aging either the ternary binder system and its individual components for 1 day (top) or 7 days (bottom) at 35 °C / 90 % RH.

When the aging period was extended from 1 to 7 days (**Figure 2**, bottom), the duration of the main hydration process roughly doubled from 24 to 48 hours with regards to reaching comparable total heat values (200–250 J/g) as displayed on the right. Concerning the heat flow maxima, the prolonged aging least affected the OPC and AH. The peak of the SLU sample with 7-days aged CAC however was much delayed to ~22 hours after the start of hydration up from ~9 hours after 1 day of exposure with the dormant period extended to ~10 hours. This appears to disproportionately affect the combined TBS which peaked at ~19 hours up from ~7 after 1 day.

In **Figure 3** the heat flow calorimetry results of model SLU samples with different chemical admixtures aged in the presence of the TBS are summarized. After 1 day of exposure, the hydration curves of the TBS aged pure and with PCE superplasticizer overlapped completely and after 7 days only a slight

#### 4.3 TOPIC 2: AGING IMPACT ON TBS AND MODEL SLU

retardation effect of the superplasticizer was observed. This is plausible with regards to the small dosage of PCE applied due to the higher w/f ratio.

On the other hand, lithium salt or tartrate admixture to the TBS before aging drastically changed the hydration behavior of the model SLU. The accelerator appears to mostly lose its effect during exposure with the hydration process lasting for 168 hours after aging for only 1 day and 240 hours after 7 days. Similarly, aging the TBS with tartrate retarder for 1 day led to a faster hydration afterwards with no dormant period being observed. After 7 days, during early hydration heat flow dropped no lower than 1.5 mW/g before rising again to above 6 mW/g, which is a result of the previously observed competing effect of TBS hydration getting increasingly delayed by longer exposure (**Figure 2**). The results signify that the prehydration of the TBS with individual admixtures can practically erase their effect in fully formulated SLUs and completely disbalance them.

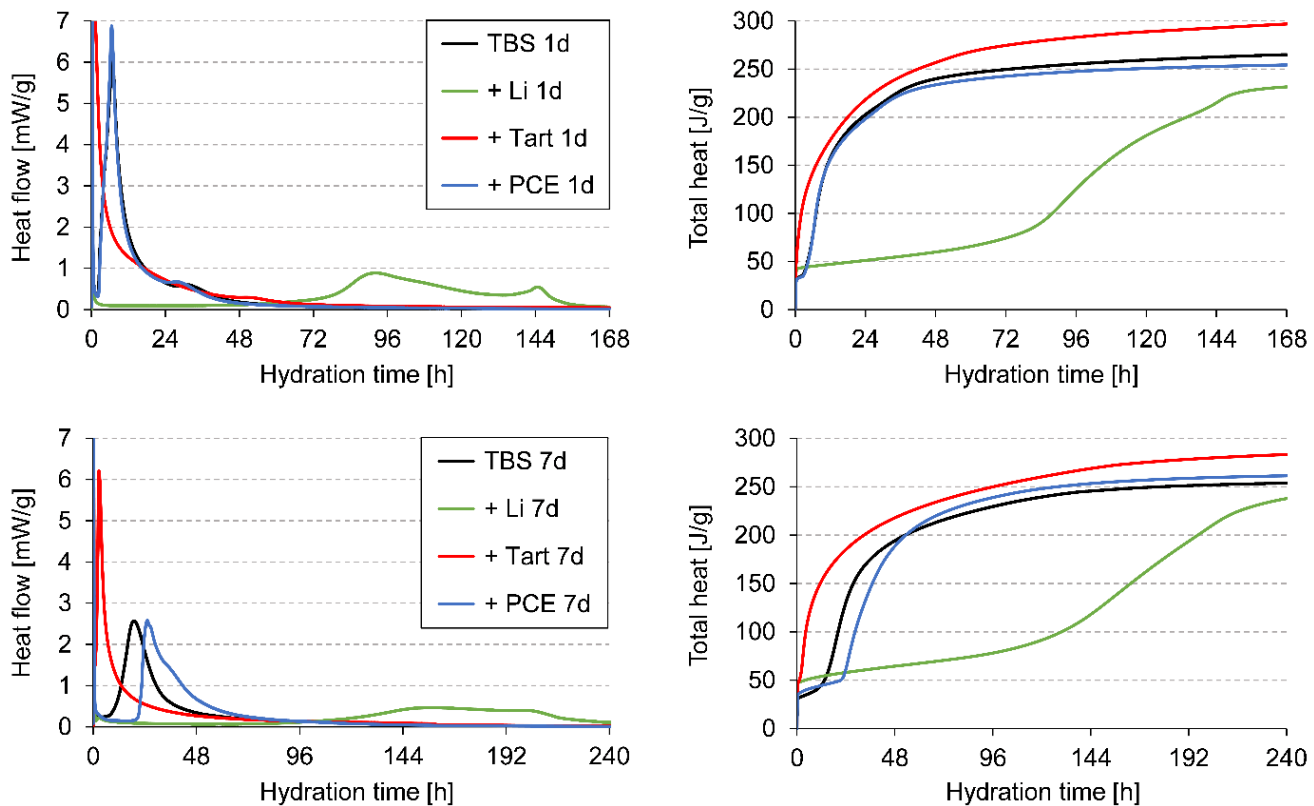


**Figure 3:** Heat flow calorimetric analysis of model SLU samples (w/f ratio = 0.50). After aging the ternary binder system with different admixtures for 1 day (top) or 7 days (bottom) at 35 °C / 90 % RH, hydration was performed in the presence of the other, non-aged admixtures.

### 3.1.3 Pore solution analysis of model SLUs with different aged components

The calorimetric analysis was supplemented by a pore solution investigation of the model SLUs using ICP-OES. **Figure 4** displays the concentration of free  $\text{Ca}^{2+}$  in the filtered supernatants after mixing the powders with deionized  $\text{H}_2\text{O}$  and centrifugation. In the fresh reference system (no components aged),  $\text{Ca}^{2+}$  concentration was  $\sim 600 \text{ mg/L}$ . This value dropped sharply had the TBS been aged for 1 day with or without admixtures, as shown on the left. Interestingly, after 7 days of exposure the free  $\text{Ca}^{2+}$  concentration was notably higher, surpassing the reference in all cases but TBS aged with lithium accelerator. The pure TBS and TBS admixed with tartrate or PCE display comparable values of 900–1000  $\text{mg/L}$  after 7 days, while the fully formulated SLU with all admixtures present during aging reached 1400  $\text{mg/L}$ . It can be assumed that in the TBS + Li sample the free  $\text{Ca}^{2+}$  concentration was kept low due to the presence of unaged tartrate and PCE which can both chelate  $\text{Ca}^{2+}$ . Correspondingly, the concentration was highest when all admixtures had been aged in the fully formulated SLU sample. The values laying in between these two outliers presumably resulted from competing effects between the  $\text{Ca}^{2+}$  enriching fresh lithium and  $\text{Ca}^{2+}$  removing fresh tartrate and/or PCE.

Had the individual components of the TBS been aged instead of the admixtures, then the initial drop in free  $\text{Ca}^{2+}$  concentration after 1 day was not observed and the values remained relatively stable, only in the SLU sample containing 7-days aged OPC was it slightly lower.

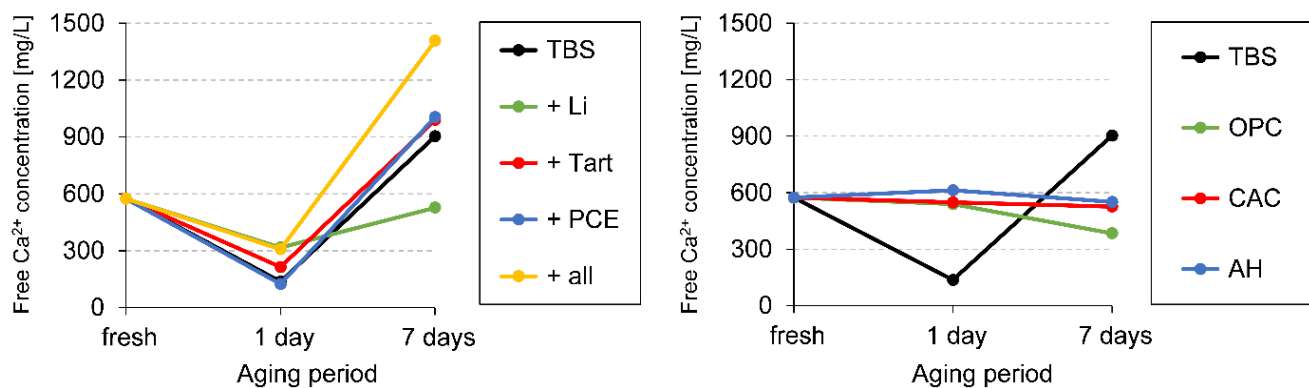


**Figure 4:** Concentration of freely dissolved  $\text{Ca}^{2+}$  present in the pore solution of model SLU samples (w/f ratio = 1.0), either fresh or with different components aged at 35 °C / 90 % RH for 1 or 7 days.

### 3.2 Aging behavior of the ternary binder system and the chemical admixtures

To gain a better understanding of its impact on hydration behavior, the SLU aging process was investigated more closely. For this purpose, the phase compositions of fresh and prehydrated SLU components were compared via TG-MS and powder XRD.

### 3.2.1 TG-MS analysis

**Figure 5** displays the TG-MS curves of the fully formulated SLU before (left) and after (right) aging for 7 days. The mass loss of the fresh sample during heating from 40 to 1000 °C was 3.3 %. The H<sub>2</sub>O plot displays three weak signals at different temperatures, labelled A (~120 °C), B (~250 °C) and C (~425 °C). In the curve representing CO<sub>2</sub> release, a peak appeared at B temperature as well besides a large and broad signal labelled D (~500–750 °C).

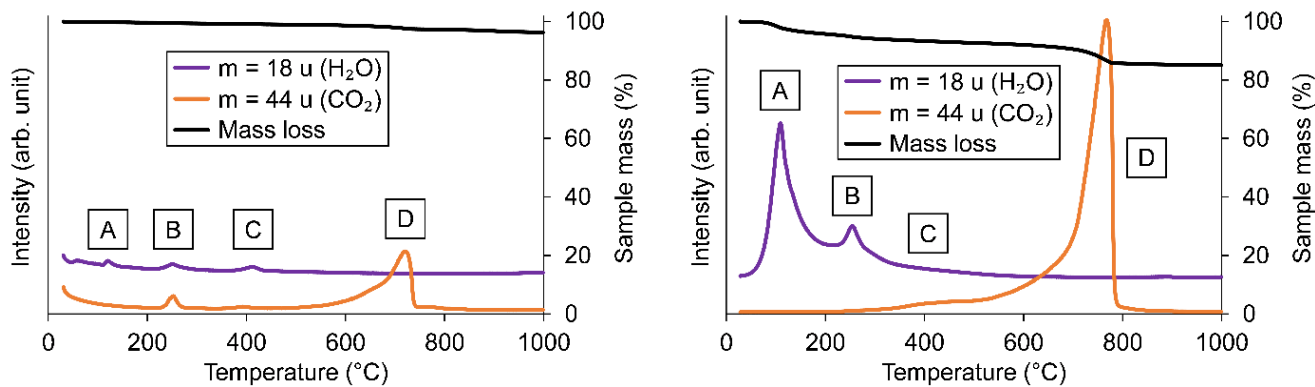


**Figure 5:** Thermogravimetric analysis of the fully formulated model SLU before (left) and after (right) aging for 7 days at 35 °C / 90 % RH.

The water evaporation signified by Peaks A and B can be attributed to the dehydration of minor calcium aluminum hydrates and calcium sulfate hydrates (from impurities in the binders and the OPC set regulator). Concurrently, some carbon-based compounds, mainly grinding agents, degraded, resulting in the release of both H<sub>2</sub>O and CO<sub>2</sub> at B temperature. The C signal marks the dehydration of portlandite which originated from the reaction of free lime with moisture during cement manufacture. Peak D signifies the decarbonation of limestone and carbonated hydrates [32–34].

After aging, the mass loss of the fully formulated SLU increased to 14.7 % with peaks A, B and D having significantly expanded both in height and width. Signal C had either disappeared or was of such low intensity that it no longer peaked out. This is in accordance with a previous study in which we found that at the applied aging conditions of 35 °C and 90 % RH portlandite quickly reacts with atmospheric CO<sub>2</sub> to calcium carbonate [35]. Had individual components been aged instead of the fully formulated model SLU, then the TG-MS plots did not change significantly. The results were thus compared in tabular form (**Table 3**). There, mass losses were separated into defined temperature intervals of 40–220 °C (only H<sub>2</sub>O released), 220–340 °C (mostly H<sub>2</sub>O released) and 340–1000 °C (mostly CO<sub>2</sub> released) [36, 37]. The prehydration index (PI), first introduced by Stoian et al. [38], subtracts the total mass loss between 20 and 1000 °C from that of the fresh SLU.

The data for the 40–220 °C interval show that for the blended TBS a significantly higher initial H<sub>2</sub>O release was recorded after 1 day of aging than for its individual components OPC, CAC and AH. Apparently, at 35 °C and 90 % RH high degrees of prehydration must be expected as soon as the binders are merged into the TBS. The high water uptake however decreased again if the aging period had been extended from 1 to 7 days while the carbon content further increased. A similar behavior had been previously observed [18, 39] where ettringite formed from pure C<sub>3</sub>A and gypsum at 35 °C and 90 % RH started to react towards longer aging periods with atmospheric CO<sub>2</sub> to CaCO<sub>3</sub>, Al(OH)<sub>3</sub> and

### 4.3 TOPIC 2: AGING IMPACT ON TBS AND MODEL SLU

gypsum [40]. Eventually, the water uptake due to H<sub>2</sub>O incorporation into the ettringite crystal lattice during ettringite formation and its re-release caused by ettringite carbonation reached an equilibrium [39].

The addition of lithium salt to the TBS during aging further increased ettringite formation due to its acceleration effect promoting hydrate formation. In comparison, with tartrate or PCE addition the balance was shifted towards a higher carbonate content in the samples.

To summarize, the aging impact on the TBS both with and without admixtures was much more severe than that on the individual binders OPC, CAC and AH as the difference in the prehydration indexes (**Table 3**) clearly shows. This might explain the similar difference in the free Ca<sup>2+</sup> concentration between SLU samples with the complete TBS aged (Ca<sup>2+</sup> decrease, then increase) and samples with either OPC, CAC or AH aged (Ca<sup>2+</sup> stable) as previously presented in **Figure 4**.

**Table 3:** Mass losses and prehydration indices for model SLU formulations with different aged components as determined via TG-MS.

Sample		Mass loss [%]			Prehydration index (PI) [%]
		40–220 °C (only H <sub>2</sub> O)	220–340 °C (mostly H <sub>2</sub> O)	340–1000 °C (mostly CO <sub>2</sub> )	
<b>SLU</b>	<b>1d</b>	5.0	1.4	6.1	9.2
	<b>7d</b>	4.3	1.7	8.7	11.4
<b>TBS</b>	<b>1d</b>	2.7	1.1	6.0	6.5
	<b>7d</b>	1.9	1.2	8.8	8.6
<b>OPC</b>	<b>1d</b>	0.7	0.3	4.8	2.5
	<b>7d</b>	1.4	0.4	5.8	4.3
<b>CAC</b>	<b>1d</b>	0.3	0.4	3.0	0.4
	<b>7d</b>	0.5	0.5	3.8	1.5
<b>AH</b>	<b>1d</b>	0.2	0.4	2.8	0.1
	<b>7d</b>	0.3	0.4	3.1	0.5
<b>TBS + Li</b>	<b>1d</b>	5.0	1.4	5.3	8.4
	<b>7d</b>	4.4	1.7	7.6	10.4
<b>TBS + Tart</b>	<b>1d</b>	2.3	0.8	5.8	5.6
	<b>7d</b>	2.3	0.9	9.1	9.0
<b>TBS + PCE</b>	<b>1d</b>	2.2	1.0	5.6	5.5
	<b>7d</b>	2.9	1.4	9.5	10.5

### 3.2.2 Powder XRD analysis

To verify the results from the TG-MS as well as characterize the prehydrates and carbonates formed during aging, powder XRD analysis was performed. Unlike in the previous experiments, here the aged components were investigated individually and not after being formulated into a SLU sample. Hence, **Figure 6** shows the X-ray diffractograms of the TBS and its individual components in pure form before and after aging for 7 days. As had been presumed during TG-MS analysis, significant ettringite formation ( $9.1^\circ 2\Theta$ , highlighted in the top left) was observed in the pure TBS, less so in the OPC due to its lower contents of calcium aluminate and sulfate phases [35]. Meanwhile, no visible change occurred in the diffractograms of CAC and AH before and after aging with the main reflexes (CA  $35.7^\circ$ , AH  $25.5^\circ 2\Theta$ ) remaining at similar intensity.

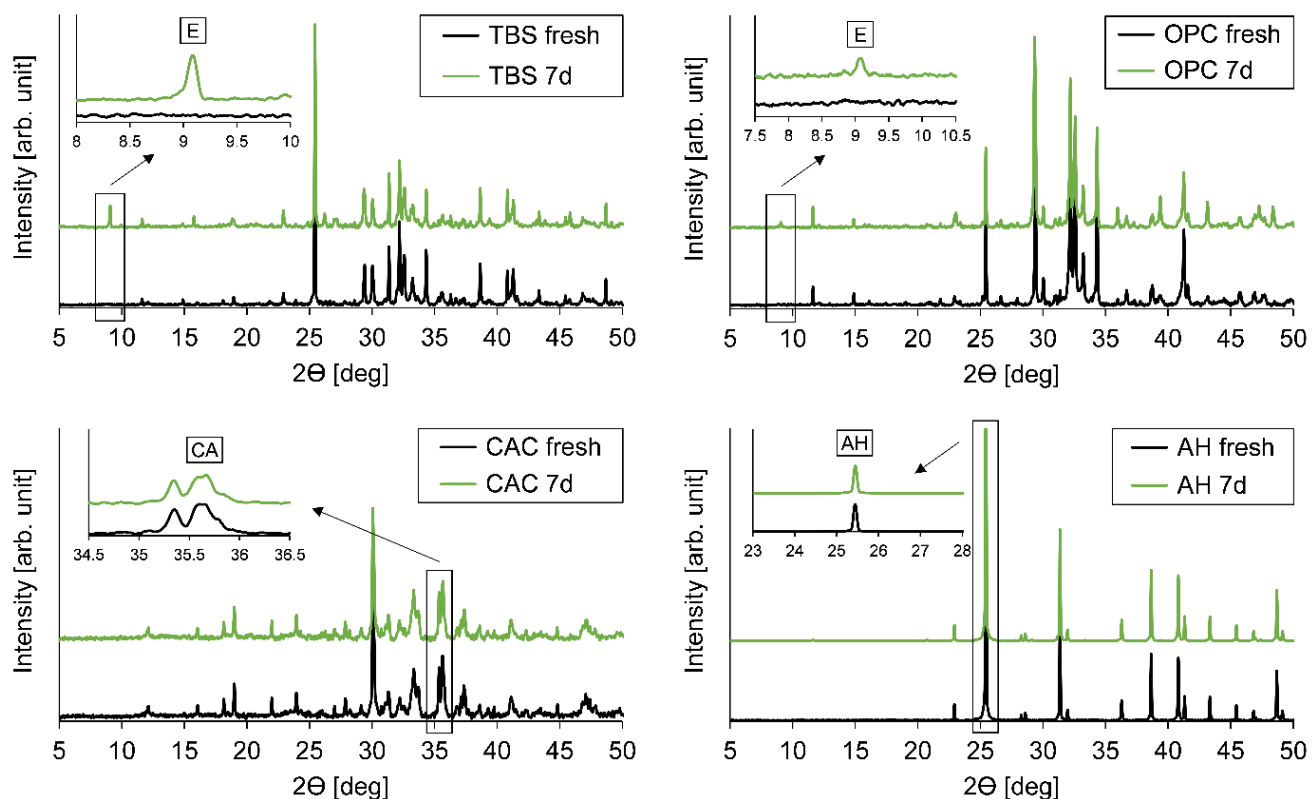


**Figure 6:** Powder XRD analysis of the ternary binder system and its individual components, before and after aging for 7 days at 90 % RH / 35 °C. E = ettringite; CA = calcium aluminate, AH = anhydrite.

Regarding the formation of carbonates during aging, **Figure 7** shows that in the TBS calcium carbonate was primarily observed in calcite ( $29.3^\circ 2\Theta$ ) and aragonite ( $26.2^\circ 2\Theta$ ) modification. The  $C_3S$  reflex ( $30.1^\circ 2\Theta$ ) correspondingly decreased in intensity over the aging period. Interestingly, the higher carbonate formation recorded via TG-MS for tartrate and PCE addition compared to lithium appears to primarily result in aragonite while calcite formation remained stable.

### 4.3 TOPIC 2: AGING IMPACT ON TBS AND MODEL SLU

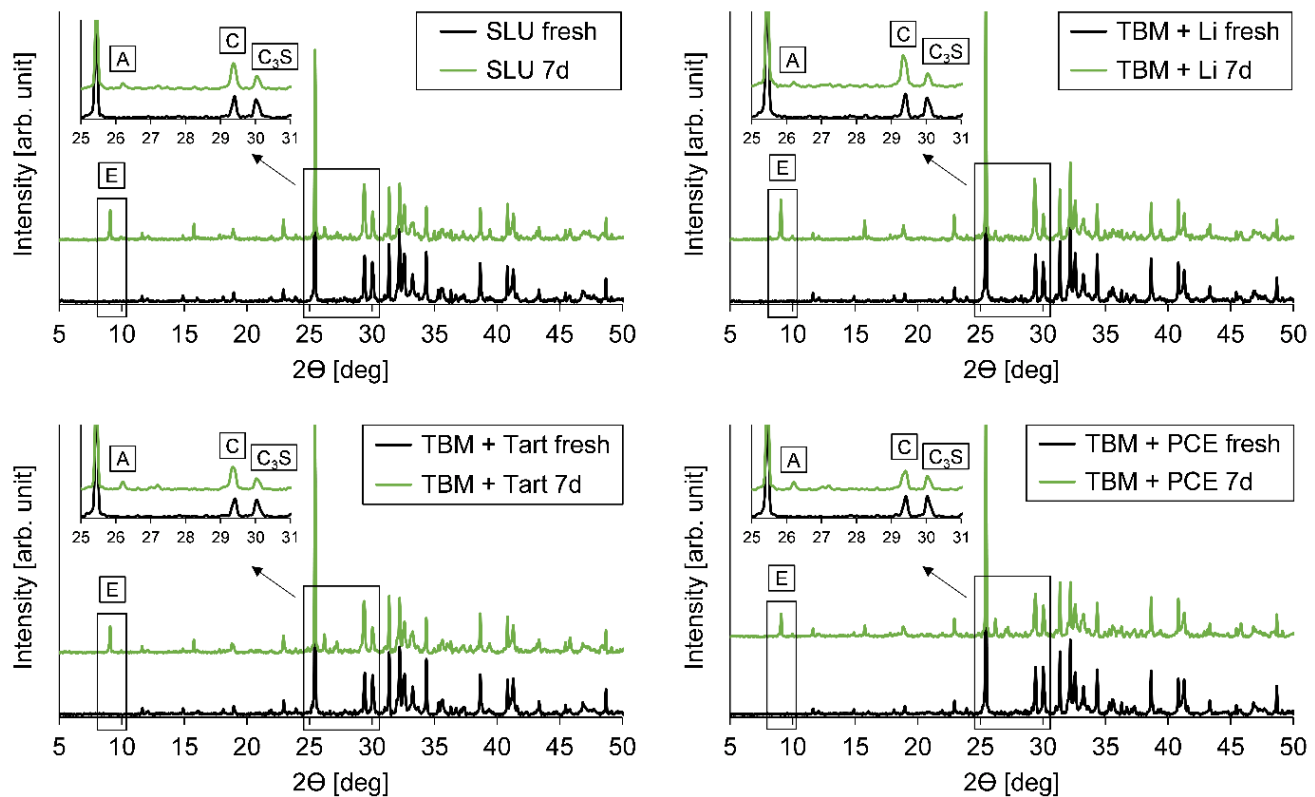


**Figure 7:** Powder XRD analysis of the fully formulated model SLU and the ternary binder system with different admixtures, before and after aging for 7 days at 90 % RH / 35 °C. A = aragonite, C = calcite;  $\text{C}_3\text{S}$  = tricalcium oxy silicate.

### 3.3 Application-related properties of aged SLUs

Against the background of SLU aging and hydration behavior, in the final part of this study engineering properties of fresh and aged SLU samples were compared. Examined were rheological and setting behavior as well as compressive strength development.

#### 3.3.1 Rheological behavior

**Figure 8** presents the spread flows of the model SLU with different aged components. In all cases the aging was either detrimental or of no consequences to the spread flow, no positive impact was observed. On the left the presence of admixtures during aging in comparison to the TBS aged in pure form is displayed. After 1 day of exposure, the spread flow reduction was worse had admixtures been added to the TBS before aging. Interestingly, the sample with 1-day aged superplasticizer (TBS + PCE) was least affected by flowability loss. On the other hand, both samples containing 7-days aged superplasticizer (TBS + PCE and TBS + all admixtures) exhibited the lowest spread flows overall. Meanwhile the samples with aged lithium salt or aged tartrate did not change significantly after a prolonged aging period of 7 days and became comparable in spread flow to the TBS aged without admixture. Therefore, at longer aging periods the accelerator and retarder became less of a factor in determining spread flow while the presence of fresh superplasticizer had a higher impact. This might explain why Winnefeld [16] observed a better performance of PCE superplasticizers in cement aged at 20 °C and 90 % RH for 2 days than Dubina et al. [17] after exposure to 35 °C and 90 % RH for 3 days.

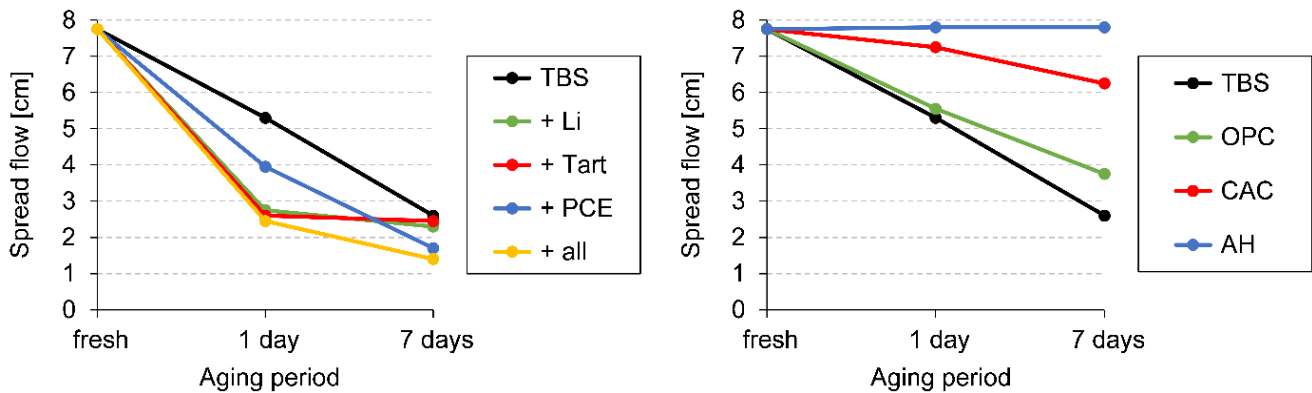


**Figure 8:** Spread flow of model SLU samples (w/f ratio = 0.50), either fresh or with different components aged at 35 °C / 90 % RH for 1 or 7 days.

Had the individual components of the TBS been aged (**Figure 8**, right), the strongest spread flow reduction was observed with aged OPC, exposure of CAC had a lesser effect and with aged AH the spread flow remained constant. This mirrors the relative reactivity of the binders towards moisture and CO<sub>2</sub> as observed via TG-MS and powder XRD.

### 3.3.2 Setting behavior

The setting behavior was investigated by determining the time-dependent penetration depth of the Vicat needle relative to the bottom of the vessel as shown in **Figure 9**. Exposing the fully formulated SLU for 1 day led to a slight acceleration as compared to the unaged reference, but after 7 days to a significant retardation of the setting process. Broken down into the individual admixtures, the aging of the TBS together with the lithium accelerator completely prevented an onset of setting for at least 18 hours after the start of hydration. This verifies the dysfunctionality of the aged accelerator as previously observed via heat flow calorimetry (**Figure 3**). In further accordance with calorimetry, had the TBS been aged with tartrate retarder for 1 day and the other admixtures been kept fresh, then the setting was drastically accelerated and not retarded. The acceleration was however less extreme after 7 days. This in combination with a strong retardation effect of 7-days aged TBS + PCE might explain the reversal of the fully formulated SLU from acceleration to retardation between 1 and 7 days. Aging TBS + PCE having no effect after 1 day but after 7 days also matches with heat flow calorimetry (**Figure 3**). It is furthermore in line with the spread flow measurements discussed in the previous **Section 3.3.1**, where longer aging periods had a more significant impact on the performance of the PCE superplasticizer (**Figure 8**). Some PCEs are known to exhibit retarding properties [41], which appear to increase at higher degrees of binder aging.

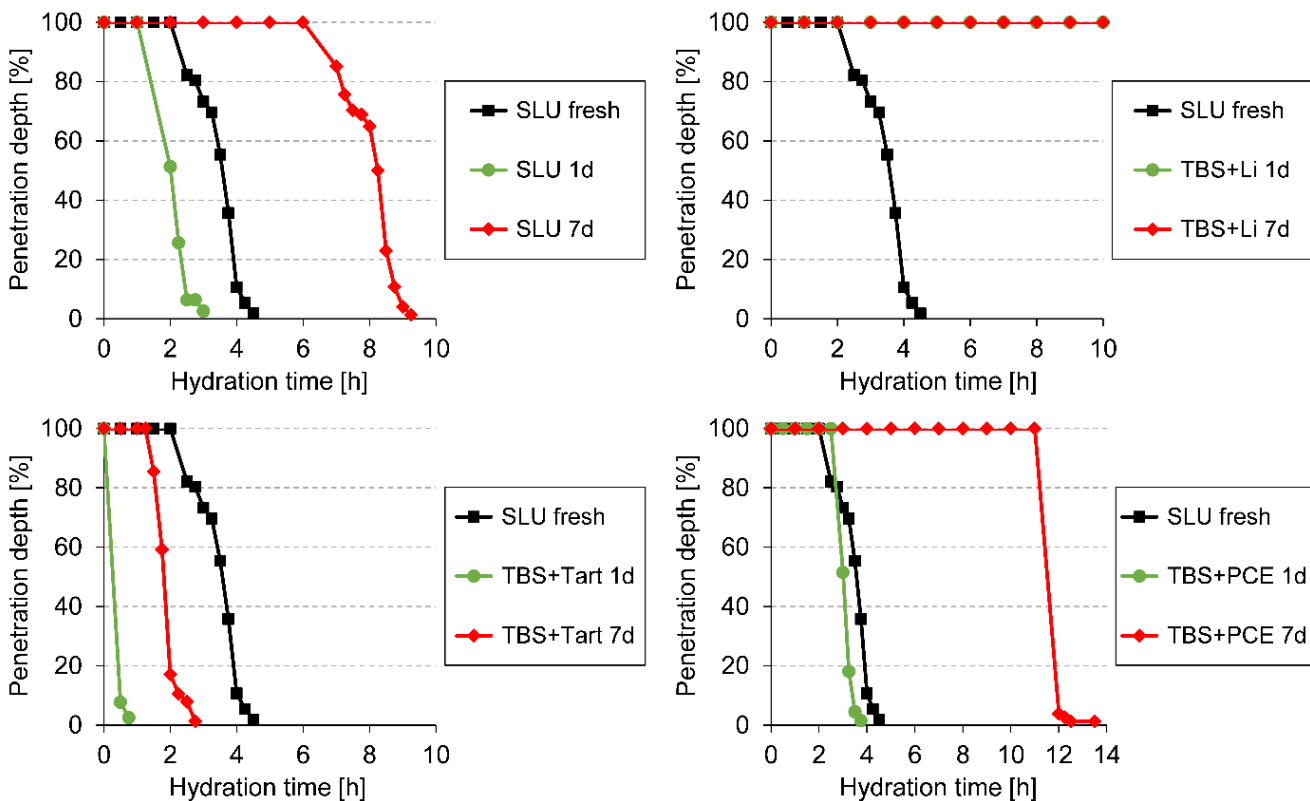


**Figure 9:** Setting behavior of the fully formulated model SLU and the ternary binder system with different admixtures, before and after aging for 7 days at 90 % RH / 35 °C.

### 3.3.3 Compressive strength development

Similar to the rheological properties, aging had an universally detrimental effect on the compressive strength of the model SLU. **Figure 10** displays the strength values after 24 hours, 72 hours and 1 week of curing. Aging the TBS in pure form for 1 day already reduced its compressive strength after 1 week from 90.7 to 29.2 N/mm<sup>2</sup>. Extending the aging period to 7 days especially affected early development with 24 hours strength being reduced from 16.2 to 3.7 N/mm<sup>2</sup> (fresh value: 23.8 N/mm<sup>2</sup>). These results signify that the reduced setting time and flowability of the TBS after aging do not translate into a faster strength development. In a previous study on the aging of pure OPC, we made similar observations [35]. There, the ettringite crystals formed on the cement during aging seeded a dense particle overgrowth in hydration. This hindered the formation of C S H phases and thus strength development.

The presence of admixtures during aging further slows strength development in subsequent hydration. The strength values of the sample produced from TBS aged together with all admixtures were already as low after 1 day of exposure as those of a 7-days aged TBS hydrated with fresh admixtures. Among the individual additives, lithium carbonate yielded the lowest values, here a measurable strength ( $\geq 3$  N/mm<sup>2</sup> for the test plant used) was only achieved after 1 week of curing the 1-day aged sample. Second worst strength was recorded with the retarder, whereas PCE displayed a similar performance as the pure TBS. The observed impacts of the admixture additions were even more pronounced after 7 days of aging.

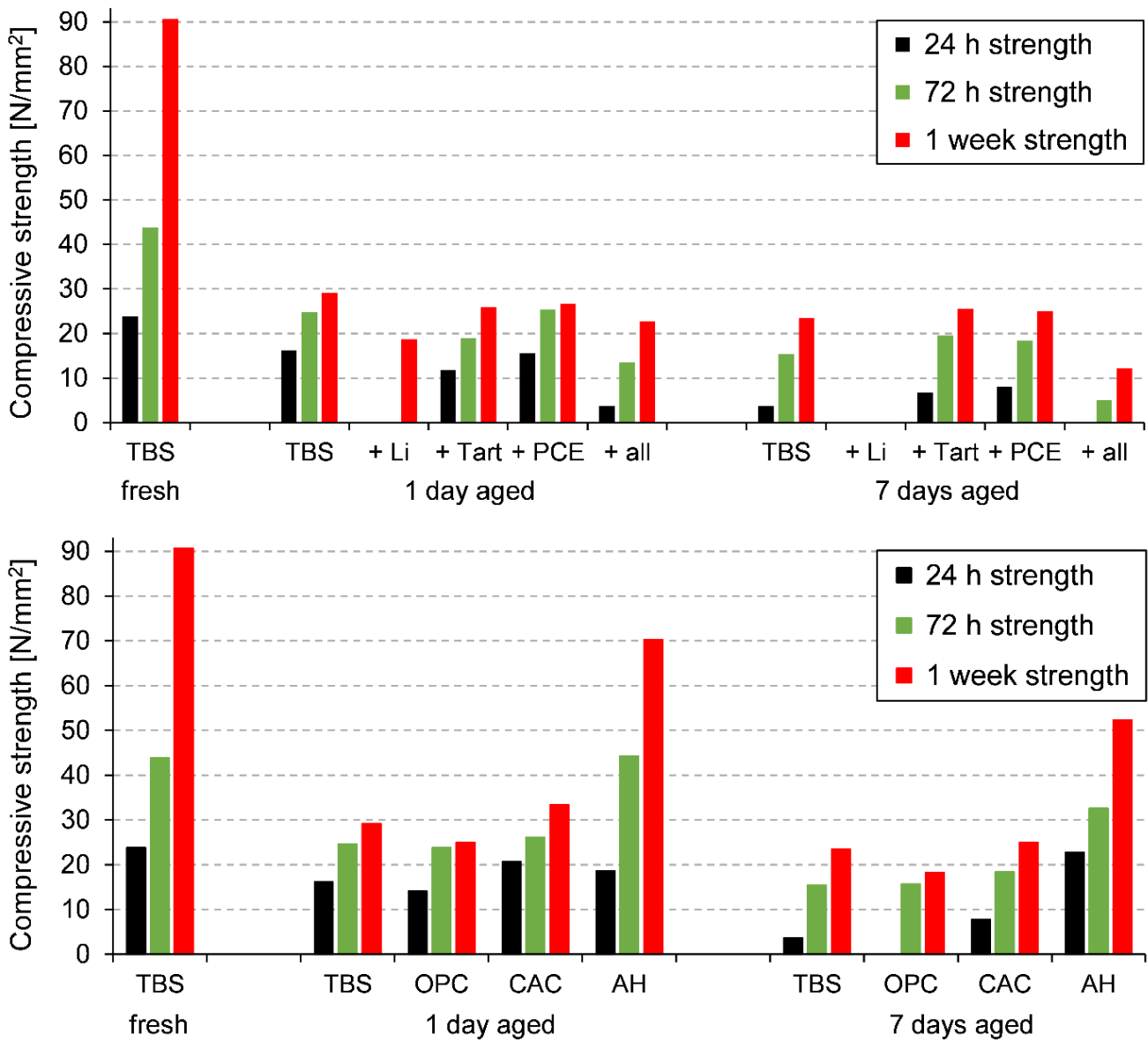


**Figure 10:** Compressive strength development of model SLU samples (w/f ratio = 0.50), either fresh or with different components aged at 35 °C / 90 % RH for 1 or 7 days. Values below 3 N/mm<sup>2</sup> are below the detection limit of the test plant used.

In comparison to the TBS, aging its individual components separately (**Figure 10**, bottom) yielded higher strengths for CAC and AH and lower values for the OPC. Aged OPC having a higher impact on a SLU sample than aged CAC or AH was to be expected with OPC presenting the main source of strength in the TBS and the most reactive binder as demonstrated via TG-MS (**Table 3**) and powder XRD (**Figure 6**). From the compressive strength experiments it is further suggested that in combination with CAC and AH the OPC appears to age slightly slower than in pure form.

### 4. Summary and conclusions

This study investigated the effects of aging on a ternary binder system and chemical admixtures applied in self-levelling underlays. Examined was a model formulation based on a TBS from OPC, CAC and AH admixed with an accelerator (lithium carbonate), retarder (sodium potassium tartrate) and superplasticizer (polycarboxylate ether). Different components were exposed individually or in combinations to 35 °C / 90 % RH for up to 7 days. Changes in the material composition, hydration behavior, and engineering properties (spread flow, setting behavior and compressive strength development) were determined. It was found that

- (1) only the blended TBS and OPC formed aging products (ettringite and calcium carbonate) under the applied aging conditions, CAC and AH did not react
- (2) Ettringite from aging induced a seeding effect during hydration which reduces flowability and accelerates setting, but also retards strength development
- (3) admixtures present during aging of the TBS further increased ettringite (accelerator) and calcium carbonate (retarder and superplasticizer) formation and worsened the impact of aging on the engineering properties
- (4) the admixtures tested completely lost their functionality after 1 day (accelerator and retarder) or after 7 days (superplasticizer) of aging

The functionality loss of the admixtures warrants further research. Accelerator and retarder fundamentally lost their properties already after a short aging period. A different mechanism appears to apply for the superplasticizer, which was less affected by aging initially but its dispersing ability decreased with increased aging duration. Coincidentally, the PCE displayed a retarding effect after aging that became stronger with increased aging duration. In future work, the potential of partial dissolution of the admixtures under high humidity, the role of atmospheric CO<sub>2</sub> and the agglomeration of the binder particles during exposure should be studied.

The results obtained in this study signify that aging has substantial impacts on the performance of SLU components. Even if their individual aging potential is low, the combination with each other or with more reactive components enables prehydration and loss of functionality. This underlines the necessity to limit exposure during all stages of manufacture, storage and transport of dry-mix formulations.

### 5. Acknowledgements

The authors are most grateful to Deutsche Forschungsgemeinschaft, Bonn, Germany (DFG) for financing this project under the grant PL-472/9-2 “Influence of aging of binder systems on the performance of additives”. We would also like to express our thanks to HeidelbergCement, Kerneos and Ardex companies for providing the cements and the commercial SLU sample.

## 6. References

- [1] G. Tzouvalas, G. Rantis, S. Tsimas, Alternative calcium-sulfate-bearing materials as cement retarders: Part II. FGD gypsum, *Cem. Concr. Res.* 34 (11) (2004) 2119–2125.  
<https://doi.org/10.1016/j.cemconres.2004.03.021>
- [2] G. Goswami, B. Mohapatra, J.D. Panda, Gypsum dehydration during comminution and its effect on cement properties, *J. Am. Ceram. Soc.* 73 (3), (1990) 721–723.  
<https://doi.org/10.1111/j.1151-2916.1990.tb06578.x>
- [3] N.B. Singh, B. Middendorf, Calcium sulphate hemihydrate hydration leading to gypsum crystallization, *Prog. Cryst. Growth Charact. Mater.* 53 (1) (2007) 57–77  
<https://doi.org/10.1016/j.pcrysgrow.2007.01.002>
- [4] O. Yamaguchi, H. Sugaya, Y. Nakajima, Effect of the cement characteristics and storing in the silo on the fluidity of cement with superplasticizer, in: Beijing International Symposium on Cement and Concrete 1998, Proceedings (Volume 2).
- [5] S. Sprung, Effect of storage conditions on the properties of cement, *ZKG Int.* 31 (1978) 305–309.
- [6] O.M. Jensen, P. Hansen, E.E. Lachowski, F.P. Glasser, Clinker mineral hydration at reduced relative humidities, *Cem. Concr. Res.* 29 (1999) 1505–1512.  
[https://doi.org/10.1016/S0008-8846\(99\)00132-5](https://doi.org/10.1016/S0008-8846(99)00132-5)
- [7] C.S. Deng, C. Breen, J. Yarwood, S. Habesch, J. Phipps, B. Craster, G. Maitland, Ageing of oilfield cement at high humidity: a combined FEG-ESEM and Raman microscopic investigation, *J. Mater. Chem.* 12 (10) (2002) 3105–3112. <https://doi.org/10.1039/B203127M>
- [8] E. Dubina, L. Wadsö, J. Plank, A sorption balance study of water vapor sorption on anhydrous cement minerals and cement constituents, *Cem. Concr. Res.* 41 (2011) 1196–1204.  
<https://doi.org/10.1016/j.cemconres.2011.07.009>
- [9] E. Dubina, J. Plank, L. Black, Impact of water vapor and carbon dioxide on surface composition of C<sub>3</sub>A polymorphs studied by X-ray photoelectron spectroscopy, *Cem. Concr. Res.* 73 (2015) 36–41. <https://doi.org/10.1016/j.cemconres.2015.02.026>
- [10] V. Starinieri, D.C. Hughes, C. Gosselin, D. Wilk, K. Bayer, Pre-hydration as a technique for the retardation of Roman cement mortars, *Cem. Concr. Res.* 46 (2013) 1–13.  
<https://doi.org/10.1016/j.cemconres.2013.01.004>
- [11] K. Theisen, V. Johansen, Prehydration and strength development of Portland cement, *J. Am. Ceram. Soc. Bull.* 54 (9) (1975) 787–791.
- [12] L. Barbic, V. Tinta, B. Lozar, V. Marincovic, Effect of storage time on the rheological behavior of oil well slurries, *J. Am. Ceram. Soc.* 74 (1991) 954–949.  
<https://doi.org/10.1111/j.1151-2916.1991.tb04326.x>
- [13] E. Dubina, L. Black, R. Sieber, J. Plank, Interaction of water vapor with anhydrous cement minerals, *Adv. Appl. Ceram.* 109 (5) (2010) 260–268.  
<https://doi.org/10.1179/174367509X12554402491029>

- [14] M. Whittaker, E. Dubina, F. Al-Mutawa, L. Arkless, J. Plank, L. Black, The effect of prehydration on the engineering properties of CEM I Portland cement, *Adv. Cem. Res.* 25 (1) (2013) 12–20. <https://doi.org/10.1680/adcr.12.00030>
- [15] C. Maltese, C. Pistolesi, A. Bravo, F. Cella, T. Cerulli, D. Salvione, A case history: Effect of moisture on the setting behavior of a Portland cement reacting with an alkali-free accelerator, *Cem. Concr. Res.* 37 (2007) 856–865. <https://doi.org/10.1016/j.cemconres.2007.02.020>
- [16] F. Winnefeld, Influence of cement aging and addition time on the performance of superplasticizers, *ZKG Int.* 61 (2008) 68–77.
- [17] E. Dubina, J. Plank, Influence of moisture- and CO<sub>2</sub>-induced aging in cement on the performance of admixtures used in construction chemistry, *ZKG Int.* 65 (2012) 60–68.
- [18] M.R. Meier, T. Napharatsamee, J. Plank, Dispersing performance of superplasticizers admixed to aged cement, *Constr. Build. Mater.* 139 (2017) 232–240. <https://doi.org/10.1016/j.conbuildmat.2016.12.126>
- [19] R. Bayer, H. Lutz, Dry Mortars, in: Ullmann's Encyclopedia of Industrial Chemistry. Vol. 11. Wiley-VCH, Weinheim (2003) 83–108.
- [20] J. Plank, Technology trends in the European dry mix mortar industry, in: 1<sup>st</sup> Conference on Research and Application of Commercial Mortar, Shanghai, 10–11 November 2005, Proceedings 26–40.
- [21] C. Winter, J. Plank, The European dry-mix mortar industry (Part 1) *ZKG Int.* 60 (2007) 62–69.
- [22] R. Harbron, A general description of flow-applied floor screeds – an important application for complex formulations based on CAC, in: R.J. Mangabhai, C.H. Fentiman (eds.), International Conference on Aluminate Cement (CAC), Edinburgh, 16–19 July 2001, Proceedings 597–604.
- [23] L. Amathieu, T.A. Bier, K.L. Scrivener Mechanisms of set acceleration of Portland cement through CAC addition, in: R.J. Mangabhai, C.H. Fentiman (eds.), International Conference on Aluminate Cement (CAC), Edinburgh, 16–19 July 2001, Proceedings 303–317.
- [24] R. Zurbriggen, F. Goetz-Neunhoeffer, Mechanism and resulting damages of prolonged retardation in aged dry mixes: A case study of mixed-binders containing tartaric acid, *GDCh-Monographie* 37, Tagung Bauchemie (2007) 111–118.
- [25] G. Schmid, T.A. Bier, K. Wutz, M. Maier, Characterization of the aging behavior of premixed dry mortars and its effect on their workability properties, *ZKG Int.* 60 (2007) 94–103.
- [26] E. Dubina, J. Plank, L. Wadsö, L. Black, H. König, Investigation of the long-term stability during storage of cement in drymix mortars, *Int. Anal. Rev. Alitinform* 20, 26 (3, 4–5) (2011–2012) 38–45, 86–99.
- [27] DIN EN 196-11 (2019). Methods of testing cement – Part 11: Heat of hydration – Isothermal Conduction Calorimetry method. German version EN 196-11.

- [28] DIN EN 12706-12 (1999), Adhesives – Test methods for hydraulic setting floor smoothing and/or levelling compounds – Part 12: Determination of flow characteristics. German version EN 12706.
- [29] DIN EN 196-3 (2017). Methods of testing cement – Part 3: Determination of setting times and soundness. German version EN 196-1.
- [30] D. Stephan, J. Plank, Einfluss von Verzögerern auf Alit und Zemente mit unterschiedlichem Gehalt an Klinkerphasen, in: J. Plank (Ed.), Bauchemie von der Forschung bis zur Praxis: 5. Tagung Bauchemie in München [9.10.2003], Gesellschaft Dt. Chemiker, Frankfurt am Main, 2003, pp. 31–38.
- [31] DIN EN 196-1 (2016). Methods of testing cement – Part 1: Determination of strength. German version EN 196-1.
- [32] D.K. Lee, An apparent kinetic model for the carbonation of calcium oxide by carbon dioxide, *Chem. Eng. J.* 100 (1) (2004) 71–77. <https://doi.org/10.1016/j.cej.2003.12.003>
- [33] D. Mess, A.F. Sarofim, J.P. Longwell, Product layer diffusion during the reaction of calcium oxide with carbon dioxide, *Energ. Fuel.* 13 (5) (1999) 999–1005. <https://doi.org/10.1021/ef980266f>
- [34] E. Ruiz-Agudo, K. Kudłacz, C.V. Putnis, A. Putnis, C. Rodriguez-Navarro, Dissolution and carbonation of portlandite  $[\text{Ca}(\text{OH})_2]$  single crystals, *Environ. Sci. Technol.* 47 (19) (2013) 11342–11349. <https://doi.org/10.1021/es402061c>
- [35] F.A. Hartmann, J. Plank, New insights into the effects of aging on Portland cement hydration and on retarder performance, *Con. Build. Mat.*, submitted on 28.09.2020.
- [36] P. Mounanga, A. Khelidj, A. Loukili, V. Baroghel-Bouny, Predicting  $\text{Ca}(\text{OH})_2$  content and chemical shrinkage of hydrating cement pastes using analytical approach, *Cem. Concr. Res.* 34 (2) (2004) 255–265. <https://doi.org/10.1016/j.cemconres.2003.07.006>
- [37] M. Thiery, G. Villain, P. Dangla, G. Platret, Investigation of the carbonation front shape on cementitious materials: Effects of the chemical kinetics, *Cem. Concr. Res.* 37 (7) (2007) 1047–1058. <https://doi.org/10.1016/j.cemconres.2007.04.002>
- [38] J. Stoian, T. Oey, J.W. Bullard, J. Huang, A. Kumar, M. Balonis, J. Terrill, N. Neithalath, G. Sant, New insights into the prehydration of cement and its mitigation, *Cem. Concr. Res.* 70 (2015) 94–103. <https://doi.org/10.1016/j.cemconres.2015.01.012>
- [39] F.A. Hartmann, J. Plank, Impact of aging on the hydration of tricalcium aluminate ( $\text{C}_3\text{A}$ )/gypsum blends and the effectiveness of retarding admixtures, *Z. Naturforsch. B* 75 (8) (2020) 739–753. <https://doi.org/10.1515/znb-2020-0087>
- [40] J. Plank, M. Zhang-Preße, N.P. Ivleva, R. Niessner, Stability of single phase  $\text{C}_3\text{A}$  hydrates against pressurized  $\text{CO}_2$ , *Const. Build. Mater.* 122 (2016) 426–434. <https://doi.org/10.1016/j.conbuildmat.2016.06.042>
- [41] L. Zhang, X. Miao, X. Kong, S. Zhou, Retardation effect of PCE superplasticizers with different architectures and their impacts on early strength of cement mortar, *Cem. Concr. Compos.* 104 (2019) 103369. <https://doi.org/10.1016/j.cemconcomp.2019.103369>

### 4.3.2 Further investigations on topic 2

#### 4.3.2.1 Compilation of the results

This section expands on the findings presented in journal article 3. Further investigations were carried out and published in conference contribution 3. Hereafter an overview of the results is given, followed by the contribution itself.

As described in journal article 3, both after 1 and 7 days of exposure, neither in CAC nor in AH were any prehydrate phases detected via powder XRD. Long-term aging experiments revealed the formation of small amounts of  $\text{Al(OH)}_3$  in CAC after 14 days. A detectable amount of gypsum from the prehydration of AH was only obtained after 2 months of continued exposure.

Inspired by the aging of  $\text{C}_3\text{A}$  / gypsum blends in the project topic on retarders, the aluminate cement clinker phases CA,  $\text{C}_{12}\text{A}_7$  and  $\text{CA}_2$  were also each mixed with gypsum and exposed to 35 °C and 90% RH. None of these three blends produced detectable amounts of ettringite over 14 days of aging. However, the TBS had formed ettringite from CAC and AH during exposure as mentioned in journal article 3. This implies that the ettringite seeds produced in the OPC component of the TBS during aging accelerate the formation of further seeds from CAC and AH.

For the model SLU admixtures, additional aging investigations were carried out as well. Instead of the whole TBS, either the OPC or the CAC were aged with one of the admixtures. The presence of  $\text{Li}_2\text{CO}_3$  massively accelerated the prehydration of the CAC which now formed ample amounts of  $\text{Al(OH)}_3$  and  $\text{CaCO}_3$  already after 1 day of exposure. In contrast,  $\text{Li}_2\text{CO}_3$  addition only slightly increased the water uptake of OPC. Powder XRD revealed that aging conditions of 35 °C and 90% RH are sufficient to convert the  $\text{Li}_2\text{CO}_3$  into  $[\text{Li}_2\text{Al}_4(\text{OH})_{12}](\text{OH})_2 \cdot 3 \text{ H}_2\text{O}$ . This layered double hydroxide is the cornerstone of the accelerating mechanism of  $\text{Li}_2\text{CO}_3$  in aluminate cements [270, 271].  $[\text{Li}_2\text{Al}_4(\text{OH})_{12}](\text{OH})_2 \cdot 3 \text{ H}_2\text{O}$  promotes both the dissolution of the CA clinker phase and the formation of  $\text{C}_2\text{AH}_8$ . This also explains why in journal article 3 the addition of  $\text{Li}_2\text{CO}_3$  to the TBS resulted in the highest water uptake among the three model SLU admixtures.

Other samples of OPC or CAC were aged with one of the retarders sodium potassium tartrate and sodium citrate. Although widely used in cement, citrate had not been considered for the model SLU due its known compatibility issues with PCE superplasticizers [261, 272]. At similar retarder dosages, the water uptakes during aging of both OPC and CAC were higher in the presence of citrate. Unlike  $\text{Li}_2\text{CO}_3$ , the retarders increased the water uptake of OPC more than that of CAC and no prehydration products from a combination of citrate or tartrate with cement constituents were detected via powder XRD.

In journal article 3, rheological properties were only determined directly after the start of hydration. Additional tests of spread flow over time were carried out with samples of the fully formulated model SLU which had been aged for 1, 3 or 7 days. The rheological properties at the start of hydration decreased with increasing exposure duration. However, the longer the SLU had been aged, the more it increased in flowability over time. 45 minutes after the start of hydration, the spread flows of all aged samples were similar, regardless of the exposure duration. This indicates that the superplasticizer does not lose its effect early in hydration due to an irreversible degradation during aging. Instead, it is

#### 4.3 TOPIC 2: AGING IMPACT ON TBS AND MODEL SLU

---

possibly enclosed at the start of hydration when the seeding materials trigger a particle overgrowth. The superplasticizer would then gradually be released as the hydrating SLU matures.

To improve the early spread flow, the addition of calcium hydroxide to the model SLU formulation before aging was tested. Calcium hydroxide had previously been suggested as an additive for ternary binder systems to combat the formation of hydrate spheres [273, 274]. Indeed, a calcium hydroxide addition of 2.5 wt.% by weight of formulation increased the spread flow for ~30 min after the start of hydration.

**4.3.2.2 Reprint of conference contribution 3**

**Towards understanding the ageing behavior of SLU formulations: Impact of prehydration on individual components and the role of admixtures**

F. A. Hartmann, A. A. Engbert, J. Plank

*5<sup>th</sup> International Conference on Calcium Aluminates (CAC)*

Cambridge, United Kingdom, 01–03 June 2020 (postponed to 18–20 July 2022)

in:

C. H. Fentiman, R. J. Mangabhai (eds.), Proceedings, part 6 – Ternary binders

Reprinted with permission from Cement and Concrete Science

## TOWARDS UNDERSTANDING THE AGEING BEHAVIOUR OF SLU FORMULATIONS: IMPACT OF PREHYDRATION ON INDIVIDUAL COMPONENTS AND THE ROLE OF ADMIXTURES

F. A. HARTMANN, A. ENGBERT and J. PLANK

Chair for Construction Chemistry, Technical University of Munich,  
Lichtenbergstrasse 4, 85748 Garching, Germany

*florian.a.hartmann@tum.de*

*sekretariat@bauchemie.ch.tum.de*

**SUMMARY:** Based on highly reactive multi-component binder systems, self-levelling underlays (SLUs) are especially vulnerable to preliminary surface hydration when exposed to humidity and CO<sub>2</sub>, in particular at elevated temperature. Such prehydrated SLUs exhibit reduced flowability and workability. Likewise, SLU performance can worsen when individual components suffer prehydration before the formulation is prepared.

The main constituents of a typical SLU ternary binder system are Portland cement (PC), calcium aluminate cement (CAC) and anhydrite. To gain a better understanding of the system's ageing behaviour, the constituents were prehydrated individually at 35°C and 90 % relative humidity. Interestingly, CAC containing about 40 wt. % Al<sub>2</sub>O<sub>3</sub> was found to age/prehydrate considerably less than Portland cement CEM I 52.5 N by measure of weight increase during storage. Anhydrite remained completely unaffected by these conditions.

In subsequent experiments, additives in powder form were mixed with the binders before ageing. The presence of lithium carbonate accelerator increased prehydration of CAC significantly. However, the common SLU retarders tartrate and citrate surprisingly accelerated CAC ageing as well.

To further investigate the impact of prehydration on flowability, a model SLU based on a PC/CAC/anhydrite ternary binder system was formulated with accelerator, retarder and PCE superplasticizer. The reduced flowability found for a prehydrated commercial SLU could be reproduced with this model system. To mitigate flowability reduction, addition of calcium hydroxide was investigated.

The results show that the individual components of a formulation exhibit different ageing behaviour, which is further changed by the presence of admixtures during ageing. **Keywords:** Admixture, ageing, cement, clinker phase, prehydration, self-levelling underlayment (SLU), ternary binder system.

## INTRODUCTION

Self-levelling underlays (SLUs) are used to obtain smooth surfaces on otherwise uneven foundations before floor coverings can be installed<sup>[1,2]</sup>. Conventionally, Portland cement (PC) is the basis for a SLU mortar. If rapid hardening is required in application, a ternary binder system of PC, calcium aluminate cement (CAC) and calcium sulphate is employed<sup>[3,4]</sup>.

Upon contact with water, CAC-rich formulations quickly form large amounts of ettringite in the presence of sulphate. The needle-shaped crystal morphology of the ettringite along with its ability to incorporate high quantities of water cause rapid stiffening of the SLU slurry. Furthermore, this water uptake leads to volume expansion which counteracts shrinkage. However, to overcome the CAC's energy barrier for ettringite formation, accelerators are required, the most common of which is lithium carbonate  $\text{Li}_2\text{CO}_3$ . Lithium ions improve the dissolution of the main  $\text{CaAl}_2\text{O}_4$  (CA) clinker phase and form lithium-aluminium layered double hydroxide (LDH) precursors, thereby decreasing the activation energy for aluminate hydrate formation<sup>[5]</sup>.

Furthermore, overly quick stiffening can reduce the workability time of the slurry to such an extent that using a mechanical pump in application is no longer feasible. Therefore, hydration retarders are applied to maintain sufficient workability. Commonly used are  $\alpha$ -hydroxycarboxylic acid salts such as tartrate and citrate. To achieve flowability and self-levelling capacity without greatly increasing the water to cement (w/c) ratio, superplasticizers are added. Thus, by design drymixed SLU formulations possess a high reaction potential towards water. While advantageous in application, it makes SLUs susceptible to premature hydration on particle surfaces upon exposure to atmospheric humidity. This "prehydration" occurs when the formulation is aged unintentionally due to insufficient protection against external environmental influences during storage. Moreover, individual components might undergo prehydration even before the SLU is formulated. An example is the milling of cement clinker after firing in the kiln. In this process water is injected into the mill for temperature regulation, resulting in a partially hydrated cement powder. Prehydration of cement can cause deficiencies in strength development as well as unpredictability in setting behaviour and interaction with additives<sup>[6, 7]</sup>.

To get a better understanding of the prehydration mechanisms, we have investigated the water sorption capabilities of Portland cement constituents in earlier works<sup>[8,9]</sup>. It was discovered that individual clinker phases start to sorb water at different levels of relative humidity. The most hygroscopic clinker phase is orthorhombic (doped)  $\text{C}_3\text{A}$  which sorbs large amounts of water from 55 % RH upwards. It is followed by the silicate phases alite ( $\text{C}_3\text{S}$ ) and belite ( $\text{C}_2\text{S}$ ) showing a comparatively minor water uptake which starts around 65 % RH. Non-doped, cubic  $\text{C}_3\text{A}$  in turn sorbs a moderate amount of water, but only at a relative humidity of 80 % and higher.

For this reason, in follow-up studies on cements and binder systems humidity levels were increased to 90 % to guarantee that all clinker phases sorb water sufficiently. A SLU model formulation based on a ternary binder system of PC, CAC and fluoroanhydrite with the essential additives as described above was investigated<sup>[10,11]</sup>. Powder XRD made evident that the high atmospheric humidity was sufficient to trigger the characteristic strong ettringite formation of ternary binder systems within the first 24 hours of prehydration. This led to an increase in the water demand due to the ettringite overgrowth consuming water while also limiting access to the non-prehydrated inner part of the particles. As a result, producing a free-flowing paste with the aged formulation required doubling the w/c ratio from 0.25 to 0.50.

Still, at w/c = 0.50 the SLU with tartrate showed a 40 % reduction in spread flow after one day of prehydration compared to the paste from the fresh formulation. After three days, this difference even increased to 70 %. Interestingly, prehydration inverted the performance of citrate. Using citrate instead of tartrate in a fresh SLU led to a higher initial spread flow but

*Towards understanding the ageing behaviour of SLU formulations: Impact of prehydration on individual components and role of admixtures*

worse fluidity retention. However, after prehydrating the formulation for three days before adding citrate, initial flowability was nearly zero but increased constantly until reaching a maximum after two hours. Such unpredictable retarder behaviour after prehydration is not unique, we have also reported about varying performances of gluconate and pyrophosphate in PC and clinker phases [12].

Thus, our previous investigations revealed the profound impact of prehydration on binder systems and their constituents. In this work, we aimed to expand on the results obtained so far by taking a closer look at the ageing of the individual components of a ternary binder system, namely PC, CAC and anhydrite. Furthermore, to complement the research on Portland cement clinker, we investigated the ageing of the major aluminato cement clinker phases. Moreover, ageing of a model SLU formulation was investigated and the results were compared with those obtained from a commercial SLU. Finally, the differences between citrate and tartrate used in the formulation were studied.

## EXPERIMENTAL PROCEDURES

### SLU formulation

The composition of the model SLU formulation used in this study as displayed in Table 1 is based on previous works [10,11]. For the PC component of the ternary binder system a CEM I 52.5 N (Milke®, HeidelbergCement AG, Ennigerloh plant, Germany) which is regularly used in drymix applications was chosen. Ciment Fondu® (Kerneos S.A., Neuilly sur Seine, France) is a common CAC with an Al<sub>2</sub>O<sub>3</sub> content of nearly 40 wt. %. Sulphate was provided in the form of fluoroanhydrite (Solvay Fluor, Bad Wimpfen, Germany), which contained a slight fluorite impurity and had a pH of 8.5 in H<sub>2</sub>O.

Added to the ternary binder system were lithium carbonate (Chemetall, Frankfurt am Main, Germany), polycarboxylate ether (PCE) superplasticiser (Melflux® 2651 F, BASF, Ludwigshafen, Germany) and either sodium potassium tartrate (Jungbunzlauer, Basel, Switzerland) or sodium citrate (Merck, Darmstadt, Germany). The SLU formulation was prepared by drymixing binders and additives together for two hours using an overhead shaker Reax 20 (Heidolph, Schwabach, Germany).

**Table 1.** Composition of simplified model SLU formulation used in this study.

Constituent	Function	Share [wt. %]
PC (CEM I 52.5 N Milke®)	Binder	47.16
CAC (Ciment Fondu®, 40 % Al <sub>2</sub> O <sub>3</sub> )	Binder	32.70
CaSO <sub>4</sub> (Fluoroanhydrite)	Binder	19.04
Lithium carbonate	Accelerator	0.30
Sodium potassium tartrate tetrahydrate or sodium citrate dihydrate	Retarder	0.40
PCE (Melflux® 2651 F)	Superplasticiser	0.40
Total		100.00

### Clinker phases

The aluminato clinker phases C<sub>3</sub>A, C<sub>12</sub>A<sub>7</sub>, CA and CA<sub>2</sub> were synthesised according to [13] in a chamber furnace (Nabertherm, Lilienthal, Germany). After sintering, the calcium aluminates were ground and sieved to match the particle size of the Ciment Fondu® CAC used in this study ( $d_{50} = 18 \mu\text{m}$ ). To enable ettringite formation, they were mixed on a 1 : 1 basis (by weight) with calcium sulphate dihydrate (gypsum).

### Ageing of samples

The drymixed model SLU formulations, the commercial SLU and the individual components of the ternary binder system were spread out on 60 x 135 cm Plexiglas® plates in portions of 250 g each. The samples were then exposed to  $35 \pm 2^\circ\text{C}$  and  $90 \pm 5\%$  RH for varying periods in a custom-built climate controllable box (Figure 1). After ageing, the powders were scraped off the plates. Weight changes of the samples were then determined on a laboratory balance (Sartorius, Göttingen, Germany).

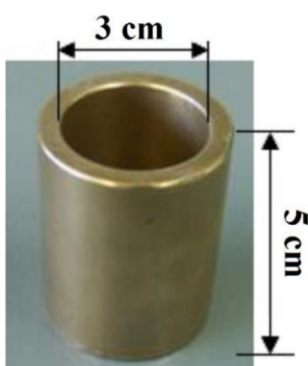


**Fig. 1:** PC powder spread on a plate (left) prior to ageing at  $35^\circ\text{C} / 90\%$ , and afterwards (right).

### Characterisation of ageing products

For monitoring the ageing progress with powder XRD, plastic sample carriers were prepared with samples of binders and clinker phases and continually aged in the climate box. XRD identification of the ageing products was carried out at a *D8 Advance* (Bruker AXS, Karlsruhe, Germany) instrument using a CuK $\alpha$  source. As the peak intensities of the ageing products increased with ageing time, the peaks of the cement constituents simultaneously receded. Quantifying the conversion by means of XRD however proved not feasible. During prehydration water is not exclusively chemically sorbed, but also physically bond to the surface, thus lowering the XRD signal intensity of aged samples.

#### Paste flow



The flowability of both fresh and prehydrated formulations was tested by a “mini slump test” according to DIN EN 12706 [14] using a brass cylinder with an inner diameter of 30 mm and a height of 50 mm (Figure 2). First, the cylinder is positioned on a neat glass plate and completely filled with paste prepared from the formulation and DI water ( $w/f = 0.45$ ). The cylinder is then lifted up and the paste allowed to flow out for ten seconds. After four minutes the paste spread on the glass plate is measured. The results for the model formulation were compared to those of a commercial SLU (*K15 DR*, Ardex, Witten, Germany).

**Fig. 2:** Slump cylinder used in flowability investigations.

## RESULTS AND DISCUSSION

### Ageing of ternary binder system components and clinker phases

#### Binders – PC, CAC and anhydrite

During ageing, cementitious materials increase in weight due to reaction with water and CO<sub>2</sub> from the atmosphere. Figure 3 shows the weight increase for the three components of a SLU ternary binder system after being individually exposed to  $35^\circ\text{C}$  and  $90\%$  relative humidity for 1, 3 and 7 days.

### 4.3 TOPIC 2: AGING IMPACT ON TBS AND MODEL SLU

*Towards understanding the ageing behaviour of SLU formulations: Impact of prehydration on individual components and role of admixtures*

Of the three components, PC displayed the largest weight increase by far. A 7 days aged sample weighed ~ 12 % more than before prehydration. In the same timeframe, the weight of the CAC sample only increased by about 3.5 %, and anhydrite did not change in weight at all.

This was unexpected, since it was believed that the aluminate-rich CAC would quickly form large amounts of calcium aluminate hydrate (C-A-H) phases upon contact with moisture. Likewise, anhydrite was assumed to incorporate water resulting in hemihydrate (basanite) or dihydrate (gypsum). On the other hand, silicate rich PC was expected to age slower based on the aforementioned earlier investigations of alite and belite. Unlike CAC, PC contains sulphate and is therefore able to produce ettringite. However, considering that PC contains only ~ 4 % C<sub>3</sub>A, this huge increase in weight after exposure to humidity is surprising.

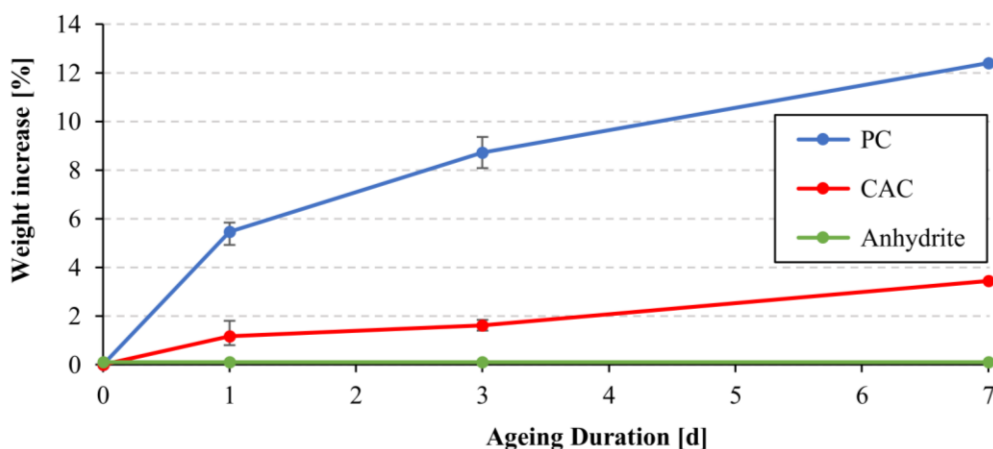


**Fig. 3:** Weight increase of components of a ternary binder system during ageing at 35 °C and 90 % RH for up to seven days.

To get a better understanding of the processes taking place during ageing, the surfaces of PC and CAC powders placed on plastic sample carriers were periodically examined by XRD, thus allowing for continuous monitoring of their surfaces. This makes the results for different ageing periods more comparable instead of samples which were prepared for every measurement individually and may show inconsistencies. Moreover, it avoids damaging the sensitive prehydrated particle surfaces which would occur during fixing aged samples onto the sample holders.

The XRD measurements of fresh and 14 days aged PC as well as CAC are displayed in Figure 4. The results match the earlier observations from determination of the weight increase, because the surface of the PC sample undergoes more significant changes than the CAC. Taking X-ray amorphous calcium silicate hydrates (C-S-H) out of the picture, PC predominantly formed calcium carbonate (CaCO<sub>3</sub>) in the calcite modification. No portlandite was detected and ettringite only in a very small amount. This is a result of carbonation. On contact with CO<sub>2</sub>, portlandite and ettringite decompose to CaCO<sub>3</sub>, aluminium hydroxide Al(OH)<sub>3</sub>, calcium sulphate and water.

The CAC in comparison formed only minor quantities of a different CaCO<sub>3</sub> modification, aragonite. No C-A-H phases were detected, the only indicator of a reaction with H<sub>2</sub>O consisted of a small amount of bayerite, an Al(OH)<sub>3</sub> polymorph. Pure anhydrite did not undergo any visible changes in the XRD during the first 14 days of ageing. Only after exposure for two months, a very low concentration of gypsum could be detected. In summary, the individual behaviours of the ternary binder system components displayed in weight increase and XRD are consistent.

Cement constituents	AH: Anhydrite	CA: $\text{CaAl}_2\text{O}_4$	$\text{C}_3\text{S}$ : $\text{Ca}_3\text{SiO}_5$	$\text{C}_3\text{A}$ : $\text{Ca}_3\text{Al}_2\text{O}_6$
Ageing products	A: Aragonite	B: Bayerite	C: Calcite	E: Ettringite

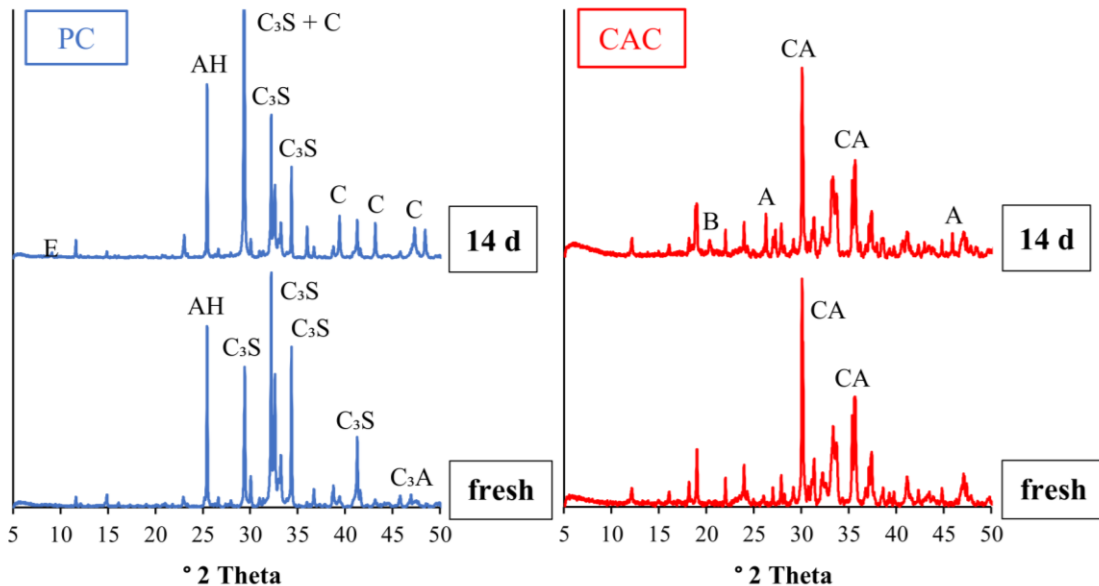


**Fig. 4:** XRD patterns of fresh and 14 days aged PC (in blue, left) as well as CAC (in red, right), shown in the range of  $5 - 50^\circ 2\theta$  with cement constituents and ageing products marked.

#### Aluminate phases – $\text{C}_3\text{A}$ , $\text{C}_{12}\text{A}_7$ , CA, $\text{CA}_2$

In the previous part, the prehydration of CAC in the absence of sulphate was studied, hence ettringite formation was not possible. For this reason, the ageing of combinations of pure aluminate phases and sulphate was investigated next. The primary aluminate phase in PC used in this study is undoped, cubic  $\text{C}_3\text{A}$ . For Cement Fondu® it is  $\text{CaAl}_2\text{O}_4$  (CA). Other aluminate phases commonly encountered in aluminate cements are  $\text{C}_{12}\text{A}_7$  and  $\text{CA}_2$ . All four phases were individually aged after drymixing with calcium sulphate dihydrate (gypsum) on a 1 : 1 basis (by weight) to enable ettringite formation. Gypsum was chosen over hemihydrate or anhydrite to eliminate sulphate hydration as a side reaction.

Figure 5 shows the XRD patterns of  $\text{C}_3\text{A}$  and CA combined with gypsum, both fresh and after 14 days of ageing. Aged  $\text{C}_3\text{A}$  exhibits strong ettringite formation while the CA does not react at all.  $\text{C}_{12}\text{A}_7$  and  $\text{CA}_2$  likewise remained unaffected after this ageing time. Only after 28 days at  $35^\circ\text{C}$  and 90 % RH did the three aluminate phases show small concentrations of  $\text{Al}(\text{OH})_3$ . In contrast, the ettringite formed by  $\text{C}_3\text{A}$  had decomposed at this point.

#### 4.3 TOPIC 2: AGING IMPACT ON TBS AND MODEL SLU

## Towards understanding the ageing behaviour of SLU formulations: Impact of prehydration on individual components and role of admixtures

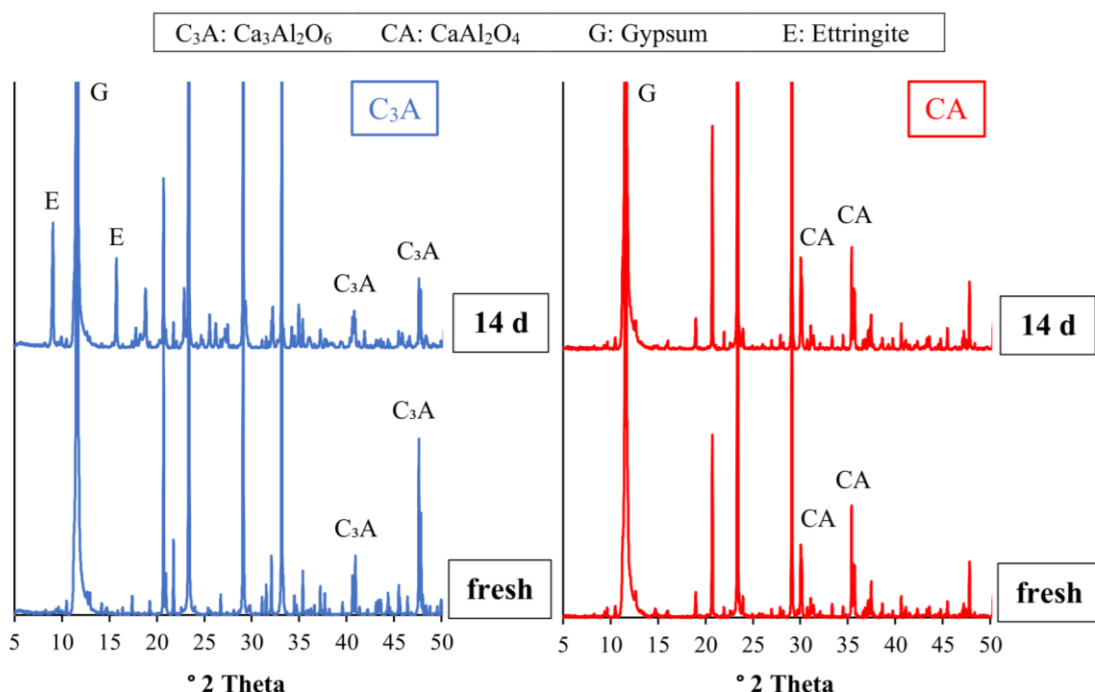


**Fig. 3:** XRD patterns of fresh and 14 days aged aluminate clinker phases mixed with gypsum to enable ettringite formation.  $C_3A$  (blue, on the left) and  $CA$  (red, on the right) are shown in the range of  $5 - 50^\circ 2\theta$ .

## Influence of additives on the ageing of PC and CAC

## *Lithium carbonate accelerator*

The results presented so far indicate a low reactivity of the aluminate phases towards humidity, both their pure form and in the presence of sulphate. This underlines the need to use accelerators to activate the CAC, as is known from actual application. We subsequently mixed PC and CAC with lithium carbonate accelerator prior to ageing. The  $\text{Li}_2\text{CO}_3$  dosage was chosen based on the relative portion of the two cements in the model SLU formulation (Table 1). PC comprises almost half of the formulation (47.16 wt.%), therefore it was mixed with 0.63 wt.%  $\text{Li}_2\text{CO}_3$ , which is slightly more than twice the 0.30 wt.% used in the SLU formulation. CAC makes up almost one third the formulation (32.70 wt.%), thus it was mixed with 0.91 wt.%  $\text{Li}_2\text{CO}_3$ .

A comparison of the weight increases with and without accelerator after 1 day of ageing at 35 °C and 90 % RH is shown in Figure 6. Lithium addition only slightly enhances weight increase of PC from 5.5 to 6.2 %. However, at 8.8 % the weight increase of CAC with accelerator is more than seven times higher than without (1.2 %). This difference was also visually observed, as the CAC sample aged with Li<sub>2</sub>CO<sub>3</sub> formed large platelets like PC (Figure 1). In contrast, the pure CAC remained in a powdery form, more closely resembling the fresh cements.

XRD investigation of the CAC aged with lithium for 1 day revealed formation of  $\text{CaCO}_3$  and  $\text{Al}(\text{OH})_3$  analogous to PC. In addition, the  $\text{Li}_2\text{CO}_3$  had converted to the accelerating  $[\text{Li}_2\text{Al}_4(\text{OH})_{12}](\text{OH})_2 \cdot 3\text{H}_2\text{O}$  layered double hydroxide (LDH). This shows that lithium acceleration does not require quantitative amounts of water and can already be activated during storage at elevated humidity.

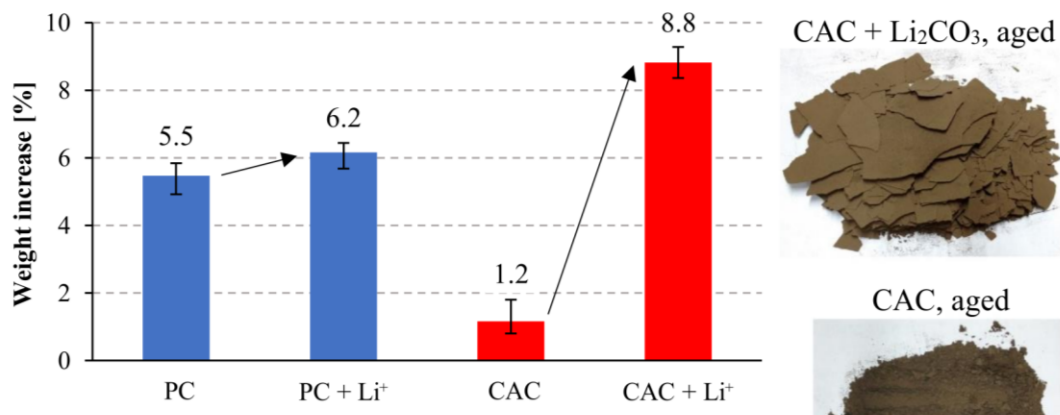


**Fig. 6:** Comparison of the weight increase after 24 hours of ageing with  $\text{Li}_2\text{CO}_3$  at  $35^\circ\text{C}$  / 90 % RH. PC (blue) and CAC (red) were aged neat as well as after addition of 0.63 % (CAC 0.91 %) bwoc  $\text{Li}_2\text{CO}_3$ .

#### Tartrate and citrate retarders

In a second series of experiments we added tartrate and citrate instead of lithium carbonate to the cements prior to ageing. Relative to the model SLU formulation, this amounted to dosages of 0.84 wt.% for PC and 1.21 wt.% for CAC respectively.

As is shown in Figure 7, both retarders surprisingly accelerated the weight increase over 24 hours, thus displaying a behaviour similar to  $\text{Li}_2\text{CO}_3$ . Tartrate had about the same effect on PC as lithium (6.4 % weight increase), whereas citrate addition led to a significantly higher weight increase of 10.0 %. Citrate had a stronger impact than tartrate in CAC as well. Unlike  $\text{Li}_2\text{CO}_3$ , the overall weight increase of CAC with retarders was lower than for PC. Furthermore, no compounds containing tartrate or citrate were detected by XRD, just  $\text{CaCO}_3$  and  $\text{Al(OH)}_3$ . This makes a unique interaction between the retarders and the CAC such as the formation of LDH intercalation compounds unlikely.

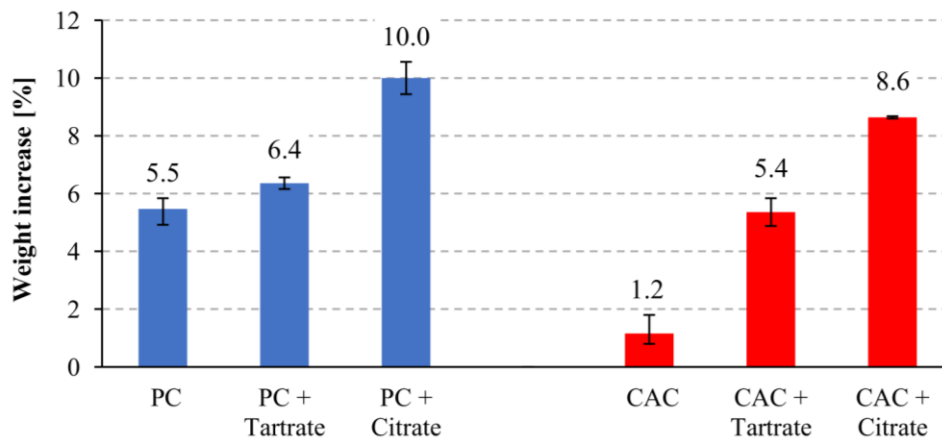


**Fig. 7:** Comparison of the weight increase after 24 hours ageing with retarders at  $35^\circ\text{C}$  / 90 % RH. PC (blue, on the left) and CAC (red, on the right) were aged neat as well as after addition of 0.84 % (CAC 1.21 %) bwoc of tartrate or citrate.

Not only did retarder addition unexpectedly accelerate ageing, it also altered the outward appearance of the samples with spotty discolourations appearing on their surfaces during ageing (Figure 8). In order to get more insight into the additives' reaction at elevated humidity and temperature, we exposed small quantities of pure  $\text{Li}_2\text{CO}_3$  and retarders to  $35^\circ\text{C}$  / 90 % RH as well.

*Towards understanding the ageing behaviour of SLU formulations: Impact of prehydration on individual components and role of admixtures*

Tartrate and citrate turned out to be hygroscopic, both increasing their weight by ~ 15 % over 7 days. The citrate even incorporated the sorbed moisture into its crystal structure, changing from a dihydrate to a pentahydrate.  $\text{Li}_2\text{CO}_3$  on the other hand remained unaffected due to its low solubility in water compared to other lithium salts.

We assume that tartrate and citrate accelerate the weight increase of PC and CAC due to a combination of their hygroscopicity and particle size. After mixing, the coarse retarder crystals are distributed in the fine cement powder. The facilitated uptake of water via these isolated particles leads to areas of strong prehydration, visible as discolourations on the powder surfaces.



**Fig. 8:** Surface discolourations of the model SLU formulation (left) and of pure PC (right), appearing when aged with citrate at 35 °C and 90 % RH.

#### Impact of ageing on SLU flowability

##### *Comparison between model SLU formulation and commercial SLU*

The most important difference between the model SLU formulation and the commercial product is that the latter is “fully formulated”, meaning it contains fillers like quartz sand and limestone as well as auxiliary additives such as redispersing polymers. The model formulation comprising the ternary binder system and its additives thus only represents the reactive key component (~ 35 wt.%) of a fully formulated SLU.

Figure 9 compares paste spread and mass increase of the model formulation (with tartrate as retarder) and the commercial SLU *K15 DR*. Before ageing, both reached a spread of 23 cm at a water-to-solid (w/s) ratio of 0.45. During ageing *K15 DR* lost flowability faster than the model formulation. It reached the minimum paste spread already after 24 hours of exposure to moisture. Increasing the ageing duration did not change the fluidity any further. This corresponds to the weight increase of the sample, which stopped after 1 day.

The model formulation on the other hand displayed a more gradual decline in flowability, the early stages of ageing still having the strongest impact. The corresponding weight increase mirrors the flowability development, similar to the commercial product.

The fillers in the *K15 DR* SLU are chemically inert towards water but can physically sorb moisture. This explains that the weight increase of the commercial product overall is lower but achieves its maximum after just 24 hours of exposure. The physical sorption of water further leads to agglomeration of filler particles which reduces initial flowability.

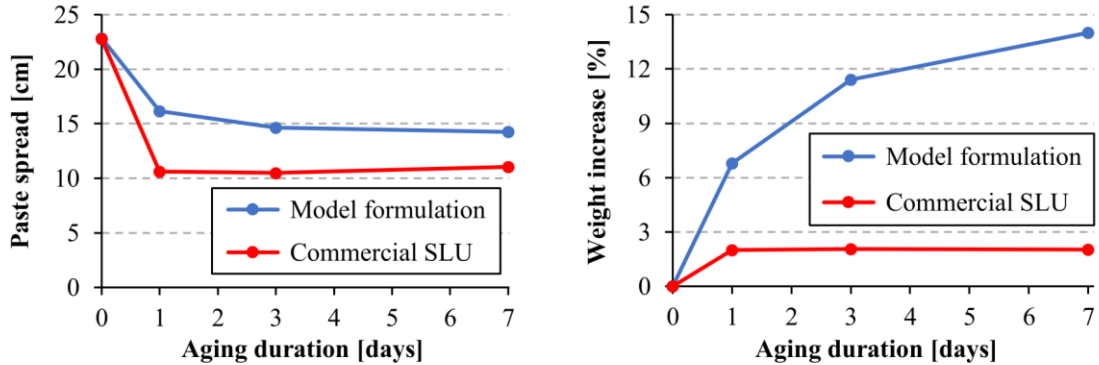


**Fig. 9:** Comparison between model SLU formulation (with tartrate as retarder) and a commercial SLU (Ardex K15 DR). Shown are paste spread at a w/s ratio of 0.45 (left) and the weight increase (right) of samples aged at 35 °C / 90 % RH for up to seven days.

#### Delayed plastification and measures to counteract ageing effects

In a previous study<sup>[11]</sup> we reported that ageing leads to delayed plastification, meaning that the flowability of a paste prepared from an aged sample of the model formulation increases over time. However there, the retarders had not been aged together with the other components of the model SLU and instead were added only during paste preparation. Now we conducted these experiments with the whole model formulation aged together. The results obtained were practically identical with those from the previous study and are shown in Figure 10 on the left for reference.

In order to find measures to mitigate the negative impact of ageing on paste flowability we investigated the impact of adding calcium hydroxide  $\text{Ca}(\text{OH})_2$  to the SLU formulation.  $\text{Ca}(\text{OH})_2$  addition has originally been suggested to prevent the formation of so-called hydrate spheres in ternary binder systems<sup>[15]</sup>. Hydrate spheres are inclusions inside the hardened matrix that develop due to inhomogeneous setting and are regularly encountered in tartrate-retarded ternary binder systems used in drymix applications<sup>[16]</sup>.

In this study, we tested the addition of 1.0 and 2.5 wt.%  $\text{Ca}(\text{OH})_2$  to the model formulation containing tartrate prior to ageing for three days. As can be seen in Figure 10 on the right,  $\text{Ca}(\text{OH})_2$  generally increased fluidity which might be owed to its high hygroscopicity which prevents other phases from prehydration. The positive effect on flowability diminished over time due to the aforementioned delayed plastification.

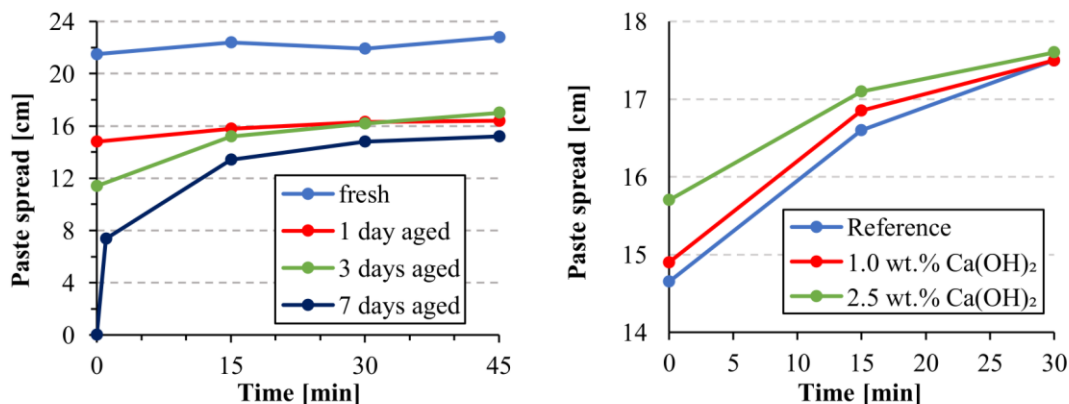


**Fig. 10:** Paste spread of the model SLU formulation before and after ageing ( $w/s = 0.45$ ). On the left, different ageing periods are compared. The results shown on the right were obtained with addition of  $\text{Ca}(\text{OH})_2$  prior to ageing for 3 days.

*Towards understanding the ageing behaviour of SLU formulations: Impact of prehydration on individual components and role of admixtures*

### CONCLUSION

The aim of this study was to further our understanding of the ageing behaviour of SLU formulations. First, we investigated the impact of prehydration on individual constituents of the ternary binder system which presents the basis of a SLU. Samples were exposed to 35 °C and 90 % RH over varying periods of time in a climate box.

Unexpectedly, PC displayed a higher weight increase during ageing than CAC, while anhydrite did not change in weight at all. This was confirmed by XRD analysis with PC samples undergoing significant changes on their surface. PC predominantly formed CaCO<sub>3</sub> (calcite modification) with atmospheric CO<sub>2</sub> and minor quantities of ettringite. CAC on the other hand produced only small amounts of CaCO<sub>3</sub> and Al(OH)<sub>3</sub>, with no C-A-H being formed under the ageing conditions applied.

We investigated potential ettringite formation during ageing by mixing pure aluminate clinker phases with gypsum prior to prehydration. As was observed for neat PC, C<sub>3</sub>A also produced quantitative amounts of ettringite during ageing while CA, C<sub>12</sub>A<sub>7</sub> and CA<sub>2</sub> remained unaffected by moisture.

These results confirmed the need to use accelerators to activate the CAC contained in the ternary binder system. While the weight increase of PC aged with Li<sub>2</sub>CO<sub>3</sub> was only slightly accelerated, the weight of CAC increased sevenfold. XRD analysis confirmed the formation of a [Li<sub>2</sub>Al<sub>4</sub>(OH)<sub>12</sub>]·(OH)<sub>2</sub> · 3 H<sub>2</sub>O LDH in CAC during ageing.

Ageing of PC and CAC with tartrate or citrate retarder instead of Li<sub>2</sub>CO<sub>3</sub> surprisingly accelerated the weight increase as well. In their pure form the retarders turned out to be hygroscopic at 90 % RH. In combination with the relatively large particle size of the retarders, this led to isolated spots of strong prehydration on the cement surface.

We compared the paste spread of a model SLU formulation with that of a commercial SLU (*K15 DR*). Before ageing, both reached a similar spread, whereas after 24 hours in the climate box the commercial product showed a stronger reduction in flowability than the model formulation. *K15 DR* contains fillers like quartz sand and limestone besides the ternary binder system. These non-hydrating fillers can physically sorb moisture, thus possibly causing particle agglomeration which results in additional flowability loss. To counteract the ageing effect on SLUs, we tested the addition of Ca(OH)<sub>2</sub> to the model formulation which had a positive impact on early flowability.

The experiments conducted in this study show that the combination of numerous components contained in a SLU increases its susceptibility to ageing. Apart from the binder system, additives and even aggregates play a role in determining ageing behaviour.

### ACKNOWLEDGEMENTS

The authors are most grateful to the Deutsche Forschungsgemeinschaft (DFG, German Research Foundation) for funding this project under the grant PL-472/9-2. Thanks go also to HeidelbergCement and Kerneos S.A. for providing the cements used in this study.

### REFERENCES

- [1] Plank J. *Technology Trends in the European Dry Mix Mortar Industry*. Proceedings of 1<sup>st</sup> Conference on Research and Application of Commercial Mortar, Shanghai/China, 2005. pp 26-40.
- [2] Winter C and Plank J. *The European Dry-Mix Mortar Industry (Part 1)*. Zement-Kalk-Gips International, 2007, 60(6), pp 62-69.

- [3] Harbron R. *A general description of flow-applied floor screeds - an important application for complex formulations based on CAC*. Calcium Aluminate Cements: Proceedings of the International Conference 2001, Edinburgh. Mangabhai R J and Glasser F P. (Eds). London: IOM Communications, 2001, pp 597-604.
- [4] Amathieu L, Bier T A and Scrivener K L. *Mechanisms of set acceleration of Portland cement through CAC addition*. Calcium Aluminate Cements: Proceedings of the International Conference 2001, Edinburgh. Mangabhai R J and Glasser F P. (Eds). London: IOM Communications, 2001, pp 303-317.
- [5] Götz-Neunhoeffer F. *Modelle zur Kinetik der Hydratation von Calciumaluminatzement mit Calciumsulfat aus kristallchemischer und mineralogischer Sicht*, Universitätsverbund Erlangen-Nürnberg, 2006.
- [6] Al-Mutawa F, Whittaker M, Arkless L, Dubina E, Plank J and Black L. *The Effects of Prehydration at Moderate Humidities on the Engineering Properties of Portland Cement*. Proceedings of Cement and Concrete Science, Birmingham, 2010.
- [7] Winnefeld F. *Influence of cement ageing and addition time on the performance of superplasticisers*. Zement-Kalk-Gips International, 2008, 61(11), pp 68-77.
- [8] Dubina E, Black L, Sieber R and Plank J. *Interaction of water vapour with anhydrous cement minerals*. Advances in Applied Ceramics 109(5), 2010, 260-268.
- [9] Dubina E, Wadsö L and Plank J. *A sorption balance study of water vapour sorption on anhydrous cement minerals and cement constituents*. Cement and Concrete Research, 2011, 41, pp 1196-1204.
- [10] Dubina E and Plank J. *Investigation of the long-term stability during storage of drymix mortars, Part 2. Influence of Moisture Exposure on the Performance of Self-levelling mortars (SLUs)*. ALITinform, 2012, 26(4-5), pp 86-99.
- [11] Plank J, Dubina E and Meier M R. *Ageing Behavior of SLU Mortar Formulations Based on a Ternary Binder System Comprising PC/CAC/Anhydrite Exposed to Environmental Moisture and CO<sub>2</sub>*. Calcium Aluminate Cements: Proceedings of the International Conference 2014, Avignon. Fentiman C H, Mangabhai R J and Scrivener K L. (Eds). London: IOM Communications, 2014, pp 407-421.
- [12] Hartmann F A, Meier M R and Plank J. *The impact of cement and clinker prehydration on retarder performance*. Proceedings of 15<sup>th</sup> International Congress on the Chemistry of Cement, Prague, 2019.
- [13] Wesselsky A and Jensen O M. *Synthesis of pure Portland cement phases*. Cement and Concrete Research, 2009, 39, pp 973-980.
- [14] DIN EN 12706. *Adhesives-test methods for hydraulic setting floor smoothing and/or levelling compounds - determination of flow characteristics*. 1999.
- [15] Zurbriggen R. *High Performing Self-Levelling Underlays - Learnings from Material Science Studies*, Proceedings of 5<sup>th</sup> American Drymix Mortar Conference, Philadelphia, 2016
- [16] Götz-Neunhoeffer F and Zurbriggen R. *Formation of hydrate spheres in ternary binder systems*. Zement-Kalk-Gips International, 2008, 61(12), pp 68-76.



## 5 Conclusion

### 5.1 Summary of the project and outlook for future research

The DFG research project PL 472 / 9-2 "Influence of aging of binder systems on the performance of additives" investigated two major topics: The effectiveness of retarding admixtures in aged OPC and clinker phases as well as the aging impact on the components of a dry-mix product at the example of a model SLU.

Concerning the retarder topic, CEM I 52.5 N as well as the clinker phases  $C_3A$  (blended with gypsum) and  $C_3S$  were exposed to water vapor and atmospheric  $CO_2$  at 35 °C and 90% RH for up to 14 days. The effectiveness of the retarders NaGluc and KPPhos, as defined by how long a certain dosage delays the hydration process, was determined for fresh and aged samples. The exposure duration of the cement was identified as the decisive factor for the retarder performance (**Figure 45**). When the aging period only lasted a few days at maximum, the effectiveness of both retarders was lower than in fresh CEM I 52.5 N. Rising again with increasing exposure duration, the retarder performance in 14 days aged CEM I 52.5 N is significantly higher than in fresh cement. This behavior is caused by the formation of ettringite during the aging in humid atmosphere from aluminate clinker phases and sulfate set regulators. Having crystallized on the surface of the cement particles, this early ettringite acts as a seeding material in the main ettringite formation during the hydration of aged OPC. This accelerating effect reduces the impact of the retarders as compared to fresh cement. However, the ettringite crystallites formed during aging are not stable towards the atmospheric  $CO_2$ . The longer the cement is aged, the more of the ettringite decomposes to  $CaCO_3$ ,  $Al(OH)_3$  and gypsum. As a result, the seeding effect is weakened and the retarder effectiveness increases again.

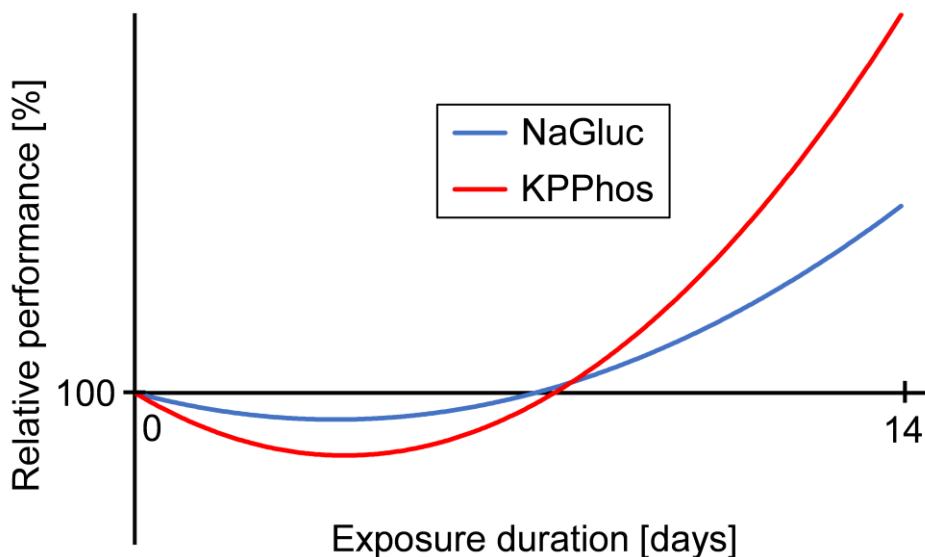


**Figure 45:** Impact of OPC aging on the performance of NaGluc and KPPhos retarders (not to scale).

## 5.1 SUMMARY AND OUTLOOK

---

In direct comparison, NaGluc performance is less negatively affected after short exposure of the cement whereas KPPhos becomes superior towards long aging periods. It was found that the dissolution of calcium is slower the longer the CEM I 52.5 N is aged. This means that with increasing exposure duration the same dosage of pyrophosphate precipitates a larger fraction of the free  $\text{Ca}^{2+}$  from pore solution, which results in a stronger retardation of the ettringite formation.

The seeds on the particle surface also trigger a rapid overgrowth of the aged CEM I 52.5 N with ettringite during hydration. This induces a fast setting, but the compressive strength development is massively slowed. The ettringite overgrowth acts as a diffusion barrier against water access to the silicate phase which impedes the formation of the strength-giving C–S–H. Gluconate, by strongly adsorbing on the particles, was found to slow this overgrowth which explains why NaGluc performs better than KPPhos after short cement exposure. In aged  $\text{C}_3\text{A}$  / gypsum blends, NaGluc even acted as a “delayed accelerator”: The slower particle overgrowth resulted in a faster dissolution of the clinker phase, thereby shortening the hydration process overall. In pure  $\text{C}_3\text{S}$  the situation was different than in OPC, with NaGluc being most potent in retarding the hydration of the fresh clinker phase. This is likely the result of a poisoning of  $\text{C}_3\text{S}$  dissolution sites by the retarder and the aging of the clinker appeared to weaken this effect.

In the second topic on the aging of a model SLU formulation, the exposure of individual components or combinations thereof and the respective impact on the hydration of the whole formulation were investigated. The SLU formulation comprised a TBS consisting of OPC, CAC and AH which would be admixed with an accelerator, a retarder and a superplasticizer. It was found that aging the TBS resulted in the formation of a significant amount of ettringite. Ettringite from the prehydration of the OPC component appears to catalyze the crystallization of additional ettringite from the combination of CAC and AH. The ettringite formed during aging accelerates the early hydration of the model SLU, similar to what was previously observed for pure OPC in the first project topic. If chemical admixtures are present during aging, they will lose their intended effect in the subsequent hydration. If the TBS is aged together with the accelerator, then the SLU formulated from this sample hydrates slower due to the presence of the fresh, functioning retarder (**Figure 46**). Likewise, if the retarder is added to the TBS prior to exposure, then the SLU formulation hydrates faster due to the intact accelerator. If the fully formulated SLU with all admixtures is aged, acceleration and retardation are balanced again since both admixtures have lost their effect simultaneously. The presence of the superplasticizer during the aging of the TBS not only reduced the flowability of the SLU formulation, it also caused a significant delay of the setting. Unlike accelerator and retarder, the effect of the superplasticizer is not irretrievably lost. The flowability of the aged SLU formulation increased again towards later stages of the hydration process, similar to a delayed addition of the admixture.

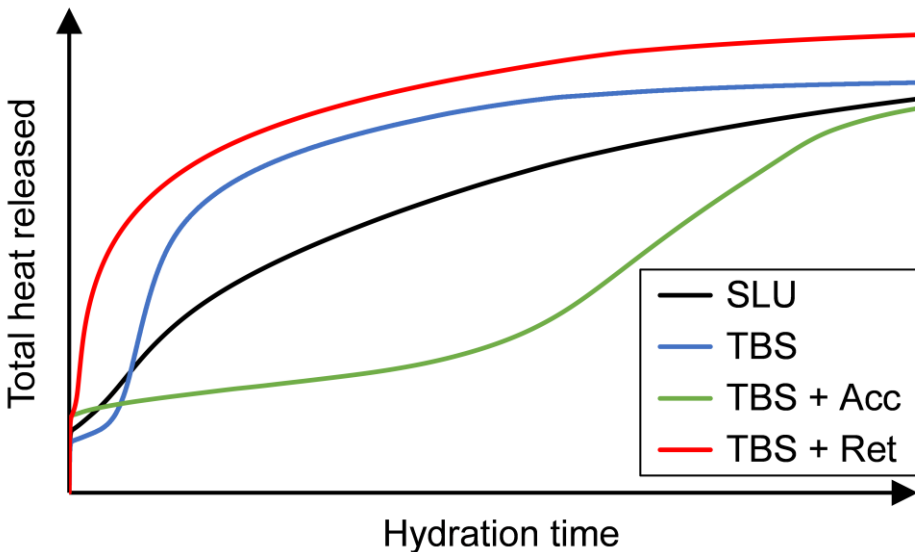


**Figure 46:** Impact of aging different TBS / admixture combinations or the fully formulated SLU on the hydration process.

Speaking of the delayed addition of admixtures to aged binders, this is a topic that warrants targeted investigation in future research. As described in chapter 2.3.1, the cement surface undergoes significant changes during the early hydration which affects its interaction with subsequently added admixtures. It would be interesting to know how aging the cement would impact this behavior. In this project, a delayed admixture addition was not examined. Due to the fast setting of the OPC after exposure, it would require a significant increase of the w/c ratio. This however reduces the comparability with cement application outside the laboratory environment, similar to what was observed for the model SLU formulation. A purely mechanistical study, limited to how delaying the admixture addition impacts the ion concentrations in the pore solution and the depletion of the admixtures, seems appropriate. The associated experiments all profit from a higher w/c ratio. It allows to separate liquid and solid phases of the hydrating aged cement over a longer period of time instead of having to centrifuge the samples shortly after the start of hydration as it was done in this project. In return for the limited scope of such a study, the pool of investigated admixtures can be easily expanded to include representatives of various admixture classes.



## 5.2 Official project report (in German)

Deutsche Forschungsgemeinschaft (DFG) - Projektnummer 224813219

### **Einfluss der Alterung von Bindemittelsystemen auf die Wirkung bauchemischer Zusatzmittel**

DFG-Geschäftszeichen PL 472/9-2

### **Abschlussbericht**

## 5.2 OFFICIAL PROJECT REPORT

---

1. Allgemeine Angaben

1.1 DFG-Verfahren:

Sachbeihilfen

1.2 Antragsteller:

Professor Dr. Johann Plank

Technische Universität München (TUM)

Fakultät für Chemie

Lehrstuhl für Bauchemie

1.3 Fachliche Zuordnung:

Baustoffwissenschaften, Bauchemie, Bauphysik

1.4 Thema des Projekts:

Untersuchung des Einflusses der Alterung von Zement und Klinkerphasen auf deren Wechselwirkung mit Verzögerern, Aufklärung des Alterungsverhaltens von ternären Bindemittelgemischen und Trockenmörtelformulierungen

1.5 Berichtszeitraum / Förderzeitraum:

Das Projekt wurde insgesamt 36 Monate durch die DFG gefördert

1.6 Durch dieses Projekt geförderten Promotionen

Florian Andreas Hartmann, geboren 15.12.1992

## 5.2 OFFICIAL PROJECT REPORT

---

### Inhaltsverzeichnis

2. Arbeits- und Ergebnisbericht
  - 2.1. Ausgangsfragen und Zielsetzung des Projekts
  - 2.2. Darstellung der erzielten Ergebnisse
    - 2.2.1. Alterung von Zement
    - 2.2.2. Alterung der Aluminat-Klinkerphase
    - 2.2.3. Interaktion mit Verzögerern
    - 2.2.4. Alterung von ternären Bindemittelgemischen
    - 2.2.5. Alterung von Trockenmörtelformulierungen
3. Zusammenfassung
4. Literaturverzeichnis

## 2. Arbeits- und Ergebnisbericht

### 2.1. Ausgangsfragen und Zielsetzung des Projekts

Ein Hauptgrund für den kommerziellen Erfolg von zementären Baumaterialien ist deren hohes Reaktionspotential gegenüber Wasser. Dadurch reichen jedoch schon geringe Feuchtigkeitsmengen, beispielsweise durch Aufnahme aus der Luft, aus, um eine Hydratationsreaktion auszulösen. Dieser Vorgang wird als „Vorhydratation“ bezeichnet, oder als „Alterung“ wenn die parallele Reaktion mit atmosphärischem CO<sub>2</sub> mitberücksichtigt wird.

Die Zementalterung kann neben unsachgemäßer Lagerung oder Transport bereits bei der Herstellung auftreten. Während des Mahlprozesses, bei dem Temperaturen bis 120 °C erreicht werden, setzen dem Klinker zugesetzte Abbinderegler, primär Gips, Kristallwasser frei [1]. Außerdem kann es vorkommen, dass zur Kühlung der Mühle zusätzliches Wasser eingespritzt wird. Nach dem Mahlprozess werden bei der Lagerung des Pulvers in Silos noch ~80 °C erreicht, wodurch sich der Wasseraustritt fortsetzt [2].

Die Reaktion mit atmosphärischer Feuchte führt zur vorzeitigen Bildung von Hydratphasen auf den Zementpartikeloberflächen [3, 4]. Diese wirken sich negativ auf Fließverhalten, Abbindezeiten und Festigkeitsentwicklung aus [5, 6]. Darüber hinaus wird die Interaktion mit chemischen Zusatzmitteln, die eng mit den Eigenschaften der Partikeloberfläche verbunden ist, signifikant und oftmals auf inkonsistente Weise beeinflusst. Eine Studie unserer Gruppe [7] fand heraus, dass in gealtertem Zement bezogen auf die Dosis-Wirkbeziehung die Effektivität von Methylcellulose als Wasserretentionsmitteln zunimmt, die der Beschleuniger Ca-Formiat und amorphem Al-Oxid jedoch abnimmt. Dagegen konnten Maltese et al. [8] von einer Steigerung der beschleunigenden Wirkung von Al-Sulfat berichten. Winnefeld [9] wies ebenfalls eine Wirkungszunahme bei Polycarboxylat- und Polykondensat-basierten Fließmitteln nach, wobei sich diese bei Verschärfung der Alterungsbedingungen und Verlängerung der Expositionsdauer ins Gegenteil umkehrt, wie unsere Gruppe feststellte [7]. Nach weiteren Untersuchungen [10, 11] kommen wir zu dem Schluss, dass die Effektivität der Polycarboxylat-Fließmittel von der Komposition des gealterten Zements abhängig ist, da Aluminatphasen bei hoher Luftfeuchte schneller und mehr Wasser sorbieren als Silikatphasen.

Aus diesem Grund war es das erste Ziel des Projekts, die Hydratationsmechanismen von gealtertem Zement und die Rolle der Klinkerphasen näher zu untersuchen. Des Weiteren wurde der Einfluss von Verzögerern auf das Abbindeverhalten analysiert, da sich bisher noch keine Studie mit der Wechselwirkung dieser Zusatzmittel mit gealtertem Zement befasst hat.

Um verschiedene gewünschte Eigenschaften in einem Bindemittel zu vereinen, werden Zemente, sulfatbasierte Binder und andere Materialien oft miteinander kombiniert. In der zweiten Projekthälfte wurde daher der Schwerpunkt von reinem Portlandzement auf Bindemittelgemische erweitert. Ein typisches Beispiel ist das ternäre System aus Portlandzement, Calciumaluminatzement und Anhydrit. Ternäre Bindemittelsysteme finden kommerzielle Anwendung in Trockenmörtelformulierungen, beispielsweise Selbstverlaufsmassen zur Beseitigung von Unebenheiten nach der Fundamentierung [12]. Dabei wird das TBS mit Verzögerern, Beschleunigern und Fließmitteln kombiniert, um kurze Abbindezeiten und hohe Frühfestigkeiten zu erzielen [13]. Die hohe Reaktivität dieser Formulierungen resultiert jedoch auch in kurzen Haltbarkeitsdauern vor der Anwendung [14]. Daher wurde neben der Alterung des ternären Systems an sich auch die Präsenz von Zusatzmitteln während der Exposition untersucht.

## 2.2. Darstellung der erzielten Ergebnisse

### 2.2.1. Alterung von Zement

In der ersten Projektphase wurde das Verständnis der Zementalterung hinsichtlich ihres Einflusses auf den Hydrationsmechanismus vertieft. Bei 35 °C und 90 % RH gealterter CEM I 52.5 N bindet über einen wesentlich kürzeren Zeitraum ab als frischer und mit zunehmender Alterungsdauer erfolgt das Abbinden früher, nach 14 Tagen Alterung bereits direkt nach dem Anmischen (Abbildung 1, links). Die Beschleunigung wird durch massive Ettringitbildung früh in der Hydratation von gealtertem Zement verursacht (Abbildung 1, rechts).

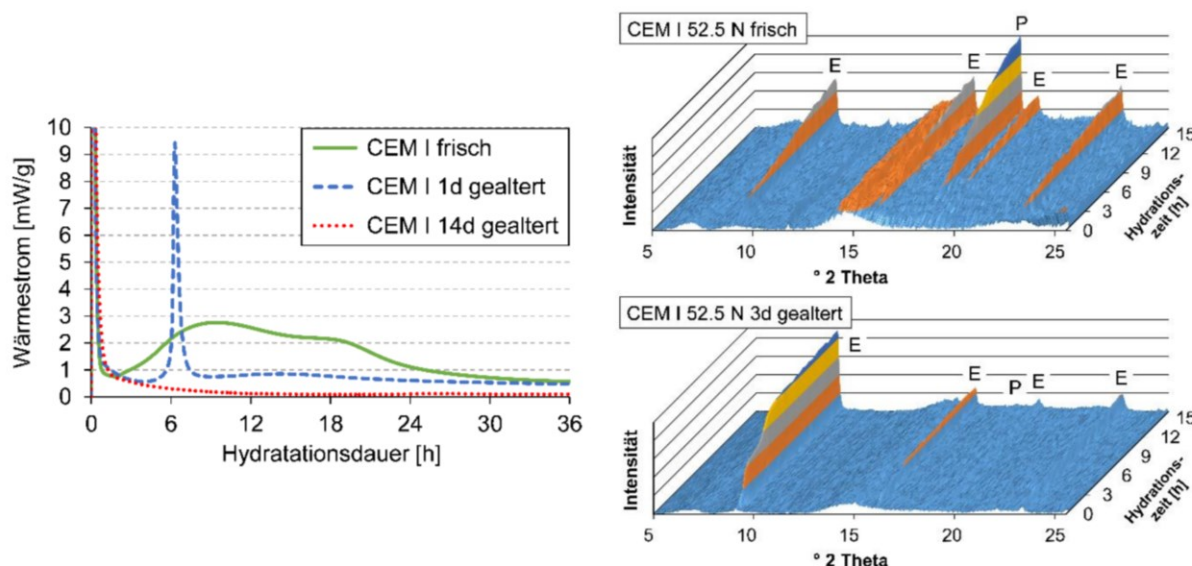


Abbildung 1: Vergleich der Hydratation von frischem und gealtertem Portlandzement CEM I 52.5 N.

Diese wird ermöglicht durch die Bildung nanoskaliger Ettringitnadeln auf den Zementpartikeloberflächen während der Alterung (Abbildung 2, Mitte), welche während der Hydratation als Kristallisationskeime agieren. Dadurch werden die Oberflächen mit einer Ettringitschicht (Abbildung 2, rechts) überzogen, die den weiteren Wasserzutritt und damit die vollständige Hydratation der Zementpartikel, insbesondere der silikatischen Phasen, verzögert. Dies erklärt die bereits in mehreren Studien berichtete [3, 6, 15, 16] verlangsamte Festigkeitsentwicklung von gealtertem Zement. Mit den in diesem Projekt gewonnen Erkenntnissen wird ein aktualisierter Ablauf der Hydratation von gealtertem Zement postuliert (Abbildung 3).

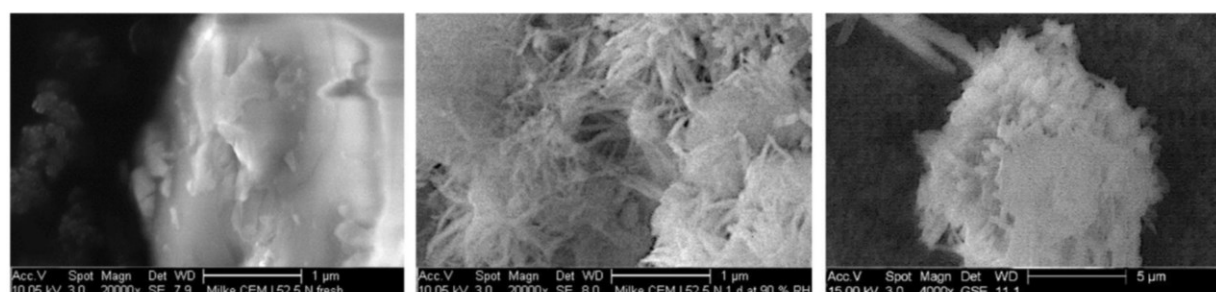


Abbildung 2: SEM-Aufnahmen von frischem (links) sowie 1 Tag bei 35 C / 90 % RH gealtertem (Mitte) CEM I 52.5 N. ESEM- Aufnahme von 1 Tag gealtertem CEM I 52.5 N nach Hydratation (w/c = 0.55) für 8 Stunden (rechts).

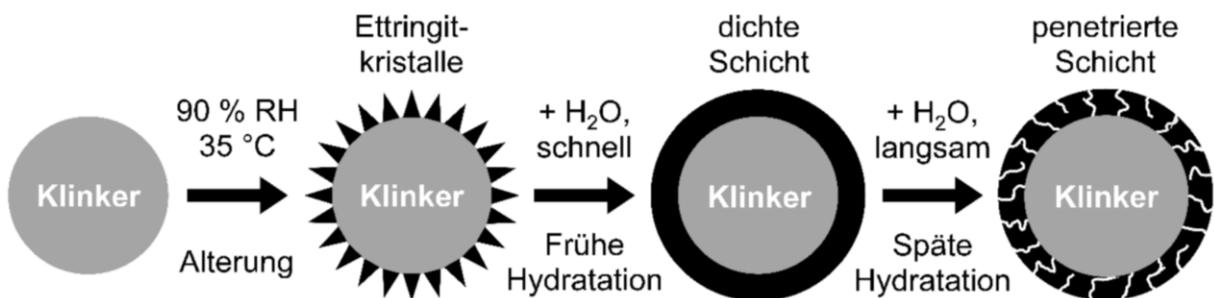


Abbildung 3: Schematischer Ablauf der Hydratation von gealtertem Portlandzement.

## 2.2.2. Alterung von C<sub>3</sub>A

Die Hauptkomponente der Ettringitbildung in Zement ist die Aluminat-(C<sub>3</sub>A)-Klinkerphase. Im zweiten Schritt dieses Projektes wurde daher ihre individuelle Rolle in der Zementalterung untersucht. Dazu wurden binäre Mischungen aus C<sub>3</sub>A und Gips unter den gleichen Bedingungen wie zuvor CEM I 52.5 N gealtert. Darüber hinaus wurde bei der Alterung zwischen kubischem (reinem) und orthorhombischem (Na<sup>+</sup>-dotiertem) C<sub>3</sub>A differenziert, den beiden am häufigsten in technischem Zement auftretenden Kristallmodifikationen.

Die Untersuchungen zeigten, dass orth. C<sub>3</sub>A deutlich schneller altert als kub. C<sub>3</sub>A. Dies äußert sich in einer Beschleunigung sowohl der Ettringitbildung als auch des Ettringitzerfalls. Nach 14 Tagen Alterung wurde von orth. C<sub>3</sub>A gebildeter Ettringit bereits nahezu vollständig von atmosphärischem CO<sub>2</sub> carbonatisiert, während kub. C<sub>3</sub>A eine Mischung von Ettringit und den Zerfallsprodukten CaCO<sub>3</sub> und Al(OH)<sub>3</sub> aufweist (Abbildungen 4, 5). Die Reaktion von Ettringit mit gasförmigem CO<sub>2</sub> wurde in einer vorangehenden Studie nachgewiesen [17].

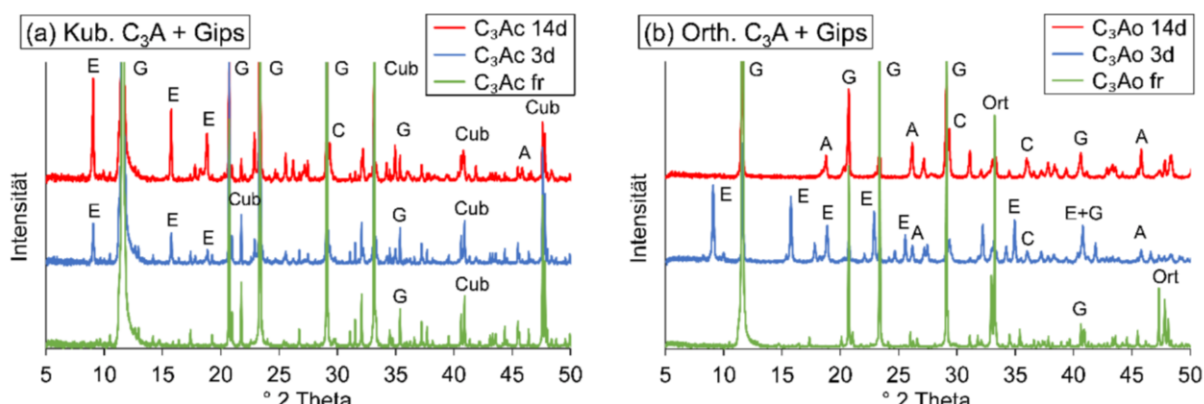


Abbildung 4: Pulver-XRD-Diffraktogramme von binären Mischungen aus kubischem (links) und orthorhombischem (rechts) C<sub>3</sub>A und Gips, vor der Exposition sowie nach 3 und 14 Tagen Alterung bei 35 °C / 90 % RH.

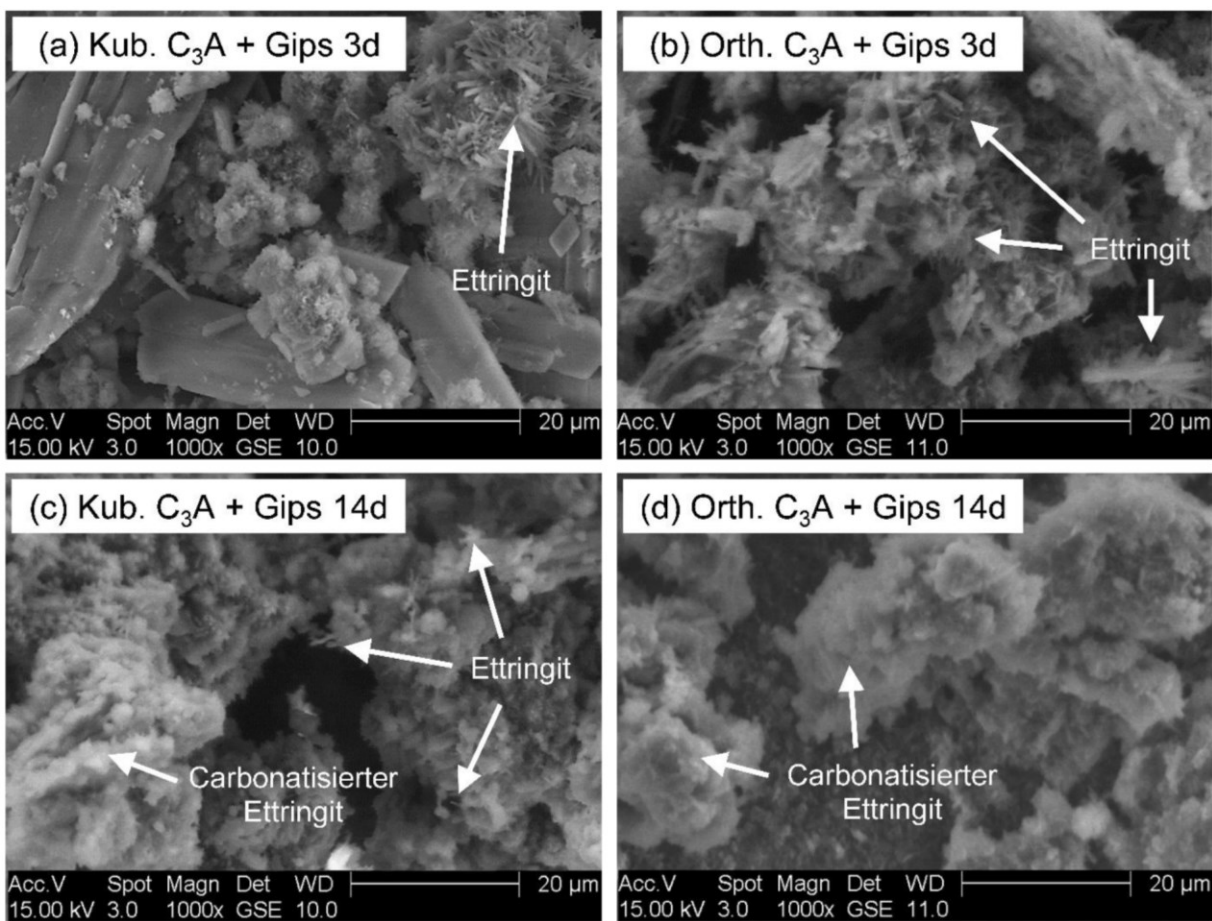


Abbildung 5: ESEM-Aufnahmen von  $\text{C}_3\text{A}$  / Gips-Mischungen nach 3 und 14 Tagen Alterung bei 35 °C / 90 % RH.

Diese Unterschiede zwischen den beiden Polymorphen haben direkte Auswirkungen auf das Abbindeverhalten. Die bei der Zementalterung beobachtete Beschleunigung der Ettringitbildung während der Hydratation ist primär von der Menge an Kristallisationskeimen auf der Partikeloberfläche abhängig. Bei kub.  $\text{C}_3\text{A}$  ist die beschleunigende Wirkung relativ unabhängig von der Alterungsdauer (Abbildung 6, links), da nanoskaliger Ettringit in vergleichbarer Geschwindigkeit gebildet wird und zerfällt. Bei orth.  $\text{C}_3\text{A}$  ist ein viel schnellerer Abschluss der Ettringitbildung (innerhalb von 2 Stunden) nach 3 Tagen Alterung zu beobachten, im Gegenzug entfällt eine beschleunigende Wirkung nach 14 Tagen aufgrund der Carbonatisierung der Kristallisationskeime (Abbildung 6, rechts).

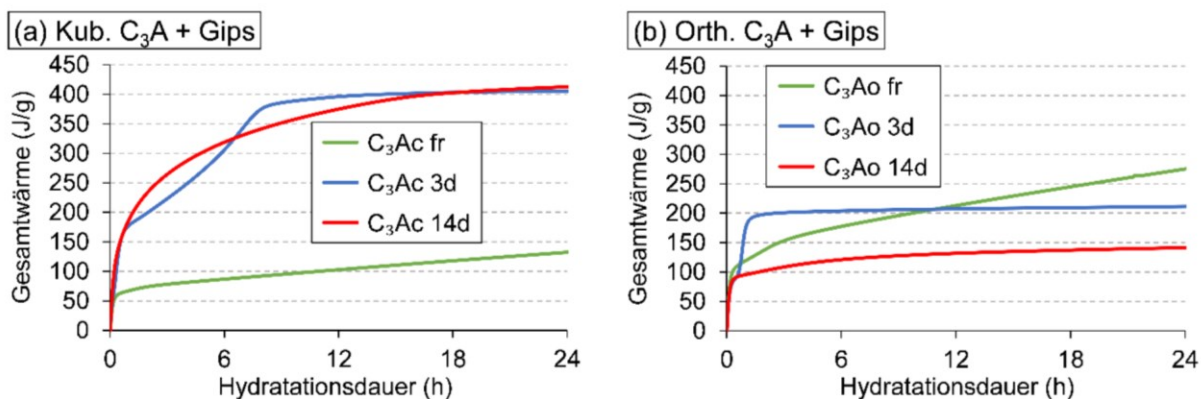


Abbildung 6: Wärmefreisetzung von frischen und gealterten  $\text{C}_3\text{A}$  / Gips Mischungen ( $w/c = 1.0$ ).

### 2.2.3. Einfluss der Alterung auf die Wirkung von Verzögerern

Das beschleunigte Ettringitbildung wurde als Hauptursache für die verringerte Verarbeitungszeit und verlangsamte Festigkeitsentwicklung von gealtertem Zement identifiziert. Im nächsten Projektabschnitt wurde daher der gezielte Einsatz von Verzögerern als Gegenmaßnahme zum Nukleationseffekt des während der Alterung gebildeten nanoskaligen Ettringits untersucht. Zur Anwendung kamen NaGluc und KPPhos, zwei Verzögerer mit unterschiedlichen primären Wirkmechanismen. NaGluc adsorbiert auf den Oberflächen von Klinker- und Hydratphasen, wodurch deren Auflösung respektive Bildung verlangsamt wird. KPPhos chelatisiert und präzipitiert Ca-Kationen aus der Porenlösung, wodurch diese Ionen dem Aufbau der Hydratphasen entzogen werden. Der Vergleich der Verzögerer soll Rückschlüsse auf die effizientesten Wirkmechanismen in gealtertem Zement ermöglichen.

Tabelle 1: Einfluss von NaGluc und KPPhos auf das Abbinden von frischem und gealtertem CEM I 52.5 N.

Probe	Referenz	Abbindezeit [h]	
		+ 0.10 % NaGluc	+ 0.40 % KPPhos
frisch	9.0	21.0	24.0
1d gealtert	6.5	16.0	17.0
3d gealtert	2.0	17.0	11.5
7d gealtert	3.0	15.0	57.0
14d gealtert	< 1*	28.5	293.0

Kalorimetrische Untersuchungen ergaben, dass die Ettringitbildung in gealtertem Zement durch beide Verzögerer verlangsamt wird (Tabelle 1). Ihre Effektivität verändert sich primär mit der Alterungsdauer, so verzögert KPPhos bis 3 Tage gealterten Zement immer schlechter, darüber hinaus jedoch steigt die verzögernde Wirkung extrem stark an. NaGluc verzögert 1 bis 7 Tage gealterten Zement in konstantem Maß, nach 14 Tagen ist die verzögernde Wirkung wie bei KPPhos erhöht, jedoch nicht annähernd so stark.

Dieses Verhalten wurde durch Untersuchung der Porenlösung nach dem Mischen des Zements mit dem Anmachwasser aufgeklärt. NaGluc wird in der eingesetzten Dosierung von 0.1 % weder von frischem noch von gealtertem Zement während des Mischprozesses (120 Sekunden) vollständig adsorbiert, die Depletion aus der Porenlösung wird durch die Alterung von 91 % auf bis zu 74 % gesenkt (Abbildung 7, links). Dadurch steht gerade bei gealtertem Zement auch nach Beginn der Hydratation noch gelöstes NaGluc zur Verfügung, um auf den Ettringitnadeln zu adsorbieren und deren Wachstum zu verzögern. 0.40 % KPPhos wird dagegen sowohl von frischem als auch 3 Tage gealtertem Zement vollständig während des Mischens präzipitiert, wodurch die verzögernde Wirkung verringert wird (Abbildung 7, rechts). Erst nach längerer Alterungsdauer verbleibt auch KPPhos partiell in Lösung.

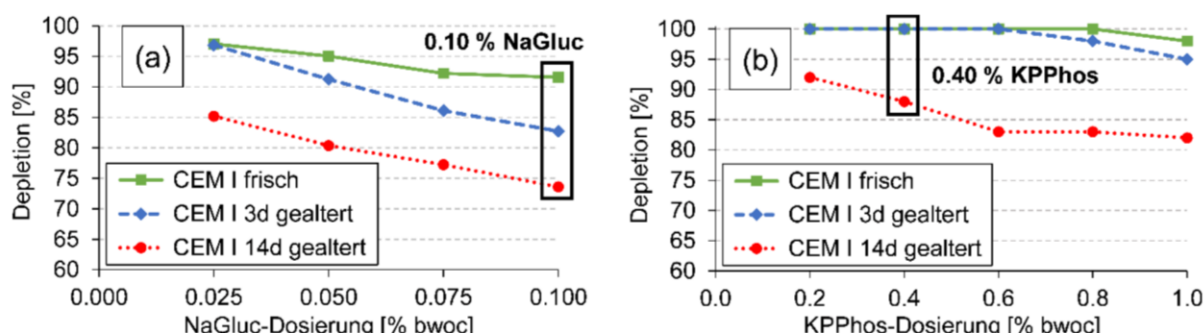


Abbildung 7: Depletion von NaGluc (a) und KPPhos (b) aus der Porenlösung von frischem und gealtertem CEM I 52.5 N (w/c = 2.0).

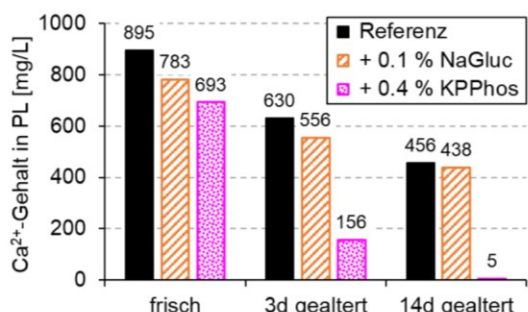


Abbildung 8: Ca<sup>2+</sup>-Gehalt in der Porenlösung von frischem und gealtertem CEM I 52.5 N.

Der Grund hierfür ist ein reduziertes Inlösungengehen von Ca-Kationen während des Mischprozesses mit zunehmender Alterungsdauer (Abbildung 8). Nach 14 Tagen Zementalterung sind 0.40 % KPPhos ausreichend, um die Porenlösung nahezu Ca<sup>2+</sup>-frei zu halten, wodurch jegliches Wachstum der Ettringitnadeln unterbunden und ein extrem langanhaltender Verzögerungseffekt erzielt wird.

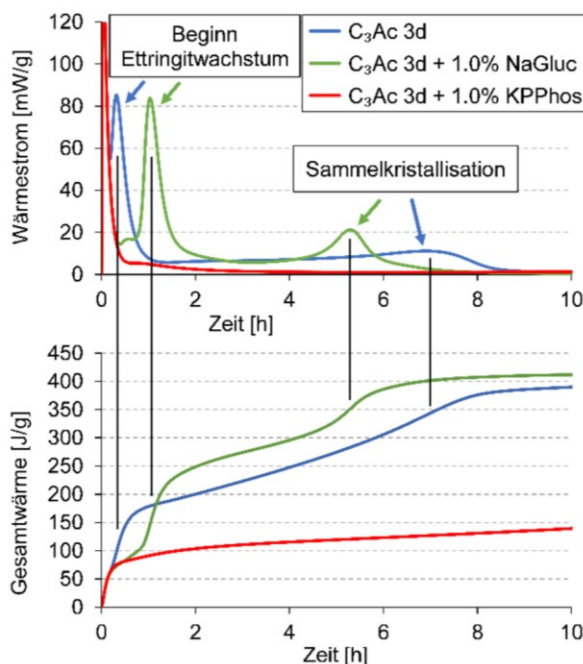


Abbildung 9: Wärmefreisetzung einer 3 Tage gealterten C<sub>3</sub>A / Gips Mischung (w/c = 1.0) mit Verzögererzusatz.

Ein direkter Vergleich zwischen Zement und C<sub>3</sub>A hinsichtlich der Wirkung der Verzögerer gestaltete sich schwierig, da die Dosierungen in der reinen Klinkerphase stark erhöht werden müssen, um eine sichtbare verzögernde Wirkung zu erzielen. Es konnten jedoch wichtige Erkenntnisse über die Wechselwirkung zwischen den Verzögerern und der Aluminatphase gewonnen werden. Wie im Zement beobachtet, wird in der Hydratation der Beginn des Wachsens der während der Alterung von C<sub>3</sub>A gebildeten Ettringitnadeln durch NaGluc verzögert (Abbildung 9). Die Wachstumsphase wiederum wird durch eine Ettringit-Sammelkristallisation aus der Porenlösung abgeschlossen, nachdem die Edukte C<sub>3</sub>A und Gips vollständig aufgelöst wurden. Diese Sammelkristallisation erfolgt nach Zusatz von

NaGluc jedoch früher als bei der unverzögerten Hydratation. Die Adsorption von NaGluc schwächt, wie erhofft, die Bildung der Ettringitschicht um die gealterten C<sub>3</sub>A-Partikel, wodurch diese schneller gelöst und die Hydratation früher abgeschlossen wird.

Vergleichend zu den C<sub>3</sub>A-Modifikationen wurde die Hydratation der Silikatphase mit dem größten Anteil im Portlandzement, Alit (monoklines C<sub>3</sub>S), betrachtet. Vor der Alterung wurde bei gleicher Dosierung eine viel stärkere verzögernde Wirkung von NaGluc auf reines C<sub>3</sub>S als auf CEM I 52.5 N beobachtet, die Hydrationsreaktion wird praktisch unterdrückt (Abbildung 10). Zum selben Ergebnis kam Milestone [18], der diesen Effekt mit einer Blockierung der aktiven Kristallisationszentren an der Partikeloberfläche begründete. Dagegen sind in gealtertem Alit die Wirkungen der beiden Verzögerer vergleichbar.

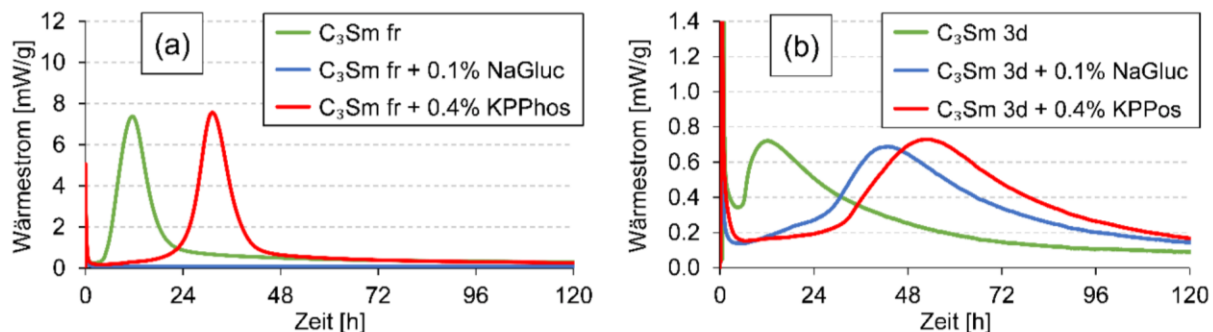


Abbildung 10: Wärmefreisetzung von frischem (a) und 3 Tage gealtertem (b)  $\text{C}_3\text{Sm}$  ( $w/c = 0.55$ ) mit Verzögererzusatz.

### 2.2.4. Alterung des ternären Bindemittelgemisches OPC / CAC / AH

Im vierten Projektschritt wurden die Alterungsuntersuchungen auf ein ternäres Bindemittelsystem (TBS) bestehend aus Portlandzement (OPC), Calciumaluminatzement (CAC) und Anhydrit (AH) erweitert.

Es konnte festgestellt werden, dass das ternäre System als Ganzes deutlich schneller altert als seine einzelnen Komponenten alleine (Abbildung 11). Wie aus dem ersten Projektabschnitt bekannt, produziert OPC bei  $35^\circ\text{C} / 90\% \text{RH}$  Ettringitnadeln auf der Partikeloberfläche, für reinen CAC oder AH konnte unter diesen Bedingungen jedoch keine Bildung von Alterungsprodukten nachgewiesen werden. Dagegen kristallisiert bei der Alterung des kompletten TBS deutlich mehr Ettringit als in reinem OPC, was bedeutet, dass die gemeinsame Alterung von CAC und AH zu quantitativer Ettringitbildung führt. Damit entsteht nicht nur aus der  $\text{C}_3\text{A}$ -Phase des OPC in Gegenwart einer Sulfatquelle Ettringit, sondern auch aus der CA- und  $\text{CA}_2$ -Phase des CAC.

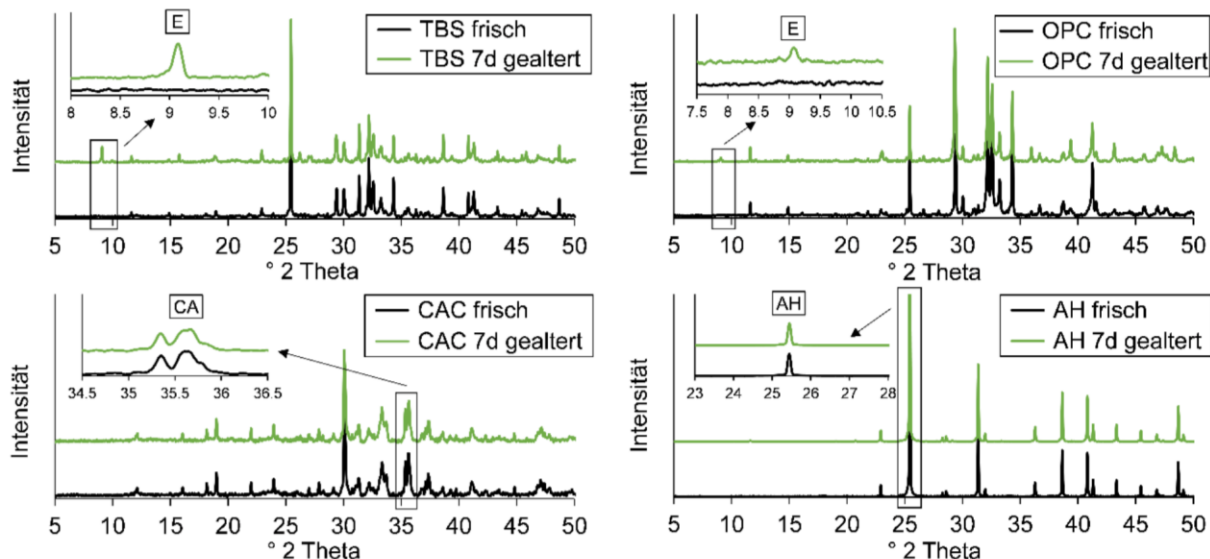


Abbildung 11: Pulver-XRD-Diffraktogramme des ternären Bindemittelsystems (TBS) und seinen Einzelkomponenten, vor der Exposition sowie nach 7 Tagen Alterung bei  $35^\circ\text{C} / 90\% \text{RH}$ . E = Ettringit, OPC = Portlandzement, CAC = Calciumaluminatzement, AH = Anhydrit.

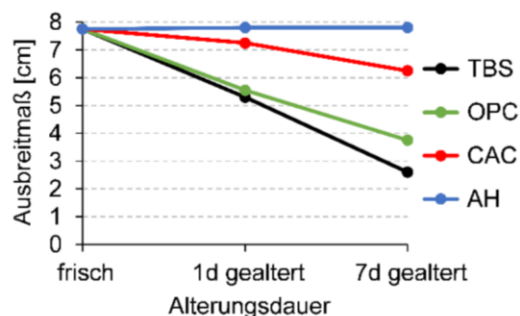


Abbildung 12: Fließmaße des ternären Bindemittelsystems nach Alterung verschiedener Komponenten.

Die Unterschiede im Alterungsverhalten zwischen dem kompletten System und seinen einzelnen Komponenten übertragen sich direkt auf das Fließverhalten und die Druckfestigkeitsentwicklung des TBS. Die Alterung wirkt sich ausschließlich negativ auf diese Eigenschaften aus, dabei ist der Effekt umso stärker, je höher die Reaktivität der gealterten Komponente gegenüber atmosphärischer Feuchte und CO<sub>2</sub> ist. Das bedeutet, dass Fließverhalten und Druckfestigkeiten des TBS am stärksten durch Alterung des kompletten Systems oder der OPC-Komponente beeinträchtigt werden (Abbildungen 12, 13). Ist dagegen nur CAC oder AH gealtert, sind die negativen Auswirkungen auf das TBS weniger gravierend.

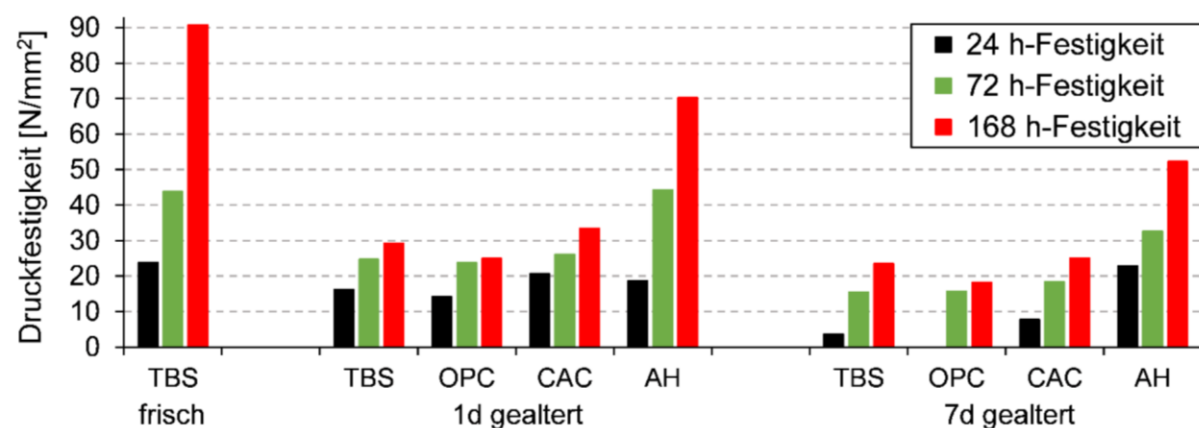


Abbildung 13: Druckfestigkeitsentwicklung des ternären Bindemittelsystems nach Alterung verschiedener Komponenten.

### 2.2.5. Alterung einer Selbstverlaufsmasse als Beispiel für Trockenmörtelformulierungen

Im finalen Schritt des Projekts wurde der Einfluss der Präsenz von Zusatzmitteln auf das Alterungsverhalten des TBS untersucht. Dieser Fall trifft auf, wenn fertige Trockenmörtelformulierungen wie Selbstverlaufsmassen (SLUs) in Kontakt mit atmosphärischer Feuchte und CO<sub>2</sub> kommen.

Dazu wurde eine Modell-SLU-Formulierung aus dem im vorangehenden Projektabschnitt betrachteten TBS und Lithiumcarbonat (Beschleuniger), Kaliumnatriumtartrat (Verzögerer) sowie Polycarboxylatether (PCE, Fließmittel) entwickelt. Die Zusatzmittel wurden entweder einzeln oder zusammen mit dem TBS gealtert. Im ersten Fall wurden die nicht mitgealterten Zusatzmittel anschließend zugemischt.

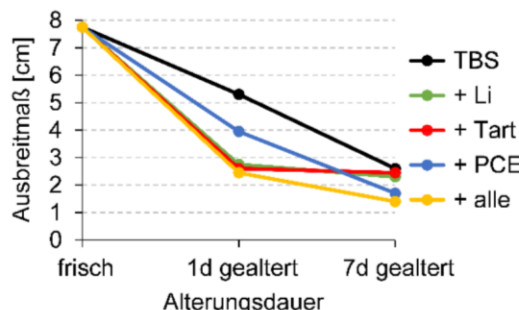


Abbildung 14: Fließmaße der Modell-SLU-Formulierung nach Alterung des TBS mit verschiedenen Zusatzmitteln.

Lithiumcarbonat erhöhte die Wasseraufnahme des TBS während der Alterung am stärksten, Grund dafür ist die Förderung der Hydratbildung, die seiner beschleunigenden Wirkung zugrunde liegt. PCE weist unter den betrachteten Zusatzmitteln das geringste Reaktionspotential gegenüber  $H_2O$  und  $CO_2$  auf. Interessanterweise führt daher eine kurze Alterung des TBS mit Lithium oder Tartrat für 1 Tag zu einer größeren Beeinträchtigung des Fließverhaltens als eine Alterung mit dem designierten Fließmittel (Abbildung 14).

Dagegen reduziert nach 7 Tagen Exposition das Mitaltern des Fließmittels das Ausbreitmaß am stärksten. Grund dafür ist der graduelle Überwuchs von Fließmittelpartikeln durch Alterungsprodukte, wie wir in einer vorangehenden Studie [11] berichten konnten.

Beschleuniger und Verzögerer verlieren durch die Alterung ihre Wirkung während der Hydratation nahezu vollständig. Modellformulierungen mit gealtertem Lithium (Abbildung 15, oben rechts) binden verspätet, mit gealtertem Tartrat (Abbildung 15, unten links) beschleunigt ab. Wie beim Fließverhalten ist auch bei der Hydratation der Einfluss des Fließmittels stark von der Alterungsdauer abhängig: Nach 7 Tagen Alterung entwickelt das PCE eine starke verzögernde Wirkung (Abbildung 15, unten rechts). Durch den Überwuchs der Fließmittelpartikel während der Alterung werden diese während der Hydratation verspätet freigesetzt, wodurch die Adsorption auf der Bindemitteloberfläche und dadurch die Fließwirkung zeitlich versetzt werden. Dieser Prozess ist mit einer nachträglichen Zugabe des PCE während der Hydratation vergleichbar. Dadurch wird die Auflösung der Zementpartikel und somit das Abbinden verzögert. Das mit allen Zusatzmitteln gealterte TBS entspricht in etwa der Addition der Alterungsverhalten der einzelnen Zusatzmittel. Nach 1 Tag Exposition wurde ein beschleunigtes Abbinden und nach 7 Tagen ein verzögertes Abbinden beobachtet (Abbildung 15, oben links).

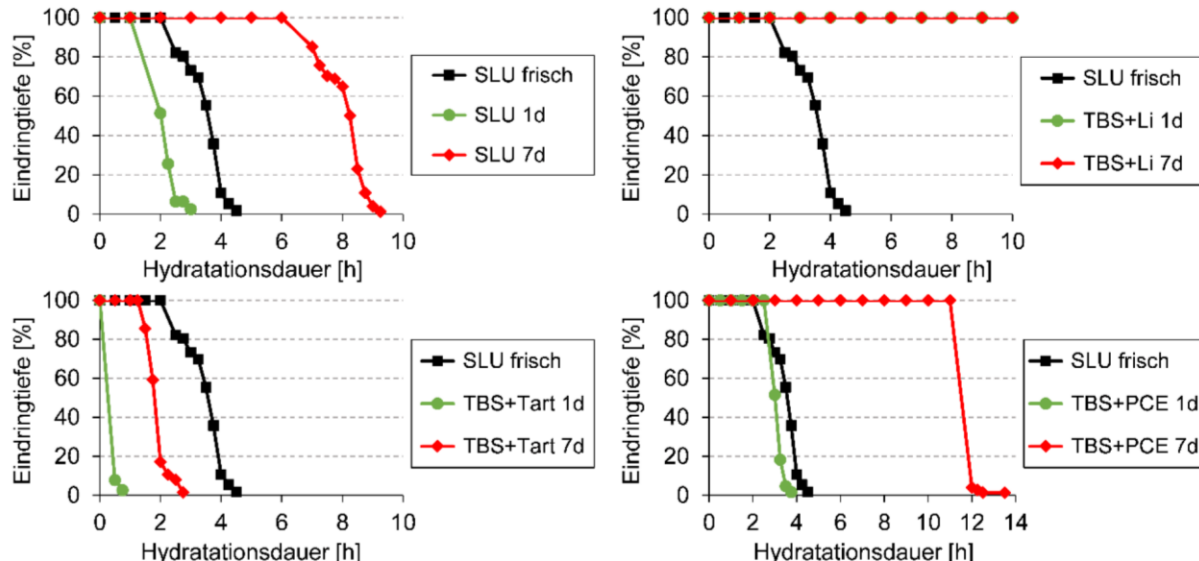


Abbildung 15: Abbindeverhalten der Modell-SLU-Formulierung vor und nach der Alterung im Vergleich mit der Alterung des TBS mit einzelnen Zusatzmitteln ( $w/f = 0.50$ ).

Vergleichbare Trends konnten auch in der Festigkeitsentwicklung beobachtet werden. Modellformulierungen mit gealtertem Lithium sowie frischem Tartrat und PCE weisen die größten beobachteten Einbußen auf (Abbildung 16). Wurde das TBS mit allen Zusatzmitteln gealtert, ist die verzögernde Wirkung von Tartrat und PCE ebenfalls herabgesetzt, wodurch wieder etwas höhere Frühfestigkeiten erreicht werden.

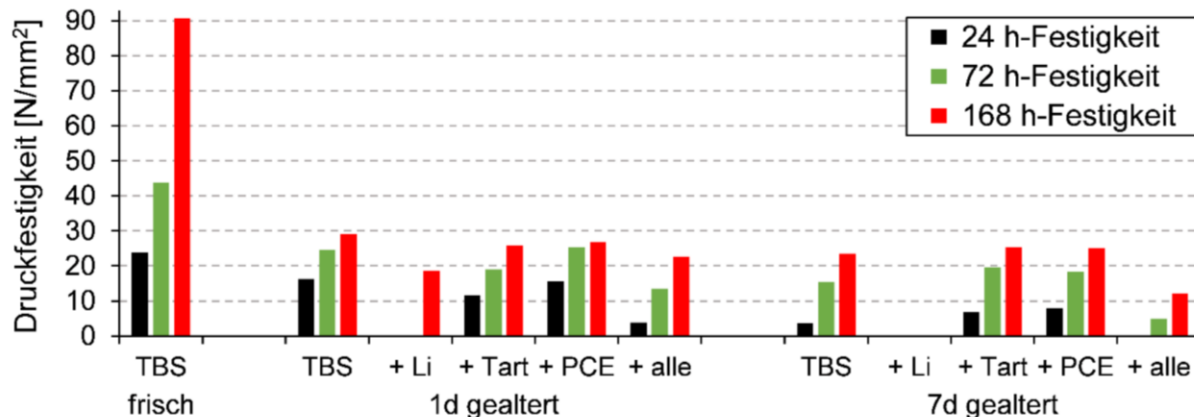


Abbildung 16: Einfluss der Alterung des TBS mit Zusatzmitteln auf die Druckfestigkeitsentwicklung der Modell-SLU-Formulierung.

### 3. Zusammenfassung

Im Rahmen dieses Forschungsprojektes zum Einfluss der Alterung auf die Hydratation zementärer Bindemittel in Gegenwart von Zusatzmitteln entstanden insgesamt 3 Publikationen in peer review Journals sowie 3 weitere Tagungsbeiträge. Das Verständnis der Alterung von Portlandzement konnte vertieft und auf die Klinkerphasen erweitert werden. Die Reaktion der Aluminatphasen mit atmosphärischer Feuchte in Gegenwart von sulfathaltigen Abbindereglern resultiert in der Bildung von nanoskaligen Ettringitkristalliten auf der Zementpartikeloberfläche. Diese agieren als Nukleationskeime für die Ettringitkristallisation während der Hydratation von gealtertem Zement, wodurch dieser deutlich schneller abbindet als frischer Zement. Die Ettringitkristallite werden bei längerer Exposition durch atmosphärisches CO<sub>2</sub> zersetzt, die Geschwindigkeit der Carbonatisierung ist abhängig von der Kristallmodifikation der Aluminatphase.

Dem beschleunigten Abbinden von gealtertem Zement kann durch Zugabe von Verzögerern während der Hydratation entgegengewirkt werden. Mit zunehmender Alterungsdauer erhöht sich dabei die Wirkung der Verzögerer bei gleichbleibender Dosis. Grund dafür sind eine bei gealtertem im Vergleich zu frischem Zement verlangsamte Adsorption der Verzögerer und dem Inlösungen gehen von Calcium.

Die beschleunigte Ettringitkristallisation in gealtertem Zement führt zur Ausbildung einer ausgeprägten Ettringitschicht um die Zementpartikel, die weiterem Wasserzutritt entgegensteht. Dadurch wird die Hydratation von gealtertem Zement und somit dessen Festigkeitsentwicklung erheblich verlangsamt. Nach Verzögererzugabe zu gealterter Aluminatphase konnte eine erhöhte Geschwindigkeit bei der Auflösung der Partikel und der Hydratbildung beobachtet werden.

Die Alterungsuntersuchungen wurden von reinem Portlandzement auf das ternäre Bindemittelsystem (OPC / CAC / AH) erweitert. Dabei konnte eine vergleichbare Ettringitbildung durch die CA- und CA<sub>2</sub>-

## 5.2 OFFICIAL PROJECT REPORT

---

Phasen des Aluminatzements in Anwesenheit einer Sulfatquelle beobachtet werden wie zuvor durch die Aluminatphasen des Portlandzements. Eine individuelle Alterung von Aluminatzement und Anhydrit führte in keinem Fall zur Bildung von Alterungsprodukten.

Abschließend wurde der Einfluss von Zusatzmitteln auf die Alterung des ternären Bindemittelsystems untersucht. Dabei konnte eine starke Erhöhung der Aufnahme von atmosphärischer Feuchte durch den Beschleuniger Lithiumcarbonat beobachtet werden. Das PCE-Fließmittel wird von Alterungsprodukten überwachsen, wodurch das Ausbreitmaß einer Formulierung des ternären Systems und PCE mit zunehmender Alterungsdauer stärker reduziert wird. Während der Hydratation wird das Fließmittel jedoch mit der Zeit wieder freigesetzt, wodurch eine zeitlich versetzte Wirkung und damit auch eine Verzögerung des Abbindens verursacht wird.

Die in diesem Projekt erarbeiteten Resultate zeigen, dass die Zementalterung ein vielschichtiges Phänomen darstellt. Das Alterungsverhalten einzelner Komponenten unterscheidet sich mitunter signifikant. Die Alterung des Gesamtsystems kann zum Teil aus der Summe seiner einzelnen Bestandteile abgeleitet werden, so wie es bei den Zusatzmitteln für Trockenmörtelformulierungen auftrat. Auf der anderen Seite kann in einem System die Kombination auch wenig reaktiver Komponenten auch zu einer deutlich stärkeren Alterung führen, wie die Untersuchung des ternären Bindemittelsystems zeigt. Für den Anwender kann die gleichbleibende Leistung eines zementären Bindemittels nur durch die sorgfältige Handhabe unter Ausschluss von Feuchte und CO<sub>2</sub> von der Herstellung bis zum Einsatz garantiert werden.

#### 4. Literaturverzeichnis

- [1] Tzouvalas, G.; Rantis, G.; Tsimas, S.: "Alternative calcium-sulfate-bearing materials as cement retarders: Part II. FGD gypsum." *Cem. Concr. Res.* 34 **2004**, pp. 2119-2125.  
<https://doi.org/10.1016/j.cemconres.2004.03.021>
- [2] Singh, N. B.; Middendorf, B.: "Calcium sulphate hemihydrate hydration leading to gypsum crystallization." *Prog. Cryst. Growth Charact. Mater.* 53 **2007**, pp. 57-77  
<https://doi.org/10.1016/j.pcrysgrow.2007.01.002>
- [3] Jensen, O. M.; Hansen, P.; Lachowski, E. E.; Glasser, F.P.: "Clinker mineral hydration at reduced relative humidities." *Cem. Concr. Res.* 29 **1999**, pp. 1505-1512.  
[https://doi.org/10.1016/S0008-8846\(99\)00132-5](https://doi.org/10.1016/S0008-8846(99)00132-5)
- [4] Deng, C. S.; Breen, C.; Yarwood, J.; Habesch, S.; Phipps, J.; Craster, B.; Maitland, G.: "Ageing of oilfield cement at high humidity: a combined FEG-ESEM and Raman microscopic investigation." *J. Mater. Chem.* 12 **2002**, pp. 3105-3112.  
<https://doi.org/10.1039/B203127M>
- [5] Barbic, L.; Tinta, V.; Lozar, B.; Marincovic, V.: "Effect of storage time on the rheological behavior of oil well slurries." *J. Am. Ceram. Soc.* 74 **1991**, pp. 954-949.  
<https://doi.org/10.1111/j.1151-2916.1991.tb04326.x>
- [6] Whittaker, M.; Dubina, E.; Al-Mutawa, F.; Arkless, L.; Plank, J.; Black, L.: "The effect of prehydration on the engineering properties of CEM I Portland cement." *Adv. Cem. Res.* 25 **2013**, pp. 12-20.  
<https://doi.org/10.1680/adcr.12.00030>
- [7] Dubina, E.; Plank, J.: "Influence of moisture- and CO<sub>2</sub>-induced aging in cement on the performance of admixtures used in construction chemistry." *ZKG Int.* 65 **2012**, pp. 60-68.
- [8] Maltese, C.; Pistolesi, C.; Bravo, A.; Cella, F.; Cerulli, T.; Salvione, D.: "A case history: Effect of moisture on the setting behavior of a Portland cement reacting with an alkali-free accelerator." *Cem. Concr. Res.* 37 **2007**, pp. 856-865.  
<https://doi.org/10.1016/j.cemconres.2007.02.020>
- [9] Winnefeld, F.: "Influence of cement aging and addition time on the performance of superplasticizers." *ZKG Int.* 61 **2008**, pp. 68-77.
- [10] Dubina, E.; Wadsö, L.; Plank, J.: "A sorption balance study of water vapor sorption on anhydrous cement minerals and cement constituents." *Cem. Concr. Res.* 41 **2011**, pp. 1196-1204.  
<https://doi.org/10.1016/j.cemconres.2011.07.009>
- [11] Meier, M. R.; Napharatsamee, T.; Plank, J.: "Dispersing performance of superplasticizers admixed to aged cement." *Constr. Build. Mater.* 139 **2017**, pp. 232-240.  
<https://doi.org/10.1016/j.conbuildmat.2016.12.126>

## 5.2 OFFICIAL PROJECT REPORT

---

- [12] Winter, C.; Plank, J.: “*The European dry-mix mortar industry (Part 1).*” ZKG Int. 60 **2007**, pp. 62-69.
- [13] Amathieu, L.; Bier, T. A.; Scrivener, K. L.: “*Mechanisms of set acceleration of Portland cement through CAC addition.*”, International Conference on Aluminate Cement (CAC), Edinburgh (United Kingdom), July 16-19 **2001**, Proceedings, pp. 303-317.
- [14] Zurbriggen, R.; Goetz-Neunhoeffer, F.: “*Mechanism and resulting damages of prolonged retardation in aged dry mixes: A case study of mixed-binders containing tartaric acid.*” GDCh-Monographie 37, Tagung Bauchemie **2007**, pp. 111–118.
- [15] Theisen, K.; Johansen, V.: “*Prehydration and strength development of Portland cement.*” J. Am. Ceram. Soc. Bull. 54 **1975**, pp. 787-791.
- [16] Sprung, S.: “*Effect of storage conditions on the properties of cement.*” ZKG Int. 31 **1978**, pp. 305-309.
- [17] Plank, J.; Zhang-Preße, M.; Ivleva, N. P.; Niessner, R.: “*Stability of single phase C<sub>3</sub>A hydrates against pressurized CO<sub>2</sub>.*” Const. Build. Mater. 122 **2016**, pp. 426-434.  
<https://doi.org/10.1016/j.conbuildmat.2016.06.042>
- [18] Milestone, N. B.: “*Hydration of tricalcium silicate in the presence of lignosulfonates, glucose and sodium gluconate.*” J. Am. Ceram. Soc. 62 **1979**, pp. 321-324.  
<https://doi.org/10.1111/j.1151-2916.1979.tb19068.x>

## 6 References

- [1] Trout, E.A.R. The history of calcareous cements. In: *Lea's chemistry of cement and concrete*. Hewlett, P.C., Liska, M., Eds.; Elsevier, **2019**; pp. 1–29.
- [2] Newman, J.B. The evolution of cement and concrete. In: *ICT Yearbook 2012-2013*. Mangabhai, R., Hewlett, P.C., Taylor, G., Domone, P., Trout, E., Berrie, I., Killoran, D., Eds.; The Concrete Society: Blackwater, **2012**; p. 60.
- [3] Halstead, P.E. The early history of Portland cement. *Transactions of the Newcomen Society*, **1961**, 34, 37–54.
- [4] Stanley, C.C. *Highlights in the history of concrete*. Cement and Concrete Association: Slough, **1979**.
- [5] Davis, A.C. *A hundred years of Portland cement, 1824-1924*; Concrete Publications: London, **1924**.
- [6] Spackman, C. Some writers on lime and cement: from Cato to the present time; W. Heffer & Sons Ltd: Cambridge, **1929**.
- [7] Aspdin, J. An improvement in the mode of producing an artificial stone. BP 5022, **1824**.
- [8] Blezard, R.G. Technical aspects of Victorian cement. *Chemistry & Industry*, **1981**, 18, 630–636.
- [9] Blezard, R.G. The history of calcareous cements. In: *Lea's chemistry of cement and concrete*. 4<sup>th</sup> edition. Hewlett, P.C., Ed.; Elsevier: London, **1998**; p. 3.
- [10] Blezard, R.G. Reflections on the history of the chemistry of cement: London (United Kingdom), **2000**.
- [11] Halliday, S. The great stink of London: Sir Joseph Bazalgette and the cleansing of the Victorian capital; The History Press: Stroud, **2011**.
- [12] Redgrave, G.R. *Calcareous cements: Their nature and uses*; Charles Griffin & Co Ltd: London, **1895**.
- [13] Skempton, A.W. Portland cements, 1843-1887. *Transactions of the Newcomen Society*, **1962**, 35, 117–152.
- [14] Livesey, P. The rise, fall and revival of natural cements in the developing pattern of binders. In: *ICT Yearbook 2013-2014*. Mangabhai, R., Hewlett, P.C., Domone, P., Taylor, G., Trout, E., Killoran, D., Berrie, I., Eds.; The Concrete Society: Blackwater, **2013**; p. 86.
- [15] Peray, K.E. *The rotary cement kiln*, 2<sup>nd</sup> ed.; Chemical Pub. Co: New York, **1986**.
- [16] *Technology roadmap: Low-carbon technology for the Indian cement industry*; International Energy Agency: Paris, France, **2013**.
- [17] Lea, F.M. Cement and building from Roman times to the twentieth century: A public lecture delivered at the University of Leeds on 6 May 1974: London, **1974**.

## 6 REFERENCES

---

- [18] Jackson, P.J. *Cement manufacture by UK companies 1914-1994*; privately published: Rugby, **1999**.
- [19] Richard C. Mielenz. History of chemical admixtures for concrete. *Concrete International*, **1984**, 6, 40–53.
- [20] Mindess, S.; Young, J.F.; Darwin, D. *Concrete*, 2<sup>nd</sup> ed.; Prentice Hall: Upper Saddle River, N.J., **2003**.
- [21] Garrison, E. A history of engineering and technology artful methods, 2<sup>nd</sup> ed.; CRC: Boca Raton, **1999**.
- [22] Jackson, F.H. An introduction and questions to which answers are thought. In: *Concretes containing Air-Entraining Agents - A Symposium, Proceedings of the American Concrete Institute*: Detroit, **1944**, Vol. 40; pp. 509–515.
- [23] Tucker, G.R. Concrete and hydraulic cement. US Patent 2141569A, **1938**.
- [24] Aïtcin, P.-C. Retarders. In: *Science and technology of concrete admixtures*. Aïtcin, P.-C., Flatt, R.J., Eds.; Woodhead Publishing / Elsevier, **2016**; pp. 395–404.
- [25] Harrison, A.M. The importance of raw materials. *International Cement Review*, **2014**, 46.
- [26] Bogue, R.H. *La Chimie du ciment Portland*; Eyrolles: Paris, **1952**.
- [27] Moranville-Regourd, M., Boikova A. I. Chemistry, structure, properties and quality of clinker. In: *Proceedings of the 9<sup>th</sup> International Congress on the Chemistry of Cement*: New Delhi, **1992**; Vol. 1; pp. 23–45.
- [28] Dunstetter, F.; Noirlontaine, M.-N. de; Courtial, M. Polymorphism of tricalcium silicate, the major compound of Portland cement clinker. *Cement and Concrete Research*, **2006**, 36, 39–53.
- [29] Maki, I. Relationship of processing parameters to clinker properties; influence of minor components. In: *Proceedings of the 8<sup>th</sup> International Congress on the Chemistry of Cement*: Rio de Janeiro, **1986**; Vol. 1; pp. 34–47.
- [30] Hahn, T.; Eysel, W.; Brenner, P.; Woerman, E. Modification of Ca<sub>3</sub>SiO<sub>5</sub>. In: *Proceedings of the 5<sup>th</sup> International Congress on the Chemistry of Cement*: Tokyo, **1968**; Vol. 1; pp. 38–39.
- [31] Takeuchi, Y.; Nishi, F. Crystal-chemical characterization of the 3CaO·Al<sub>2</sub>O<sub>3</sub>—Na<sub>2</sub>O solid-solution series. *Zeitschrift für Kristallographie - Crystalline Materials*, **1980**, 152.
- [32] Herfort, D.; MacPhee, D.E. Components in Portland cement clinker and their phase relationships. In: *Lea's chemistry of cement and concrete*. Hewlett, P.C., Liska, M., Eds.; Elsevier, **2019**; pp. 57–86.
- [33] Bredig, M.A. Polymorphism of calcium orthosilicate. *Journal of the American Ceramic Society*, **1950**, 33, 188–192.

## 6 REFERENCES

---

- [34] Niesel, K.; Thorman, P. Die Stabilitätsbereiche der Modifikationen des Dicalciumsilikats: The stability ranges of the modifications of dicalcium silicate. *Tonindustrie-Zeitung*, **1967**, *91*, 362–369.
- [35] Regourd, M. Cristallisation et réactivité de l'aluminate tricalcique dans les ciments portland. // *Cemento*, **1978**, *3*, 323–336.
- [36] Moranville-Regourd, M., Boikova, A.I. Chemistry, structure, properties and quality of clinker. In: *Proceedings of the 9<sup>th</sup> International Congress on the Chemistry of Cement*: New Delhi, **1992**; Vol. 1; pp. 407–414.
- [37] Richardson, I.; Taylor, H.F.W. *Cement Chemistry*, 3<sup>rd</sup> ed.; Ice Publishing: London, **2018**.
- [38] Wesselsky, A.; Jensen, O.M. Synthesis of pure Portland cement phases. *Cement and Concrete Research*, **2009**, *39*, 973–980.
- [39] Mondal, P.; Jeffery, J.W. The crystal structure of tricalcium aluminate,  $\text{Ca}_3\text{Al}_2\text{O}_6$ . *Acta Crystallographica Section B: Structural Crystallography and Crystal Chemistry*, **1975**, *31*, 689–697.
- [40] Takeuchi, Y.; Nishi, F.; Maki I. Structural aspects of the  $\text{C}_3\text{A}-\text{Na}_2\text{O}$  solid solutions. In: *Proceedings of the 7<sup>th</sup> International Congress on the Chemistry of Cement*: Paris, **1980**; Vol. 4; pp. 426–431.
- [41] Nishi, F.; Takeuchi, Y. The  $\text{Al}_6\text{O}_{18}$  rings of tetrahedra in the structure of  $\text{Ca}_{8.5}\text{NaAl}_6\text{O}_{18}$ . *Acta Crystallographica Section B: Structural Crystallography and Crystal Chemistry*, **1975**, *31*, 1169–1173.
- [42] Aggarwal, P.S.; Gard, J.A.; Glasser, F.P.; Biggar, G.M. Synthesis and properties of dicalcium aluminate,  $2\text{CaO}\cdot\text{Al}_2\text{O}_3$ . *Cement and Concrete Research*, **1972**, *2*, 291–297.
- [43] Harrisson, A.M. Constitution and specification of Portland cement. In: *Lea's chemistry of cement and concrete*. Hewlett, P.C., Liska, M., Eds.; Elsevier, **2019**; pp. 87–155.
- [44] Moore, A.E. The sequence of compound formation in Portland cement rotary kilns. *Cement Technology*, **1976**, *7*, 85–91.
- [45] Aïtcin, P.-C. Binders for Durable and Sustainable Concrete; CRC Press, **2007**.
- [46] Aïtcin, P.-C. Portland cement. In: *Science and technology of concrete admixtures*. Aïtcin, P.-C., Flatt, R.J., Eds.; Woodhead Publishing / Elsevier, **2016**; pp. 27–52.
- [47] Strother, P. de. Manufacture of Portland cement. In: *Lea's chemistry of cement and concrete*. Hewlett, P.C., Liska, M., Eds.; Elsevier, **2019**; pp. 31–56.
- [48] Mould, A.E.; Williams, D.W. The effects of high ambient temperatures on gypsum plasters. *Building Science*, **1974**, *9*, 243–245.
- [49] Bied, J. British patent 8193, **1909**.

## 6 REFERENCES

---

- [50] Houghton, S.J.; Scrivener, K.L. A microstructural study of a 60 year old calcium aluminate cement concrete. In: *Proceedings of the 3<sup>rd</sup> CANMET / ACI International Conference on the Durability of Concrete*: Nice, **1994**; pp. 133–146.
- [51] Dunster, A.M.; Crammond, N.J.; Pettifer, K.; Rayment, D.L. An assessment of ageing calcium aluminate concrete from marine structures. In: *Mechanisms of chemical degradation of cement-based systems*. Scrivener, K.L., Young, J.F., Eds.; E & FN Spon: London, **1997**.
- [52] Scrivener, K.L.; Lewis, M.C.; Houghton, S.J. Microstructural investigation of calcium aluminate cement concrete form structures. In: *Proceedings of the 10<sup>th</sup> International Congress on the Chemistry of Cement*: Gothenburg, **1997**.
- [53] Ideker, J.H.; Scrivener, K.L.; Fryda, H.; Touzo, B. Calcium aluminate cements. In: *Lea's chemistry of cement and concrete*. Hewlett, P.C., Liska, M., Eds.; Elsevier, **2019**; pp. 537–584.
- [54] Ushiro, M.; Higuchi, T.; Arano, N.; Morioka, M. Carbonation of quick-hardening cement containing  $\gamma$ -C<sub>2</sub>S. *Cement Science and Concrete Technology*, **2016**, *70*, 209–214.
- [55] Kosmatka, S.H. In defense of the water-cement ratio. *Concrete International*, **1991**, *13*, 65–69.
- [56] Feret, R. Sur la compacité des mortiers hydrauliques. *Annales des Ponts et Chaussées*, **1892**, *4*, 5–164.
- [57] Abrams, D.A. *Design of concrete mixtures. Bulletin No. 1*; Lewis Institute: Chicago, IL, **1918**.
- [58] Bentz, D.P.; Aïtcin, P.-C. The hidden meaning of the water-cement ratio. *Concrete International*, **2018**, *30*, 51–54.
- [59] Granju, J.L.; Maso, J.C. Hardened portland cement pastes, modelisation of the micro-structure and evolution laws of mechanical properties II- compressive strength law. *Cement and Concrete Research*, **1984**, *14*, 303–310.
- [60] Granju, J.L.; Grandet, J. Relation between the hydration state and the compressive strength of hardened Portland cement pastes. *Cement and Concrete Research*, **1989**, *19*, 579–585.
- [61] Richardson, I.G. Tobermorite/jennite- and tobermorite/calcium hydroxide-based models for the structure of C-S-H: applicability to hardened pastes of tricalcium silicate,  $\beta$ -dicalcium silicate, Portland cement, and blends of Portland cement with blast-furnace slag, metakaolin, or silica fume. *Cement and Concrete Research*, **2004**, *34*, 1733–1777.
- [62] Aïtcin, P.-C. The importance of the water-cement and water-binder ratios. In: *Science and technology of concrete admixtures*. Aïtcin, P.-C., Flatt, R.J., Eds.; Woodhead Publishing / Elsevier, **2016**; pp. 3–13.
- [63] Aïtcin, P.-C. The influence of the water/cement ratio on the sustainability of concrete. In: *Lea's chemistry of cement and concrete*. Hewlett, P.C., Liska, M., Eds.; Elsevier, **2019**; pp. 807–826.
- [64] Powers, T.C. *The properties of fresh concrete*; Wiley: New York, **1968**.
- [65] Powers, T.C.; Brownyard, T. L. Studies of the physical properties of hardened portland cement paste. *ACI Journal Proceedings*, **1946**, *43*, 101–132.

## 6 REFERENCES

---

- [66] Aïtcin, P.-C. Phenomenology of cement hydration. In: *Science and technology of concrete admixtures*. Aïtcin, P.-C., Flatt, R.J., Eds.; Woodhead Publishing / Elsevier, **2016**; pp. 15–25.
- [67] Jensen, O.M.; Hansen, P.F. Water-entrained cement-based materials. *Cement and Concrete Research*, **2001**, *31*, 647–654.
- [68] Tang, F.J.; Glasser, F.P. Influence of sulphate source on Portland cement hydration. *Advances in Cement Research*, **1988**, *1*, 67–74.
- [69] Gartner, E.J., Young, J.F., Damidot, D.A., Jawed, I. Hydration of Portland cement. In: *Structure and Performance of Cements*. 2<sup>nd</sup> ed. Bensted, J., Barnes, P. (Eds.); CRC Press, **2001**.
- [70] Marchon, D., Flatt, R.J. Mechanisms of cement hydration. In: *Science and technology of concrete admixtures*. Aïtcin, P.-C., Flatt, R.J., Eds.; Woodhead Publishing / Elsevier, **2016**; pp. 129–146.
- [71] Damidot, D.; Nonat, A. In: *Hydration and setting of cements*. Nonat, A., Mutin, J.C., Eds., 2<sup>nd</sup> ed.; E&FN Spon: London, **1992**; p. 23.
- [72] Trettin, R.; Wiecker, W. Zur Hydratation von Trikalziumsilikat: I. Ursachen der Induktionsperiode. *Silikattechnik*, **1986**, *37*, 75–78.
- [73] Barret, P.; Ménétrier, D.; Bertrandie, D. Mechanism of C<sub>3</sub>S dissolution and problem of the congruency in the very initial period and later on. *Cement and Concrete Research*, **1983**, *13*, 728–738.
- [74] Grutzeck, M.W.; Ramachandran, A.R. An integration of tricalcium silicate hydration models in light of recent data. *Cement and Concrete Research*, **1987**, *17*, 164–170.
- [75] Tadros, M.E.; Skalny, J.A.N.; Kalyoncu, R.S. Early hydration of tricalcium silicate. *Journal of the American Ceramic Society*, **1976**, *59*, 344–347.
- [76] Young, J.F.; Tong, H.S.; Berger, R.L. Compositions of solutions in contact with hydrating tricalcium silicate pastes. *Journal of the American Ceramic Society*, **1977**, *60*, 193–198.
- [77] Skalny, J.; Young, J.F. In: *Proceedings of the 7th International Congress on the Chemistry of Cement*: Paris, **1980**; Vol. 2.
- [78] Locher, F.W.; Richartz, W.; Sprung, S. Erstarren von Zement. I: Reaktion und Gefügeentwicklung: Setting of cement. Part I: Reaction and development of structure. *Zement-Kalk-Gips*, **1976**, *29*, 435–442.
- [79] Chen, Y.; Odler, I. In: *Proceedings of the 9<sup>th</sup> International Congress on the Chemistry of Cement*: New Delhi, **1992**; Vol. 4; p. 24.
- [80] Taylor, H.F.W.; Barret, P.; Brown, P.W.; Double, D.D.; Frohnsdorff, G.; Johansen, V.; Menetrier-Sorrentino, D.; Odler, I.; Parrott, L.J.; Pommersheim, J.M.; Regourd, M.; Young, J.F. The hydration of tricalcium silicate. *Materiaux et Constructions*, **1984**, *17*, 457–468.
- [81] Brown, P.W.; Franz, E.; Frohnsdorff, G.; Taylor, H.F.W. Analyses of the aqueous phase during early C<sub>3</sub>S hydration. *Cement and Concrete Research*, **1984**, *14*, 257–262.

## 6 REFERENCES

---

- [82] Regourd, M.; Thomassin, J.H.; Baillif, P.; Touray, J.C. Study of the early hydration of  $\text{Ca}_3\text{SiO}_5$  by X-ray photoelectron spectrometry. *Cement and Concrete Research*, **1980**, *10*, 223–230.
- [83] Jennings, H.M. Aqueous solubility relationships for two types of calcium silicate hydrate. *Journal of the American Ceramic Society*, **1986**, *69*, 614–618.
- [84] Gartner, E.M.; Jennings, H.M. Thermodynamics of calcium silicate hydrates and their solutions. *Journal of the American Ceramic Society*, **1987**, *70*, 743–749.
- [85] Bellmann, F.; Damidot, D.; Möser, B.; Skibsted, J. Improved evidence for the existence of an intermediate phase during hydration of tricalcium silicate. *Cement and Concrete Research*, **2010**, *40*, 875–884.
- [86] Bellmann, F.; Sowoidnich, T.; Ludwig, H.-M.; Damidot, D. Analysis of the surface of tricalcium silicate during the induction period by X-ray photoelectron spectroscopy. *Cement and Concrete Research*, **2012**, *42*, 1189–1198.
- [87] Rodger, S.A.; Groves, G.W.; Clayden, N.J.; Dobson, C.M. Hydration of tricalcium silicate followed by  $^{29}\text{Si}$  NMR with cross-polarization. *Journal of the American Ceramic Society*, **1988**, *71*, 91–96.
- [88] Stein, H.N.; Stevels, J.M. Influence of silica on the hydration of  $3 \text{ CaO} \cdot \text{SiO}_2$ . *Journal of Applied Chemistry*, **1964**, *14*, 338–346.
- [89] Kantro, D.L.; Brunauer, S.; Weise, C.H. Development of surface in the hydration of calcium silicates. II. Extension of investigations to earlier and later stages of hydration. *Journal of Physical Chemistry*, **1962**, *66*, 1804–1809.
- [90] Dent Glasser, L.S. Osmotic pressure and the swelling of gels. *Cement and Concrete Research*, **1979**, *9*, 515–517.
- [91] Birchall, J.D.; Howard, A.J.; Double, D.D. Some general considerations of a membrane / osmosis model for portland cement hydration. *Cement and Concrete Research*, **1980**, *10*, 145–155.
- [92] Lasaga, A.C.; Luttge, A. Variation of crystal dissolution rate based on a dissolution stepwave model. *Science (New York, N.Y.)*, **2001**, *291*, 2400–2404.
- [93] Juillard, P.; Gallucci, E.; Flatt, R.; Scrivener, K. Dissolution theory applied to the induction period in alite hydration. *Cement and Concrete Research*, **2010**, *40*, 831–844.
- [94] Wu, Z.; Young, J.F. Formation of calcium hydroxide from aqueous suspensions of tricalcium silicate. *Journal of the American Ceramic Society*, **1984**, *67*, 48–51.
- [95] Odler, I.; Dörr, H. Early hydration of tricalcium silicate: II. The induction period. *Cement and Concrete Research*, **1979**, *9*, 277–284.
- [96] Sierra, R. In: *Proceedings of the 6th International Congress on the Chemistry of Cement*: Moscow, **1974**; Vol. 2; p. 138.
- [97] Barret, P.; Bertrandie, D. Fundamental hydration kinetic features of the major cement constituents :  $\text{Ca}_3\text{SiO}_5$  and  $\beta\text{Ca}_2\text{SiO}_4$ . *Journal de Chimie Physique*, **1986**, *83*, 765–775.

## 6 REFERENCES

---

- [98] Bullard, J.W.; Flatt, R.J. New insights into the effect of calcium hydroxide precipitation on the kinetics of tricalcium silicate hydration. *Journal of the American Ceramic Society*, **2010**, *93*, 1894–1903.
- [99] Beaudoin, J.; Odler, I. Hydration, setting and hardening of Portland cement. In: *Lea's chemistry of cement and concrete*. Hewlett, P.C., Liska, M., Eds.; Elsevier, **2019**; pp. 157–250.
- [100] Gartner, E.M., Gaidis, J.M. Hydration mechanisms I. In: *Materials Science of Concrete*, Skalny, J.P., Ed., The American Ceramic Society, **1989**, pp. 95–125.
- [101] Thomas, J.J.; Jennings, H.M.; Chen, J.J. Influence of nucleation seeding on the hydration mechanisms of tricalcium silicate and cement. *Journal of Physical Chemistry C*, **2009**, *113*, 4327–4334.
- [102] Alizadeh, R.; Raki, L.; Makar, J.M.; Beaudoin, J.J.; Moudrakovski, I. Hydration of tricalcium silicate in the presence of synthetic calcium–silicate–hydrate. *Journal of Materials Chemistry*, **2009**, *19*, 7937–7946.
- [103] Lippmaa, E.; Mägi, M.; Tarmak, M.; Wieker, W.; Grimmer, A.R. A high resolution  $^{29}\text{Si}$  NMR study of the hydration of tricalciumsilicate. *Cement and Concrete Research*, **1982**, *12*, 597–602.
- [104] Comotti, A.; Castaldi, G.; Gilioli, C.; Torri, G.; Sozzani, P. Step-by-step observation of the hydration of  $\text{C}_3\text{S}$  by magic-angle spinning  $^{29}\text{Si}$  nuclear magnetic resonance: The masking effect of  $\text{D}_2\text{O}$ . *Journal of Materials Science*, **1994**, *29*, 6427–6433.
- [105] Bonaccorsi, E.; Merlino, S.; Taylor, H. The crystal structure of jennite,  $\text{Ca}_9\text{Si}_6\text{O}_{18}(\text{OH})_6 \cdot 8\text{H}_2\text{O}$ . *Cement and Concrete Research*, **2004**, *34*, 1481–1488.
- [106] Bonaccorsi, E.; Merlino, S.; Kampf, A.R. The crystal structure of Tobermorite 14 Å (Plombierite), a C-S-H Phase. *Journal of the American Ceramic Society*, **2005**, *88*, 505–512.
- [107] Nonat, A. The structure and stoichiometry of C-S-H. *Cement and Concrete Research*, **2004**, *34*, 1521–1528.
- [108] Katz, A.; Bentur, A.; Kovler, K. A novel system for in-situ observations of early hydration reactions in wet conditions in conventional SEM. *Cement and Concrete Research*, **2007**, *37*, 32–37.
- [109] Garrault, S.; Nonat, A. Hydrated layer formation on tricalcium and dicalcium silicate surfaces: Experimental study and numerical simulations. *Langmuir*, **2001**, *17*, 8131–8138.
- [110] Garrault, S.; Finot, E.; Lesniewska, E.; Nonat, A. Study of C-S-H growth on  $\text{C}_3\text{S}$  surface during its early hydration. *Materials and Structures*, **2005**, *38*, 435–442.
- [111] Mohan, K.; Taylor, H.F.W. Analytical electron microscopy of cement pastes: IV. Beta-dicalcium silicate pastes. *Journal of the American Ceramic Society*, **1981**, *64*, 717–719.
- [112] Tong, Y.; Du, H.; Fei, L. Comparison between the hydration processes of tricalcium silicate and beta-dicalcium silicate. *Cement and Concrete Research*, **1991**, *21*, 509–514.
- [113] Boikova, A.I.; Grishchenko, L.V.; Domanski, A.I. In: *Proceedings of the 7<sup>th</sup> International Congress on the Chemistry of Cement*: Paris, **1980**; Vol. 4; pp. 460–464.

## 6 REFERENCES

---

- [114] Plowman, C.; Cabrera, J.G. Mechanism and kinetics of hydration of C<sub>3</sub>A and C<sub>4</sub>AF extracted from cement. *Cement and Concrete Research*, **1984**, *14*, 238–248.
- [115] Pommersheim, J.; Chang, J. Kinetics of hydration of tricalcium aluminate. *Cement and Concrete Research*, **1986**, *16*, 440–450.
- [116] Regourd, M. Crystallization and reactivity of tricalcium aluminate in Portland cements. *II Cemento*, **1978**, *75*, 323–336.
- [117] Schwiete, H.E.; Ludwig, U.; Jager, P. *Highway Research Board*; Special report #90, **1966**.
- [118] Tumidajski, P.J.; Thomson, M.L. Influence of cadmium on the hydration of C<sub>3</sub>A. *Cement and Concrete Research*, **1994**, *24*, 1359–1372.
- [119] Corstanje, W.A.; Stein, H.N.; Stevles, J.M. Hydration reactions in pastes C<sub>3</sub>S+C<sub>3</sub>A+CaSO<sub>4</sub>·2aq+H<sub>2</sub>O at 25°C.I. *Cement and Concrete Research*, **1973**, *3*, 791–806.
- [120] Breval, E. C<sub>3</sub>A hydration. *Cement and Concrete Research*, **1976**, *6*, 129–137.
- [121] Regourd, M.; Hornain, H.; Montureux, B. In: *Proceedings of the 7<sup>th</sup> International Congress on the Chemistry of Cement*: Paris, **1980**; Vol. 4; p. 437.
- [122] Collepardi, M.; Baldini, G.; Pauri, M.; Corradi, M. Tricalcium aluminate hydration in the presence of lime, gypsum or sodium sulfate. *Cement and Concrete Research*, **1978**, *8*, 571–580.
- [123] Pommersheim, J.; Chang, J. Kinetics of hydration of tricalcium aluminate in the presence of gypsum. *Cement and Concrete Research*, **1988**, *18*, 911–922.
- [124] Collepardi, M.; Baldini, G.; Pauri, M.; Corradi, M. Retardation of tricalcium aluminate hydration by calcium sulfate. *Journal of the American Ceramic Society*, **1979**, *62*, 33–35.
- [125] Odler, I.; Chen, Y. Effect of grinding in high pressure roller mill on properties of Portland cement. *Zement-Kalk-Gips*, **1990**, *43*, 188–191.
- [126] Odler, I.; Chen, Y. In: *Verfahrenstechnik der Zementherstellung: Proceedings of the congress on cement technology*; Bauverlag: Düsseldorf, **1993**; p. 78.
- [127] Locher, F.W.; Richartz, W.; Sprung, S. Erstarren von Zement. II: Einfluss des Calciumsulfatzusatzes: Setting of cement. Part II: Effect of adding calcium sulfate. *Zement-Kalk-Gips*, **1980**, *33*, 271–277.
- [128] Minard, H.; Garrault, S.; Regnaud, L.; Nonat, A. Mechanisms and parameters controlling the tricalcium aluminate reactivity in the presence of gypsum. *Cement and Concrete Research*, **2007**, *37*, 1418–1426.
- [129] Gaidis, J.M., Gartner, E.M. Hydration mechanism II. In: *Materials Science of Concrete*. Skalny, J., Mindess, S., Ed., **1989**; Vol. 2; pp. 9–39.
- [130] Brown, P.W.; Liberman, L.O.; Frohnsdorff, G. Kinetics of the early hydration of tricalcium aluminate in solutions containing calcium sulfate. *Journal of the American Ceramic Society*, **1984**, *67*, 793–795.

## 6 REFERENCES

---

- [131] Gupta, P.S., Chatterji, S., Jeffrey, W. Studies of the effect of different additives on the hydration reaction of tricalcium aluminate - Part 5: A mechanism of retardation of tricalcium aluminate hydration. *Cement Technology*, **1973**, 4, 146–149.
- [132] Skalny, J.A.; Tadros, M.E. Retardation of tricalcium aluminate hydration by sulfates. *Journal of the American Ceramic Society*, **1977**, 60, 174–175.
- [133] Feldman, R.F.; Ramachandran, V.S. Character of hydration of  $3\text{CaO}\cdot\text{Al}_2\text{O}_3$ . *Journal of the American Ceramic Society*, **1966**, 49, 268–273.
- [134] Manzano, H.; Dolado, J.S.; Ayuela, A. Structural, mechanical, and reactivity properties of tricalcium aluminate using first-principles calculations. *Journal of the American Ceramic Society*, **2009**, 92, 897–902.
- [135] Odler, I.; Wonnemann, R. Effect of alkalies on portland cement hydration: I. Alkali oxides incorporated into the crystalline lattice of clinker minerals. *Cement and Concrete Research*, **1983**, 13, 477–482.
- [136] Odler, I.; Wonnemann, R. Effect of alkalies on portland cement hydration: II. Alkalies present in form of sulphates. *Cement and Concrete Research*, **1983**, 13, 771–777.
- [137] Gartner, E.M.; Gaidis, J.M. In: *Materials Science of Concrete*. Skalny, J.P., Ed.: Westerville, OH, **1989**; Vol. 1; p. 95.
- [138] Odler, I.; Abdul-Maula, S. Reactivity of industrial clinkers. *Zement-Kalk-Gips*, **1984**, 37, 311–315.
- [139] Kuzel, H.-J.; Pöllmann, H. Hydration of  $\text{C}_3\text{A}$  in the presence of  $\text{Ca}(\text{OH})_2$ ,  $\text{CaSO}_4\cdot 2\text{H}_2\text{O}$  and  $\text{CaCO}_3$ . *Cement and Concrete Research*, **1991**, 21, 885–895.
- [140] Mehta, P.K. Morphology of calcium sulfoaluminate hydrates. *Journal of the American Ceramic Society*, **1969**, 52, 521–522.
- [141] Meredith, P.; Donald, A.M.; Meller, N.; Hall, C. Tricalcium aluminate hydration: Microstructural observations by in-situ electron microscopy. *Journal of Materials Science*, **2004**, 39, 997–1005.
- [142] Chatterji, S.; Jeffery, J.W. Studies of early stages of paste hydration of cement compounds, I. *Journal of the American Ceramic Society*, **1962**, 45, 536–543.
- [143] Negro, A.; Stafferi, L. Über die Hydratation der Calcium-Ferrite und Calciumaluminat-Ferrite: The hydration of calcium ferrites and calcium aluminoferrites. *Zement-Kalk-Gips*, **1979**, 32, 83–88.
- [144] Collepardi, M.; Monosi, S.; Moriconi, G.; Corradi, M. Tetracalcium aluminoferrite hydration in the presence of lime and gypsum. *Cement and Concrete Research*, **1979**, 9, 431–437.
- [145] Drabik, M.; Smrcok, L.; Stevula, L.; Kapralik, I. Study of brownmillerite prepared at 1200°C. II: Reactivity with water. *Silikáty*, **1987**, 31, 299–307.
- [146] Brown, P.W. Early hydration of tetracalcium aluminoferrite in gypsum and lime-gypsum solutions. *Journal of the American Ceramic Society*, **1987**, 70, 493–496.

## 6 REFERENCES

---

- [147] Ramachandran, V.S.; Beaudoin, J.J. In: *Proceedings of the 7<sup>th</sup> International Congress on the Chemistry of Cement*: Paris, **1980**; Vol. 2; pp. 11–25.
- [148] Liang, T.; Nanru, Y. Hydration products of calcium aluminoferrite in the presence of gypsum. *Cement and Concrete Research*, **1994**, *24*, 150–158.
- [149] Fukuhara, M.; Goto, S.; Asaga, K.; Daimon, M.; Kondo, R. Mechanisms and kinetics of C<sub>4</sub>AF hydration with gypsum. *Cement and Concrete Research*, **1981**, *11*, 407–414.
- [150] Odler, I.; Abdul-Maula, S. Investigations on the relationship between porosity structure and strength of hydrated portland cement pastes III. Effect of clinker composition and gypsum addition. *Cement and Concrete Research*, **1987**, *17*, 22–30.
- [151] Odler, I.; Abdul-Maula, S.; Zhongya, L. Effect of hydration temperature on cement paste structure. *MRS Proceedings*, **1986**, *85*.
- [152] P.C. Kreijger. Plasticizers and dispersing admixtures. In: *Admixtures. Proceedings of the International Congress on Admixtures, London, 16–17 April 1980*; Construction Press: Lancaster, **1980**; pp. 1–46.
- [153] Patel, R.G.; Killoh, D.C.; Parrott, L.J.; Gutteridge, W.A. Influence of curing at different relative humidities upon compound reactions and porosity in Portland cement paste. *Materials and Structures*, **1988**, *21*, 192–197.
- [154] Uchikawa, H.; Uchida, S.; Hanehara, S. Flocculation structure of fresh cement paste determined by sample freezing-back scattered electron image method. // *Cemento*, **1987**, *84*, 3–21.
- [155] Lothenbach, B.; Pelletier-Chaignat, L.; Winnefeld, F. Stability in the system CaO–Al<sub>2</sub>O<sub>3</sub>–H<sub>2</sub>O. *Cement and Concrete Research*, **2012**, *42*, 1621–1634.
- [156] Scherer, G.W. Stress from crystallization of salt. *Cement and Concrete Research*, **2004**, *34*, 1613–1624.
- [157] Scherer, G.W. Crystallization in pores. *Cement and Concrete Research*, **1999**, *29*, 1347–1358.
- [158] Bizzozero, J.; Gosselin, C.; Scrivener, K.L. Expansion mechanisms in calcium aluminate and sulfoaluminate systems with calcium sulfate. *Cement and Concrete Research*, **2014**, *56*, 190–202.
- [159] Aïtcin, P.-C. Accelerators. In: *Science and technology of concrete admixtures*. Aïtcin, P.-C., Flatt, R.J., Eds.; Woodhead Publishing / Elsevier, **2016**; pp. 405–414.
- [160] Nkinamubanzi, P.-C., Mantellato, S., Flatt, R.J. Superplasticizers in practice. In: *Science and technology of concrete admixtures*. Aïtcin, P.-C., Flatt, R.J., Eds.; Woodhead Publishing / Elsevier, **2016**; pp. 353–378.
- [161] Palacios, M., Flatt, R.J. Working mechanism of viscosity-modifying admixtures. In: *Science and technology of concrete admixtures*. Aïtcin, P.-C., Flatt, R.J., Eds.; Woodhead Publishing / Elsevier, **2016**; pp. 415–432.

## 6 REFERENCES

---

- [162] Flatt, R.J.; Roussel, N.; Cheeseman, C.R. Concrete: An eco material that needs to be improved. *Journal of the European Ceramic Society*, **2012**, 32, 2787–2798.
- [163] Gagne, R. Air entraining agents. In: *Science and technology of concrete admixtures*. Aïtcin, P.-C., Flatt, R.J., Eds.; Woodhead Publishing / Elsevier, **2016**; pp. 379–392.
- [164] Gagne, R. Shrinkage-reducing admixtures. In: *Science and technology of concrete admixtures*. Aïtcin, P.-C., Flatt, R.J., Eds.; Woodhead Publishing / Elsevier, **2016**; pp. 457–470.
- [165] Aïtcin, P.-C.; Flatt, R.J., Eds. *Science and technology of concrete admixtures*; Woodhead Publishing / Elsevier, **2016**.
- [166] Dodson, V.H. *Concrete Admixtures*; Springer US: Boston, MA, **1990**.
- [167] Hewlett, P.C.; Justnes, H.; Edmeades, R.M. Cement and concrete admixtures. In: *Lea's chemistry of cement and concrete*. Hewlett, P.C., Liska, M., Eds.; Elsevier, **2019**; pp. 641–698.
- [168] Gelardi, G., Mantellato, S., Marchon, D., Palacios, M., Eberhardt, A.B., Flatt, R.J. Chemistry of chemical admixtures. In: *Science and technology of concrete admixtures*. Aïtcin, P.-C., Flatt, R.J., Eds.; Woodhead Publishing / Elsevier, **2016**; pp. 149–218.
- [169] Hewlett, P.C. *Cement admixtures: Use and applications*, 2<sup>nd</sup> ed.; Longman Group UK Ltd: Harlow, Essex, England, **1988**.
- [170] Engbert, A.; Gruber, S.; Plank, J. The effect of alginates on the hydration of calcium aluminate cement. *Carbohydrate polymers*, **2020**, 236, 116038.
- [171] Engbert, A.; Plank, J. Templating effect of alginate and related biopolymers as hydration accelerators for calcium alumina cement - A mechanistic study. *Materials & Design*, **2020**, 195, 109054.
- [172] Ramachandran, V.S. 17 - Admixture formulations. In: *Concrete Admixtures Handbook*, 2<sup>nd</sup> ed. Ramachandran, V.S., Ed.; William Andrew Publishing: Park Ridge, NJ, **1996**; pp. 1045–1076.
- [173] Ramachandran, V.S., Ed. *Concrete Admixtures Handbook*, 2<sup>nd</sup> ed.; William Andrew Publishing: Park Ridge, NJ, **1996**.
- [174] Abdelrazig, B.E.I.; Bonner, D.G.; Nowell, D.V.; Dransfield, J.M.; Egan, P.J. Effects of accelerating admixtures on cement hydration. In: *Admixtures for concrete, improvement of properties, RILEM symposium*; Chapman & Hall: London, **1990**; pp. 106–109.
- [175] Fletcher, K.E.; Roberts, M.H. The performance in concrete of admixtures with accelerating, retarding or water-reducing properties. *Concrete Journal*, **1971**, 5, 175–179.
- [176] Marchon, D., Flatt, R.J. Impact of chemical admixtures on cement hydration. In: *Science and technology of concrete admixtures*. Aïtcin, P.-C., Flatt, R.J., Eds.; Woodhead Publishing / Elsevier, **2016**; pp. 279–304.
- [177] Ramachandran, V.S.; Lowery, M.S. Conduction calorimetric investigation of the effect of retarders on the hydration of Portland cement. *Thermochimica Acta*, **1992**, 195, 373–387.

## 6 REFERENCES

---

- [178] Justnes, H. Aspects of replacing gypsum with other calcium salts in Portland cement. *Advances in Cement Research*, **2013**, *25*, 44–50.
- [179] Justnes, H. Properties of gypsum-free Portland cement. *Journal of Sustainable Cement-Based Materials*, **2014**, *3*, 128–139.
- [180] Milestone, N.B. Hydration of tricalcium silicate in the presence of lignosulfonates, glucose, and sodium gluconate. *Journal of the American Ceramic Society*, **1979**, *62*, 321–324.
- [181] Smith, R.M., Martell, A.E., Motekaitis, R.J. *NIST Critically Selected Stability Constants of Metal Complexes Database*, **2003**.
- [182] Young, F. Reaction mechanisms of organic admixtures with hydrating cement compounds, *Transportation Research Record No. 564*: Washington DC, USA, **1976**.
- [183] Cheung, J.; Jeknavorian, A.; Roberts, L.; Silva, D. Impact of admixtures on the hydration kinetics of Portland cement. *Cement and Concrete Research*, **2011**, *41*, 1289–1309.
- [184] Bishop, M.; Barron, A.R. Cement hydration inhibition with sucrose, tartaric acid, and lignosulfonate: Analytical and spectroscopic study. *Industrial & Engineering Chemistry Research*, **2006**, *45*, 7042–7049.
- [185] Collepardi, M. 6 - Water Reducers / Retarders. In: *Concrete Admixtures Handbook*, 2<sup>nd</sup> ed. Ramachandran, V.S., Ed.; William Andrew Publishing: Park Ridge, NJ, **1996**; pp. 286–409.
- [186] Ramachandran, V.S.; Lowery, M.S.; Wise, T.; Polomark, G.M. The role of phosphonates in the hydration of Portland cement. *Materials and Structures*, **1993**, *26*, 425–432.
- [187] Bruijn, J.M. de; Kieboom, A.P.G.; van Bekkum, H. Alkaline degradation of monosaccharides III. Influence of reaction parameters upon the final product composition. *Recueil des Travaux Chimiques des Pays-Bas*, **1986**, *105*, 176–183.
- [188] Yang, B.Y.; Montgomery, R. Alkaline degradation of glucose: Effect of initial concentration of reactants. *Carbohydrate Research*, **1996**, *280*, 27–45.
- [189] Thomas, N.L.; Birchall, J.D. The retarding action of sugars on cement hydration. *Cement and Concrete Research*, **1983**, *13*, 830–842.
- [190] Smith, B.J.; Rawal, A.; Funkhouser, G.P.; Roberts, L.R.; Gupta, V.; Israelachvili, J.N.; Chmelka, B.F. Origins of saccharide-dependent hydration at aluminate, silicate, and aluminosilicate surfaces. *Proceedings of the National Academy of Sciences of the United States of America*, **2011**, *108*, 8949–8954.
- [191] Smith, B.J.; Roberts, L.R.; Funkhouser, G.P.; Gupta, V.; Chmelka, B.F. Reactions and surface interactions of saccharides in cement slurries. *Langmuir*, **2012**, *28*, 14202–14217.
- [192] Luke, K.; Luke, G. Effect of sucrose on retardation of Portland cement. *Advances in Cement Research*, **2000**, *12*, 9–18.

## 6 REFERENCES

---

- [193] Zhang, L.; Catalan, L.J.J.; Balec, R.J.; Larsen, A.C.; Esmaeili, H.H.; Kinrade, S.D. Effects of saccharide set retarders on the hydration of ordinary Portland cement and pure tricalcium silicate. *Journal of the American Ceramic Society*, **2010**, 93, 279–287.
- [194] Young, J.F. A review of the mechanisms of set-retardation in portland cement pastes containing organic admixtures. *Cement and Concrete Research*, **1972**, 2, 415–433.
- [195] Marchon, D., Mantellato, S., Eberhardt, A., Flatt, R.J. Adsorption of chemical admixtures. In: *Science and technology of concrete admixtures*. Aïtcin, P.-C., Flatt, R.J., Eds.; Woodhead Publishing / Elsevier, **2016**; pp. 219–256.
- [196] Gelardi, G., Flatt, R.J. Working mechanisms of water reducers and superplasticizers. In: *Science and technology of concrete admixtures*. Aïtcin, P.-C., Flatt, R.J., Eds.; Woodhead Publishing / Elsevier, **2016**; pp. 257–278.
- [197] Ramachandran, V.S. *Superplasticizers: Properties and applications in concrete*; Canada Centre for Mineral and Energy Technology: Ottawa, **1998**.
- [198] Aïtcin, P.-C. *High Performance Concrete*; Spon Press / Routledge: New York, **2002**.
- [199] Süddeutsche Kalkstickstoffwerke (SKW). British patent 1 169 582, **1969**.
- [200] Kao Soap Co. (Ltd.). Additive composition for hydraulic cement-based mixtures. British Patent 1 286 798, **1970**.
- [201] Marchon, D.; Sulser, U.; Eberhardt, A.; Flatt, R.J. Molecular design of comb-shaped polycarboxylate dispersants for environmentally friendly concrete. *Soft Matter*, **2013**, 9, 10719.
- [202] Hanehara, S.; Yamada, K. Interaction between cement and chemical admixture from the point of cement hydration, absorption behaviour of admixture, and paste rheology. *Cement and Concrete Research*, **1999**, 29, 1159–1165.
- [203] Robeyst, N., De Belie, N. Effect of superplasticizers on hydration and setting behavior of cements. In: *9<sup>th</sup> CANMET / ACI International Conference on Superplasticizers and Other Chemical Admixtures in Concrete*: Sevilla, Spain, **2009**; pp. 61–73.
- [204] Wang, Z.-M., Zhao, L., Tian, N. The initial hydration behaviors of cement pastes with different types of superplasticizers. In: *9<sup>th</sup> CANMET / ACI International Conference on Superplasticizers and Other Chemical Admixtures in Concrete*: Sevilla, Spain, **2009**; pp. 267–278.
- [205] Okamura, H., Ouchi, M. Self-compacting concrete. Development, present and future. In: *First International RILEM Symposium on Self-Compacting Concrete*, **1999**; pp. 3–14.
- [206] Tsubakimoto, T., Hosoidi, M., Tahara, H. Copolymer and method for manufacture thereof. European Patent 0056627 B1, **1984**.
- [207] Palacios, M.; Puertas, F. Effect of superplasticizer and shrinkage-reducing admixtures on alkali-activated slag pastes and mortars. *Cement and Concrete Research*, **2005**, 35, 1358–1367.

## 6 REFERENCES

---

- [208] Ferrari, L.; Kaufmann, J.; Winnefeld, F.; Plank, J. Multi-method approach to study influence of superplasticizers on cement suspensions. *Cement and Concrete Research*, **2011**, *41*, 1058–1066.
- [209] Plank, J.; Zhimin, D.; Keller, H.; Hössle, F.v.; Seidl, W. Fundamental mechanisms for polycarboxylate intercalation into C<sub>3</sub>A hydrate phases and the role of sulfate present in cement. *Cement and Concrete Research*, **2010**, *40*, 45–57.
- [210] Yamamoto, M., Uno, T., Onda, Y., Tanaka, H., Yamashita, A., Hirata, T., Hirano, N. Copolymer for cement admixtures and its production process and use. US Patent 6727315 B2, **2004**.
- [211] Plank, J.; Sachsenhauser, B. Impact of molecular structure on zeta potential and adsorbed conformation of α-allyl-ω-methoxypolyethylene glycol-maleic anhydride superplasticizers. *Journal of Advanced Concrete Technology*, **2006**, *4*, 233–239.
- [212] Müller, M.W.; Plank, J. Influence of diol and diester content on the performance of MPEG-based superplasticisers. In: *1<sup>st</sup> International Conference on the Chemistry of Construction Materials*, Berlin, 7 October **2013**; pp. 293–296.
- [213] Flatt, R.J.; Schober, I.; Raphael, E.; Plassard, C.; Lesniewska, E. Conformation of adsorbed comb copolymer dispersants. *Langmuir*, **2009**, *25*, 845–855.
- [214] Nawa, T., Ichiboji, H., Kinoshita, M. Influence of temperature on fluidity of cement paste containing superplasticizer with polyethylene oxide graft chains. In: *6<sup>th</sup> CANMET / ACI International Conference on Superplasticizers and Other Chemical Admixtures in Concrete*, **2000**; Vol. 195; pp. 181–194.
- [215] Pourchet, S., Compart, C., Nicoleau, L., Nonat, A. Influence of PC superplasticizers on tricalcium silicate hydration. In: *Proceedings of the 12<sup>th</sup> International Congress on the Chemistry of Cement*, Montréal, **2007**.
- [216] Winnefeld, F.; Becker, S.; Pakusch, J.; Götz, T. Effects of the molecular architecture of comb-shaped superplasticizers on their performance in cementitious systems. *Cement and Concrete Composites*, **2007**, *29*, 251–262.
- [217] Winnefeld, F., Zingg, A., Holzer, L., Figi, R., Pakusch, J., Becker, S. Interaction of polycarboxylate-based superplasticizers and cements: Influence of polymer structure and C<sub>3</sub>A-content of cement. In: *Proceedings of the 12<sup>th</sup> International Congress on the Chemistry of Cement*, Montréal, **2007**.
- [218] Yamada, K.; Takahashi, T.; Hanehara, S.; Matsuhisa, M. Effects of the chemical structure on the properties of polycarboxylate-type superplasticizer. *Cement and Concrete Research*, **2000**, *30*, 197–207.
- [219] Heeb, R.; Lee, S.; Venkataraman, N.V.; Spencer, N.D. Influence of salt on the aqueous lubrication properties of end-grafted, ethylene glycol-based self-assembled monolayers. *ACS Applied Materials & Interfaces*, **2009**, *1*, 1105–1112.

## 6 REFERENCES

---

- [220] Tasaki, K. Poly(oxyethylene)-cation interactions in aqueous solution: A molecular dynamics study. *Computational and Theoretical Polymer Science*, **1999**, *9*, 271–284.
- [221] Masuda, Y.; Nakanishi, T. Ion-specific swelling behavior of poly(ethylene oxide) gel and the correlation to the intrinsic viscosity of the polymer in salt solutions. *Colloid & Polymer Science*, **2002**, *280*, 547–553.
- [222] Plank, J.; Sachsenhauser, B. Experimental determination of the effective anionic charge density of polycarboxylate superplasticizers in cement pore solution. *Cement and Concrete Research*, **2009**, *39*, 1–5.
- [223] Robeyst, N.; Schutter, G. de; Grosse, C.; Belie, N. de. Monitoring the effect of admixtures on early-age concrete behaviour by ultrasonic, calorimetric, strength and rheometer measurements. *Magazine of Concrete Research*, **2011**, *63*, 707–721.
- [224] Lei, L.; Plank, J. A study on the impact of different clay minerals on the dispersing force of conventional and modified vinyl ether based polycarboxylate superplasticizers. *Cement and Concrete Research*, **2014**, *60*, 1–10.
- [225] Ng, S.; Plank, J. Interaction mechanisms between Na montmorillonite clay and MPEG-based polycarboxylate superplasticizers. *Cement and Concrete Research*, **2012**, *42*, 847–854.
- [226] Lei, L.; Plank, J. A concept for a polycarboxylate superplasticizer possessing enhanced clay tolerance. *Cement and Concrete Research*, **2012**, *42*, 1299–1306.
- [227] Lei, L.; Plank, J. Synthesis and properties of a vinyl ether-based polycarboxylate superplasticizer for concrete possessing clay tolerance. *Industrial & Engineering Chemistry Research*, **2014**, *53*, 1048–1055.
- [228] Li, R.; Lei, L.; Sui, T.; Plank, J. Effectiveness of PCE superplasticizers in calcined clay blended cements. *Cement and Concrete Research*, **2021**, *141*, 106334.
- [229] Havard, J.; Gjorv, O.E. Effect of gypsum-hemihydrate ratio in cement on rheological properties of fresh concrete. *Materials Journal*, **1997**, *94*, 142–146.
- [230] Sprung, S. Einfluß der Mühlentemperatur auf das Erstarren und die Festigkeit von Zement: Effect of mill atmosphere on the setting and strength of cement. *Zement-Kalk-Gips*, **1974**, *27*, 259–267.
- [231] Hills, L.M. Water spray in cement finish mills: A literature review: Skokie, IL, **2006**.
- [232] Hansen, F.E.; Clausen, H.J. Zementfestigkeit und Kühlung durch verdüstes Wasser beim Mahlen: Cement strength and cooling by water injection during grinding. *Zement-Kalk-Gips*, **1974**, *27*, 333–336.
- [233] Theisen, K.; Johansen, V. Prehydration and strength development of Portland cement. *American Ceramic Society Bulletin*, **1975**, *54*, 787–791.
- [234] Matouschek, F. Beitrag zur Erklärung der Knollenbildung im Zement. *Zement-Kalk-Gips*, **1972**, *25*, 395–396.

## 6 REFERENCES

---

- [235] Meyers, S.L. Heat developed by cement while setting and hardening. *Rock Products*, **1932**, 35, 22.
- [236] Woods, H.; Steinour, H.H.; Starke, H.R. Effect of composition of Portland cement on heat evolved during hardening. *Industrial & Engineering Chemistry*, **1932**, 24, 1207–1214.
- [237] Davis, R.E.; Carlson, R.W.; Troxell, G.E.; Kelly, J.W. Cement investigations for the Hoover Dam. *Proceedings of the American Concrete Institute*, **1933**, 29, 413–431.
- [238] Hornibrook, F.B.; Kalousek, G.L.; Jumper, C.H. Effects of partial prehydration and different curing temperatures on some of the properties of cement and concrete. *Journal of Research of the National Bureau of Standards*, **1936**, 16, 487.
- [239] Sprung, S. Einfluß der Lagerungsbedingungen auf die Zementeigenschaften: Effect of storage conditions on the properties of cements. *Zement-Kalk-Gips*, **1978**, 31, 305–309.
- [240] Silk, I.M. Exposure to moisture alters well cement. *Petroleum Engineer International*, **1986**, 58, 45–49.
- [241] Barbic, L.; Tinta, V.; Lozar, B.; Marinkovic, V. Effect of storage time on the rheological behavior of oil well cement slurries. *Journal of the American Ceramic Society*, **1991**, 74, 945–949.
- [242] Schmidt, G.; Bier, T.; Wutz, K.; Maier, M. Characterization of the ageing behaviour of premixed dry mortars and its effect on their workability properties. *ZKG International*, **2007**, 60, 94–103.
- [243] Weithase, H. Über Änderung der Bindezeit von Portlandzement. *Zement*, **1931**, 20, 187–192.
- [244] Hansen, W.C. Aeration cause of false set in Portland cement. *ASTM Proceedings*, **1955**, 58, 1044–1050.
- [245] Kalousek, G.L. Abnormal set of Portland cement, causes and correctives. *U. S. Department of the Interior, Bureau of Reclamation, General Report No. 45*, Denver, CO, **1969**.
- [246] Kalousek, G.L. Hydration processes at the early stages of cement hardening. In: *Proceedings of the 6<sup>th</sup> International Congress on the Chemistry of Cement: Moscow*, **1974**.
- [247] Richartz, V.W.; Eick, H. Effects of storage on the properties of cement. *Zement-Kalk-Gips*, **1973**, 2, 67–74.
- [248] Dubina, E.; Wadsö, L.; Plank, J. A sorption balance study of water vapour sorption on anhydrous cement minerals and cement constituents. *Cement and Concrete Research*, **2011**, 41, 1196–1204.
- [249] Jensen, O.M.; Hansen, F.P.; Lachowski, E.E.; Glasser, F.P. Clinker mineral hydration at reduced relative humidities. *Cement and Concrete Research*, **1999**, 29, 1505–1512.
- [250] Breval, E. Gas-phase and liquid-phase hydration of C<sub>3</sub>A. *Cement and Concrete Research*, **1977**, 7, 297–303.

## 6 REFERENCES

---

- [251] Dubina, E.; Plank, J.; Wadsö, L.; Black, L. The effects of prehydration of a combination of cubic C<sub>3</sub>A with β-hemihydrate on the adsorption of BNS superplasticizer. In: *13<sup>th</sup> International Congress on the Chemistry of Cement (ICCC), Madrid, 3-8 July 2011, Abstracts and Proceedings: Cementing a sustainable future*. Palomo, A., Zaragoza, A., López Agüí, J.C., Eds.; Instituto de Ciencias de la Construcción: Madrid, **2011**; p. 250.
- [252] Dubina, E.; Plank, J.; Black, L.; Wadsö, L. Impact of environmental moisture on C<sub>3</sub>A polymorphs in the absence and presence of CaSO<sub>4</sub>·0.5H<sub>2</sub>O. *Advances in Cement Research*, **2014**, *26*, 29–40.
- [253] Dubina, E.; Plank, J.; Black, L. Impact of water vapour and carbon dioxide on surface composition of C<sub>3</sub>A polymorphs studied by X-ray photoelectron spectroscopy. *Cement and Concrete Research*, **2015**, *73*, 36–41.
- [254] Dubina, E.; Korat, L.; Black, L.; Strupi-Šuput, J.; Plank, J. Influence of water vapour and carbon dioxide on free lime during storage at 80 °C, studied by Raman spectroscopy. *Spectrochimica Acta Part A: Molecular and Biomolecular Spectroscopy*, **2013**, *111*, 299–303.
- [255] Breval, E. The effects of prehydration on the liquid hydration of 3CaO·Al<sub>2</sub>O<sub>3</sub> with CaSO<sub>4</sub>·2H<sub>2</sub>O. *Journal of the American Ceramic Society*, **1979**, *62*, 395–398.
- [256] Stoian, J.; Oey, T.; Bullard, J.W.; Huang, J.; Kumar, A.; Balonis, M.; Terrill, J.; Neithalath, N.; Sant, G. New insights into the prehydration of cement and its mitigation. *Cement and Concrete Research*, **2015**, *70*, 94–103.
- [257] Dubina, E.; Plank, J. Influence of moisture- and CO<sub>2</sub>-induced ageing in cement on the performance of admixtures used in construction chemistry. *ZKG International*, **2012**, *65*, 60–68.
- [258] Maltese, C.; Pistoletti, C.; Bravo, A.; Cella, F.; Cerulli, T.; Salvioni, D. A case history: Effect of moisture on the setting behaviour of a Portland cement reacting with an alkali-free accelerator. *Cement and Concrete Research*, **2007**, *37*, 856–865.
- [259] Winnefeld, F. Influence of cement ageing and addition time on the performance of superplasticizers. *ZKG International*, **2008**, *61*, 68–77.
- [260] Meier, M.R.; Napharatsamee, T.; Plank, J. Dispersing performance of superplasticizers admixed to aged cement. *Construction and Building Materials*, **2017**, *139*, 232–240.
- [261] Dubina, E.; Plank, J. Investigation of the long-term stability during storage of drymix mortars, Part 2: Influence of moisture exposure on the performance of self-levelling mortars (SLUs). *ALITinform*, **2012**, *4-5*, 86–99.
- [262] Zurbriggen, R.; Götz-Neunhoeffer, F. Mechanisms and resulting damages of prolonged retardation in aged dry mixes: A case study of mixed-binders containing tartaric acid. In: *GDCh-Tagung Bauchemie, 27-28 September 2007, Siegen*. Trettin, R., Ed., 1<sup>st</sup> ed.; Gesellschaft Deutscher Chemiker: Frankfurt, **2007**; pp. 111–118.
- [263] Deutsche Forschungsgemeinschaft (DFG). *Funding Atlas 2018: Key indicators for publicly funded research in Germany*, 1<sup>st</sup> ed.; Wiley-VCH: Weinheim, **2020**.

## 6 REFERENCES

---

- [264] DIN EN 196-11:2019-03, Prüfverfahren für Zement - Teil 11: Hydratationswärme - Isotherme Wärmeflusskalorimetrie-Verfahren; Deutsche Fassung EN 196-11:2018; Beuth Verlag GmbH: Berlin, **2019**.
- [265] Nagul, E.A.; McKelvie, I.D.; Worsfold, P.; Kolev, S.D. The molybdenum blue reaction for the determination of orthophosphate revisited: Opening the black box. *Analytica Chimica Acta*, **2015**, 890, 60–82.
- [266] Luecke, W. Systematic investigation of aluminium interferences with the alkaline earths in flame atomic absorption spectrometry. *Fresenius' Journal of Analytical Chemistry*, **1992**, 344, 242–246.
- [267] DIN EN 12706:1999-12, Klebstoffe - Prüfverfahren für hydraulisch erhärtende Boden-Spachtelmassen - Bestimmung des Fließverhaltens; Deutsche Fassung EN 12706:1999; Beuth Verlag GmbH: Berlin, **1999**.
- [268] DIN EN 196-3:2017-03, Prüfverfahren für Zement - Teil 3: Bestimmung der Erstarrungszeiten und der Raumbeständigkeit; Deutsche Fassung EN 196-3:2016; Beuth Verlag GmbH: Berlin, **2017**.
- [269] DIN EN 196-1:2016-11, Prüfverfahren für Zement - Teil 1: Bestimmung der Festigkeit; Deutsche Fassung EN 196-1:2016; Beuth Verlag GmbH: Berlin, **2016**.
- [270] Luong, T.; Mayer, H.; Eckert, H.; Novinson, T.I. In situ  $^{27}\text{Al}$  NMR studies of cement hydration: The effect of lithium-containing setting accelerators. *Journal of the American Ceramic Society*, **1989**, 72, 2136–2141.
- [271] Matusinovic, T.; Vrbos, N.; Curlin, D. Lithium salts in rapid setting high-alumina cement materials. *Industrial & Engineering Chemistry Research*, **1994**, 33, 2795–2800.
- [272] Plank, J.; Winter, C. Competitive adsorption between superplasticizer and retarder molecules on mineral binder surface. *Cement and Concrete Research*, **2008**, 38, 599–605.
- [273] Götz-Neunhoeffer, F.; Zurbriggen, R. Formation of hydrate spheres in ternary binder systems. *ZKG International*, **2008**, 61, 68–76.
- [274] Zurbriggen, R.; Bühler, E.; Waser, H.; Aberle, T.; Bachmann, R.; Herwegh, M. High performing self-levelling underlays - Learnings from material science studies. In: *5<sup>th</sup> American Drymix Mortar Conference*: Philadelphia, PA, **2016**.